BC
Province of British Columbia
Ministry of Energy, Mines
and Petroleum Resources
Hon. Anne Edwards, Minister

MINERAL RESOURCES DIVISION
Geological Survey Branch

THE GEOLOGY AND MINERAL DEPOSITS OF THE HEDLEY GOLD SKARN DISTRICT, SOUTHERN BRITISH COLUMBIA

By G.E. Ray, P.Geo. and G.L. Dawson, P.Geo.

**With contributions by M.J. Orchard (GSC),
J.E. Gabites (U.B.C.) and E.C. Prosh**

BULLETIN 87

Canadian Cataloguing in Publication Data
Ray, G.E. (Gerald E.)
The geology and mineral deposits of the Hedley gold skarn district, southern British Columbia

(Bulletin, ISSN 0226-7497; 87)

Issued by Geological Survey Branch.
Includes bibliographical references; p.
ISBN 0-7726-1977-8

1. Geology - British Columbia - Similkameen River Region. 2. Geochemistry - British Columbia - Similkameen River Region. 3. Geology, Economic - British Columbia - Similkameen Region. 4. Mines and mineral resources - British Columbia - Similkameen Region. I. Dawson, G.L. II. British Columbia. Ministry of Energy, Mines and Petroleum Resources. III. British Columbia. Geological Survey Branch. IV. Title. V. Series: Bulletin (British Columbia. Ministry of Energy, Mines and Petroleum Resources) ; 87.

QE187.R39 1993 557.11'5' C93-092420-7

VICTORIA
BRITISH COLUMBIA
CANADA

January 1994

Fieldwork for this research was carried out during the period 1985 to 1987

ABSTRACT

The Hedley mining district of British Columbia lies within the allochthonous Quesnel Terrane of the Intermontane Belt. It is situated at the eastern edge of the Upper Triassic Nicola Group, close to the group's contact with Paleozoic and Triassic oceanic rocks of the Apex Mountain Complex.

The Nicola Group is a westerly thickening, late Carnian to late Norian calcareous sedimentary and arc-related volcaniclastic sequence that was deposited on a tectonically active, west-dipping paleoslope. Sedimentary facies changes and paleocurrent indicators suggest that the sediments in the group were derived largely from an eastern source. The Nicola Group in the Hedley area was laid down across a structural hinge zone that marked the rifted margin of the westerly deepening, shallow-marine Nicola basin.

A sedimentary succession is recognized in the Nicola Group. This includes an upper, widely developed and thick (at least 1200m) unit, the Whistle Formation, which consists largely of alkalic and subalkalic tuffs and tuffaceous sediments. The base of the formation is marked by an extensive limestone-clast-bearing unit, the Copperfield breccia, which reaches 200 metres in thickness and 16 kilometres in strike length. The unit is an important stratigraphic marker horizon in the district, and is believed to represent a gravity-slide megabreccia deposit.

The Whistle Formation is underlain by a succession in which four sedimentary facies are distinguished: from east to west, the thin (up to 200m), shallow-marine, limestone-dominant French Mine Formation; the thicker, siltstone-dominant Hedley and Chuchuwayha formations in the central part of the area; and the thick (up to 2200m), deeper water and argillite-dominant Stemwinder Formation. Conodonts from the French Mine, Hedley and Chuchuwayha formations indicate they are Late Triassic (Carnian-Norian) in age. The sedimentary facies were separated from one another by long-lived faults that marked syn-sedimentation scarp slopes related to rifting along the Nicola basin margin.

The Chuchuwayha, Hedley and French Mine formations are underlain by a sequence of mafic tuffs with minor flows, limestone and chert-pebble conglomerate, the Oregon Claims Formation. The age of this unit and its contact relationship with the overlying rocks are uncertain. The formation may represent the oldest exposed section of the Nicola Group, but it is more likely to be an older basement, and it may represent a western extension of the Apex Mountain Complex.

A newly recognized mid-Jurassic unit, the Skwel Peken Formation, overlies the Nicola Group. It consists of a 1900-metre succession of calcalkaline andesitic to dacitic tuffs with minor amounts of epiclastic sediments, and pyroclastic surge deposits. It was laid down in a nonmarine, subaerial to shallow water environment and is believed to represent volcanism related to the mid-Jurassic plutonism represented by the Cahill Creek and Lookout Ridge plutons.

Minor amounts of Cretaceous Spences Bridge Group and the Eocene Springbrook and Marron formations are also present in the area.

Several episodes of plutonism are recognized. The oldest resulted in the quartz dioritic and gabbroic Hedley intrusions that are associated with widespread gold skarn mineralization. Equivocal radiometric U-Pb dating and field evidence suggest they were intruded during Late Triassic to Early Jurassic time (219−194 Ma). The intrusions occur as large and small stocks, as abundant sills, or as rare dikes; the sills are preferentially developed in the thinly bedded Chuchuwayha and Hedley formations.

A slightly younger intrusive episode produced the large, granodioritic Bromley batholith and a related marginal body, the granodioritic to gabbroic Mount Riordan stock. The latter is genetically associated with the Mount Riordan (Crystal Peak) skarn that is being evaluated as a potential industrial garnet deposit. A radiometric U-Pb zircon age of 194.6±1.2 Ma (Early Jurassic) is indicated for the Mount Riordan stock, and a similar age has been obtained from the Bromley batholith.

A subsequent phase of granodioritic to quartz monzonitic magmatism is represented by the Lookout Ridge and Cahill Creek plutons; the latter, which commonly separates the Nicola Group to the west from the Apex Mountain Complex farther east, yielded a U-Pb zircon date of 168.8±9 Ma (mid Jurassic). These high-level plutons are spatially related to a suite of aplites and quartz porphyry minor intrusions that yielded a U-Pb zircon date of 154.5 +8 −43 Ma (Late Jurassic).

The youngest major intrusion in the district, the Verde Creek stock, is coeval with the Early Cretaceous Spences Bridge Group; it intrudes the Nicola Group in the western part of the district. A rare suite of leucocratic, calcalkaline minor intrusions (or possible volcanic flows) is spatially associated with the Skwel Peken Formation. These rocks contain magmatic garnet phenocrysts with almandine-rich cores and spessartine-rich margins that are chemically distinct from the grossular-andradite garnets in the gold skarns.

Two deformational episodes are identified in the Apex Mountain Complex, the first and predominant of which resulted in tight to isoclinal folds with moderate to strong penetrative axial planar fabrics.

Two structural phases are also recognized in the Nicola Group, neither of which produced dominant penetrative fabrics. These predate both the Skwel Peken Formation and the Cahill Creek pluton which suggests they are pre mid-Jurassic in age. A younger phase of folding has gently deformed the Skwel Peken Formation. The first phase, which was only locally developed in the Nicola Group, produced minor flexure folds, that were probably related to the forcible emplacement of the Hedley intrusions. At Nickel Plate, these structures partly controlled the gold skarn mineralization.

The second deformational phase to overprint the Nicola Group was the dominant structural event in the district. It resulted in overturned minor and major asymmetric folds, including the large Hedley anticline. The youngest (post mid-Jurassic) fold phase has only been identified in the Skwel Peken Formation; it produced open minor flexure folds.

The Hedley district has important skarn deposits as well as some minor gold-bearing quartz-carbonate veins. The skarns are separable into two types, the most important being gold skarns which are characteristically pyroxene dominant. The second and less common type is garnet dominant and contains some tungsten and copper but little or no gold; the Mount Riordan skarn represents the largest of this second type.

Between 1904 and 1991 the gold skarns produced over 62 tonnes of gold from 8.4 million tonnes of ore mined, of which over 97% was won from the Nickel Plate deposit; lesser amounts were recovered from gold skarns at the French, Canty and Good Hope mines. The overall gold grade of all the gold skarn deposits mined (by underground and open pit) in the district is 7.43 grams per tonne.

The gold skarns are genetically and spatially related to the dioritic stocks and sill-dike swarms of the Hedley intrusions. Economic gold skarns are hosted only by the Nicola Group, and are structurally, stratigraphically and lithologically controlled; they favour areas where the Hedley intrusions cut the calcareous, shallower marine sedimentary facies rocks of the Hedley and French Mine formations.

Skarn alteration varies from narrow zones less than 10 metres wide to large envelopes hundreds of metres thick. The largest skarn envelope is at Nickel Plate where it outcrops over 4 square kilometres. Prograde skarn development is characterized by an early phase of K-feldspar-biotite-albite alteration which is replaced subsequently by pyroxene-garnet-carbonate-scapolite assemblages. Mineralogical zoning is present in both the mineralized and barren skarns; this zoning generally consists of coarser grained garnet-rich proximal assemblages and finer grained pyroxene-rich distal assemblages. Gold-pyrrhotite-arsenopyrite mineralization is preferentially developed in the distal, pyroxene-dominant skarn.

Bismuth tellurides, arsenopyrite and high pyrrhotite/pyrite ratios characterize the auriferous ore, and the gold-sulphide mineralization is generally coeval with widespread scapolitization. The close temporal and spatial association between gold and scapolite suggests that chlorine-rich fluids may have been important in the transportation and precipitation of gold.

The proposed model for the Nickel Plate deposit involves the injection of large volumes of magmatic fluid derived from the Hedley intrusions into the calcareous sediments to produce an early, high-temperature mineral sequence of biotite and orthoclase, followed by manganese-poor clinopyroxene, and finally grandite garnet. The overall compositional zoning in the Nickel Plate garnets is from grossularitic cores to andraditic margins. Subsequently, sulphides, gold and scapolite were introduced at lower temperatures. Fluid inclusion studies (Ettlinger, 1990a) at Nickel Plate indicate the main pyroxene-garnet skarn formed at temperatures between 460° and 480°C with average fluid salinities of 18.3 and 9.7 wt% NaCl equivalent for garnet and pyroxene respectively.

The Hedley intrusions, compared to other magmatic rocks related to base metal skarns, have the lowest amounts of total alkalis and silica, and the highest amounts of calcium, magnesium and iron. Low Fe_2O_3/FeO ratios and the presence of ilmenite and pyrrhotite in the unaltered Hedley intrusions, and abundant pyrrhotite in the ore suggest the skarns formed in a strongly reduced environment.

Skarn overprinting of the intrusions to produce endoskarn was accompanied by an increase in the potassium content and declines in total iron and the Fe_2O_3/FeO ratios. Initial skarn alteration of the sediments, to produce weakly altered exoskarn, was accompanied by gains in potassium, sodium and iron, with crystallization of K-feldspar, biotite, albite and minor pyroxene. As exoskarn alteration became more intense, the early minerals were replaced by hedenbergitic pyroxene and andraditic garnet, with corresponding losses of potassium, sodium, silica and aluminum and continuing gains in iron. It is believed that the breakdown of the ferromagnesian minerals in the endoskarn was the source for much of the iron enrichment in the exoskarn.

It is postulated that a large thermal cell formed around the Nickel Plate skarn. This probably resulted in the influx of meteoric waters into the base of the system which mixed with the magmatic fluids and resulted in the deposition of sulphides and gold. Consequently, ore horizons are preferentially developed close to the base and lateral margins of the alteration envelope. By contrast, the upper and interior portions of the skarn tend to be barren This zoning has relevance regarding future exploration of other, apparently barren, skarn outcrops that may mask mineralization at depth.

A district-wide, east-to-west change in the metallogeny, mineralogy and oxidation state of the skarns is suggested. Pyroxene-dominant and highly reduced skarns containing gold, arsenopyrite and bismuth tellurides occur in the west and central parts of the district, while more oxidised tungsten-bearing and garnet-dominant skarn such as the Mount Riordan skarn occur in the east. This zoning is partly due to the different sedimentary protoliths of the various skarns which reflects the original sedimentary facies changes in the Nicola Group across the district. It is also related to the different ages and compositions of the associated intrusions.

The district has good exploration potential for new gold-skarn discoveries, and the deposit model and ore controls postulated for the Hedley district are applicable to other areas of the Cordillera.

TABLE OF CONTENTS

Abstract iii
Regional Geology and Previous Work 1
  Introduction 1
  Previous work 1
  Regional geology 3
  Acknowledgements 7
Lithology and Stratigraphy in the Hedley District 9
  Introduction 9
  Apex Mountain Complex (Unit 1) 11
  Nicola Group (Units 2 − 7) 12
    Oregon Claims Formation (Unit 2) 13
    French Mine Formation (Unit 3) 15
    Hedley Formation (Unit 4) 16
    Stemwinder Formation (Unit 5) 17
    Chuchuwayha Formation (Unit 6) 17
    Whistle Formation (Unit 7) 18
    Rocks of uncertain age (Unit 8) 21
    Depositional environment of the Nicola Group at Hedley 21
  Skwel Peken Formation (Unit 15) 22
  Spences Bridge Group (Unit 17) 25
  Springbrook Formation (Unit 18) 25
  Marron Formation (Unit 19) 26
  Intrusive rocks 27
    Hedley Intrusions (Unit 9) 27
      Stemwinder stock 31
      Pettigrew stock 33
      Banbury stock 33
      Toronto stock 33
      Climax Bluff and Larcan stocks 34
      Hedley sills and dikes 34
      Comparison of Hedley intrusion geochemistry with other skarn-related igneous rocks 35
    Bromley batholith (Unit 10) 35
    Mount Riordan stock (Unit 11) 35
    Cahill Creek pluton (Unit 12) 36
    Lookout Ridge pluton (Unit 13) 38
    Quartz porphyry (Unit 14) 39
    Verde Creek stock (Unit 16) 40
    Minor intrusions Unit 20) 40
Structural Evolution of the Hedley District 43
  Introduction 43
  Apex Mountain Complex 43
  Nicola Group and Skwel Peken Formation 43
Economic Geology 47
  Introduction 47
  Major skarn deposits and prospects 47
    Nickel Plate and Hedley Mascot mines 47
      Mineralogical and geochemical variations at Nickel Plate 50
      Skarn mineralogy at Nickel Plate 51
      Mineral paragenesis at Nickel Plate 51
      Ore controls at Nickel Plate 57
      Genetic model for Nickel Plate deposit 59
  French mine 59
  Canty mine 61
  Good Hope mine 62
  Peggy 63
  Mount Riordan and Patricia 65
    Mineralogy of the Mount Riordan skarn 66
  Minor skarn occurrences 67
    Don and Speculator 67
    Duffy 67
    Florence 68
    Hedley North 68
    JJ 68
    Kel 68
    Kingston 68
    Lost Horse 69
    Sweden 69
    Red Mountain 69
    Red Top 69
    Rollo 69
    Stag Fraction 69
    Sunnyside 69
    Tough Oaks 70
    Winters Gold 70
    Unnamed skarn occurrences 70
  Veins and other mineral prospects 70
    Bradshaw 70
    Hedley Star 70
    Golden Oaks 70
    Gold Hill 71
    Golden Zone 71
    Hed 72
    Iota 72
    Ile 72
    Maple Leaf and Pine Knot 72
    Mission 73
    Patsy No.1 73
    Patsy No.2 74
    Snowstorm 74
    Toronto 74
    Victoria 74
  Other Mineral Resources 74
    Hedley Tailings 74
Changes in Geochemistry and Oxidation State in the Gold Skarns 75
  Introduction 75
  Changes in the endoskarn 75
  Changes in the exoskarn 75
  Conclusions 80
Mineralogical Zoning in the Gold Skarns 81
Conclusions 85
References 87

LIST OF APPENDICES

Appendix 1. Data concerning U-Pb zircon geochronology of the Hedley area 93
Appendix 2. Fossils collected from the Hedley area 98

Appendix 3. Geochemical analyses of Oregon Claims Formation tuffs 107
Appendix 4. Geochemical analyses of Nicola Group sedimentary rocks 108
Appendix 5. Geochemical analyses of the Whistle Formation tuffs 109
Appendix 6. Geochemical analyses of Skwel Peken Formation tuffs — lower and upper members 109
Appendix 7. Geochemical analyses of Spences Bridge Group rocks 110
Appendix 8. Geochemical analyses of the Marron Formation volcanics 110
Appendix 9. Geochemical analyses of the unaltered Hedley intrusions 111
Appendix 10. Geochemistry of the Toronto stock and other skarn-altered Hedley intrusions 113
Appendix 11. Geochemistry of the Mount Riordan stock 114
Appendix 12. Geochemistry of the Cahill Creek pluton 115
Appendix 13. Geochemistry of garnet-bearing intrusions (Unit 20a) and garnet crystals 116
Appendix 14. Major element analyses of "aplite"(Unit 20b) 120
Appendix 15. Microprobe analyses of exoskarn garnets and exoskarn clinopyroxenes: Nickel Plate deposit 120
Appendix 16. Geochemistry of exoskarn and endoskarn samples collected from drill hole 401: Nickel Plate deposit 125
Appendix 17. Geochemistry of exoskarn and endoskarn samples collected from drill holes 261 and 195: Nickel Plate deposit 127
Appendix 18. Microprobe analyses of exoskarn garnets and exoskarn clinopyroxenes: French deposit. 130
Appendix 19. Microprobe analyses of exoskarn garnets and exoskarn clinopyroxenes: Canty deposit 132
Appendix 20. Microprobe analyses of exoskarn garnets and exoskarn clinopyroxenes: Good Hope deposit 136
Appendix 21. Microprobe analyses of exoskarn garnets and exoskarn clinopyroxenes: Peggy skarn 140
Appendix 22. Microprobe analyses of exoskarn garnets and exoskarn clinopyroxenes: Mount Riordan skarn 145
Appendix 23. Microprobe analyses of exoskarn garnets: JJ skarn 150
Appendix 24. Assay results on mineralized grab samples 151
Appendix 25. UTM locations of lithogeochemical samples listed in Appendices 3 to 14 152
Appendix 26. Description of lithogeochemical samples 153

LIST OF FIGURES

Figure 1. Location of the Hedley gold skarn district 1
Figure 2. Regional geology of the southern part of the Intermontane Belt 4
Figure 3. Schematic east-west section through the Nicola marginal basin 5
Figure 4. Geology of the Hedley district 6
Figure 5. Schematic east-west section across the Hedley district 11
Figure 6. Age range of conodont microfossils collected from the Nicola Group, Hedley district 13
Figure 7. Various chemical plots of the Oregon Claims and Whistle formations 14
Figure 8. Depositional history of the Nicola Group in the Hedley area 20
Figure 9. Various chemical plots of the Skwel Peken Formation 24
Figure 10. Various chemical plots of the Spences Bridge Group, Marron Formation and garnet-bearing rhyodacite (Unit 20a) 26
Figure 11. Various chemical plots comparing the Hedley intrusions to other skarn-related plutons 27
Figure 12. Geology of the Banbury stock area 32
Figure 13. Various chemical plots of the Cahill Creek pluton, Mount Riordan stock, and the garnet-bearing rhyodacite (Unit 20a) 36
Figure 14. Distribution of the Cahill Creek pluton and its thermal metamorphic aureole 37
Figure 15. Composition of garnets from the Hedley gold skarns and garnet-bearing rhyodacite (Unit 20a) compared to garnets developed in plutonic, volcanic, and regional metamorphic environments 40
Figure 16. Compositional variation across individual garnet crystals from garnet-bearing rhyodacite (Unit 20a) 41
Figure 17. Computer generated stereoplots of various structural data in the Apex Mountain Complex and Nicola Group 44–45
Figure 18. Outcrop distribution of the skarn envelopes surrounding the Nickel Plate and Canty deposits 49
Figure 19. General paragenesis of skarn minerals in the Nickel Plate gold skarn 52
Figure 20. Composition of exoskarn pyroxenes in the Hedley skarns 52
Figure 21. Composition variation across individual exoskarn pyroxene crystals from the Hedley skarns 53
Figure 22. Composition of exoskarn garnets in the Hedley skarns 55
Figure 23. Compositional variation across various types of small birefringent exoskarn garnet crystals from the Nickel Plate deposit 56
Figure 24. Compositional variation across large garnet crystals with isotropic cores and birefringent margins, Nickel Plate deposit 56
Figure 25. Postulated development of the Nickel Plate skarn envelope 58

Figure 26. Compositional variation across individual garnet crystals from the Hedley skarns 64
Figure 27. Distribution of zones of high-grade garnet in the Mount Riordan skarn 65
Figure 28. Lithologies and skarn alteration in drill holes 401, 261 and 195 76
Figure 29. Plot illustrating changes in K_2O with progressive endoskarn alteration at Nickel Plate 77
Figure 30. Plot illustrating changes in oxidation state and iron content with progressive endoskarn alteration at Nickel Plate 78
Figure 31. Plot illustrating changes in Na_2O and K_2O with progressive exoskarn alteration at Nickel Plate 78
Figure 32. Plot illustrating changes in oxidation state and iron content with progressive exoskarn alteration at Nickel Plate 79
Figure 33. Plot of mole fraction hedenbergite versus mole fraction andradite of the Hedley skarns 79
Figure 34. Plot illustrating changes in total iron and SiO_2 with progressive exo and endoskarn alteration at Nickel Plate 79
Figure 35. Idealized mineralogical zoning associated with small-scale exoskarn alteration in the Hedley district 82
Figure 36. Sequence of exoskarn formation at Hedley 82
Figure 37. Geology and mineral occurrences in NTS 092H/8E .... (In pocket)
Figure 38. Geology and mineral occurrences NTS 082E/5W .... (In pocket)
Figure 39. Geological cross-sections across the Hedley area .... (In pocket)

LIST OF PLATES

Plate 1. The Nickel Plate mill and mine site under construction in 1987 2
Plate 2. The Nickel Plate mill and mine site after completion of construction in 1987 2
Plate 3. Marble skarn breccia, French mine 16
Plate 4. Chuchuwayha Formation siltstones 17
Plates 5 and 6. Copperfield breccia 18
Plate 7. Photomicrograph of crystal and ash tuff — Whistle Formation 20
Plate 8. Skwel Peken Formation, lower member tuffs 22
Plates 9 and 10. Photomicrograph of Skwel Peken Formation, lower member tuffs 23
Plate 11. Skwel Peken Formation, upper member tuffs 25
Plate 12. Porphyritic Hedley intrusions 30
Plates 13, 14, 15, 16 and 17. Photomicrographs: Hedley intrusions 30–31
Plate 18. Cahill Creek pluton 38
Plate 19. Photomicrograph: Quartz Porphyry 39
Plate 20. Photomicrograph: garnet-bearing rhyodacite 39
Plate 21. Nickel Plate deposit sulphide-rich ore 52
Plates 22 and 23. Photomicrograph: Nickel Plate exoskarn garnets 54
Plate 24. French deposit: various mineralogical zones 60
Plate 25. French deposit exoskarn alteration 61
Plate 26. Photomicrograph: French deposit garnet enclosed by late sulphides 61
Plate 27. Photomicrograph: Good Hope deposit pyroxene overgrown by garnet 63
Plate 28. Photomicrograph: Mount Riordan zoned garnet 66
Plate 29. Gold Hill property tectonic breccia 71

LIST OF TABLES

Table 1: Table of formations, Hedley district 10
Table 2: Chemical compositions of the Hedley intrusions compared to igneous rocks associated with base and ferrous metal skarns 35
Table 3: Production from skarn deposits — Hedley district 48
Table 4: Production from veins — Hedley district 73
Table 5A: Comparative chemistry of the unaltered Hedley intrusions and moderately and intensely altered endoskarn 77
Table 5B: Comparative chemistry of the unaltered Nicola Group sedimentary rocks and moderately and intensely altered exoskarn 77
Table 5C: Major element analyses of biotite "hornfels" altered Oregon Claims Formation tuffs — French Mine 77
Table 6: Comparison of the Nickel Plate and Mount Riordan skarns 83

REGIONAL GEOLOGY AND PREVIOUS WORK

INTRODUCTION

This bulletin describes the geology, geochemistry and mineralization in the Hedley mining district. The district is centred close to the Similkameen River valley approximately 40 kilometres east-southeast of Princeton and 230 kilometres east of Vancouver in southern British Columbia (Figure 1). The area lies within the allochthonous Quesnel Terrane of the Intermontane Belt in the Canadian Cordillera (Wheeler *et al.*, 1991). This terrane comprises mostly Paleozoic to Jurassic marine volcanic and sedimentary rocks and comagmatic intrusions formed in an island arc or marginal back-arc basin environment.

Gold-skarn mineralization throughout the district is hosted in the Nicola Group and is genetically related to a suite of calcalkaline dioritic rocks, the Hedley intrusions, that are probably Late Triassic in age.

The district has had a long history of gold production and between 1904 and 1991 approximately 62 tonnes of gold were won from several auriferous skarn deposits. More than 97% of the gold produced came from a single gold-skarn deposit that was worked at the Nickel Plate and Hedley-Mascot mines. Smaller production came from the French, Good Hope and Canty gold skarns, and from the Maple Leaf and Pine Knot quartz-carbonate veins.

During its mining history the district has had three major episodes of gold production. Mining initially took place between the early 1900s and 1930, after which the Nickel Plate mine closed down due to lack of ore. After new reserves were outlined, mining recommenced in 1934 and continued until the 1950s. Exploration interest in the district revived in the early 1970s due to the increased price of gold. In 1987 Mascot Gold Mines Limited reopened the Nickel Plate mine as a 2450 tonne per day open pit operation (Plates 1 and 2). Later, Corona Corporation took over the operation, and the mine is currently owned by Homestake Mining Company.

Fieldwork for this study was carried out from 1985 to 1987, and the preliminary results were published by Ray *et al.*, (1986, 1987, 1988) and Ettlinger and Ray (1988, 1989). An area of 450 square kilometres, which includes all the gold skarn deposits, was geologically mapped at a scale of 1:20 000. This mapping is compiled at a scale of 1: 30 000 (Figures 37 and 38). The geochemistry, mineral alteration, ore controls and regional settings of the gold deposits were examined, and the ages of some sedimentary and intrusive rocks were determined using conodont microfossils and U-Pb zircon dating methods.

PREVIOUS WORK

Placer gold was worked along the Similkameen River from the 1860s and a brief mention of the geology of the Hedley area was made by Dawson (1879; *see* pages 84B−85B). He sketched the geology on Nickel

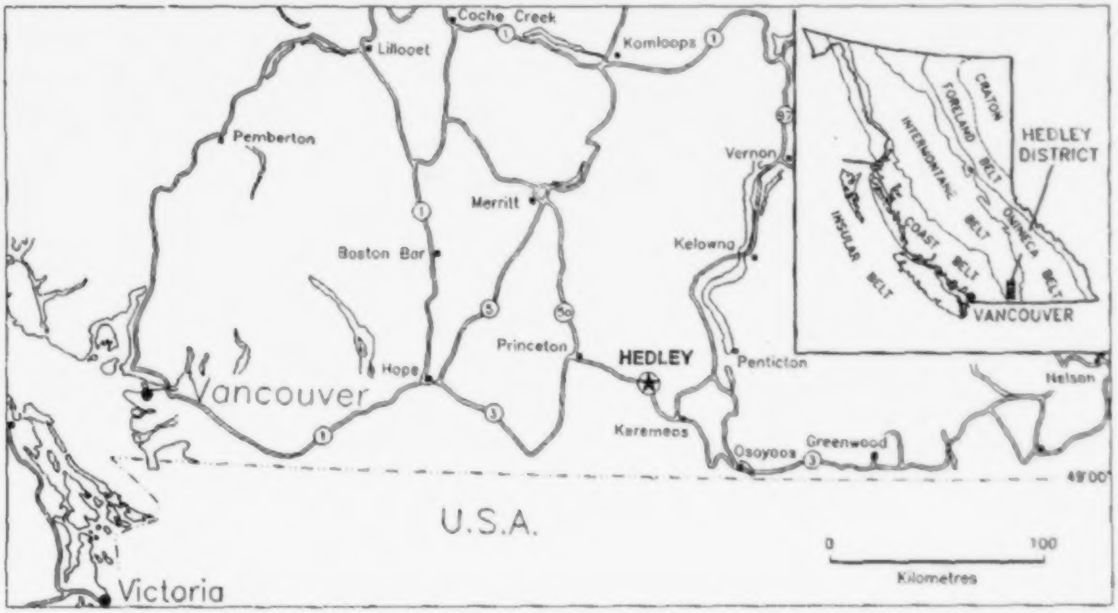

Figure 1. Location of the Hedley gold skarn district, southern British Columbia.

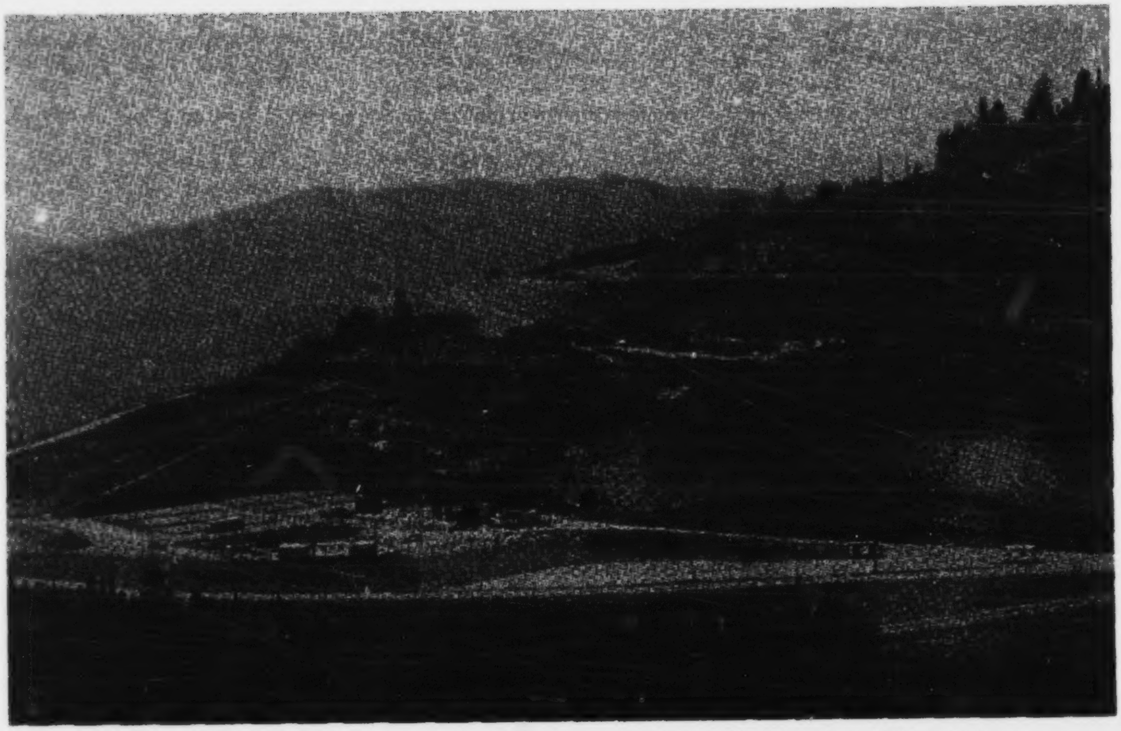

Plate 1. View of the Nickel Plate mill and mine site under construction in 1987. Photo taken looking southwest.

Plate 2. The Nickel Plate mill and mine site after completion of construction in 1987.

Plate Mountain (then called Striped Mountain), noted the limestones and measured a section in the Hedley Formation which he estimated to total 320 metres (1050 feet) in thickness. In 1894, claims were recorded on Nickel Plate Mountain. Exploration resulted in the discovery of the Nickel Plate orebody that was put into production in 1902. Winchell (1902) wrote one of the earliest reports on the mine geology and later Camsell (1910), working for the Geological Survey of Canada, completed a classical mapping study of the Hedley mining district. He outlined a stratigraphic succession, recognized the contact metamorphic nature of the mineralization, described the mineralogy of the alteration and concluded that the ores were genetically related to the Hedley dioritic intrusions.

Subsequently, Bostock (1930, 1940a, 1940b) mapped the regional geology at a scale of 1:63 360; later this work was compiled in a memoir by Rice (1947). Warren and Cummings (1936) and Warren and Peacock (1945) described the ore mineralogy at the Nickel Plate and Good Hope mines, noted the fineness of the gold and outlined a paragenetic sequence for the silicate and sulphide minerals. Warren and Peacock also recognized and described the first natural occurrence of the bismuth telluride, hedleyite, at the Good Hope mine. In 1939 a rockslide hit the outskirts of Hedley township and killed several people. This incident and the potential danger of landslides in the area was examined by Hedley (1939).

After lack of ore forced closure of the Nickel Plate mine in 1930, the well known American geologist Paul Billingsley re-examined the geology of the deposit; his work (Billingsley and Hume, 1941) resulted in the discovery of sufficient new reserves to allow reopening of the mine in 1934. Billingsley recognized that the auriferous skarn orebodies are structurally controlled and that the richest ore tended to be concentrated along fold hinges or at dike-sill intersections. Billingsley and Hume (1941) and Dolmage and Brown (1945) stressed the genetic and spatial association between gold mineralization and the Toronto stock, a large mass of generally bleached, skarn-altered, dioritic Hedley intrusion that outcrops on the mine property. Billingsley and Hume also recognized the importance of the "marble line" that marks the outer boundary of the skarn envelope; most of the ore occurs within 70 metres of this line. They were also intrigued by some coarse clastic rocks, the Copperfield breccias, which outcrop immediately north and northeast of the Nickel Plate deposit. They concluded that these rocks marked low-angle, westerly dipping thrusts, related to the major Bradshaw fault. However, recent work (Ray *et al.*, 1987, 1988), has demonstrated that these rocks comprise an extensive stratigraphic marker horizon, believed to represent a chaotic mass gravity slide deposit.

Lee (1951) completed a Ph.D. project on the Nickel Plate mountain area. He produced a detailed geological map and completed optical studies on the Hedley intrusions. Contrary to the conclusions of other workers, he tentatively concluded that the younger Similkameen granodiorites (now renamed the Cahill Creek pluton, Ray *et al.*, 1987) were more likely to be responsible for the gold skarns than the Hedley intrusions.

After the Nickel Plate mine reopened in 1987 (Plates 1 and 2), for the third time in its history, further studies on the deposit were undertaken. A mineral chemistry and fluid inclusion study of Nickel Plate by Ettlinger (1990a; 1990b) and Ettlinger *et al.*, (1992), concluded that the calcsilicate alteration and related gold mineralization are zoned about both the Toronto stock and a related suite of Hedley intrusion dikes. This study also indicated that the main pyroxene-garnet skarn formed at an average temperature (pressure corrected) of between 460° and 480°C, whereas the scapolite and coeval sulphide mineralization were deposited at temperatures in the range of 320° to 400°C. Fluid salinities averaged 18.3 and 9.7 wt% equivalent for garnet and pyroxene respectively.

Geochronometric studies of the Hedley intrusions and the Cahill Creek pluton have been conducted by Roddick *et al.* (1972) and Peto and Armstrong (1976).

Other recent publications relevant to the geology of the Hedley area include those by Peto (1973a, 1973b), Preto (1979), Preto *et al.*, (1979), Tempelman-Kluit and Parkinson (1986) and Ray and Dawson (1987, 1988). Recent data about either the Nickel Plate, French or Mount Riordan (Crystal Peak) deposits are given by Ettlinger and Ray (1989), Dawson *et al.*, (1990a), Grond *et al.*, (1991), Mathieu *et al.*, (1991) and Ray *et al.*, (1992, 1993)

REGIONAL GEOLOGY

The regional geology of the Hedley district is shown on Figure 2. The district lies at the easternmost margin of the Nicola belt, close to its contact with highly deformed, Upper Devonian to Upper Triassic ophiolitic rocks of the Apex Mountain Complex (Milford, 1984). Elsewhere in south-central British Columbia the Nicola Group unconformably overlies this ophiolitic package (Read and Okulitch, 1977) but at Hedley the nature of the original relationship is uncertain because the contact is now either faulted or intruded by the mid-Jurassic Cahill Creek pluton.

The Nicola belt comprises mainly Upper Triassic island-arc supracrustal rocks of the Nicola Group. They include subaerial and submarine rocks that were deposited within an elongate, structurally controlled marginal marine basin (Preto, 1979) formed above an easterly dipping subduction zone (Figure 3; Mortimer, 1986, 1987). Approximately 50 kilometres west of the Hedley area, along the main axis of the arc, the group reaches 6000 metres in thickness. It consists predominantly of a mafic, subaerial and submarine volcanic and volcaniclastic succession that includes potassium-enriched shoshonitic volcanic rocks (Preto, 1979). Limestones are uncommon in this main section of the arc.

Farther east in the Hedley area, the Nicola Group succession is thinner (maximum 3000 m) and is dominated by tuffs, calcareous siltstones, turbidites and some extensive limestone horizons.

Immediately following the termination of Nicola arc volcanism, a variety of intrusions ranging from sills and dikes to major batholiths were emplaced into the Nicola Group (Figure 2). These intermediate to high-level intru-

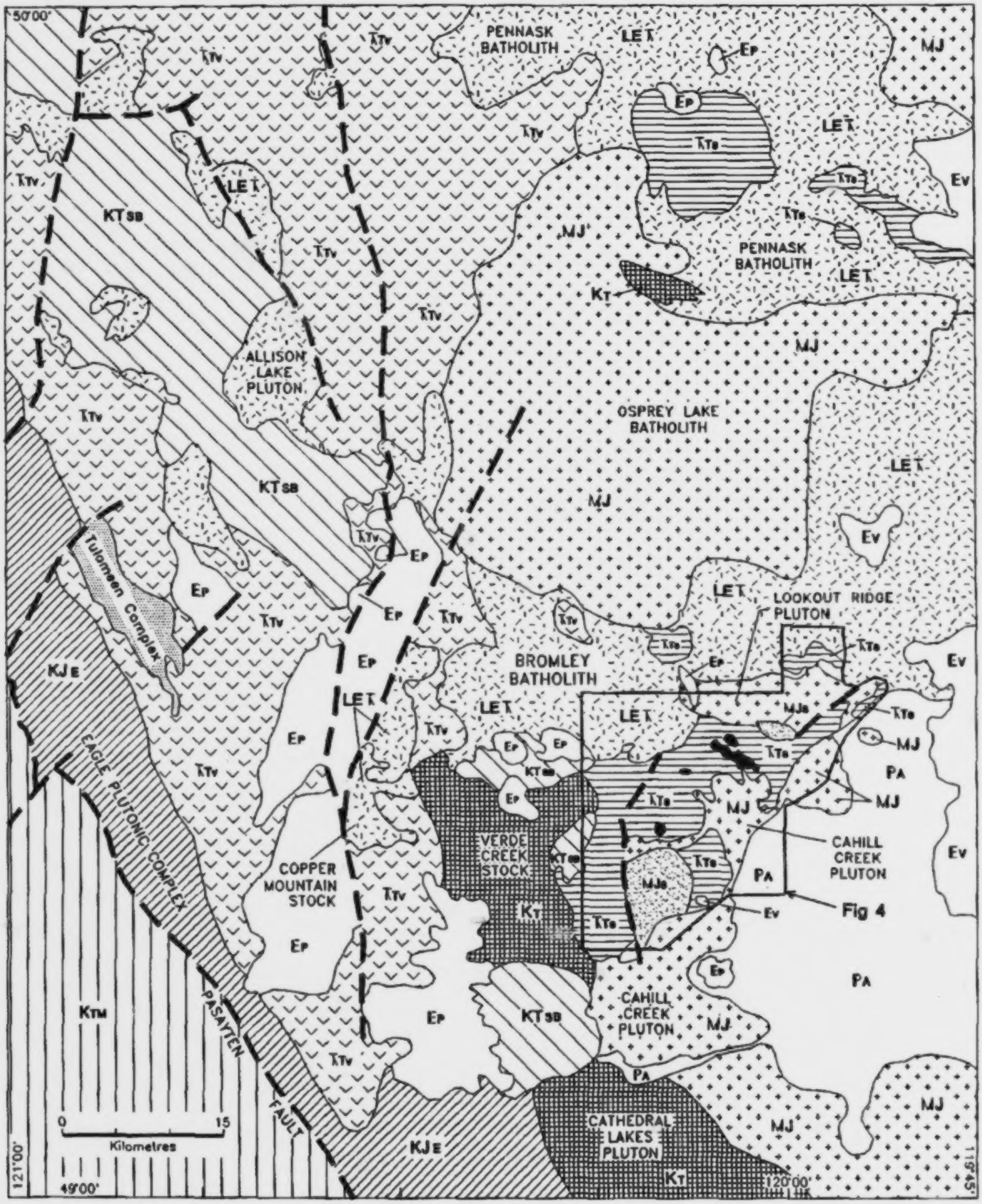
50°00'
ŦTv
PENNASK BATHOLITH
LEŦ
Ep
MJ
ŦTb
Ev
KTsb
MJ
Kt
PENNASK BATHOLITH
ALLISON LAKE PLUTON
OSPREY LAKE BATHOLITH
Tulameen Complex
KJe
LOOKOUT RIDGE PLUTON
BROMLEY BATHOLITH
MJb
Pa
EAGLE PLUTONIC COMPLEX
VERDE CREEK STOCK
COPPER MOUNTAIN STOCK
CAHILL CREEK PLUTON
Fig 4
Ktm
PASAYTEN FAULT
CATHEDRAL LAKES PLUTON
0
15
Kilometres
121°00'
49°00'
120°00'
119°45'

Figure 2. Regional geology of the southern part of the Intermontane Belt, southern British Columbia (adapted after Monger, 1989).

LEGEND FOR FIGURE 2

EP	Princeton Group
Ev	Penticton Group
CRETACEOUS AND TERTIARY	
KT	Assorted felsic intrusions
KTM	Mainly Methow Trough sedimentary rocks
KTSB	Spences Bridge Group
CRETACEOUS AND JURASSIC	
KJE	Eagle Plutonic Complex
MIDDLE JURASSIC	
MJs	Skwel Peken Formation
MJ	Assorted Felsic intrusions, including the Osprey Lake, Cahill Creek and Lookout Ridge bodies
LATE TRIASSIC TO EARLY JURASSIC	
LET	Assorted felsic intrusions including the Bromley, Pennask, Allison Lake and Copper Mountain bodies
●	Hedley Intrusions
▨	Tulameen Complex
TRIASSIC	
NICOLA GROUP	
ŦTv	Mostly volcanic and tuffaceous rocks
ŦTs	Mostly sedimentary and tuffaceous rocks
PALEOZOIC AND TRIASSIC	
PA	Apex Mountain Complex

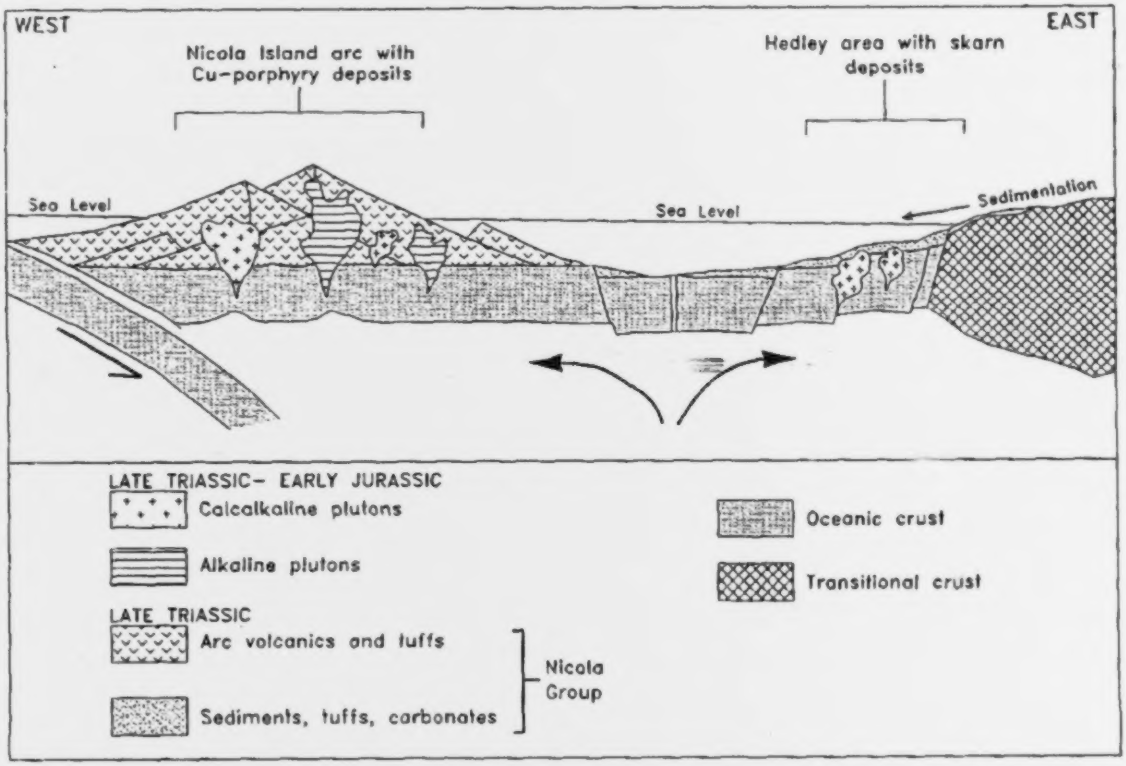
WEST
EAST
Nicola Island arc with Cu-porphyry deposits
Hedley area with skarn deposits
Sea Level
Sea Level
Sedimentation
LATE TRIASSIC- EARLY JURASSIC
Calcalkaline plutons
Alkaline plutons
LATE TRIASSIC
Arc volcanics and tuffs
Sediments, tuffs, carbonates
Nicola Group
Oceanic crust
Transitional crust

Figure 3. Schematic east-west section through the Late Triassic-Early Jurassic Nicola marginal basin showing the postulated location of the Hedley area in relation to the Nicola island arc.

sions generally range from gabbro to granodiorite and alkaline to calcalkaline in composition. Major bodies include the Pennask, Bromley, Allison Lake and Copper Mountain intrusions (Figure 2), as well as the Thuya, Wildhorse, Iron Mask and Guichon Creek bodies. Ages range from 194 to 210 Ma (Preto *et al.*, 1979; Monger, 1989; Parrish and Monger, 1992). Some of the alkalic intrusions (*e.g.*, Copper Mountain) are related to porphyry copper-gold deposits, while some of the calcalkaline plutons are associated with gold-poor porphyry copper-molybdenum mineralization (Carr, 1968; Preto, 1972; Soregaroli and Whitford, 1976). In the Hedley district, the Bromley batholith, the Hedley intrusions and the Mount Riordan stock were emplaced during this Late Triassic to Early Jurassic episode (Figure 4).

The Nicola Group in the Hedley area is overlain by a newly recognized package, the Skwel Peken Formation. The formation largely comprises mid-Jurassic calcalkaline andesitic to dacitic tuffs that total 1200 to 1900 metres in thickness. These may represent down-faulted volcaniclastic supracrustal rocks related to the deeper level emplacement of the Lookout Ridge and Cahill Creek plutons; the latter has been dated by U-Pb zircon methods at 168.8±9 Ma (Appendices 1A and 1B).

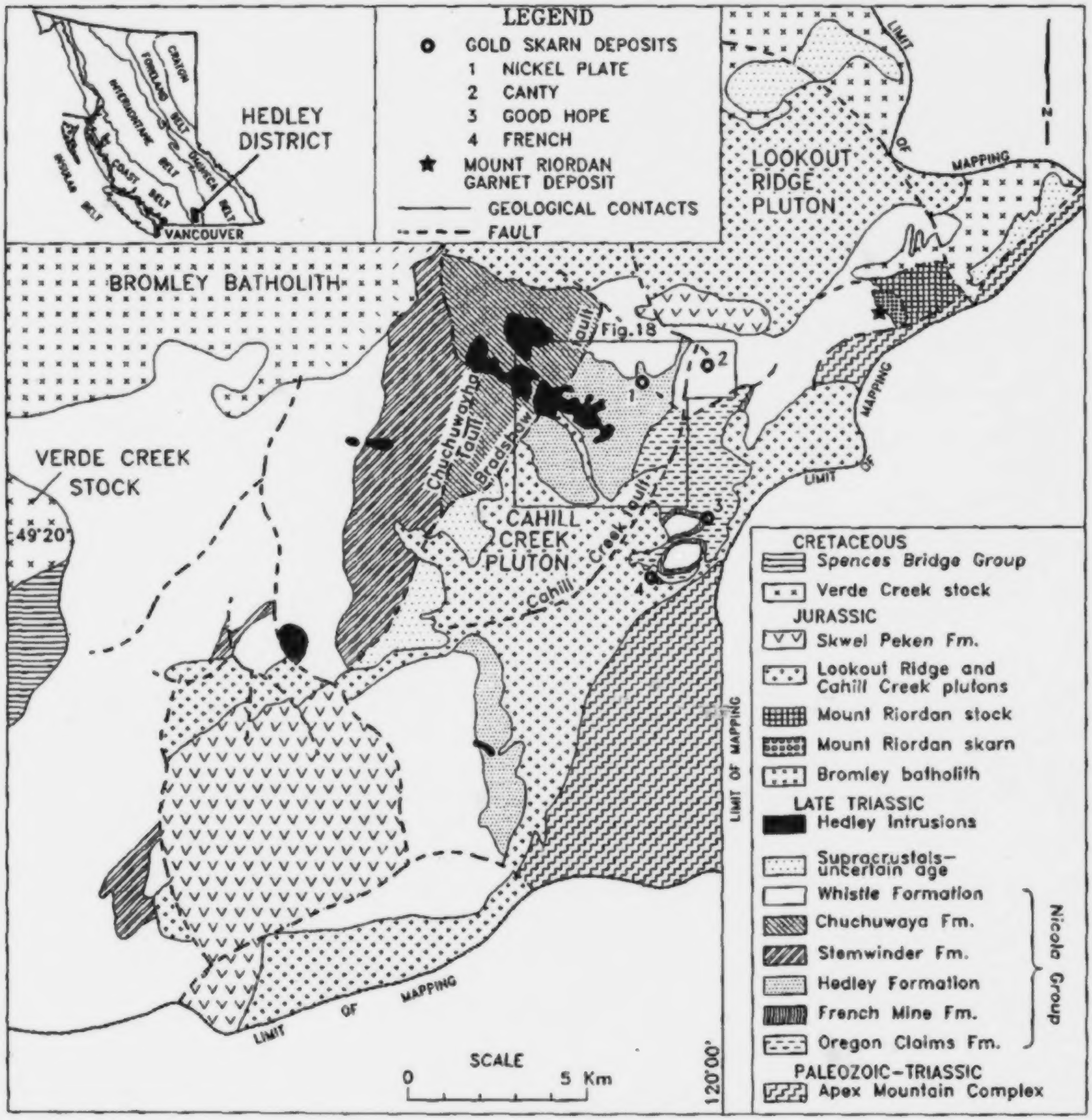
HEDLEY DISTRICT
CRATON
FORELAND BELT
OMINECA BELT
INTERMONTANE BELT
COAST BELT
INSULAR BELT
VANCOUVER
LEGEND
GOLD SKARN DEPOSITS
1 NICKEL PLATE
2 CANTY
3 GOOD HOPE
4 FRENCH
MOUNT RIORDAN GARNET DEPOSIT
GEOLOGICAL CONTACTS
FAULT
N
LIMIT OF MAPPING
LOOKOUT RIDGE PLUTON
BROMLEY BATHOLITH
Fig.18
fault
Chuchuwayha fault
Bradshaw fault
VERDE CREEK STOCK
49°20'
CAHILL CREEK PLUTON
Cahill Creek fault
1
2
3
4
SCALE
0
5 Km
120°00'
CRETACEOUS
Spences Bridge Group
Verde Creek stock
JURASSIC
Skwel Peken Fm.
Lookout Ridge and Cahill Creek plutons
Mount Riordan stock
Mount Riordan skarn
Bromley batholith
LATE TRIASSIC
Hedley Intrusions
Supracrustals–uncertain age
Whistle Formation
Chuchuwaya Fm.
Stemwinder Fm.
Hedley Formation
French Mine Fm.
Oregon Claims Fm.
Nicola Group
PALEOZOIC–TRIASSIC
Apex Mountain Complex

Figure 4. Geology of the Hedley district, southern British Columbia.

West of the Hedley area, the Nicola Group is unconformably overlain by a Lower Cretaceous, largely subaerial succession of volcanic flows, tuffs, agglomerates, lahars and tuffaceous sediments. These rocks have been variously assigned to either the Spences Bridge or Kingsvale groups (Drysdale, 1914; Rice, 1947, 1960; Preto, 1979). More recently, Thorkelson and Rouse (1989) have recommended that the entire package be called the Spences Bridge Group and that use of the term Kingsvale Group be discontinued. Some Spences Bridge rocks, together with the coeval intrusives of the Verde Creek stock, outcrop in the western parts of the Hedley map area. The area also contains minor erosional outliers of Eocene sedimentary and volcanic rocks of the Marron and Springbrook formations.

ACKNOWLEDGMENTS

We wish to thank the management, staff and former staff of the following companies and organizations for their considerable assistance and co-operation: Corona Corporation (formerly Mascot Gold Mines Limited.), particularly J. Bellemy, H.G. Ewanchuk, A.H. Ransom, L.W. Saleken, R.G. Simpson, and W. Wilkinson; Polestar Exploration Inc., particularly H.C. Grond and R. Wolfe; Banbury Gold Mines Ltd., particularly M.R Sanford; Chevron Canada Resources Limited, particularly E.D. Dodson and L.A. Dick; and the Similkameen Indian Band, particularly Chief B. Allison and G. Douglas. M.J. Orchard and F. Cordey, of the Geological Survey of Canada, identified the conodont and radiolarian microfossils respectively. The zircon U-Pb analyses were completed at the Department of Geology, The University of British Columbia, by J.E. Gabites, D. Murphy and P. van der Hayden. Microprobe analyses were undertaken by the authors at The University of British Columbia, and we thank P. Micheal, J. Knight and M. Piranian for their help. Assistance in the field was given by I.C.L. Webster, M.E. MacLean, M. Mills and M. Fournier. Informative discussions with J.W.H. Monger, A.D. Ettlinger, I.C.L. Webster, L.A. Dick, K.M. Dawson and J.L. Hammack are appreciated. The bulletin was improved by the editing of J.M. Newell and B. Grant and the scientific comments of A.D. Ettlinger, who reviewed the manuscript.

LITHOLOGY AND STRATIGRAPHY IN THE HEDLEY DISTRICT

INTRODUCTION

The geology of the district is shown on Figure 4. The various nomenclatures used by previous workers to describe the stratigraphy are summarized in Table 1. These are correlated with our newly proposed stratigraphic succession, which is influenced by the recognition of four distinct sedimentary facies in the Nicola Group.

The southeastern part of the area is underlain by deformed, Upper Devonian to Upper Triassic oceanic rocks of the Apex Mountain Complex. The complex is dominated by chert, argillite, tuffaceous siltstone, greenstone and minor limestone and gabbro. It is separated from the supracrustal rocks farther west by either intrusive rocks of the Cahill Creek pluton or by faults.

Most of the district west of the Apex Mountain Complex is underlain by sedimentary and volcaniclastic rocks of the Upper Triassic Nicola Group. The uppermost part is represented by the Whistle Formation, a thick (1200m), widely developed unit made up of alkalic and subalkalic tuff and tuffaceous sedimentary rocks with an extensive basal limestone-boulder gravity slide deposit, the Copperfield breccia.

The Whistle Formation is underlain by a succession in which four sedimentary facies are recognized (Figure 5): the thin (200m), shallow-marine limestone-dominant French Mine Formation in the east; the thicker (400 to 1500m), siltstone-dominant Hedley and Chuchuwayha formations in the central part of the district; and the thick (1000 to 2200m), deeper marine, argillite-dominant Stemwinder Formation in the west. These sedimentary facies are separated from one another by major, long-lived faults that are believed to have originally marked syn-sedimentation scarp slopes related to rifting along the Nicola basin margin.

The French, Hedley and Chuchuwayha formations are underlain by the Oregon Claims Formation (Figure 5), a 500 metres thick and poorly understood sequence of mafic tuffs with minor flows, limestone and chert pebble conglomerate. The formation may represent either the oldest section of the Nicola Group, or western extensions of the Apex Mountain Complex exposed beneath the Nicola Group.

Nicola Group rocks in the Hedley area are overlain by calcalkaline waterlain tuffs, and derived epiclastic sedimentary rocks that were formerly correlated with the Cretaceous Spences Bridge Group (Ray *et al.*, 1988). They are now thought to represent a newly recognized mid-Jurassic supracrustal succession, the Skwel Peken Formation. Many of these rocks are flat lying to moderately inclined but it is uncertain whether their contact with the underlying Nicola Group is a thrust or an unconformity, although we favour the latter interpretation. The Skwel Peken Formation, which has yielded an age of 187±9 Ma by U-Pb zircon methods (Appendices 1A and 1C), is exposed in two erosional outliers in the Hedley area (Figure 4). The largest and southernmost outlier is centred on Skwel-Kwel-Peken Ridge* and the other lies northeast of the Nickel Plate deposit.

The western margin of the map area (Figure 4) is partly underlain by the Early Cretaceous Spences Bridge Group which, farther west, has been mapped and described in detail by Preto (1972, 1979; Thorkelson and Rouse, 1989). Dacitic flows, tuffs, lahars, ignimbrites and minor sediments predominate in this unit, which is presumed to unconformably overlie the Whistle Formation. Granitic rocks immediately adjacent to the Spences Bridge Group in the Hedley area are believed to be the eastern part of the Verde Creek stock (Figures 2 and 4; Dolmage, 1934; Rice, 1947, 1960).

The youngest rocks in the area are represented by several small erosional outliers of Eocene strata of the Springbrook and Marron formations. The former are poorly consolidated, siliciclastic sediments while the latter are calcalkaline intermediate volcanics.

Several episodes of plutonism are recognized in the Hedley area. The oldest produced the quartz dioritic and gabbroic Hedley intrusions, which are widespread throughout the district, and are related to the gold skarns. They form both large stocks and swarms of sills and dikes. Attempts to date such bodies as the Toronto and Stemwinder stocks accurately have been unsuccessful (Appendices 1A and 1D). One body however, the Banbury stock (Figure 37,) has yielded a U-Pb zircon date indicating a maximum age of 215±4 Ma (Appendices 1A and 1E).

A slightly younger episode resulted in the granodioritic to quartz monzonitic Bromley batholith and a related marginal body, the Mount Riordan stock. We believe the latter is genetically related to the Mount Riordan garnet deposit in the northeast part of the district. A radiometric U-Pb zircon age of 194.6±1.2 Ma (Early Jurassic) is indicated for the stock (Appendices 1A and 1F) and a similar age has been obtained from the Bromley batholith (Parrish and Monger, 1992).

A subsequent episode resulted in the Lookout Ridge and Cahill Creek plutons which resemble the Bromley batholith compositionally and texturally. However, U-Pb zircon dating suggests a mid-Jurassic age of 168±9 Ma (Appendices 1A and 1B). This plutonism is thought to be related to the surface eruption of the volcaniclastic Skwel Peken Formation. Another episode was responsible for a widespread suite of quartz porphyries (Unit 14) that mostly form dikes and sills throughout the area. Field and textural evidence suggests these rocks are related to the Cahill Creek pluton and Skwel Peken Formation although they yielded a younger U-Pb zircon age of 154.5 +8 −43 Ma (Appendices 1A and 1G).

The youngest major intrusion in the district is the Early Cretaceous Verde Creek granitoid stock which was

---

* This name is taken from the traditional aboriginal usage (G. Douglas, personal communication 1990). The summit of the ridge, at 49° 16' 50"; 120° 08' 10" is occupied by a microwave tower.

TABLE 1
TABLE OF FORMATIONS — HEDLEY DISTRICT

Age	Camsell (1910)	Bostock (1930)	Bostock (1940a)	Ray & Dawson (this bulletin)
Tertiary Mid-Eocene	aplite, rhyolite & andesite dikes, granodiorite		basalt flows, pyroclastics	Unit 19: Marron Formation; andesite, trachyandesite
			conglomerate, sandstone	Unit 18: Springbrook Formation; conglomerate, sandstone
		----------	unconformity ----------	----------
Early Cretaceous				Unit 17: **Spences Bridge Group;** andesitic-rhyodacitic flows and tuffs, minor lahar and sedimentary rocks
			---------- Intrusive contact	----------
				Unit 16: Verde Creek stock; granite to quartz monzonite
Middle Jurassic				Unit 15: Skwel Peken Formation; andesitic ash and lapilli tuffs, minor sedimentary rocks
				Unit 14: Quartz porphyry intrusion
				Unit 13: Lookout Ridge pluton; granodiorite, quartz monzonite
				Unit 12: Cahill Creek pluton; quartz monzodiorite, granodiorite
Late Triassic(?) to Early Jurassic				Unit 11: Mount Riordan stock; granodiorite, gabbro, diorite
		granite	granite	Unit 10: Bromley batholith; granodiorite, diorite
		diorite, gabbro	diorite, gabbro	Unit 9: Hedley intrusions; quartz gabbro, quartz diorite
		----------	Intrusive contact ----------	----------
Late Triassic				Unit 8: rocks of uncertain age: includes rocks that may belong to the Oregon Claims, French Mine or Whistle formations
		Nicola Group: Unnamed section, volcanic and sedimentary rocks	**Nicola Group:** Wolfe Creek formation; andesite, basalt, tuff, minor sedimentary rocks	Unit 7: Whistle Formation: (**Nicola Group**); andesite ash & lapilli tuff (includes Unit 7a: Copperfield breccia)
		Aberdeen formation; quartzite	Henry formation; argillite, tuft	Unit 6: Chuchuwayha Formation: (**Nicola Group**); siltstone, argillite minor limestone
		Red Mountain formation; tuffs, breccias	Hedley formation; siltstone, limestone, argillite, tuff	Unit 5: Stemwinder Formation: (**Nicola Group**); argillite, siltstone
		Nickel Plate formation; limestone, quartzite	Sunnyside formation; limestone	Unit 4: Hedley Formation: (**Nicola Group**); siltstone, limestone
		Redtop formation; limestone, quartzite, argillite, tuff	Redtop formation; limestone, argillite	Unit 3: French Mine Formation: (**Nicola Group**); limestone, breccia, conglomerate
				----- uncertain contact ----------
				Unit 2: Oregon Claims Formation: (**Nicola Group or Apex Mountain Complex**) basaltic tuff and flows, minor conglomerate and limestone
		Contact faulted or occupied by Cahill Creek pluton	----------	----------
Middle to Late Paleozoic and Triassic	**Cache Creek Group:** Aberdeen formation; limestone, quartzite, argillite tuff, volcanic breccia		Independence formation; chert, argillite, basalt-andesite flows, breccia	Unit 1: **Apex Mountain Complex;** argillite, greenstone, chert, tuff, minor limestone
	Red Mountain formation; tuff, volcanic breccia, quartzite, argillite		Bradshaw formation; limestone, andesite, breccia	
	Nickel Plate formation; limestone, quartzite, argillite, tuff			
	Redtop formation; limestone, quartzite, argillite, tuff, breccia			

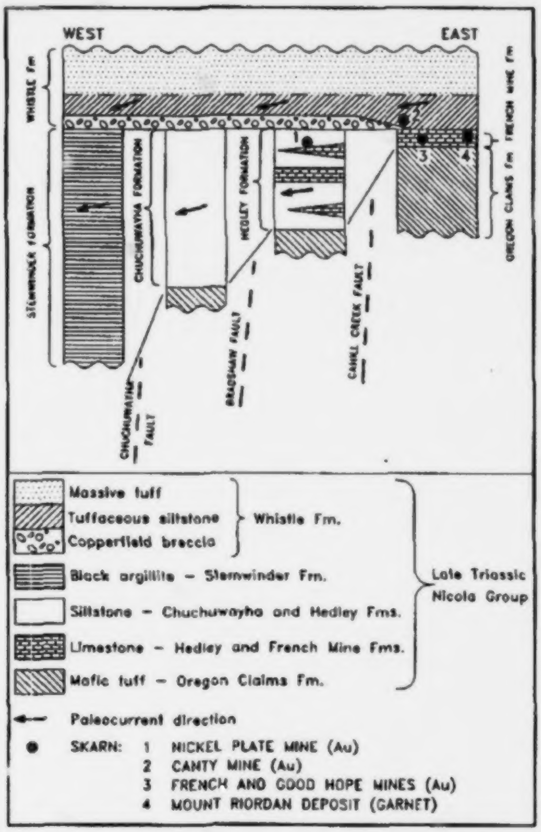
WEST
EAST
WHISTLE Fm
STEMWINDER FORMATION
CHUCHUWAYHA FORMATION
HEDLEY FORMATION
FRENCH MINE Fm
OREGON CLAIMS Fm
1
2
3
4
CHUCHUWAYHA FAULT
BRADSHAW FAULT
CAHILL CREEK FAULT
Massive tuff
Tuffaceous siltstone
Copperfield breccia
Whistle Fm.
Black argillite - Stemwinder Fm.
Siltstone - Chuchuwayha and Hedley Fms.
Limestone - Hedley and French Mine Fms.
Mafic tuff - Oregon Claims Fm.
Late Triassic Nicola Group
Paleocurrent direction
SKARN: 1 NICKEL PLATE MINE (Au)
2 CANTY MINE (Au)
3 FRENCH AND GOOD HOPE MINES (Au)
4 MOUNT RIORDAN DEPOSIT (GARNET)

Figure 5. Schematic east-west section across the Hedley district showing sedimentary facies changes in the Nicola Group and stratigraphic location of the skarn deposits.

probably coeval with the Spences Bridge Group. Farther west this stock has yielded K-Ar biotite ages of 101 and 98 Ma (Preto, 1972).

APEX MOUNTAIN COMPLEX (Unit 1)

Rocks of the Apex Mountain Complex outcrop at the eastern edge of the map area (Figures 4 and 37), south and southeast of Winters and Larcan creeks. To the west they are intruded by the Cahill Creek pluton which separates them from the Nicola Group, but farther north, near Mount Riordan, the complex is presumed to be in fault contact with Nicola Group rocks. The complex consists of strongly deformed rocks that were formerly subdivided into the Independence, Bradshaw, Old Tom and Shoemaker formations (Bostock, 1940a; Little, 1961). More recently Milford (1984) assigned them to the "Apex Mountain Group" but Monger (1989) suggested that the package should be termed the Apex Mountain Complex, due to its structural complexity and diversity of ages. Microfossils of Ordivician, Early to Late Devonian, Carboniferous and Middle to Late Triassic (Ladinian to Carnian) age have been collected from the Apex Mountain limestones and cherts (Appendices 2A and 2B; Milford, 1984; M.J.Orchard, personal communication, 1988). A large part of the complex was probably deposited during the Triassic, and the various older fossils possibly represent material derived from the erosion of older source rocks. Milford concluded that the complex represents a deformed accretionary wedge formed above an easterly dipping subduction zone during a process of eastward-directed underthrusting. Trace element discrimination plots (Milford, 1984) suggest that greenstones in the complex are typical of an oceanic spreading ridge; they represent ocean-floor basalts formed either in an open-ocean or back-arc basin. Milford also noted that the rocks in the western part of the complex are younger and are structurally overlain by older rocks farther east. Locally however, sedimentary indicators show that some rocks within presumed individual slices young to the east.

Within the present study area, the complex includes turbiditic siltstone (Unit 1a), argillite (Unit 1b), greenstone (Unit 1c), andesitic to basaltic ash and lapilli tuff (Unit 1d), limestone and marble. (Unit 1e), chert (Unit 1f), gabbro (Unit 1g) and rare conglomerate and limestone breccia (Unit 1h). Turbiditic tuffaceous siltstone (Unit 1a) with thin chert-pebble beds and minor tuff and argillite is well developed north of Winters Creek and between Paul and Larcan creeks farther south, but the status of this siltstone package is problematic. It was originally mapped by Bostock (1940a) and later by Milford (1984) as part of the Nicola Group although, on lithological grounds, we assign it either to the Apex Mountain Complex (as shown on Figure 37) or the Oregon Claims Formation. Along Winters Creek the siltstones are mostly northwesterly dipping and contain well-preserved grading, load casting, micro-crossbedding, slump, scour and flame structures. The unit probably represents distal turbidites. Individual graded beds generally comprise coarser grained bottoms of fine crystal tuff that pass upwards into dark-coloured argillaceous tops. These indicate that the unit faces west and is not tectonically inverted; the few flame structures observed suggest the sediments were deposited by south to southwesterly directed currents. Thin section studies reveal that the coarser silty layers contain abundant broken quartz and plagioclase crystals with minor amounts of tuffaceous debris. Adjacent to the southeastern margin of the Cahill Creek pluton the turbiditic siltstone unit is intensely hornfelsed and spotted with abundant grey cordierite crystals. In thin section, the hornfelsic siltstones consist of very fine gained, recrystallized quartz and feldspar, with secondary biotite and minor chlorite, sericite, and pyrite; magnetite is also present although it is uncertain whether it is detrital or secondary. Unlike most of the contact metamorphic hornfelses developed elsewhere in the district, which are characterized by decussate textures, the flakes of red biotite in these siltstones have a subparallel orientation which imparts a pronounced foliation. It is possible that contact metamorphism was accompanied by local strain to produce this weak schistosity, or that the orientation of the biotite was controlled by the bedding. Cordierite forms anhedral, rounded to elongate crystals up to 4 millimetres in length. It displays sector twinning and the crystal margins are locally altered and partially replaced by chlorite. The cordierite contains abundant inclusions and has overgrown the biotite; partial rotation of the crystals is indicated by deformation of the biotite fabric.

Argillite (Unit 1b) is commonly interbedded with chert and minor siltstone; it forms dark, massive to weakly foliated rocks in which bedding structures are uncommon and no tops have been determined. The crude foliation, which is subparallel to bedding, is marked by an alignment of chlorite and elongate grains of quartz, plagioclase, chert and probable organic opaque material. Some beds contain angular fragments of chert, quartz or tuffaceous debris set in an argillaceous matrix.

Greenstones (Unit 1c) usually form thin (5 to 100 m thick) units, but in the upper parts of Bradshaw Creek they are thicker and intimately associated with coarse-grained hornblende gabbro and diorite (Unit 1g). Elsewhere they are interlayered with thin chert, tuff, argillite, or more rarely, limestone units. Most greenstones are massive, but some outcrops contain amygdules and volcanic fragments; no pillow structures were positively identified although Milford (1984) reported pillow lavas in the complex farther east. Greenstones are strongly altered; the original coarse, pale-coloured hornblende phenocrysts are variably replaced by chlorite, tremolite-actinolite and minor biotite, and the matrix consists mainly of altered plagioclase laths, chlorite, epidote and opaque iron oxides. Some plagioclase crystals are acicular and branched; these textures are interpreted to be due to rapid quenching that took place during submarine extrusion. Abundant secondary albite and some minor quartz are present locally. Amygdules are oval to markedly elongate, up to 5 millimetres long, and filled with chlorite and minor carbonate. Other minor minerals include biotite, sericite, carbonate, sphene, rutile, anthophyllite, magnetite, ilmenite and some sulphides.

The mafic ash and lapilli tuffs (Unit 1d) vary from massive to well layered, and some are extensively reworked and interbedded with beds of tuffaceous siltstone. Fine-grained ash tuffs are more common than lapilli tuffs; in the latter the angular lithic fragments reach 3 centimetres in diameter and mainly comprise greenstone with minor amounts of chert. Some very rare fragments of limestone and silty, bedded sediments are also seen.

Limestones (Unit 1e) are widespread but relatively rare in the Apex Mountain complex. They generally occur as thin, deformed, light grey, massive to weakly bedded units, usually less than 5 metres thick; within the thermal aureole of the Cahill Creek pluton the limestones are recrystallized and bleached to marble, occasionally silicified, and rarely altered to garnet-pyroxene skarn. Generally, limestones make up stratiform units but where they are interbedded with chert, they form irregular lenses that reach 1 metre in thickness and 10 metres in length. Such limestones are exposed between Bradshaw and Shoemaker creeks, and it is uncertain whether these represent small reefs, boudins or olistostromal blocks.

Thicker limestone and marble units are present locally, notably near the mouth of Winters Creek and south of the Similkameen River valley between Larcan and Paul creeks. At the second locality the marble exceeds 60 metres in thickness and is believed to have a strike length of more than a kilometre. The marble north of Winters Creek is thicker, locally silicified and weakly altered to skarn, and malachite stained. It contains thin silicious beds as well as fragments of crinoid ossicles and bivalve shells that were too broken for specific identification. All limestones mapped in the Apex Mountain Complex were sampled for microfossils but no conodonts were recovered (M.J.Orchard, personal communication, 1988).

Chert (Unit 1f) is most common southeast of Bradshaw Creek. It forms pale to dark grey, massive to bedded outcrops; the ribbon cherts consist of 1 to 5-centimetre beds of chert interlayered with thin, sheared horizons of argillite. In thin section they are seen to consist of a fine-grained aggregate of cryptocrystalline silica, intergrown with randomly orientated needles of tremolite-actinolite and lesser amounts of chlorite, dark organic material, finely disseminated sulphides and minor altered plagioclase. Trace to accessory minerals include apatite, anthophyllite, sphene, biotite, epidote, carbonate and zircon.

A distinctive limestone boulder conglomerate and breccia (Unit 1h) is exposed at one locality on a ridge between Bradshaw and Shoemaker creeks. This 5 to 10-metre-thick unit lies within a predominantly chert unit, although the breccia itself is directly overlain, in turn, by a 20 metres thick sequence of deformed phyllitic argillite and a thin limestone bed. The breccia contains well-rounded to sharply angular clasts of grey massive limestone that reach 0.3 metre in diameter but average between 2 and 8 centimetres. The limestone clasts, which are supported by a massive, tuffaceous matrix, contain inarticulate brachiopods, phosphatic tubes and nowakiid tentaculites; the latter are mid-Early to early Late Devonian in age (Appendix 2B).

NICOLA GROUP (Units 2-7)

The Nicola Group outcrops in the western and central parts of the district (Figure 4) and is economically important as it hosts all of the gold-skarn deposits and occurrences, as well as the Mount Riordan garnet deposit. To the north, east and south it is either intruded by the Bromley batholith and Cahill Creek pluton, or faulted against rocks of the Apex Mountain Complex. Westwards, it can be traced discontinuously into the main Nicola belt (Figure 2).

The Nicola Group in the project area is believed to have been laid down along the eastern tectonic margin of a marine back-arc basin that deepened westward and derived its sediments from an eastern source (Figure 3). During the Late Triassic, the Hedley district and the main volcanic arc farther west were separated by an area of back-arc spreading, although evidence for this has been obliterated by closure of the basin and Early Jurassic intrusions. The structurally controlled basin margin influenced the Late Triassic sedimentation and subsequent emplacement of the Hedley intrusions and associated gold skarns.

The nomenclature applied to the Nicola Group in the Hedley district has evolved and changed over time (*see* Table 1. Both Camsell (1910) and Bostock (1930, 1940a) considered the group to represent an essentially continuous succession across the district with a total thickness of approximately 2900 metres. Our studies, however, suggest that the group includes four lithologically distinct but essentially coeval packages that exhibit changes in thickness and lithology from east to west across the district (Figure 5).

Overall, the Nicola succession in the Hedley area is believed to comprise three distinct stratigraphic units, although the oldest, the Oregon Claims Formation (Unit 2), is of uncertain status and age, and may represent a western extension of the Apex Mount Complex. The formation consists mainly of mafic tuff with minor flows, and some sedimentary rocks.

Overlying the Oregon Claims Formation is a predominantly sedimentary unit that varies from 200 to 2200 metres in thickness across the district. This unit is marked by the previously mentioned series of fault-bounded, east-to-west sedimentary facies changes. It thickens progressively westward (Figure 5); this thickening and the accompanying facies changes reflect sedimentary deposition across the tectonic hinge zone that marked the eastern edge of the Nicola basin. The eastern and thinnest facies, the French Mine Formation (Unit 3), has an estimated maximum thickness of 200 metres. It is dominated by massive limestone, breccia and impure calcareous sediments with minor tuffs and conglomerates, and is interpreted to represent a proximal facies deposited within a topographically uneven, fore-reef to lagoonal environment. This sequence hosts the French and Good Hope gold skarn deposits, as well as the Mount Riordan garnet deposit (Figure 5).

Farther west, between the Cahill Creek and Bradshaw faults, rocks believed to be stratigraphically equivalent to the French Mine Formation are represented by the Hedley Formation (Unit 4), which hosts the Nickel Plate deposit. The formation is 400 to 800 metres thick and consists mainly of calcareous, turbiditic siltstone with subordinate limestone, calcareous argillite, conglomerate and tuff. The massive to bedded limestones form extensive units up to 75 metres thick and several kilometres in strike length.

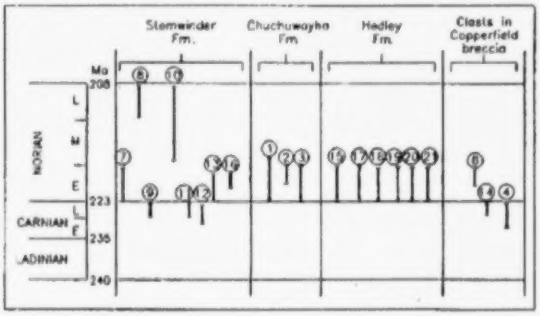

Figure 6. Age range of conodont microfossils collected from the Nicola Group, Hedley district. Numbers in circles refer to fossil sample numbers listed in Figure 37 (fossils identified by M.J.Orchard).

Between the Bradshaw and Chuchuwayha faults lies the predominantly calcareous siltstone sequence of the Chuchuwayha Formation (Unit 6); it is believed to be a thicker (up to 1500 metres) stratigraphic equivalent of the more proximal Hedley Formation farther east (Figure 5) but contains only thin, impersistent limestone units that seldom exceed 5 metres in thickness. Its base is probably exposed immediately west of the Bradshaw fault where it overlies a small inlier of Oregon Claims Formation.

The westernmost facies is represented by the Stemwinder Formation (Unit 5) which is estimated to be between 800 and 2200 metres thick. It is separated from the Chuchuwayha Formation to the east by the Chuchuwayha fault, and it is dominated by a monotonous sequence of black calcareous argillite and thinly bedded calcareous siltstone. Also present are minor, generally thin, interbeds of crystal tuff, fine conglomerate, and limestone that rarely exceed 3 metres in thickness.

The French, Hedley, Chuchuwayha and Stemwinder formations are all overlain by the Whistle Formation (Unit 7). This unit consists mainly of alkalic and calcalkalic basaltic tuffs and tuffaceous sediments, and ranges from 700 to 1200 metres in thickness . Unlike the underlying sequence, limestones are exceedingly rare and no east-to-west facies changes have been identified (Figure 5). However, the base of the formation is commonly marked by an extensive limestone boulder-sequence, the Copperfield breccia (Unit 7a).

Calcareous units throughout the Nicola Group were sampled for microfossils, but none were obtained from either the French Mine or Oregon Claims formations. However, a number of identifiable conodont microfossils were recovered from the Stemwinder, Chuchuwayha and Hedley formations and from limestone clasts in the Copperfield breccia. These range from late Carnian to late Norian (Late Triassic) in age and are summarized in Figure 6.

OREGON CLAIMS FORMATION (Unit 2)

The Oregon Claims Formation represents either the oldest part of the Nicola Group or older basement rocks possibly belonging to the Apex Mountain Complex. If the latter theory is accepted, it raises important questions concerning the contact relationship between the Nicola Group and Apex Mountain Complex.

The Oregon Claims Formation is poorly exposed and its base is not seen, but a measured section (Figure 39, Section 1-2) indicates it is at least 500 metres thick. No fossils have been obtained from the formation and consequently its age is unknown. It is best exposed near French and Good Hope mines, and between Nickel Plate mine and Cahill Creek. It is also believed to outcrop as a thin unit along the west side of the Bradshaw fault approximately 2 kilometres north of Hedley. In these three areas the formation structurally underlies the French, Hedley and Chuchuwayha formations, respectively. Contacts between

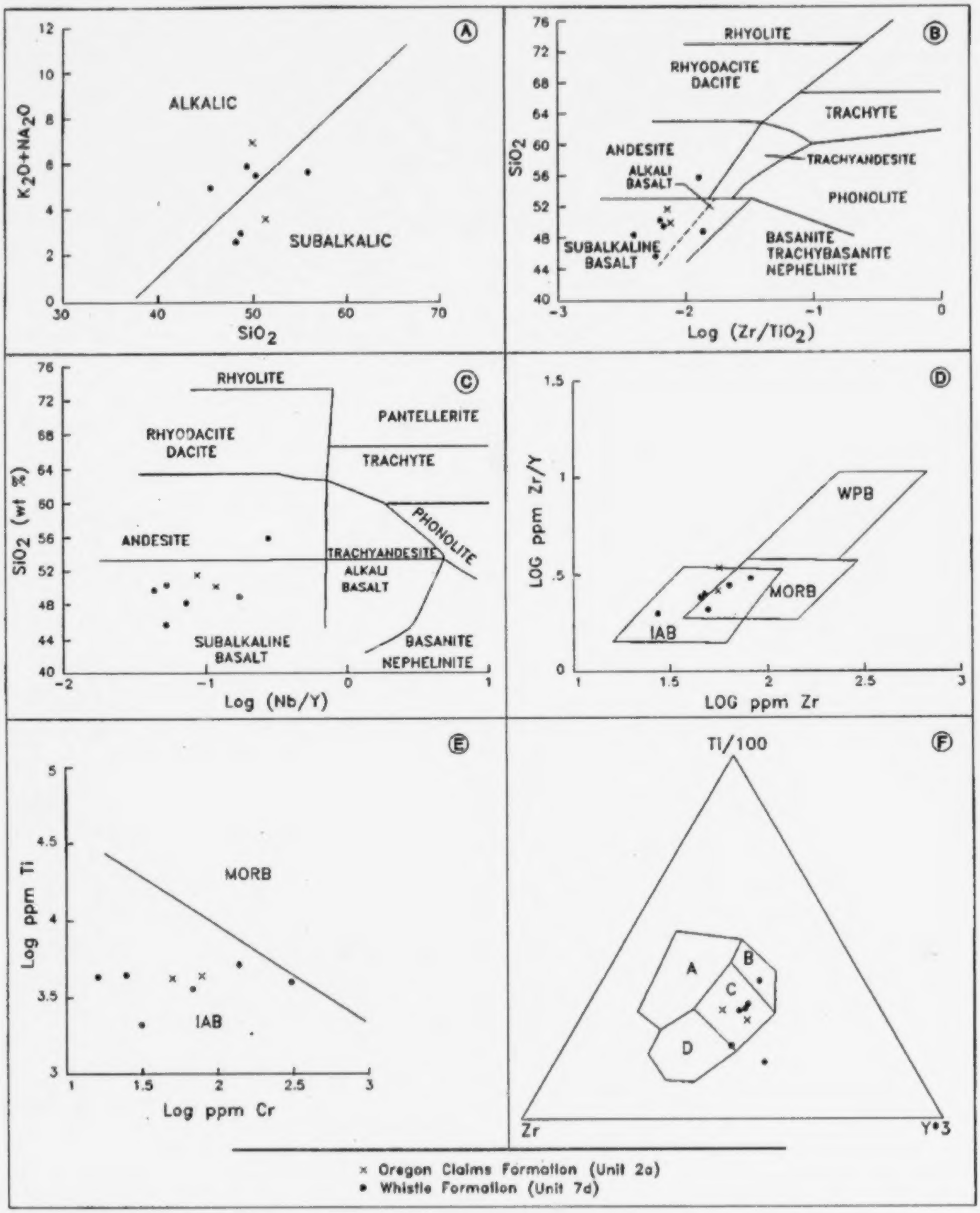

Figure 7. A. Alkali-silica plot (after MacDonald, 1968; Irvine and Baragar 1971) of tuffs from the Oregon Claims and Whistle formations. B. SiO_2 vs. log (Zr/TiO_2) plot (after Winchester and Floyd, 1977; Floyd and Winchester, 1978) of tuffs from the Oregon Claims and Whistle formations. C. SiO_2 vs. log (Nb/Y) plot (after Winchester and Floyd, 1977; Floyd and Winchester, 1978) of tuffs from the Oregon Claims and Whistle formations. D. Log Zr/Y vs. log Zr plot (after Pearce and Cann, 1973) of tuffs from the Oregon Claims and Whistle formations. E. Log Ti vs. log Cr plot (after Pearce, 1975) of tuffs from the Oregon claims and Whistle formations. F. Zr-Ti-Y ternary plot (after Pearce and Cann, 1973; Pearce, 1975) of tuffs from the Oregon Claims and Whistle formations. A = Within-plate basalts; B + C = Low-K tholeiites; C = Ocean-floor basalts; C + D = Calcalkaline basalts.

the Oregon Claims Formation and the overlying rocks are poorly exposed but appear to be sharp, and they may represent an unconformity occupied by an easterly directed and gently west dipping thrust.

The original nature of the rocks in the formation is difficult to determine in many localities, due either to local skarn alteration by the Hedley intrusions or to extensive hornfelsing related to the Cahill Creek pluton. Moreover, many of the mafic tuffs in the Oregon and Whistle formations are similar in both appearance and chemistry, making it difficult to differentiate these formations in poorly exposed localities. Compared to the Whistle Formation however, the tuffs in the Oregon Claims Formation are generally darker, and locally contain either rare, angular chert or quartz fragments, or minor beds of chert-pebble conglomerate. However, the tuffs in the two formations are chemically indistinguishable; whole rock and trace element plots (Figure 7; *see* Appendix 3) indicate that the Oregon Claims tuffs include both subalkalic and alkalic basalts that are probably arc related. In some areas where the tuffs of the two formations are indistinguishable, they have been mapped as rocks of uncertain age (Unit 8).

The Oregon Claims Formation is a heterolithic unit dominated by mafic tuffs, volcanic sandstone, siltstone and argillite, with subordinate amounts of mafic, amygdaloidal flows, limestone and polymictic or chert-pebble conglomerate. The mafic tuffs (Unit 2a) are characterized by their very dark green to black colour; massive to weakly bedded ash tuffs are most common, although some minor lapilli tuff and tuff breccia are present west and northwest of the French mine. The lapilli tuffs and tuff breccias contain mostly angular fragments of amygdaloidal and feldspar porphyry basalt, up to 15 centimetres in diameter, with rarer clasts of limy sediment, chert, broken quartz grains and recrystallized quartz crystals. Some tuff breccias have a mudstone-rich matrix with well-preserved slump structures, which suggests that they were deposited in an unstable sedimentary environment and may represent reworked gravity-slide deposits. The mafic tuffs include amphibole-rich and pyroxene-rich types. In thin section the pyroxene-rich tuff is seen to consist mainly of weak to moderately altered, well-twinned plagioclase laths (An_{42-55}), intermixed with augite crystals and some rounded lithic clasts. The augites are generally less than 0.5 millimetre across, but occasional larger crystals up to 2 millimetres in diameter are present. Although many of the plagioclase and pyroxene grains are broken, well-preserved, euhedral to subhedral crystals are also common. In the amphibole-rich tuffs, the remnant, subhedral hornblende crystals are partially altered to chlorite and epidote. In some tuffs, the volcanic fragments contain branched, acicular plagioclase crystals set in a fine-grained matrix of chlorite and opaque iron oxides; these textures suggest the fragments were derived from quenched volcanic flows. Adjacent to the Cahill Creek pluton, these rocks are hornfelsed and characterized by abundant, randomly orientated, red biotite, and rare, small porphyroblasts of cordierite and pale pink garnet; x-ray defraction analysis indicates the latter are almandine garnets (M. Chaudry, personal communication, 1989).

The mafic ash-tuffs locally contain angular to subrounded fragments of chert and lesser amounts of clear quartz (Unit 2b). These fragments are generally less than 3 millimetres across, but rarer clasts up to 0.5 centimetre are seen. The locally rare but widespread presence of the quartz and chert fragments in the Oregon Claims tuffs distinguishes them from the volcaniclastic rocks in the Whistle Formation (Unit 7).

The road section that cuts the Oregon Claims Formation west and northwest of French mine crosses a varied sequence that includes coarse, mafic lapilli tuff, minor tuff-breccia and quench-textured basaltic flows, as well as strongly altered, thinly bedded tuffaceous sediment (Unit 2c) in which the bedding is preserved as alternating light and dark layers, generally less than 2 centimetres thick; slump structures and soft-sediment deformation features are also seen. Locally these rocks contain disrupted, subangular blocks of massive marble and bedded limestone (Unit 2d), up to 20 metres in thickness and 40 metres in length, that contain possible remnant algal mats. The blocks are interpreted to be olistoliths of limestone formed in a shallow lagoonal environment that subsequently slid down a paleoslope into unconsolidated sediments; this action produced chaotic and disrupted soft-sediment structures that are commonly seen in siltstones and bedded tuffs adjacent to the marbles. The argillites and siltstones also locally contain abundant small spherical calcareous nodules of unknown origin that reach 2 centimetres in width.

The Oregon Claims Formation includes thin, impersistent beds of chert-pebble conglomerate (Unit 2e) that contain subrounded to angular pebbles generally less than 3 centimetres in diameter. Most of the pebbles are grey to white cryptocrystalline quartz, although rare clasts of limestone and volcanic rock are also present.

The character of the Oregon Claims Formation rocks indicates indicate they were laid down in a high-energy and unstable slope environment and that sedimentation was accompanied by active tectonism and explosive basic volcanism.

FRENCH MINE FORMATION (Unit 3)

The French Mine Formation is interpreted to represent the easternmost, more proximal facies equivalent to the thicker Hedley, Chuchuwayha and Stemwinder formations developed farther west (Figure 5). It is only found east of the Cahill Creek fault zone, and is a predominantly calcareous sedimentary sequence that has a maximum thickness of 200 metres. The formation hosts the gold-skarn mineralization at the French and Good Hope mines, and may also host the tungsten-copper-bearing garnet skarn at Mount Riordan farther east. It is best exposed near the French and Good Hope mines, where it forms a unit, 100 to 200 metres thick, that is sandwiched between the Oregon Claims and Whistle formations. Chert-pebble conglomerates and massive limestones outcropping along Broken Creek, approximately 6 kilometres north of Nickel Plate Lake (Figure 38), may also belong to the French Mine Formation.

The French Mine Formation consists mainly of massive to thick-bedded limestone (Unit 3a), some of which contains possible remnant algal mats and spongiomorphs, as well as lesser amounts of limestone conglomerate and breccia (Unit 3b), and minor chert-pebble conglomerate, argillite, tuff and calcareous siltstone. Many of the rocks are extensively hornfelsed or overprinted by reaction skarn, and most of the original limestones are recrystallized to white, coarse-grained marble. In the French mine area, the marbles are interbedded with conglomerate units that reach 30 metres in thickness. These contain angular to subrounded pebbles and cobbles up to 0.3 metre in diameter. Some conglomerates and breccias are monomictic; the clasts are coarse white marble with sporadic wollastonite. Even in the polymictic conglomerates, over 95% of the clasts are marble, some of which contain small remnant fragments of solitary corals, bryazoa and bivalve shells. In addition, there are pebbles and cobbles of chert, mafic volcanics, bedded argillite and rare porphyritic diorite. Some conglomerates at the French mine are bedded and display grading. A spectacular monomictic marble breccia that comprises sharply angular fragments of white, crystalline marble, up to 0.4 metre across, set in a brown garnet-rich matrix is also exposed at this locality (Plate 3). This is interpreted to be a mud-matrix-supported limestone breccia that has been overprinted by reaction skarn alteration.

Plate 3. Marble skarn breccia, French mine. Angular fragments of white marble (originally limestone) enclosed in a garnet-rich matrix (originally mudstone).

The age of the French Mine Formation is unknown and attempts to extract microfossils from the calcareous units have been unsuccessful. It is believed to have been deposited contemporaneously with the Hedley, Chuchuwayha and Stemwinder formations in a shallow-marine, possibly lagoonal or fore-reef environment.

HEDLEY FORMATION (Unit 4)

The Hedley Formation is a sedimentary sequence, 400 to 800 metres thick, that generally youngs to the west; it is best developed northeast of the Similkameen River, between the Bradshaw and Cahill Creek faults. We believe it represents a thicker, more distal facies equivalent of the French Mine Formation and includes rocks originally separated into the Redtop and Nickel Plate formations by Camsell (1910); (Table 1). The formation is characterized by thinly bedded, turbiditic, calcareous siltstone (Unit 4a), with lesser amounts of calcareous or silicious argillite (Unit 4b), limestone (Unit 4c) and thin beds of tuff and conglomerate. The siltstones and argillites appear to largely represent DE-sequence turbidites (Bouma, 1962); they locally exhibit graded bedding, scour structures, micro-crossbedding, ripple crosslaminations and occasional soft-sediment slump features and overturned flame structures. The few measurements obtained on crossbedding and overturned flames indicate the Hedley Formation was deposited by westerly directed paleocurrents.

Individual units of massive to bedded limestone reach 75 metres in thickness and are traceable along strike for several kilometres. They are best exposed approximately 1.5 kilometres south-southwest of the Nickel Plate mine, where limestone units with minor siltstone interbeds are traceable over a 600-metre outcrop distance. To the west and north, however, the amount of limestone in the section decreases, and north of the Nickel Plate deposit the limestone beds are less common and generally less than 10 metres thick. Limestone varies from light grey to dark blue-grey in colour; marble or skarn-altered limestone is generally bleached. Whole rock analytical results for limestone (Appendix 4A) and marble (Appendix 4C) from the Hedley Formation indicate they have a low dolomitic content.

Macrofossils in the Hedley limestones are rare but crinoid ossicles, bivalve fragments, solitary horn corals and belemnites have been seen. The basal sections of some thinner limestone beds are gritty and contain a few chert pebbles and shell fragments. Six limestone samples from various parts of the formation yielded conodonts of early Norian age (Figure 6; Appendix 2A); the locations of these samples are shown in Figure 37.

Thin interbeds of dark, chlorite and epidote-altered ash tuff (Unit 4d) are present in the formation, particularly toward the top of the sequence. In thin section they are seen to contain abundant fragments of altered andesitic volcanics with minor clasts of limestone, siltstone and rare quartz and chert.

Thin beds of polymictic conglomerate and breccia (Unit 4e) are also rarely present in the Hedley Formation, particularly within some limestone-rich sections. The poorly sorted, angular to rounded clasts in the breccias and conglomerates, which reach 6 centimetres across, comprise limestone and calcareous sediments, with lesser amounts of volcanic and chert pebbles.

STEMWINDER FORMATION (Unit 5)

The Stemwinder Formation is a sedimentary succession, estimated to be a 1000 to 2200 metres thick, that generally youngs to the west. It includes rocks originally designated as the Aberdeen Formation (Camsell, 1910) and the Henry Formation (Bostock, 1940a; Table 1). It is best developed immediately west of the Chuchuwayha fault where it forms a steeply dipping, southerly thinning unit that is intruded by the Bromley batholith to the northwest and stratigraphically overlain by the Whistle Formation to the west (Figure 4). To the east it is either cut by the Chuchuwayha fault or intruded by apophyses of the Cahill Creek pluton. It hosts several mineral occurrences, including the auriferous Maple Leaf and Pine Knot veins at the Banbury mine.

The formation is a monotonous sequence of thinly bedded, black and organic-rich calcareous argillite (Unit 5a), with lesser amounts of lighter coloured calcareous siltstone (Unit 5b). Whole rock analyses of unaltered samples of Stemwinder siltstone and argillite are given in Appendix 4B; the siltstone sample is highly calcareous and contains nearly 4 wt% magnesium.

The formation also includes thin beds of andesitic ash tuff (Unit 5d) as well as minor dust tuff and rare polymictic conglomerate. Beds of impure, black to dark grey limestone, (Unit 5c) up to 3 metres in thickness, are widespread. Many of the limestone beds are graded turbidites with coarse-grained bottoms that contain chert and quartz grains, bivalve shell and crinoid ossicle fragments and tuffaceous debris. Whole rock analyses of two unaltered Stemwinder limestone samples are given in Appendix 4A.

The formation faces west (Figure 39, Section 1-2) and was deposited in a more anoxic, deeper water environment than the Chuchuwayha and Hedley formations farther east. The Stemwinder rocks are conformably overlain to the west by the Whistle Formation.

No identifiable macrofossils were found in the Stemwinder rocks. However, eight carbonate-rich samples collected from throughout the formation yielded conodonts ranging in age from late Carnian to late Norian (Figure 6; Appendix 2A). Thus, the Stemwinder Formation has the longest time span of any of the sedimentary facies, and it includes sections that are both younger and older than the early Norian Chuchuwayha and Hedley formations further east. Microfossil data indicate that sediments at the base of the Stemwinder Formation, adjacent to the Chuchuwayha fault, are older than the structurally underlying rocks of the Chuchuwayha Formation; this suggests easterly directed thrusting or reverse movement along the fault.

CHUCHUWAYHA FORMATION (Unit 6)

The Chuchuwayha Formation forms a steeply dipping, wedge-shaped unit between the Stemwinder and Hedley formations. To the west and east it is bounded respectively by the Chuchuwayha and Bradshaw faults while to the north it is intruded by the Lookout Ridge pluton. In its southern part it is at least 1500 metres thick (Figure 39, Section 1-2) but is probably considerably thicker farther north. It hosts a number of mineral occurrences including the Peggy (Hedley Amalgamated) gold skarn, situated approximately 1.5 kilometres north-northwest of Hedley township.

The Chuchuwayha Formation is a predominantly thin-bedded calcareous siltstone sequence (Unit 6b; Plate 4) that closely resembles the siltstones in the Hedley Formation. Unlike the Hedley Formation, however, it does not contain thick or extensive limestone units. Instead the limestone beds (Unit 6c) seldom exceed 5 metres in thickness and are commonly graded with broken bivalve shells and crinoid ossicles. North of Hedley township the siltstones are pale coloured due to thermal alteration by the Stemwinder and Aberdeen stocks. Analyses of unaltered limestone and siltstone samples from the formation are presented in Appendices 4A and B.

The formation also includes minor argillite (Unit 6a) and some large units of dark, siliceous and tuffaceous argillite (Unit 6d). Conglomerate beds are uncommon and generally less than 2 metres thick; they contain rounded pebbles of limestone, andesitic volcanic rocks and minor chert.

Microfossils in three limestone samples collected from the formation indicate an early Norian age (Appendix 2A), similar to those in the Hedley Formation (Figure 6). The Chuchuwayha Formation is believed to

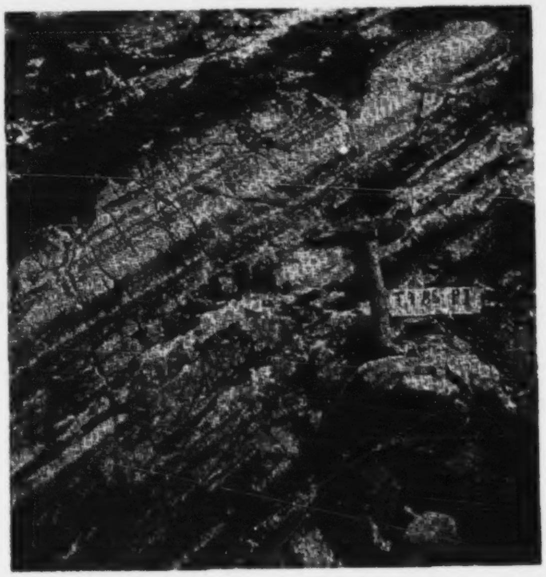

Plate 4. Chuchuwayha Formation (Unit 6b). Turbiditic, graded calcareous siltstone, 1 km west of Hedley.

have been deposited in a slightly deeper water environment than the adjoining Hedley Formation but at less depth and in more aerobic conditions than the Stemwinder sediments.

WHISTLE FORMATION (Unit 7)

The Whistle Formation is widespread throughout the district. It is well developed along Whistle Creek, where it stratigraphically overlies the Stemwinder Formation, and east of Skwel-Kwel-Peken Ridge and north of the Nickel Plate and French mines where it overlies both the Hedley and French Mine formations. The attitude of the formation throughout the district is influenced by the major, northerly trending Hedley anticline and Good Hope syncline. Along Whistle Creek and east of Skwel-Kwel-Peken Ridge, the formation generally dips steeply and youngs to the west; north of the Nickel Plate mine, around Lookout Mountain, it is gently dipping to subhorizontal, whereas east of the Cahill Creek fault it is steeply overturned and youngs to the east (Figure 39, Section 5-6). Northeast of the French mine, however, the formation is again gently dipping, indicating the proximity of the Good Hope synclinal axis.

The average true thickness of the Whistle Formation is unknown; it is estimated to be between 1000 and 1200 metres thick but the top is not exposed. Some sections along Whistle Creek, however, exceed 4000 metres in thickness although it is uncertain whether this is due to structural repetition. The formation is distinguishable from the underlying rocks by the almost total absence of limestone and the abundance of basaltic to andesitic volcaniclastic material. Unlike the underlying rocks, virtually no district-wide sedimentary or volcaniclastic facies changes are seen in the Whistle Formation (Figure 5).

A broad stratigraphic succession is recognized in the formation (Figure 5). The Copperfield breccia is commonly the basal unit; it is overlain by tuffaceous and turbiditic siltstone and minor argillite, which pass stratigraphically upwards into massive to poorly bedded crystal, ash and lapilli tuffs. Overall, there is a decrease in sediments and bedding structures up the succession and a corresponding increase in the development of massive and coarse grained tuffs. Coarser volcanic breccias and lapilli tuffs are common in the upper parts of the sequence.

The Copperfield breccia was formerly termed the Copperfield conglomerate (Ray *et al.*, 1987,1988); it is characterized by the presence of large limestone boulders and is the most important stratigraphic marker horizon in the district, due to its distinctive appearance and widespread development. West of Hedley, it forms a steeply dipping, northerly striking unit that is discontinuously traceable southwards for 16 kilometres. It is well developed on Lookout Mountain north of the Nickel Plate mine, and is also exposed within upfaulted slices at two localities along Pettigrew Creek, approximately 8 and 16 kilometres southwest of Hedley. The breccia is also preserved as a gently dipping unit within a down-faulted block approximately 1.5 kilometres east of Hedley.

The Copperfield breccia generally forms a single stratigraphic unit, but in some parts of the district there are two breccia units that are separated from each other by coarse tuffaceous sediments. The basal and thicker main unit is widely developed across the district but the thinner horizon, which lies several hundred metres higher in the sequence, is impersistent. This upper breccia rarely exceeds 40 metres in thickness; it crops out south and southwest of Lookout Mountain and on the north side of the Similkameen valley, 4.3 kilometres west-northwest of Hedley. South of the Larcan stock, the main breccia unit which separates the Whistle and Hedley formations is underlain by several thin, discontinuous breccia horizons.

The thickness of the main Copperfield breccia unit varies greatly throughout the district. West and northwest of the Banbury stock it reaches 200 metres in thickness, north of the Nickel Plate mine it is locally up to 100 metres thick, and southeast of Skwel-Kwel-Peken Ridge it is

Plate 5. Copperfield breccia (Unit 7a). Rounded to angular clasts of varied limestone and limestone conglomerate in a lime-rich tuffaceous matrix. West side of Henri Creek valley, 4.6 km west-southwest of Hedley.

Plate 6. Copperfield breccia (Unit 7a). Angular to subangular clasts of limestone with rare clasts of chert. Location as in Plate 5.

approximately 80 metres thick. Elsewhere, however, it is often less than 15 metres thick, and at many localities it appears to be absent. The breccia varies from clast to matrix supported, and is characterized by abundant, well-rounded to angular clasts of limestone generally up to 1 metre in diameter (Plates 5 and 6). In some localities, limestone blocks up to 15 metres in diameter are present, usually close to the stratigraphic base of the unit. Limestone comprises more than 95% of the clasts but rare fragments of argillite, siltstone, wacke, chert, crystalline quartz and carbonate, tuff, felsic intrusive rocks and intermediate to felsic volcanic rocks are also present. Volcanic clasts range from equigranular to coarsely feldspar porphyritic. The limestone clasts vary considerably in appearance, from grey to buff to pink in colour, from fine to coarse grained, from massive to thin bedded, and from pure to impure. Some limestone boulders contain fragments of bivalve shells and crinoid ossicles, and a few are composed of a limestone conglomerate consisting of grey limestone clasts in a calcareous matrix (Plate 5). Other less common clasts consist of chert-pebble conglomerate with a gritty calcareous matrix. Some of the larger, elongate, siltstone clasts (up to 3m long) are deformed and exhibit soft-sediment deformation structures, suggesting that they were unlithified when incorporated into the breccia. The breccia locally exhibits reverse grading, but is generally graded with larger blocks and boulders toward the base, and finer grained, moderately bedded grits and conglomerates toward the top of the unit. North of the Nickel Plate mine the breccia apparently contains a large flat-lying siltstone clast that reaches 10 metres in thickness.

The breccia matrix varies from massive to thin bedded and from siliceous and gritty, with abundant chert fragments, to very fine grained and calcareous or finely tuffaceous with small clasts of plagioclase, quartz and volcanic debris. Locally the matrix displays evidence of soft-sediment deformation and chaotic slumping.

Bivalve specimens collected from one limestone boulder at the Stemwinder Provincial Park, 3.5 kilometres west of Hedley (GSC Location No. C-143201; UTM 5471200 N, 708200 E) were identified as *Palaeocardita sp.* of probable Late Triassic age (E.T. Tozer, personal communication, 1987; Appendix 2C). Samples collected from three limestone boulders in the breccia contained conodonts that range in age from late Carnian to early Norian (Figure 6; Appendix 2A). Two of these limestone boulders are slightly older than the middle to late Norian age of the Stemwinder limestone horizon that immediately underlies the breccia (Appendix 2A). One chert clast collected from the breccia approximately 1 kilometre southwest of the Banbury stock yielded radiolarians of Permian age (F. Cordey, personal communication, 1985).

The Copperfield breccia near Nickel Plate mine was originally believed to be a tectonic breccia formed during low-angle thrust faulting (Billingsley and Hume, 1941). Our work establishes its stratigraphic nature, and it is now interpreted to be a gravity-slide deposit that is analogous to some modern megabreccias described in the Western Caribbean (Hine *et al.*, 1992). It probably resulted from the seismically triggered collapse of an unstable, shallow marine carbonate platform that originally lay along the Nicola basin margin east of the Hedley district. After the mass of carbonate debris had slumped down the submarine paleoslope, it was deposited on the unconsolidated deeper water sediments of the Hedley, Chuchuwayha and Stemwinder formations (Figure 8). Many of the sedimentary rocks immediately underlying the Copperfield breccia show chaotically disturbed bedding features similar to those seen in parts of the Oregon Claims Formation. These features were presumably caused by the breccia and limestone blocks ploughing into the unconsolidated sediments. North of the Nickel Plate mine, some of the very large and angular limestone blocks were apparently autobrecciated during their downslope movement. They are now represented by sharply angular, closely interlocking clasts, separated from one another by a matrix of limy gouge. In other instances, some of the rounded limestone clasts show evidence of milling.

Stratigraphically overlying the Copperfield breccia is a thick sequence of turbiditic siltstones (Unit 7b) and minor argillites (Unit 7c). The siltstones differ from those in the underlying Hedley and Stemwinder formations in being less calcareous and containing abundant, fine-grained tuffaceous material. They are thinly bedded and commonly graded. Individual beds have pale bottoms dominated by plagioclase-rich crystal tuff debris; they pass upwards into dark, fine-grained, argillaceous tops that contain considerable dust-tuff material. Scours, ripple marks, micro-crossbedding and flame structures are present. Overturned flames and crossbedding indicate the lower, turbiditic sediments of the Whistle Formation were deposited by westerly directed paleocurrents, similar to the underlying Hedley and Stemwinder formations.

The siltstones are intercalated with massive to weakly bedded crystal-lithic tuffs (Unit 7d). Toward the base of the Whistle Formation, these units are between 5 and 40 metres thick, but higher in the sequence, siltstone becomes gradually less abundant and tuffs predominate. Tuffs form pale to dark green outcrops that occasionally contain small, elongate, dark lithic fragments up to 75 millimetres in length. In thin section the crystal-lithic tuffs are seen to contain up to 50% twinned and optically zoned plagioclase crystals (An_{35-45}) set in a fine-grained chloritic matrix (Plate 7). The feldspars are up to 1.5 millimetres long, and vary from euhedral crystals to sharply angular, broken fragments. Colourless to very pale green augite comprises up to 20% of some specimens; the pyroxene crystals are mostly euhedral to subhedral and are up to 1 millimetre in diameter (Plate 7). The lithic clasts are generally less than 2 millimetres across and mostly represent equigranular to porphyritic basalt-andesite; clasts of carbonate and argillite are less common and one fragment of felsic volcanic rock was also identified. The euhedral, pristine nature of many augite and plagioclase crystals shows that they have undergone very little mechanical abrasion or transportation.

Whole rock and trace element compositional and discrimination plots on six samples of relatively unaltered ash tuff (Appendix 5) indicate that they include both alkaline and calcalkaline volcanics of largely basaltic composition (Figures 7A to 7C) and island-arc origin (Figures 7D to 7F).

In the upper parts of the Whistle Formation the tuffs become coarser grained and there is an increase in lapilli tuff (Unit 7e) and tuff-breccia (Unit 7f). Lapilli tuffs form thick and extensive units, but the coarser tuff-breccias are only locally developed. The angular clasts are mostly andesitic to basaltic volcanic rocks that include varieties with coarse feldspar phenocrysts. Rarer limestone, siltstone, quartz and pale, equigranular dacite clasts also occur. Impure limestone beds (Unit 7g) are extremely rare in the Whistle Formation. Thin beds, a few metres thick, are interbedded with argillite and tuff at one locality on the west side of Whistle Creek, approximately 2 kilometres south of its confluence with the Similkameen River. No microfossils were recovered from these beds. Limestones are also reported near the Canty deposit where drilling indicates the skarn mineralization overprints thin limestone horizons in coarse lapilli tuffs of the Whistle Formation (R.G. Simpson, personal communication, 1989).

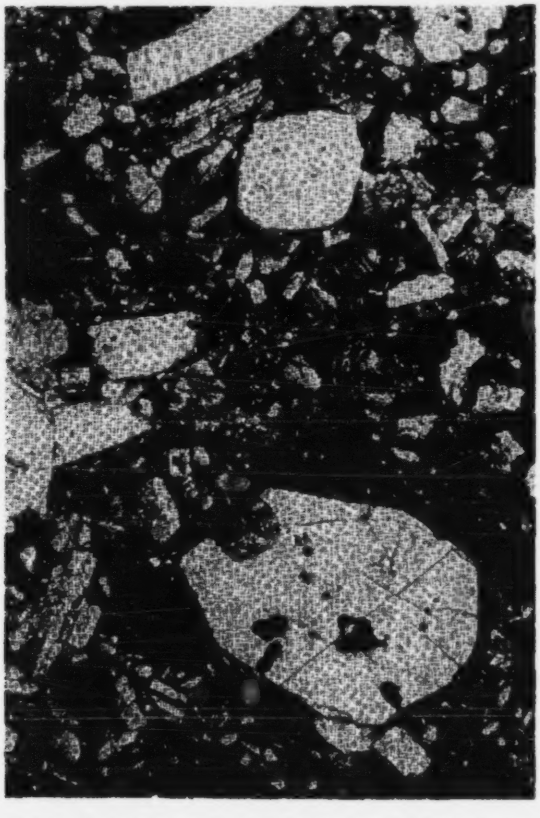

Plate 7. Crystal and ash tuff; Whistle Formation (Unit 7d). Photomicrograph (X polars) showing euhedral to subhedral crystals of augite and plagioclase in a chloritic matrix (field of view is 3 mm wide).

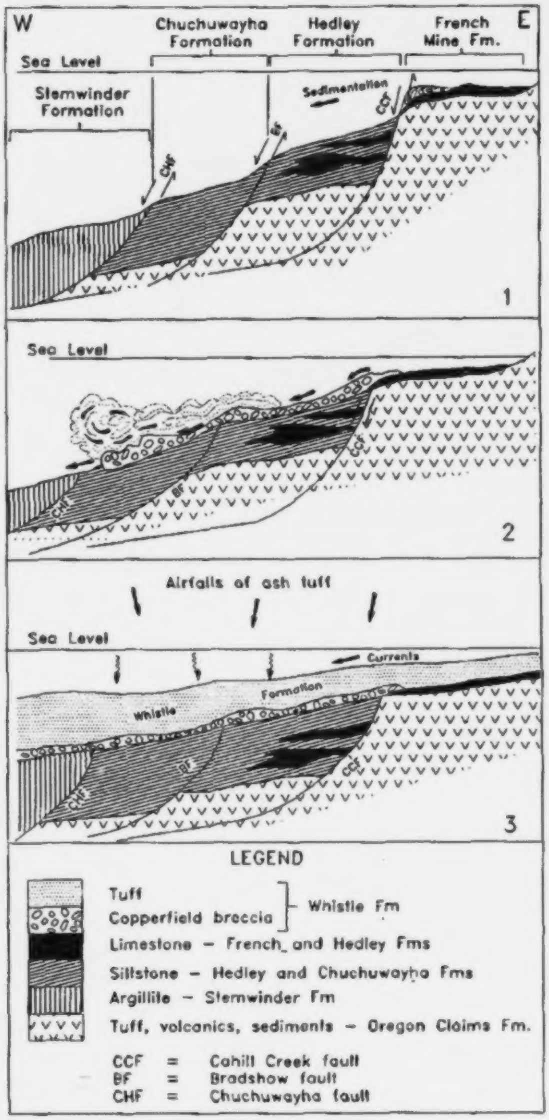
W
Chuchuwayha Formation
Hedley Formation
French Mine Fm.
E
Sea Level
Stemwinder Formation
Sedimentation
CHF
BF
CCF
1
Sea Level
CHF
BF
CCF
2
Airfalls of ash tuff
Sea Level
Currents
Formation
Whistle
CHF
BF
CCF
3
LEGEND
Tuff
Copperfield breccia
Whistle Fm
Limestone – French and Hedley Fms
Siltstone – Hedley and Chuchuwayha Fms
Argillite – Stemwinder Fm
Tuff, volcanics, sediments – Oregon Claims Fm.
CCF = Cahill Creek fault
BF = Bradshaw fault
CHF = Chuchuwayha fault

Figure 8. Depositional history of the Nicola Group in the Hedley area: 1. Carnian-Norian — Deposition of the French, Hedley, Chuchuwayha and Stemwinder formations onto the Oregon Claims Formation adjacent to the fault-bounded eastern margin of the Nicola basin. Sedimentation was from an eastern source and the facies were controlled by active normal faults that were precursor structures for the Chuchuwayha, Bradshaw and Cahill Creek faults. 2. Late Triassic — Catastrophic deposition of the Copperfield breccia into the basin as a chaotic mass gravity slide, from shallow marine facies to the east. This was possibly triggered by earth movements associated with development of the main Nicola arc farther west. 3. Late Triassic — Major airfalls of Whistle Formation ash and lapilli tuffs from an unknown source. Sedimentary currents were still from the east but conditions did not allow limestone deposition.

ROCKS OF UNCERTAIN AGE (Unit 8)

Due either to poor exposure or thermal metamorphic overprinting, some supracrustal rocks in the area cannot be assigned to any designated formation and are consequently of uncertain age and status. Such rocks are exposed in extensive areas north and northwest of Mount Riordan (Figure 38) as well as an area south of the Similkameen River and west of the Cahill Creek pluton (Figure 37). Rocks in the latter area were regarded by Bostock (1940a) as the same package that host the Nickel Plate deposit, the "Sunnyside Formation" (now part of our Hedley Formation; *see* Table 1). Like that package, the rocks south of the Similkameen River contain some thick limestone and marble units (Unit 8c). However, unlike the Hedley Formation, the siltstones are predominantly tuffaceous, and they include some chert-pebble conglomerate and limestone-breccia horizons (Units 8g and 8h) as well as argillite (Unit 8e). Locally, the tuffaceous and argillaceous sedimentary rocks adjacent to the limestones display disrupted bedding features. Similar features are seen in the Oregon Claims Formation northwest of the French mine, and the package south of the Similkameen River may belong to this formation. Moreover, this package contains some thermal metamorphic cordierite, similar to that seen in the Oregon Claims Formation and Apex Mountain Complex (Figure 14). However, this interpretation raises problems concerning the nature of the fracture (believed to be a southern continuation of the Bradshaw fault) that separates the package from Stemwinder rocks farther west (Figure 37). North of the Similkameen River, the Bradshaw fault appears to be downthrown to the east. South of the river, however, the presence of Oregon Claims Formation (or Apex Mountain Complex) against Stemwinder Formation suggests the opposite sense of movement.

DEPOSITIONAL ENVIRONMENT OF THE NICOLA GROUP AT HEDLEY

The Nicola belt west of the Hedley district (Figures 2 and 3) represents an Upper Triassic island-arc succession (Preto, 1972; 1979) that formed above an easterly dipping subduction zone (Mortimer, 1986, 1987) A shallow-marine back-arc basin is believed to have formed inboard of the main belt, and the Hedley district probably lies close to the eastern margin of this basin. The character of the Nicola Group sediments, together with the sedimentary facies changes present at Hedley, suggests that the basin edge was rifted and tectonically controlled by northerly striking and reactivated faults that marked a structural hinge zone (Figures 3 and 8).

The basin deepened westwards and derived most of its sediment from an easterly source. Nicola Group sedimentation at Hedley, throughout much of its history, was strongly influenced by both the westerly dipping paleoslope and the faults (Figure 8). The latter were probably the precursors of the Chuchuwayha, Bradshaw and Cahill Creek faults that now separate different facies represented by the Stemwinder, Chuchuwayha, Hedley and French Mine formations. Proximal volcanic activity during this time was negligible as most of the tuffaceous material in all the four facies is fine grained and reworked. The French Mine sedimentation took place in a shallow-marine, possibly fore-reef or lagoonal environment that included an irregular, locally steep topography; this resulted in the formation of reefal and algal limestones together with aprons of accumulated reef debris.

The essentially coeval Hedley, Chuchuwayha and Stemwinder sedimentation was characterized by calcareous turbidites that, to the west in the deeper, anoxic part of the basin, became progressively finer grained and organic rich (Figure 8). The occasional presence of rich conodont microfossil faunas in the Stemwinder Formation (M.J. Orchard, personal communication, 1988) suggests either lag deposits or periods of extremely slow sedimentation in the more distal part of the basin. The presence of current-induced sedimentary structures, general absence of macrofossils, and a lack of bioturbation in the Stemwinder and Chuchuwayha formations suggest that the marine basin was relatively shallow (<150 m) but was extensively anaerobic. Turbiditic sedimentation in the Hedley and Chuchuwayha formations was occasionally interrupted by influxes of coarse conglomerate and fine-grained tuff, as well as quieter periods when extensive and thick limestones were laid down. The source of these coarser sediments was presumably from the upslope French Mine Formation and the eroding uplands farther east.

Deposition of the Copperfield breccia across the area marked a profound change in the sedimentary environment. These changes were possibly related to major movements that resulted in the collapse of the basin margin (Figure 8) and the onset of volcanic activity responsible for the Whistle Formation tuffs. Some local auto brecciation and milling occurred in the Copperfield breccia, but most clasts lack significant abrasion which suggests they were supported by a fluid-rich matrix. During its initial transport down slope, the gravity slide may have been contained in submarine channels, but as it reached the deeper, more gentle slopes in the Hedley, Chuchuwayha and Stemwinder facies it coalesced into a broad fan of variable thickness (Figure 8). This fan ploughed into the unlithified basin floor causing scouring and chaotic disturbance of the underlying, water-saturated sediments; fragments of unconsolidated sea-floor sediment were ripped up and incorporated in the conglomerate and are now represented by large clasts of strongly deformed siltstone and mudstone.

After the Copperfield breccia was laid down the sedimentary environment across the area changed drastically and never returned to conditions suitable for widespread carbonate sedimentation. Sedimentary structures indicate that the fine-grained, well-bedded tuffaceous turbidites in the lower part of the Whistle Formation, like those in the underlying sediments, were deposited by west-directed paleocurrents. Later, the Whistle Formation sedimentation was largely dominated by airfalls of basic to intermediate, arc-related tuff. With time, the amount of coarse volcaniclastic deposition increased, resulting in thick, massive lapilli and ash tuffs that rarely display bedding. The tuffaceous airfalls were widespread and no facies changes similar to those in the underlying sediments are recognized in the Whistle Formation. The fine grained tuffs in the formation may represent long-travelled airborne material derived from the Nicola arc to the west. However, the coarser lapilli tuffs presumable originated from a nearer but unidentified volcanic source.

SKWEL PEKEN FORMATION (Unit 15)

The Skwel Peken Formation is a predominantly volcaniclastic sequence that was originally mapped as part of the Nicola Group (Bostock, 1940a). Later, during reconnaissance mapping by the Geological Survey of Canada (J.W.H. Monger, personal communication, 1986), it was recognized as a younger, distinct package that Ray *et al.*, (1988) tentatively assigned to the Early Cretaceous Spences Bridge Group. However, further study suggests that these rocks are significantly different from the true Spences Bridge rocks that outcrop farther west. Moreover, radiometric dating indicates the package is Jurassic rather than Cretaceous in age, and consequently, the name Skwel Peken Formation is formally proposed for these rocks. The formation is interpreted to have been laid down in a nonmarine, subaerial to shallow-water environment and is believed to represent largely volcaniclastic deposits related to the emplacement of the Cahill Creek and Lookout Ridge plutons. It is believed to represent the first example of mid-Jurassic supracrustal rocks recognized in south-central British Columbia, although plutonism of this age is widespread.

The formation contains two predominantly volcaniclastic members that also include minor epiclastic rocks. No flows have been positively identified, although it is possible that the rare, thin units of garnet-bearing rhyodacite (Unit 20a) spatially associated with the formation are flows rather than intrusions as shown in Figure 37. The boundary between the two volcaniclastic members is generally gradational. Skwel Peken rocks are exposed in two separate outliers; the northern outlier covers less than 4 square kilometres on Lookout Ridge, east of Lookout Mountain, while the other, surrounding Skwel-Kwel-Peken Ridge, exceeds 30 square kilometres in area (Figure 37).

The lower member, which is present in both outliers, has an estimated thickness of 1500 metres (Figure 39, Section 9-10). It consists largely of pale grey to dark green to maroon ash and lapilli tuffs (Unit 15a) that are massive (Plate 8) to well layered. These rocks contain abundant plagioclase crystals and lithic clasts; many of the tuffs characteristically include variable amounts of glassy quartz crystals, either as fragments in the matrix (Plate 9), or as phenocrysts in some volcanic clasts. Lesser amounts of coarse lapilli tuff and tuff-breccia (Unit 15b) are present, as well as rare examples of maroon-coloured, welded tuffs with fiamme textures (Unit 15c). Some of the layered tuffs are graded, and are interpreted to represent pyroclastic surge deposits laid down relatively close to the source vents. In addition, minor quantities of dust tuff, tuffaceous siltstone, argillite and thin beds of conglomerate (Unit 15d), as well as some andesitic ash and lapilli tuff (Unit 15e) are also present in the member.

In thin section, the lower member tuffs are seen to contain abundant lithic fragments, generally up to 5 millimetres in diameter; the fragments are strongly altered and mostly represent porphyritic and equigranular volcanic rocks of andesitic and dacitic composition. In addition to dacitic clasts with quartz phenocrysts, there are fragments of fine-grained, devitrified rhyodacite with zoned and altered phenocrysts of plagioclase and orthoclase. Less commonly, fragments of flow-banded rhyodacite, and ignimbrite with welded and compacted pumice fragments are also seen, as well as clasts of a quartz porphyry that closely resemble the quartz porphyry intrusive suite (Unit 14), and rare clasts of pyrite-rich andesite.

The groundmass of the lower member tuffs commonly contains abundant crystals and fragments of feldspar and quartz (Plate 9) with lesser amounts of hornblende and very rare augite. The feldspars are mostly twinned plagioclase (An_{7-34}) with lesser amounts of strongly altered orthoclase and very minor microcline; some plagioclase crystals have bent twin lamellae. The rare, subhedral and extensively chloritized hornblende crystals are up to 1.5 millimetres in length. Quartz in the groundmass forms unstrained, clear crystals that are mostly less than 1 millimetre across, although some reach up to 4 millimetres in diameter. They range from sharply angular fragments to whole, subhedral crystals; many are well rounded (Plates 9 and 10) and some have partially resorbed (Plate 10) or deeply embayed margins. Most contain no inclusions and are unzoned, but one example of a rounded quartz core overgrown by a subhedral quartz margin was noted. Many crystals appear to have been fractured after their deposition, as adjacent fragments often match and interlock. Zircons extracted from a lower

Plate 8. Skwel Peken Formation, lower member (Unit 15a). Lapilli tuffs with abundant clasts of andesite and rhyodacite.

member tuff sample containing abundant quartz phenocrysts gave a maximum U-Pb date of 187±9 Ma (Appendix 1A) suggesting a mid-Jurassic age for these rocks.

The fine-grained matrix in the lower member tuffs consists of chlorite, carbonate, quartz, sericite and minor devitrified glass, epidote and opaques. Locally, the tuffs are extensively epidotized, particularly on and around the summit of Skwel-Kwel-Peken Ridge. The ash and coarse lapilli tuffs at this locality contain abundant veins and disseminations of coarse-grained epidote, and many mafic clasts are rimmed or entirely replaced by epidote.

The coarser lapilli tuffs and tuff-breccias (Unit 15b) contain angular to subrounded clasts (Plate 8) that consist mainly of intermediate to felsic volcanic rock; the dacitic lapilli are pale coloured and contain quartz, plagioclase and orthoclase phenocrysts. Rarer lapilli of mafic volcanics, limestone and calcareous siltstone are also present.

Tuffaceous siltstones in Unit 15d form thin units within the lower member. They, and the waterlain bedded tuffs, are locally characterized by well-developed graded bedding, crossbeds and ripple marks which indicate that the Skwel Peken Formation is not tectonically inverted. Dust tuffs are also common in this unit; they are well bedded and grey to maroon in colour. In thin section they are seen to contain abundant small laths of elongate, altered plagioclase together with chlorite and opaque minerals. The plagioclase laths are less than 0.2 millimetre in length and generally orientated subparallel to the bedding. Conglomerates are rare and form impersistent beds up to 2 metres thick. They contain subangular to subrounded pebbles and cobbles of mainly andesitic tuffs and flows, with minor to rare amounts of chert, quartz, limestone, granodiorite and jasper.

Major and trace element analyses on eight samples of quartz-bearing crystal and lapilli tuff (Unit 15a) from the lower member are given in Appendix 6A. Plots of these data indicate that the lower member tuffs are subalkalic rocks (Figure 9A) of andesitic to dacitic composition (Figure 9B and C) and largely of calcalkaline affinity (Figure 9D).

In the southern outlier, west of Skwel-Kwel-Peken Ridge, the lower member is stratigraphically overlain by a sequence of mainly dark to medium green tuff (Unit 15f) up to 400 metres thick. These rocks are generally massive and homogeneous, although in rare instances weak bedding or crystal alignment is recognizable (Plate 11) and grading of the feldspar crystals is evident in some beds.

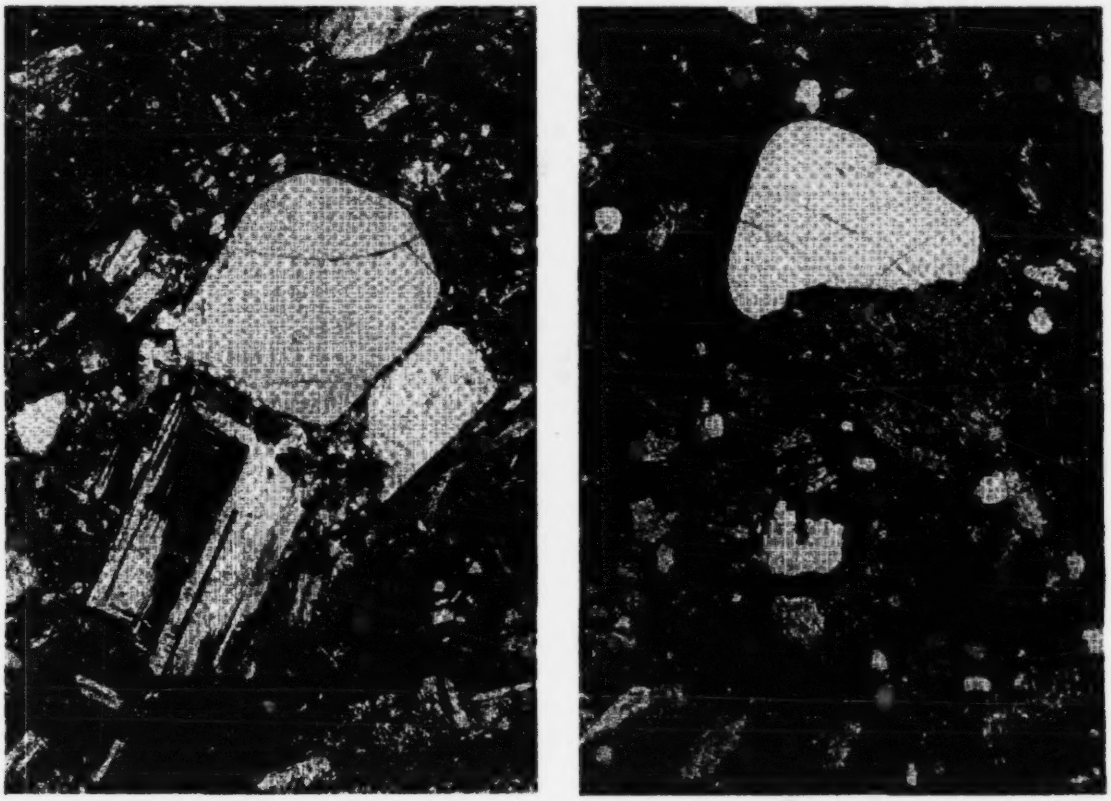

Plates 9 and 10. Skwel Peken Formation, lower member, (Unit 15a). Photomicrographs (X polars) showing ash tuff with crystals of plagioclase and quartz; the latter vary from subrounded and partially resorbed, with embayment features, to fractured and angular (field of view is 2.5 mm wide).

They are mainly crystal and ash tuffs; coarse lapilli fragments are uncommon in the upper member and, where present, are mainly of andesitic volcanics. Unlike the lower member, no clasts of limestone and dacite were identified, and quartz fragments are exceedingly rare. The abundant euhedral plagioclase in the crystal tuffs indicates that the upper member was deposited in a low-energy sedimentary environment.

In thin section the crystal tuffs of the upper member are seen to contain over 90% coarse euhedral, tabular feldspar crystals up to 4 millimetres in length, set in a fine-grained, altered matrix. Minor amounts of strongly zoned orthoclase are present, but most of the feldspar comprises zoned and twinned plagioclase that has sausseritized, calcic cores and fresher, more sodic rims. The plagioclase is mostly oligoclase (An_{14-30}), but occasionally fresher crystals of andesine (up to An_{49}) are present. Chloritized hornblende is seen occasionally, and rare, fractured and extensively altered remnants of twinned augite up to 2 millimetres long are present. The groundmass is a mixture of chlorite, tremolite-actinolite, carbonate, epidote and opaque minerals.

Major and trace element analyses on six samples of feldspar crystal tuff (Appendix 6B) indicate that the upper

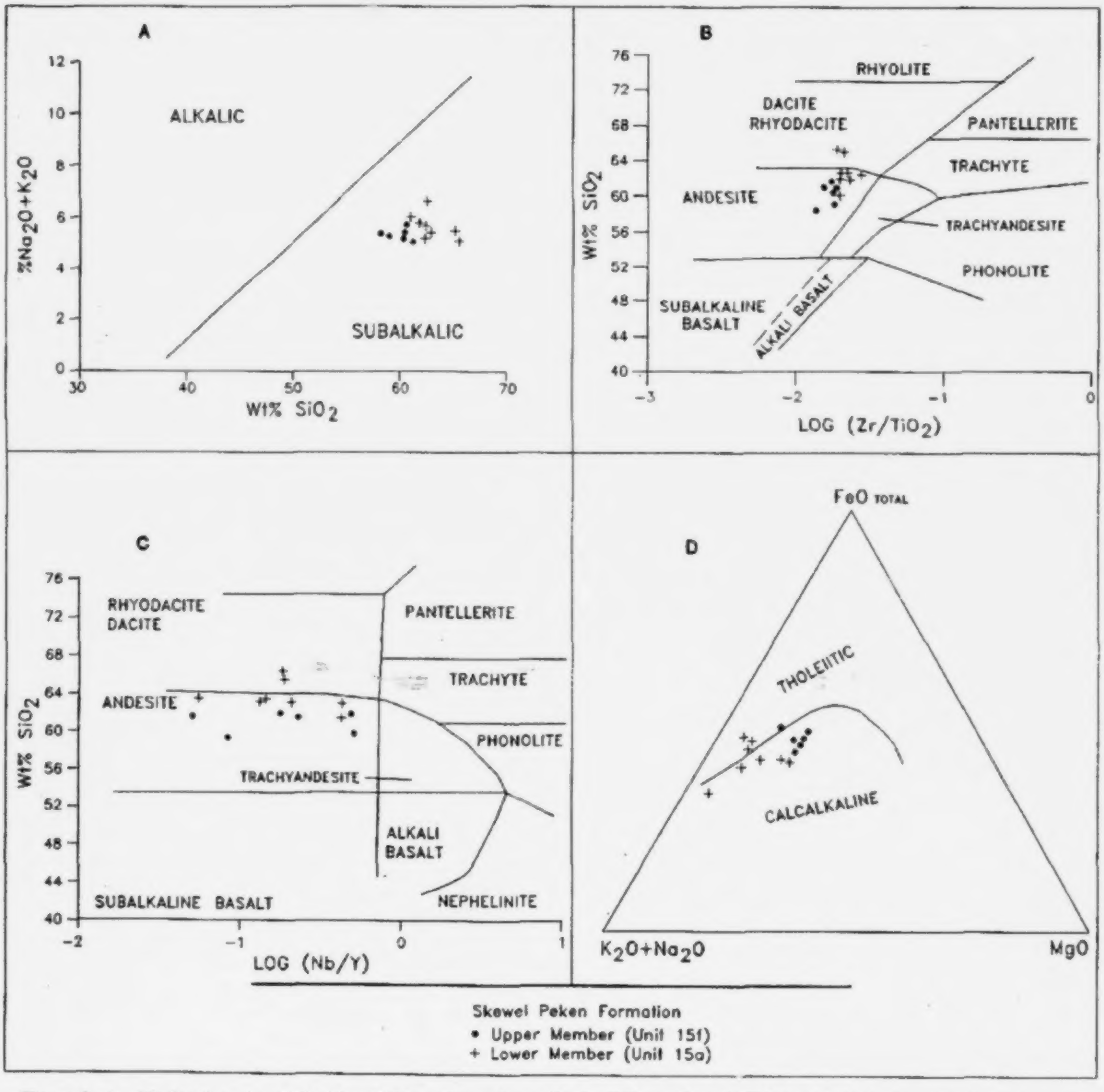

Figure 9. A. Alkali-silica plot of the Skwel Peken Formation tuffs. B. SiO_2 vs. log (Zr/TiO_2) plot of the Skwel Peken Formation tuffs. C. SiO_2 vs. log (Nb/Y) plot of the Skwel Peken Formation tuffs. D. AFM plot of the Skwel Peken Formation tuffs.

member comprises subalkalic, largely calcalkaline rocks of andesitic composition (Figure 9).

The northern outlier is a thin, subhorizontal sheet that structurally overlies both the Whistle Formation and the Lookout Ridge pluton. However, unlike the Whistle rocks, the Skwel Peken Formation is apparently not affected by contact metamorphism by the pluton. The southern outlier occupies a broad syncline that plunges north, and it too shows no evidence of thermal overprinting from the adjacent Cahill Creek pluton. The contact between the Skwel Peken Formation and the structurally underlying Hedley and Whistle formations is not exposed, and there are no signs of paleoweathering in the underlying rocks. Consequently, it is uncertain whether the base of the Skwel Peken Formation is a thrust or an unconformity.

SPENCES BRIDGE GROUP (Unit 17)

Rocks of the Early Cretaceous Spences Bridge Group outcrop at the extreme western margin of the map area, in the upper part of the Whistle Creek watershed. They consist of volcanic flows and tuffs, with lesser amounts of lahar, volcanic breccia and ignimbrite, and are similar to the Spences Bridge rocks described by Preto (1972, 1979) farther west (Figure 2). However, unlike that package, no basal conglomerate or unconformity has been identified in the Hedley area.

In the Hedley district the group includes massive flows and weakly bedded tuffs (Unit 17a) which analyses (Appendix 7) indicate are subalkalic, calcalkaline rocks of largely andesitic and rhyodacitic composition (Figure 10). The andesitic flows are pale green, equigranular to porphyritic and generally massive rocks; the coarsely porphyritic varieties are similar to some porphyritic dikes and sills that are interpreted to be subvolcanic feeders. In thin section many of the andesites are seen to contain coarse phenocrysts of euhedral, twinned plagioclase (An_{32-56}) set in a dark, altered fine-grained groundmass of small plagioclase laths, devitrified volcanic glass, carbonate, epidote, chlorite and iron oxides. The plagioclase phenocrysts are stubby crystals up to 2 millimetres long. Phenocrysts of fresh to weakly altered, twinned augite up to 3 millimetres in length, and small, chloritized remnants of dark green hornblende are less common.

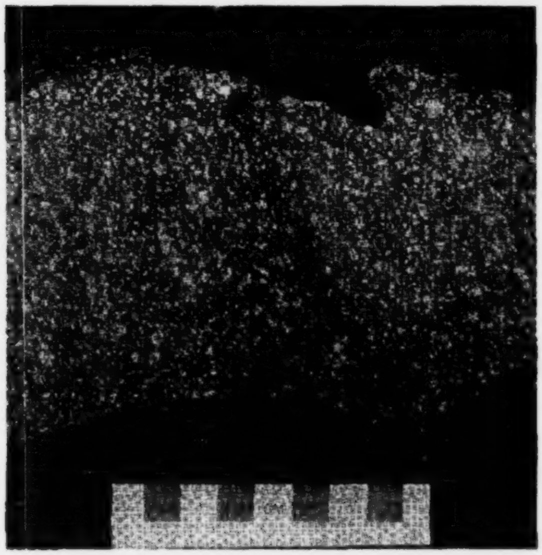

Plate 11. Skwel Peken Formation, upper member (Unit 15f). Weakly layered to massive andesitic feldspar crystal tuff.

The rhyodacitic volcanics contain euhedral phenocrysts of plagioclase (An_{8-34}), lesser amounts of orthoclase together with strongly altered hornblende and green pleochroic mica; these are set in an altered groundmass of chlorite, quartz and minor carbonate. The andesitic ash and lapilli tuffs are massive to weakly bedded and are similar in mineralogy to the andesitic flows.

West of Whistle Creek, a thin, northerly striking, westerly dipping layer of lahar and minor volcanic breccia (Unit 17b) stratigraphically overlies Unit 17a. The lahar forms pale, silicious outcrops that contain numerous subrounded to well-rounded clasts up to 0.3 metre in diameter. Clast lithologies include andesitic and dacitic volcanics, tuff, siltstone and impure calcareous sediments. Rarer, generally small clasts of dark chert and jasper were also noted. Lahars include both clast-supported and matrix-supported varieties; the matrix is a fine to medium-grained heterolithic, reworked tuff. Some coarse heterolithic breccias containing angular to subrounded clasts up to 25 centimetres wide are associated with the lahars. Clasts include green to maroon, flow-banded dacites, andesitic tuffs, and rare fragments of hornblende diorite.

A northerly striking, west-dipping unit of welded tuff and ignimbrite (Unit 17c) appears to stratigraphically overlie the laharic unit. It forms grey, pale pink, green and maroon outcrops containing dark fiammé that average 2 centimetres, and reach 10 centimetres in length. The welded tuff and ignimbrite contain abundant fragments of flattened and unflattened pumice, quartz and feldspar crystals, as well as numerous angular to subrounded fragments of pink to brown felsic, volcanic rock. The volcanic clasts are up to 7 centimetres long and include equigranular and porphyritic varieties. In thin section the ignimbrites are seen to contain abundant fractured crystals of orthoclase, plagioclase (An_{18-34}) and quartz; the latter have inclusions of apatite. Many of the welded glass shards are devitrified, and the fiamme are extensively chloritized and contain minor carbonate and epidote. Whole rock analyses on one sample of welded tuff (Sample HD 424, Appendix 7) indicate it is a subalkaline, calcalkaline rock of ryhodacite composition.

SPRINGBROOK FORMATION (Unit 18)

The Springbrook Formation was named and described by Bostock (1940a, 1941a and b). In the Hedley district it forms a thin unit of poorly consolidated conglomerate, sandstone, alluvium, talus, and stream and lake deposits that unconformably overlies the Nicola Group and Bromley batholith. Numerous exposures of gently dipping conglomerate and bedded sandstone of this formation were observed at one locality, approximately 1 to 2 kilometres northwest of Stemwinder Mountain. Bostock (1940a) also recorded some Springbrook Formation rocks underlying Marron Formation west of Smith Creek, in the western part of the map area, but these were not visited during the present survey. The erosional outlier of Marron volcanic rocks 4 kilometres southeast of Skwel-Kwel-Peken Ridge is presumed to be underlain by the Springbrook Formation, although no outcrops were observed in the field.

Church (1973) tentatively assigned a mid-Eocene age to the formation, and these siliciclastic deposits are believed to have been laid down in topographic depressions related to graben structures that formed during Eocene crustal extension.

MARRON FORMATION (Unit 19)

Erosional outliers of mid-Eocene Marron Formation (Bostock, 1941a, 1941b; Church, 1973) outcrop at three widely separated localities in the district, namely west of Smith Creek at the western edge of the map area, north of Paul Creek 4 kilometres southeast of Skwel-Kwel-Peken Ridge, and north and northwest of Stemwinder Mountain.

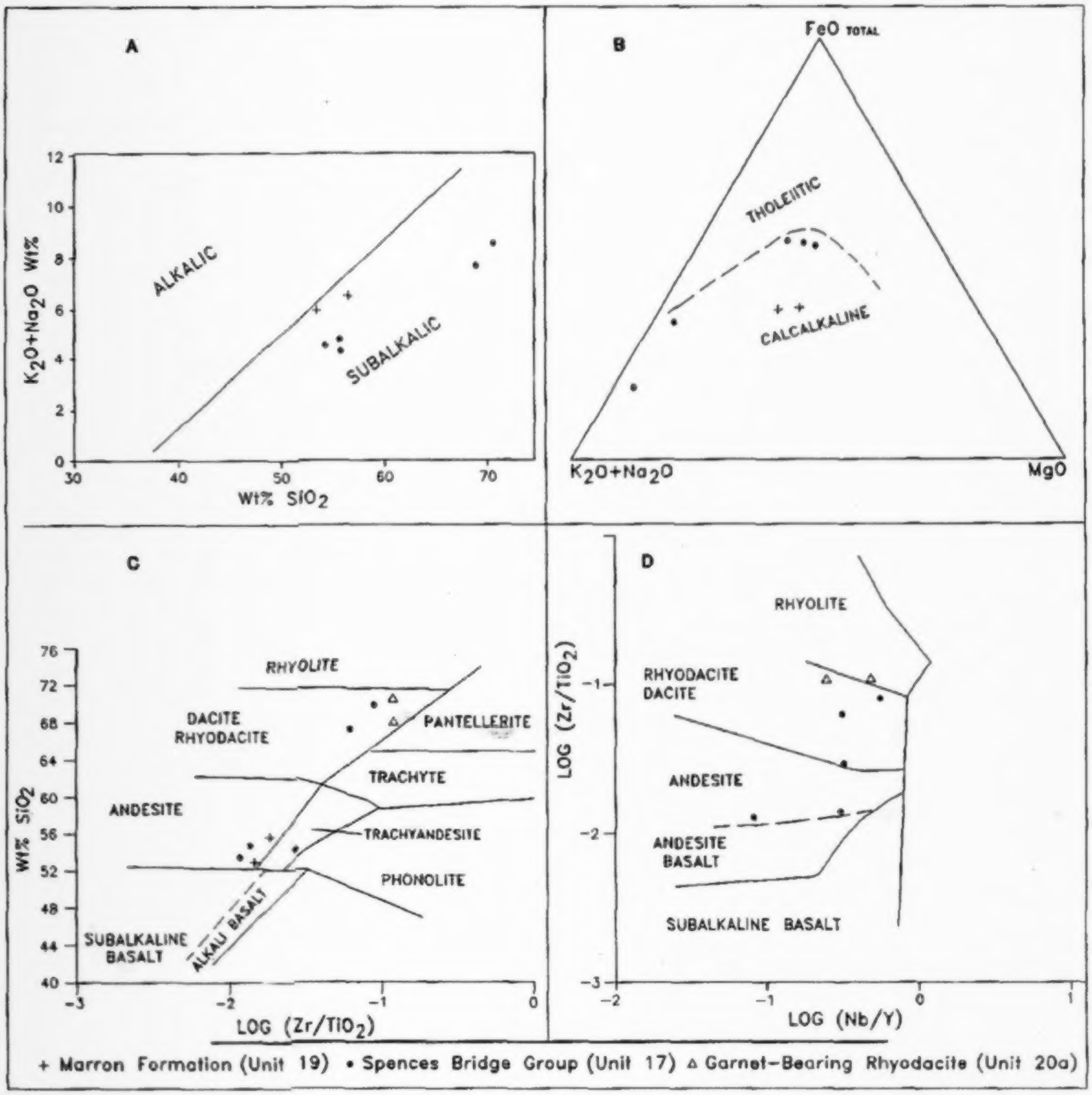

Figure 10. A. Alkali-Silica plot of the Spences Bridge Group and Marron Formation. B. AFM plot of the Spences Bridge Group and Marron Formation. C. SiO_2 vs. log (Zr/TiO_2) plot of the Spences Bridge Group, Marron Formation and garnet-bearing intrusions (Unit 20a). D. Log (Zr/TiO_2) vs. log (Nb/Y) plot of the Spences Bridge Group and garnet-bearing intrusions (Unit 20a).

The Marron Formation rocks that cap a hill west of Smith Creek, and those north of Stemwinder Mountain were previously mapped by Bostock (1940a), but the outlier southeast of Skwel-Kwel-Peken Ridge was first recognized during this survey. Farther east, in the White Lake basin, the Marron Formation mainly comprises a series of andesite, trachyandesite and phonolite flows with a total thickness of between 600 to 1500 metres (Church, 1973), but in the Hedley area it is much thinner.

The Marron Formation in the Hedley district unconformably overlies poorly exposed sediments of the Springbrook Formation. It consists of grey to green, massive to flow-banded, amygdaloidal volcanic rocks that locally exhibit spheroidal weathering. Analyses on two samples (Appendix 8) indicate they are subalkalic, calcalkaline and of andesitic composition (Figure 10). The mineralogy of some thin sections suggests trachyandesites may also be present.

The outlier west of Smith Creek extends farther west outside the map area; in the Hedley district it is at least 2 square kilometres in area and has an estimated maximum thickness of 120 metres. It consists mainly of andesite that in thin section is seen to contain numerous phenocrysts of elongate augite up to 1 millimetre long. The dark groundmass consists of abundant parallel-oriented plagioclase laths up to 0.3 millimetre long, together with altered amphibole, volcanic glass and minor biotite, carbonate, epidote, chlorite and opaques. The elongate amygdules are filled with quartz and are surrounded by reaction coronas containing radiating clinopyroxene crystals. Very rare, small and corroded remnants of olivine were also noted.

The erosional outlier southeast of Skwel-Kwel-Peken Ridge covers approximately 1 square kilometre and is up to 180 metres thick. The volcanic rocks differ slightly from those west of Smith Creek; they are more coarsely porphyritic and thin sections reveal they have marked trachytic or fluxion textures; they contain corroded, subhedral phenocrysts of twinned augite up to 5 millimetres long that are optically zoned and carry numerous inclusions of plagioclase. Phenocrysts of twinned plagioclase (An_{12-38}), up to 3 millimetres long, are rimmed with sanidine. The groundmass comprises a subparallel arrangement of small plagioclase laths, together with biotite, augite and opaque iron oxide minerals.

INTRUSIVE ROCKS

HEDLEY INTRUSIONS (Unit 9).

The economically important Hedley intrusive suite is believed to be Late Triassic to Early Jurassic in age. It forms major stocks up to 1.5 kilometres in diameter as well as swarms of thin sills and rare dikes up to 100 metres in thickness and over 1 kilometre in strike length.

Whole rock and trace element analyses of 27 samples of unaltered Hedley intrusions are presented in Appendix 9; major oxide plots indicate that they are sub-alkalic, calcalkaline rocks (Figures 11A and B) of mainly quartz diorite to gabbro composition (Figure 11C).

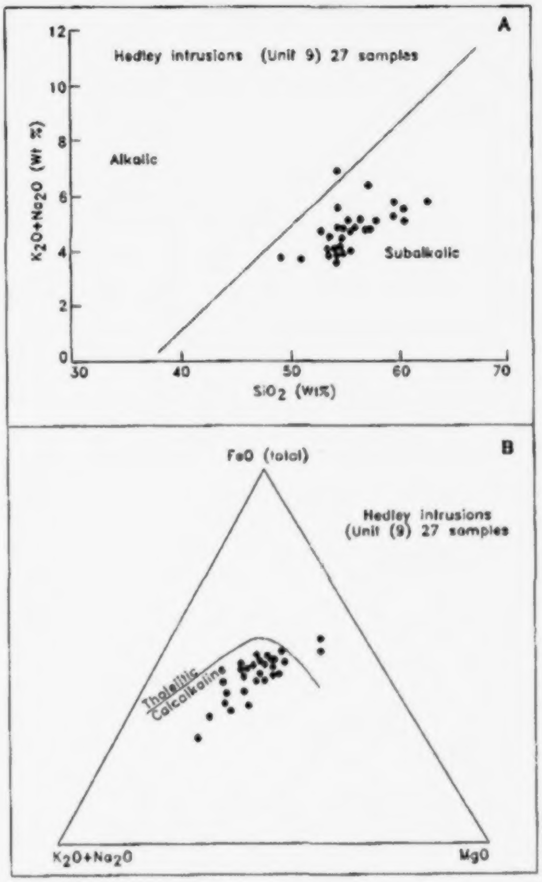

Figure 11. A. Alkali-silica plot of the unaltered Hedley intrusions. B. AFM plot of the unaltered Hedley intrusions. C. K_2O/Na_2O vs. SiO_2 plot (after Mason, 1978) illustrating the compositions of the unaltered Hedley intrusions and various rocks in the Mount Riordan stock. D to M: Plots comparing the geochemistry of the Hedley intrusions to igneous rocks associated with the other subclasses of skarn deposits. Dots represent mean values for each deposit subclass. For data *see* Table 2; *Note:* insufficient data for molybdenum skarn subclass. D. Principal oxide plot (after Church, 1975) illustrating the variable composition of intrusions associated with various skarn deposit subclasses. Note: the Hedley intrusions lie in the gabbro-diorite field. E. Alkali vs. silica plot illustrating that the Hedley intrusions, compared to other skarn-related igneous rocks, have the lowest average silica and total alkali contents. F. AFM plot comparing the Hedley intrusions to other skarn-related intrusions. G. Iron-magnesium-alumina plot comparing the Hedley intrusions to other skarn-related intrusions. H. Total iron vs. silica plot. *Note:* the Hedley intrusions are relatively enriched in iron. I. K_2O/Na_2O vs. calcium plot. *Note:* the Hedley intrusions are the most calcic and, with intrusions related to Fe skarns, have the lowest K_2O/Na_2O ratios. J. FeO vs. total iron plot. K. MgO/MgO + total iron vs. SiO_2 plot. Note: the Hedley intrusions are the most ferromagnesium-rich. L. TiO_2/Fe_2O_3 vs. total iron. M. Fe_2O_3/FeO vs. total iron. *Note:* the Hedley intrusions have the highest ferrous/ferric ratios suggesting they are the most reduced of all the skarn-related plutonic suites.

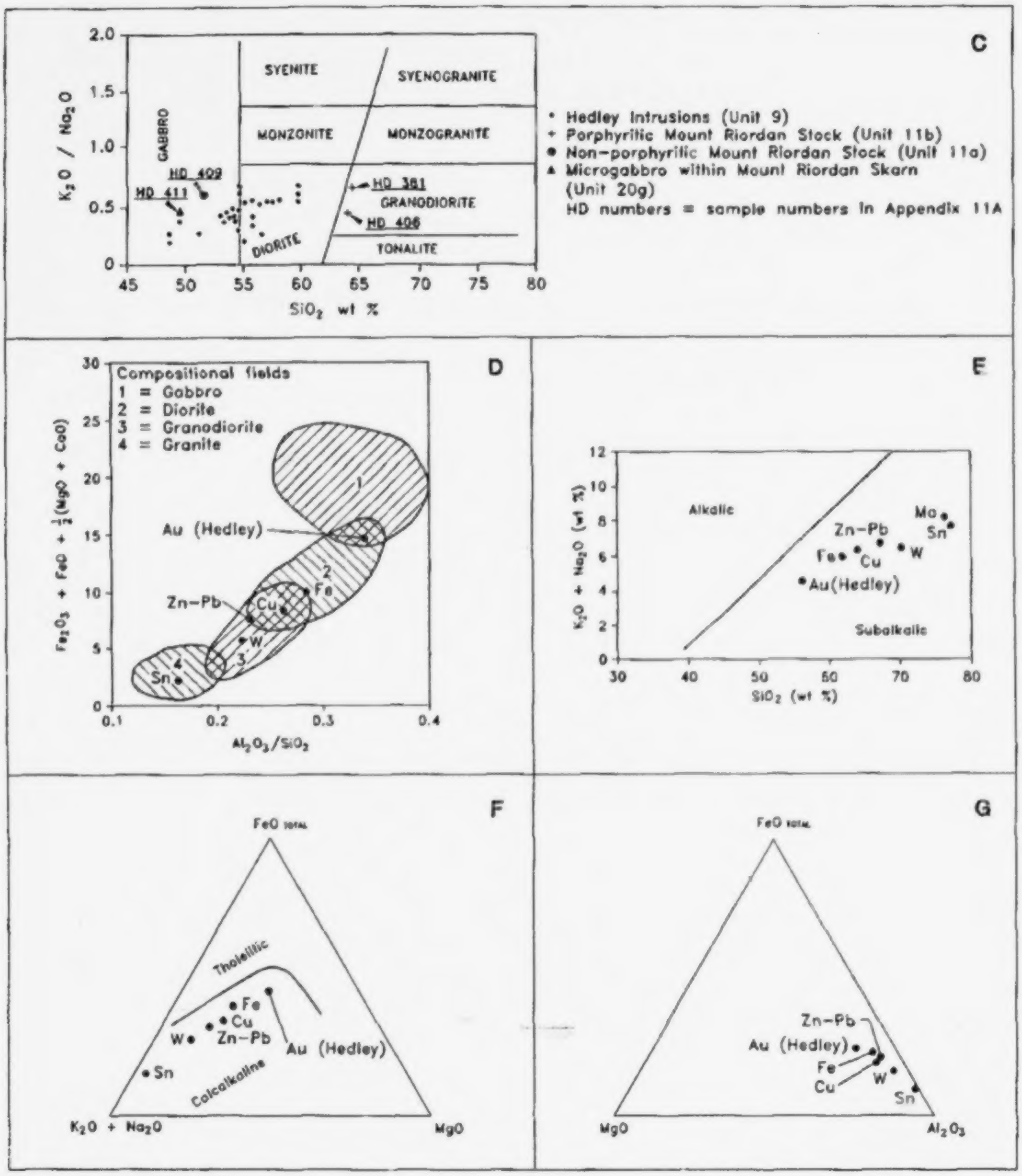

Figure 11—*Continued*

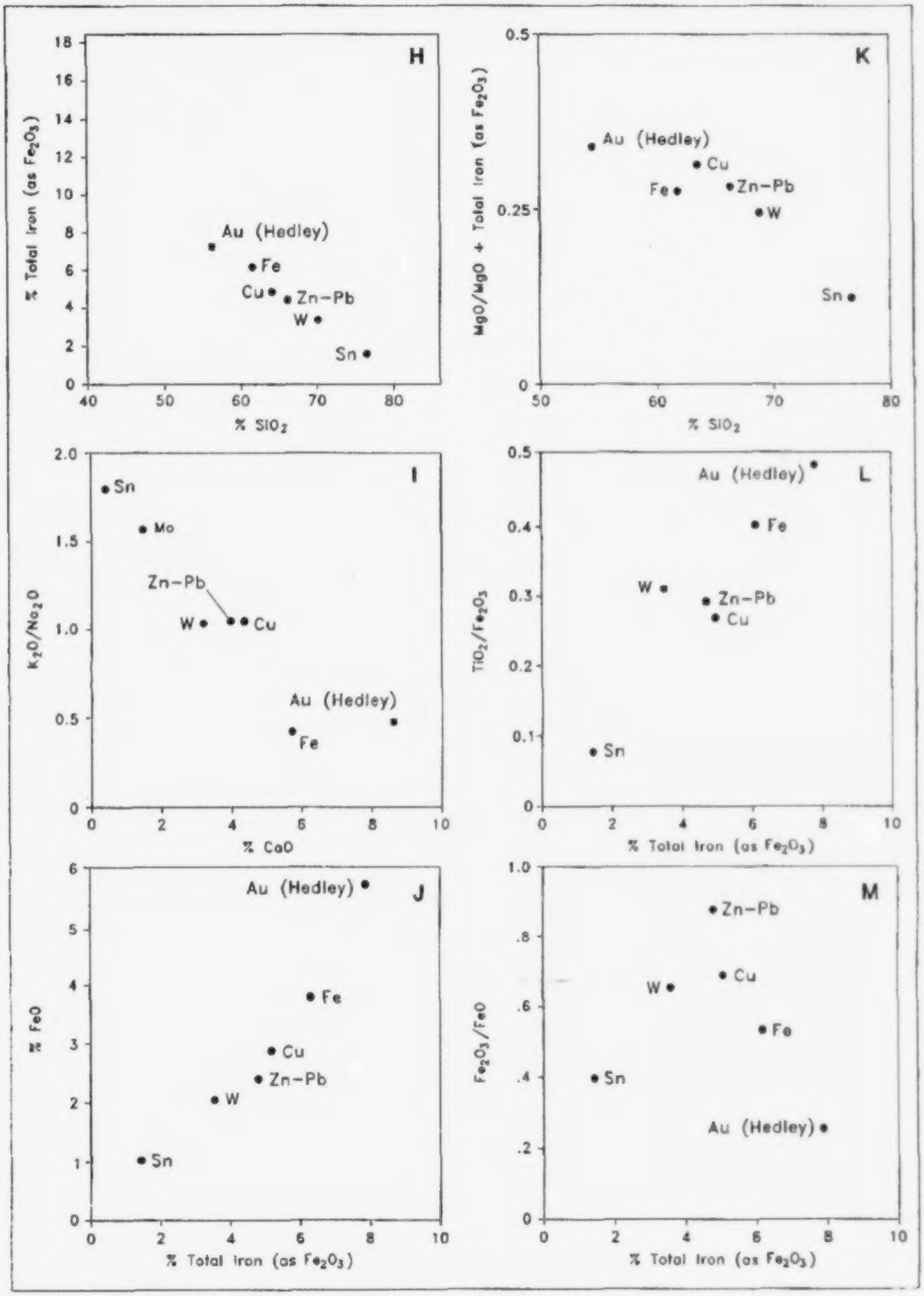

Figure 11—*Continued*

Plate 12. Porphyritic Hedley intrusions (Unit 9a). Diorite with phenocrysts of plagioclase and hornblende. One kilometre north of Hedley township.

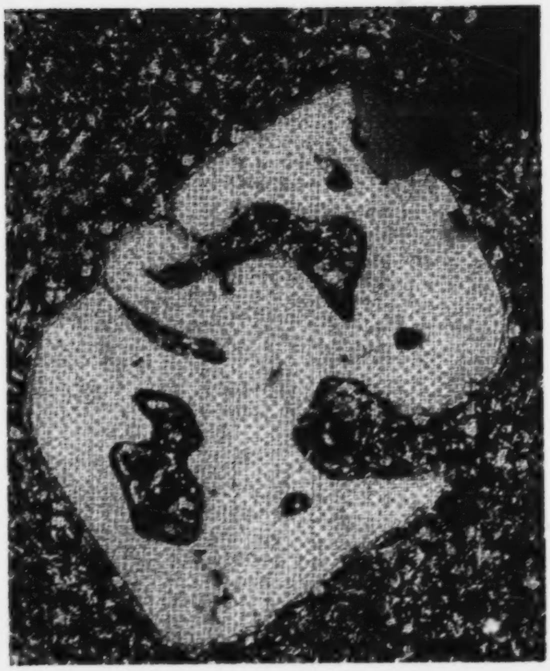

Plate 14. Hedley intrusions (Unit 9a). Photomicrograph (X polars) of a rare quartz phenocryst showing extensive resorption (field of view is 2 mm wide).

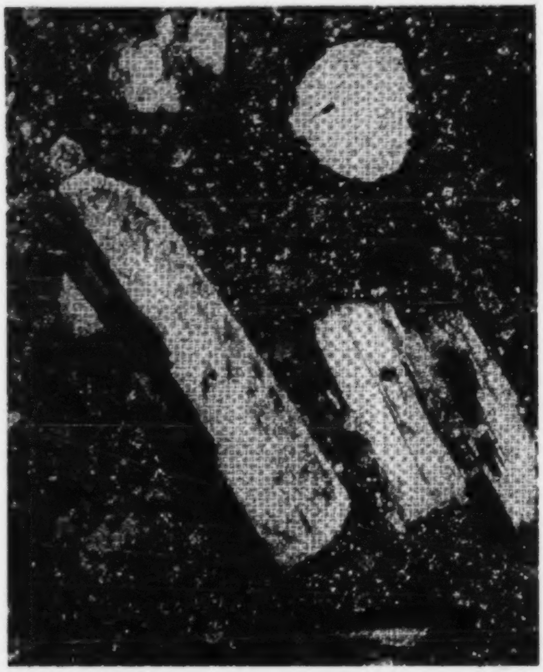

Plate 13. Hedley intrusions (Unit 9a). Photomicrograph (X polars) showing phenocrysts of euhedral plagioclase and a rare, rounded quartz crystal (field of view is 2 mm wide).

Plate 15. Hedley intrusions (Unit 9). Photomicrograph (X polars), plagioclase crystal with altered core and fine optical zoning in the margins (field of view is 2 mm wide).

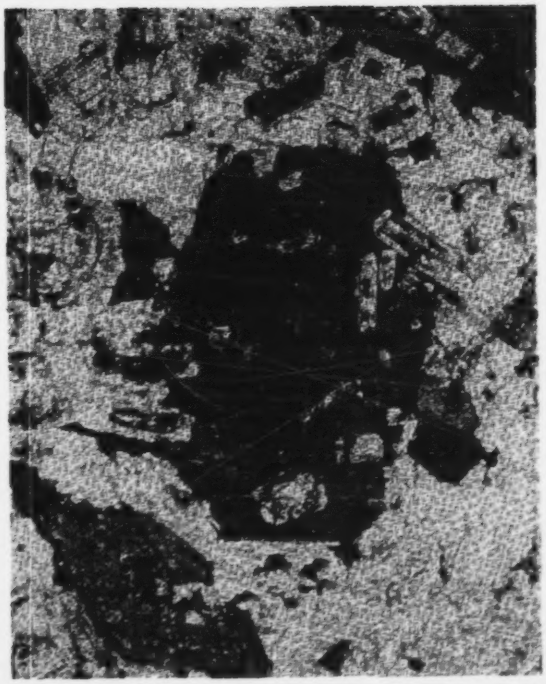

Plate 16. Hedley intrusions (Unit 9a). Photomicrograph (X polars) showing poikilitic hornblende phenocryst overgrowing euhedral crystals of plagioclase (field of view is 2 mm wide).

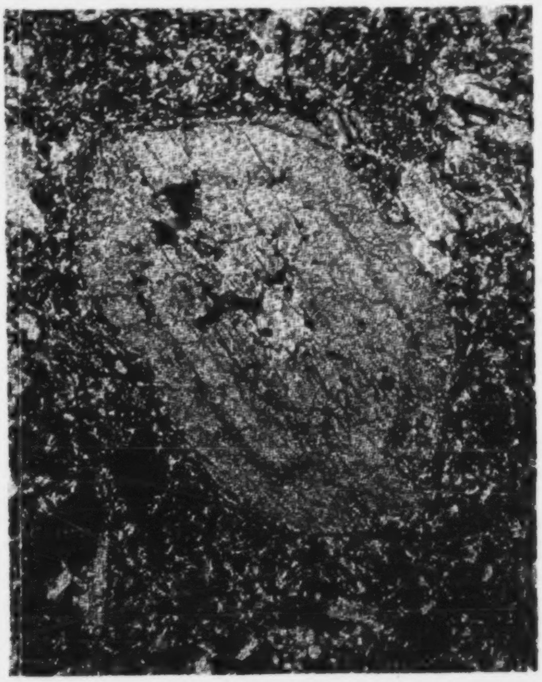

Plate 17. Hedley intrusions (Unit 9a). Photomicrograph (X polars) showing rare optical zoning in a hornblende phenocryst (field of view is 2 mm wide).

The Hedley intrusions generally form coarse-grained, porphyritic to equigranular, dark coloured and massive rocks in which xenoliths are very rare, particularly in the larger bodies. Porphyritic textures tend to be more common in the dikes and sills than in the larger stocks; they are marked by coarse, euhedral to subhedral phenocrysts of plagioclase, hornblende (Plate 12) and, less commonly, augite. A few examples include very rare, rounded to extensively resorbed phenocrysts of quartz (Plates 13 and 14). The plagioclase phenocrysts are characterized by altered cores and marked oscillatory and reverse compositional zoning, particularly in the outer parts of the crystal (Plate 15). The hornblende phenocrysts vary from subhedral to anhedral; many of the latter are markedly poikilitic and enclose numerous subhedral crystals of plagioclase (Plate 16). Rarely, some of the hornblende and pyroxene phenocrysts also show moderate optical zoning (Plate 17). Many of the unaltered dikes and sills contain minor disseminations of pyrrhotite that weathers to give these rocks a rusty appearance, whereas many of the skarn-altered intrusions are bleached.

The Hedley intrusions have not been positively identified in the Apex Mountain Complex, but they invade the Nicola Group over a wide area. Varying degrees of sulphide-bearing calcic skarn alteration are developed within and adjacent to many dikes and sills, and less commonly against the stocks. Some previous workers (Billingsley and Hume, 1941; Dolmage and Brown, 1945) considered this plutonic suite to be genetically related to the skarn-hosted gold mineralization in the district, including that at the Nickel Plate, Hedley Mascot, French and Good Hope mines. The geochemical and mapping results presented in this bulletin, together with recent studies by Ettlinger (1990a), support this conclusion.

The larger intrusions in the district include the Larcan, Pettigrew, Banbury, Stemwinder, Aberdeen, Climax and Toronto stocks (Figure 37). They are widely distributed and intrude rocks of the Oregon Claims, French Mine, Hedley, Chuchuwayha, Stemwinder and Whistle formations. The degree of alteration in the stocks is highly variable; the Pettigrew and Stemwinder stocks are generally unaltered, whereas most parts of the Toronto and Climax stocks are overprinted by varying amounts of skarn alteration.

STEMWINDER STOCK

This stock, which outcrops over an area of 2 square kilometres, was extensively sampled during this study; major and trace element analyses are included in Appendix 9, and the stock exhibits a calcalkaline differentiation trend similar to the other unaltered Hedley intrusions. It is rarely skarn altered and provides a useful geochemical and mineralogical comparison with the skarn-altered Toronto stock and sill-dike swarm at the Nickel Plate mine (Appendix 10A and B). It is a coarse-grained, massive, equigranular to moderately porphyritic, unaltered diorite-quartz diorite. It is interpreted to have originally been a subvertical, oval-shaped body that was subsequently tilted westward, which accounts for its current elongate shape in outcrop.

The margins of the Stemwinder stock are sporadically marked by minor silicification and chloritic alteration; whole rock and trace element analyses of silicified samples from the stock, together with those from other Hedley intrusions, are given in Appendix 10C and D. The southern margin of the stock is steeply inclined and is associated with several small skarns including the Peggy (Hedley Amalgamated) gold-skarn occurrence. The central parts of the stock tend to contain more hornblende than biotite, whereas at the margins the reverse is seen.

In thin section the Stemwinder stock is characterized by plagioclase crystals with a pronounced optical and compositional zoning that is enhanced by the selective alteration and clouding of certain zones. Most crystals show oscillatory or reverse zoning; the more sodic cores are generally altered and packed with minute inclusions, while the calcic rims tend to be unaltered and clear; some feldspar phenocrysts have thin, recrystallized rims consisting of numerous very small orthoclase crystals. Plagioclase phenocrysts are up to 2 millimetres long, and tend to be untwinned and more extensively altered than the smaller crystals of twinned plagioclase (An_{22-45}) in the groundmass. Hornblende is the most common and widespread mafic mineral, forming between 6 and 20% of the rock. The green to brown pleochroic hornblende forms poikilitic, subhedral to anhedral, corroded crystals up to 3 millimetres long that contain abundant small, euhedral laths of altered plagioclase (An_{30-55}). The hornblende phenocrysts are partially replaced and rimmed with tremolite-actinolite. Phenocrysts of colourless, poikilitic clinopyroxene are less common; they are rimmed and extensively replaced by green hornblende. Biotite is uncommon and when present forms less than 4% of the rock. It is locally altered to chlorite along cleavages. Quartz is generally less than 2% by volume but may locally exceed 10%; it mostly occurs as a clear, late, interstitial mineral. Trace amounts of microcline and orthoclase are also widespread; like most of the quartz they are late and interstitial. Other minerals identified include variable amounts of epidote and chlorite together with traces of carbonate, sericite, sphene, apatite, zircon, pyrrhotite, arsenopyrite, rutile, magnetite, ilmenite and rare pyrite. The pyrrhotite is often rimmed with chlorite.

Attempts to date the Stemwinder stock using U-Pb methods were unsuccessful, either due to insufficient zircons in the samples or spurious analytical results. Four

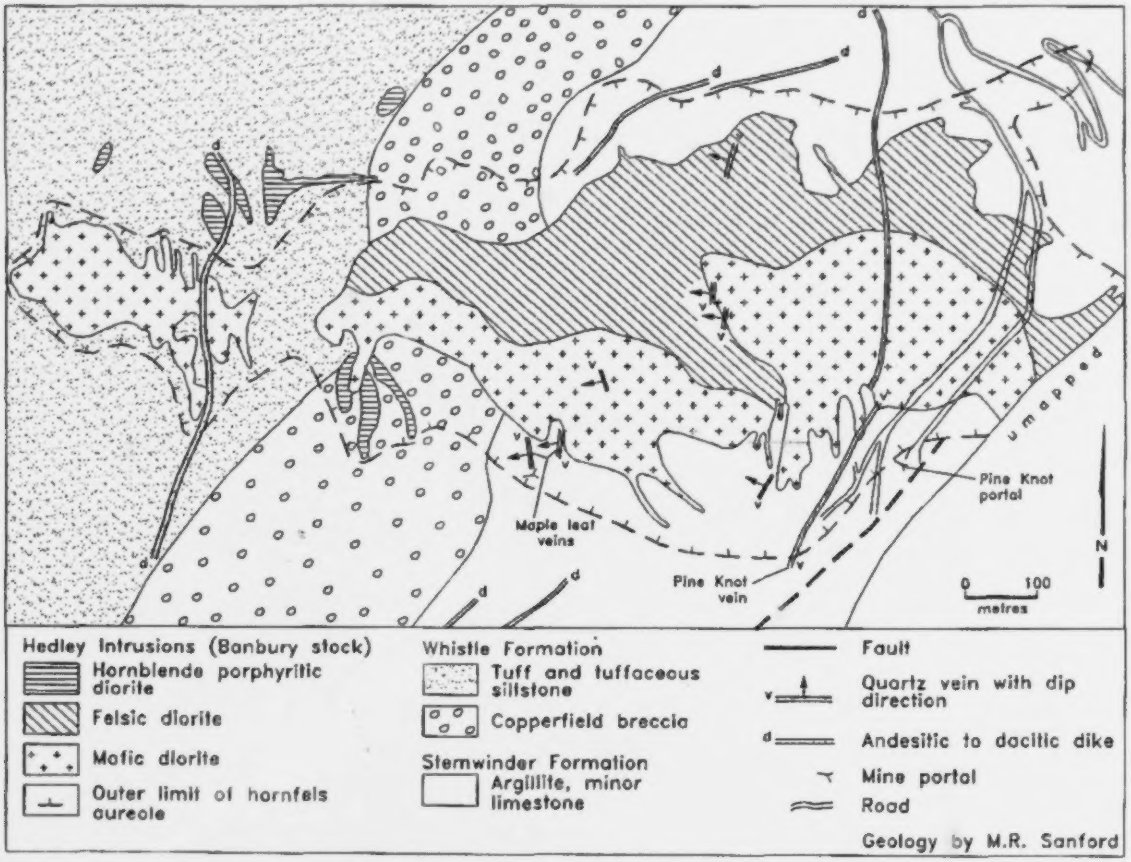
d
d
d
d
d
d
v
v
v
Maple leaf veins
Pine Knot vein
Pine Knot portal
unmapped
N
0 100
metres
Hedley Intrusions (Banbury stock)
Hornblende porphyritic diorite
Felsic diorite
Mafic diorite
Outer limit of hornfels aureole
Whistle Formation
Tuff and tuffaceous siltstone
Copperfield breccia
Stemwinder Formation
Argillite, minor limestone
Fault
Quartz vein with dip direction
Andesitic to dacitic dike
Mine portal
Road
Geology by M.R. Sanford

Figure 12. Geology of the Banbury stock area (mapping by M.R. Sanford, courtesy Banbury Gold Mines Ltd.)

zircon fractions extracted from one sample (HD 81) give inconclusive results indicating a maximum age of 219 and minimum age of 175 Ma (Appendix 1) due to combined lead loss and inheritance; the inherited lead is believed to be Paleozoic or older (J.E. Gabites, written communication, 1990).

PETTIGREW STOCK

The poorly exposed Pettigrew stock outcrops about 8 kilometres southwest of Hedley. It is believed to total 0.5 square kilometre in outcrop area, and varies from a leucocratic quartz diorite to a mafic hornblende-bearing diorite and gabbro. Zoned and altered plagioclase is abundant in all phases of the stock. The leucocratic varieties contain up to 5% colourless augite that forms phenocrysts reaching 4 millimetres in length. Quartz forms up to 7% by volume, and minor amphibole and chlorite-altered biotite are also present. The mafic varieties contain up to 25% of very coarse, brown, poikilitic hornblende that contains inclusions of plagioclase and rare augite. No skarn alteration was seen in or adjacent to the Pettigrew stock.

BANBURY STOCK

The Banbury stock is an elongate body, approximately 1 kilometre long, that crosscuts the Whistle and Stemwinder formations (Figure 12). A small satellite body, which probably represents a western extension of the stock, outcrops immediately to the west; both intrusions are surrounded by a hornfelsic aureole up to 150 metres wide.

The Banbury stock is associated with both unmineralized skarn and several quartz-carbonate veins, including the gold-bearing Mapleleaf and Pine Knot veins. The elongate shape of the stock is partly due to its current tilted orientation, although the intrusion may have been partly controlled by an easterly to northeasterly striking fracture and attendant fold structures; drilling indicates that the northern and southern margins of the body are subvertical to steeply south dipping (M.R. Sanford, personal communication, 1987).

The stock includes a northern, highly leucocratic and felsic phase, and a southern mafic dioritic phase that contains between 20 and 60% amphibole (Figure 12). Some small, dioritic apophyses of the stock are characterized by coarse hornblende phenocrysts. Drilling shows that the contact between the mafic and felsic phases is complex and that locally the two phases interfinger with each other.

In thin section the mafic diorite is seen to contain large crystals of poikilitic, greenish brown hornblende. Some amphiboles have undergone two episodes of growth; these crystals contain large, rounded cores of brown, inclusion-free hornblende that are overgrown with wide rims of paler amphibole that poikilitically encloses abundant small inclusions of plagioclase. The contacts between these two phases are often marked by coronas of small, radially arranged feldspar crystals. The mafic diorites contain up to 7% interstitial quartz as well as traces of late interstitial orthoclase. Samples of the leucocratic phase yielded insufficient zircons for geochronometric analysis, but U-Pb analysis on zircons extracted from the mafic phase of the Banbury stock suggests a maximum age of 215.4±4Ma (Appendix 1).

TORONTO STOCK

The Toronto stock intrudes the Hedley Formation 1.5 kilometres northeast of Hedley and is economically important because it is believed to be the parent of an extensive diorite sill-dike swarm and the associated skarn envelope that hosts the Nickel Plate gold deposit. Samples from the stock and from a skarn-altered sill at the deposit (the "Hot sill") were collected for geochronometric analyses but no age dates were obtainable due to insufficient zircons. Major and trace element analyses on samples collected from surface exposures of the Toronto stock and underground samples of skarn-altered intrusions at Nickel Plate are presented in Appendix 10A and B. Most outcrops of the Toronto stock display varying degrees of pale-coloured skarn alteration.

Emplacement of the stock was structurally controlled; it is elongate in an easterly to east-southeasterly direction, having a width of up to 500 metres and a length of approximately 2 kilometres. Its western margin abuts the Bradshaw fault and it is uncertain whether the adjoining lobe of diorite immediately west of the fault is part of the Toronto stock or an up-faulted segment of another Hedley intrusion. If it is a western extension of the Toronto stock it indicates that the main movement along the Bradshaw fault predated the emplacement of the Hedley intrusions.

The margins of the Toronto stock are steeply dipping, and adjacent to the northern and southern contacts, the sediments are more strongly deformed and turned sharply upwards. This suggests that the sediments were either deformed by the forcible intrusion of the stock, or the body was emplaced into a pre-existing fold structure (Dolmage and Brown, 1945). Underground mining revealed that numerous apophyses and swarms of sills and dikes were injected into the folded Hedley Formation along the northern, northeastern and eastern margins of the stock (Billingsley and Hume, 1941).

The Toronto stock consists of massive, medium to coarse-grained rocks that vary from weakly to intensely porphyritic; the porphyritic variety contains large euhedral to subhedral phenocrysts of black hornblende and smaller phenocrysts of oscillatory zoned plagioclase. Analyses of weakly altered samples, presented in Appendix 10A and B, indicate the stock is subalkalic and calcalkaline similar to other Hedley intrusions. Dolmage and Brown (1945) describe a vertical compositional zoning in the stock. Quartz diorite comprises the lower and main portion of the body, whereas quartz gabbro and lesser diorite occupy the uppermost parts of the intrusion; the intervening transitional rocks are augite diorite. Dolmage and Brown considered the parent magma to have been dioritic, and the upward vertical change to gabbro was thought to be due to a reaction between the intrusion and the calcareous country rocks. A vertical increase in the quartz content is also apparent. Both Billingsley and Hume (1941), and Dolmage and Brown (1945) describe the dioritic rocks as dark coloured and the gabbroic rocks in the upper part of the stock as very light coloured. Our study suggests that these vertical colour changes are not wholly due to original compositional differences in the magma but are also a reflection of increasing skarn alteration and bleaching in the upper parts of the intrusion. Moreover, most previous workers described the presence of abundant primary augite in the Toronto stock, but our thin section studies indicate that although igneous augite is present, much of the pyroxene is secondary, skarn-related and has overgrown and replaced the primary amphibole.

In thin section the least skarn-altered Toronto quartz diorite is seen to contain abundant compositionally and optically zoned andesine (An_{32-47}) as well as between 10 and 15% primary hornblende and 1 and 2% augite. The poikilitic amphibole phenocrysts average 2 millimetres in length but may exceed 5 millimetres. Dolmage and Brown noted the presence of two varieties of amphibole, a dark green to black hornblende (hastingsite?) and a pale tremolite-actinolite. Primary augite is partially altered to chlorite, amphibole or clinopyroxene, and usually occuppies cores in some hornblende crystals. Late, interstitial quartz and orthoclase make up to 10 and 5% of the rock, respectively. Biotite occurs as large chloritized crystals; also present are minor to trace amounts of orthoclase, sphene, carbonate, epidote, chlorite, sericite, magnetite, ilmenite, rutile, apatite, arsenopyrite and pyrrhotite.

The gabbroic and dioritic rocks in the upper part of the Toronto stock are generally more quartz rich than the dioritic rocks at depth, but it is uncertain whether this reflects an original compositional feature or is related to later silicification during skarn alteration. Quartz averages 26% (Dolmage and Brown, 1945) but ranges from 2 to 30% by volume. These rocks contain abundant andesine-labradorite plagioclase (An_{34-60}) which, as in all the Hedley intrusions, is compositionally and optically zoned. The primary augite forms colourless to very pale green prismatic crystals that are often rimmed with and partially altered to tremolite-actinolite. Other primary minerals include accessory hornblende and biotite, and trace ilmenite, sphene, rutile, orthoclase, microcline, pyrrhotite and rare magnetite.

CLIMAX BLUFF AND LARCAN STOCKS

The so-called Climax Bluff stock was first mapped by Camsell (1910) and later described by Billingsley and Hume (1941) and Dolmage and Brown (1945). It was originally considered to be a separate, elongate body but it is now believed to be a lobe of the Toronto stock, and to comprise a large sill or series of sills. It is largely plagioclase and hornblende porphyritic and in thin section it closely resembles the upper part of the Toronto stock, ranging from diorite to gabbro in composition.

The Larcan stock intrudes the Hedley and Whistle formations approximately 9 kilometres south of Hedley. It is about 400 metres long and 150 metres wide and consists largely of grey, fine to medium-grained, equigranular quartz-hornblende-biotite diorite (Duba *et al.*, 1988). Together with a related swarm of sills, it is associated with an extensive but discontinuous skarn envelope.

HEDLEY SILLS AND DIKES

Hedley sills, and to a much lesser extent dikes, are widely distributed throughout the district both as isolated bodies and as swarm complexes that locally make up to 30% of the stratigraphic section. Individual sills intrude all formations of the Nicola Group, but sill-dike swarms are preferentially developed in the thinly bedded units such as the Hedley and Chuchuwayha formations, particularly in areas adjacent to the Bradshaw fault. The largest and economically most important sill-dike swarm is developed in the Hedley Formation immediately east and north of the Toronto stock. South of the Similkameen valley, however, apart from the sills associated with the Larcan stock, swarms are less common. Many of the sills in the swarms adjacent to the Toronto stock and the Bradshaw fault are altered to skarn, but unaltered sills are also abundant in the district. Passage along strike from dark-coloured, unaltered diorite to bleached endoskarn is seen in many individual sills.

Sills are more common than dikes, and at the Nickel Plate mine the two are mineralogically indistinguishable. Dolmage and Brown (1945) recognized three different groups of sills within the Hedley Formation. Sills cut F_1 structures and yet locally they are deformed by F_1 folds; this indicates they were intruded during a continuing episode of F_1 folding. Emplacement of the dikes was also controlled by this deformation event. Where sills intrude folded sediments at Nickel Plate mine they frequently follow the bedding on the more gentle fold limbs and crosscut the sediments on the steeper limbs. Sills and dikes are medium to coarse-grained, porphyritic rocks that contain phenocrysts of zoned plagioclase and subhedral laths of black hornblende averaging 3 millimetres in length but locally 2 centimetres long. A few sills contain rare phenocrysts of fractured, rounded quartz (Plate 13), some of which are intensely corroded (Plate 14) and surrounded by resorption halos. These quartz-bearing porphyry sills, which have only been seen at Nickel Plate, are invariably skarn altered and often contain less amphibole.

Like the Toronto stock, most Hedley sills and dikes are characterized by fine optical zoning in the plagioclase crystals, and many of the unaltered sills and dikes are characterized by minor disseminations of pyrrhotite. Analyses of these rocks (Appendix 9) indicate they are similar in composition to the stocks.

Individual sills may be highly irregular and they do not always follow a single bedding plane; periodically along strike, they step upward, cutting across bedding at a high angle. This change in stratigraphic position is often accompanied by a local increase in sill thickness (Dolmage and Brown, 1945). Sills pinch, swell and bifurcate along strike, and contacts with the sedimentary rocks vary from straight to irregular to lobate. Some sills contain rare, elongate xenoliths of country rock, but no evidence of pronounced chilling is seen at the contacts. Where chilled margins are present they seldom exceed 30 centimetres in thickness. In some sills the coarse hornblende phenocrysts immediately adjacent to the margins are orientated subparallel to the contacts.

TABLE 2
CHEMICAL COMPOSITIONS OF THE HEDLEY INTRUSIONS COMPARED TO IGNEOUS ROCKS ASSOCIATED WITH BASE AND FERROUS METAL SKARNS

	Au (Hedley)		Fe		Cu		Zn-Pb		W		Mo		Sn	
	mean	range	mean	range	mean	range	mean	range	mean	range	mean	range	mean	range
SiO2	54.8	(49.1-59.5)	61.5	(47.2-74.7)	63.5	(55.2-73.7)	66.2	(57.1-76.3)	68.9	(62.6-72.8)	74.8	(73.1-76.0)	76.6	(75.4-78.0)
TiO2	0.66	(0.5-1.0)	0.8	(0.2-3.1)	0.5	(0.0-1.0)	0.6	(0.2-1.6)	0.4	(0.1-0.7)	0.2	(0.1-0.3)	0.03	(0.01-0.04)
Al2O3	18.6	(16.7-20.2)	17.3	(13.1-22.3)	16.6	(14.3-20.4)	15.4	(12.1-16.3)	15.5	(14.0-16.8)	14.3	(13.0-15.1)	12.6	(10.5-13.8)
Fe2O3	1.28	(0.3-2.2)	2	(0.5-5.6)	1.9	(0.03-3.2)	2.1	(1.0-3.0)	1.3	(0.2-2.3)	-	-	0.4	(0.0-0.9)
FeO	5.81	(4.1-7.9)	3.8	(0.4-11.2)	2.8	(0.7-5.8)	2.4	(0.2-5.0)	2	(0.8-3.2)	0.5	(0.0-1.5)	1	(0.2-1.4)
Fe2O3T	7.74	(5.8-10.1)	6.2	-		5	-	4.7	-	3.5	-	-	-	1.5
MnO	0.14	(0.07-0.17)	0.1	(0.0-0.3)	0.2	(0.0-1.8)	0.1	(0.0-0.3)	0.1	(0.0-1.0)	0.03	(0.0-0.05)	0.1	(0.0-0.2)
MgO	3.82	(2.5-5.0)	2.3	(0.2-4.9)	2.2	(0.7-4.2)	1.8	(0.1-4.2)	1.1	(0.1-2.6)	0.5	(0.3-0.9)	0.2	(0.1-0.4)
CaO	8.4	(6.5-11.5)	5.7	(0.7-11.4)	4.3	(1.8-7.6)	4	(0.4-6.3)	3.2	(1.9-4.6)	1.2	(0.5-2.0)	0.5	0.4-0.7)
Na2O	3.21	(2.5-4.8)	4.4	(2.9-7.7)	3.3	(1.0-5.3)	3.5	(1.6-4.3)	3.4	(2.7-4.0)	3.1	(1.9-4.2)	2.8	(0.8-3.6)
K2O	1.43	(0.6-2.5)	1.7	(0.3-3.4)	3.4	(1.3-5.4)	3.6	(2.0-5.2)	3.5	(2.4-5.4)	5	(2.8-7.9)	4.6	(4.2-5.0)
P2O5	0.18	(0.14-0.26)	0.27	(0.0-0.4)	0.25	(0.0-0.4)	0.26	(0.0-0.6)	0.15	(0.1-0.3)	0.08	(0.0-0.1)	0.01	(0.0-0.03)
Fe2O3/Fe	0.23	(0.04-0.37)	0.53	(0.12-2.36)	0.68	(0.01-1.04)	0.87	(0.49-6.18)	0.65	(0.09-1.23)	-	-	0.4	(0.01-1.35)
K2O/Na2O	0.44	(0.2-0.66)	0.39	(0.05-0.85)	1.03	(0.38-1.71)	1.03	(0.53-3.06)	1.03	(0.61-1.87)	1.61	(0.67-4.16)	1.64	(1.17-6.25)
# of samples	27		18		17		9		17		3		9	

Major oxide values in percent: Fe2O3T = total iron as Fe2O3
(Data for base and ferrous metal skarns compiled by Meinert, 1983)

The amount of thermal metamorphism developed in the country rocks adjacent to individual sills is highly variable and in some cases no thermal aureoles are recognized. Where the sills cut limestone, a 0.5 to 5-metre zone of marble may be developed and occasionally the adjacent limestone contains small, randomly orientated needles of black amphibole. Where they intrude siltstones, the contact aureole is commonly narrow and silicious, varying from a few centimetres to 5 metres wide. No biotite-rich hornfels has been identified in any of the thermal aureoles adjacent to the unaltered sills and dikes.

COMPARISON OF THE HEDLEY INTRUSION GEOCHEMISTRY WITH OTHER SKARN-RELATED IGNEOUS ROCKS.

The mean and range of geochemical values of 27 samples of Hedley intrusions analysed during this study are listed in Table 2. Also listed for comparison are the mean values of the igneous rocks associated with Fe, Cu, Zn-Pb, W, Mo and Sn skarns as compiled by Meinert (1983), and these data are plotted in Figures 11D to M. Alkali *versus* silica and AFM plots illustrate that all the skarn deposit subclasses, including the Hedley gold skarn, are related to subalkalic, calcalkaline intrusions. However, compared to the other skarn subclasses, the Hedley intrusions contain the least silica and the most calcium, ferrous iron, total iron, alumina and magnesium. This probably reflects their derivation from primitive oceanic crust and their relatively undifferentiated character.

Igneous rocks related to Sn, Mo, and Zn-Pb skarns have the highest mean total alkali content (>7 wt% Na_2O + K_2O), those related Fe, Cu and W skarns have intermediate mean values (6 to 7 wt%) whereas the Hedley intrusions have the lowest mean total alkali content (4.6 wt%). Together with the intrusions associated with iron skarns, they have the lowest K_2O/Na_2O ratios.

Systematic variations also exist in the TiO_2/Fe_2O_3 and Fe_2O_3/FeO ratios, as well as the FeO content of the various intrusions (Figure 11); the low ferric/ferrous ratios of the Hedley intrusions suggest they have the lowest oxidation state of all the skarn-related igneous rocks (Figure 11M).

BROMLEY BATHOLITH (Unit 10)

A southern lobe of the large Bromley batholith intrudes the Nicola Group rocks in the northern part of the map area (Figures 2 and 4). Field evidence suggests it is younger than the Hedley intrusions and U-Pb radiometric dating of zircons from the batholith gave an age of 193±1 Ma (Parrish and Monger, 1992), indicating it is an Early Jurassic intrusion. It mostly comprises equigranular, pale grey to pink, medium to coarse-grained, massive granodiorite (Unit 10a) that locally contains rounded mafic xenoliths of altered country rock. Its main constituents are oligoclase-andesine plagioclase with lesser amounts of orthoclase, quartz, green hornblende and biotite. The amphibole and biotite generally make up between 4 and 15% by volume and are locally chloritized. Accessory to trace minerals include sericite, apatite, epidote, carbonate, ilmenite, magnetite and pyrite. The margins of the batholith are locally more mafic and of diorite to quartz diorite composition (Unit 10b). These hybrid rocks contain between 20 and 45% hornblende and biotite, and in places they are porphyritic and indistinguishable from the Hedley intrusions. The country rocks adjacent to the batholith are overprinted by a hornfelsic aureole, 500 to 1000 metres wide, that is locally marked by silicification and red-brown biotite. Skarn alteration is generally not observed adjacent to the batholith. However, the Mount Riordan stock (Unit 11), which may represent a marginal or satellitic body to the Bromley batholith, is related to the Crystal Peak garnet skarn deposit and some tungsten-copper mineralization.

MOUNT RIORDAN STOCK (Unit 11)

The Mount Riordan stock is exposed approximately 7 kilometres east-northeast of the Nickel Plate mine and immediately east of Mount Riordan (Figures 4 and 38). Outcrop is sparse and the nature and precise location of its margins are uncertain. To the south it is presumed to be in fault contact with rocks of the Apex Mountain Complex, while to the north and east it passes either gradationally into, or is faulted against the Bromley batholith. To the west, the stock is flanked by the large, garnet-rich Crystal Peak skarn deposit that underlies Mount Riordan. The exposed contact between massive garnet and bleached Mount Riordan stock is steeply dipping and gradational over a few metres.

Although all rocks in the stock are massive and coarse grained, there are textural and compositional variations throughout the body. The western part of the stock, adjacent to the garnet skarn, consists mostly of equigranular, mafic quartz gabbro (Unit 11a) that is moderately skarn altered with epidote and rare garnet. Analysis of a single, slightly altered sample (Sample No. HD 409; Figure 11C) indicates it has a gabbroic composition. By contrast, most of the stock is generally unaltered, quartz-rich and porphyritic (Unit 11b) with euhedral hornblende phenocrysts up to 1 centimetre long. Analyses of two unaltered samples (Sample Nos. HD 381 and 406) indicate they are granodiorite (Figure 11C) and subalkalic, calc-alkaline (Figure 13). The porphyritic granodiorite commonly contains disseminations and veinlets of pyrite, and rounded, mafic xenoliths up to 3 centimetres in diameter are present in some outcrops.

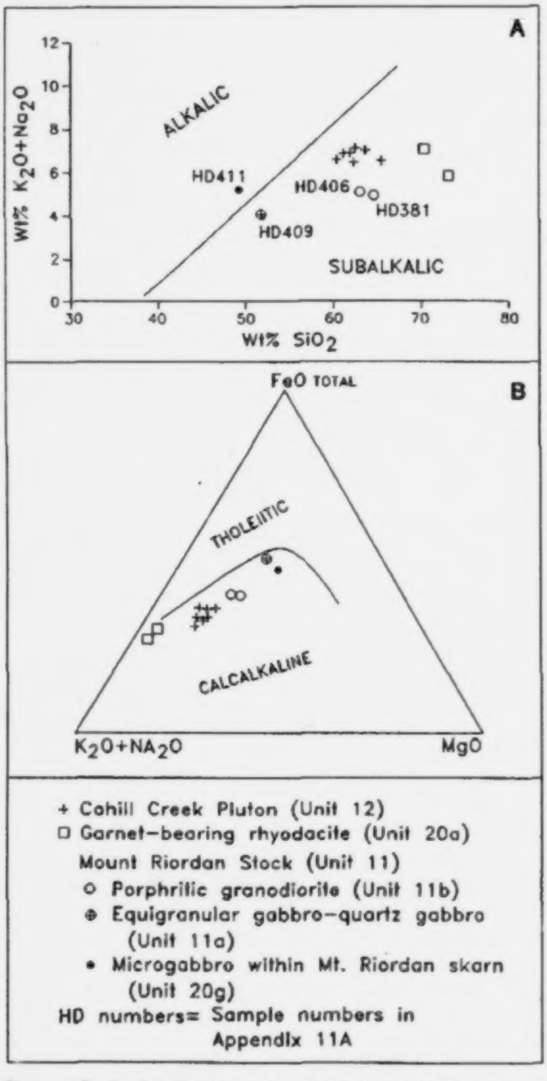

Figure 13. A. Alkali-silica plot of the Cahill Creek pluton, Mount Riordan stock and the garnet-bearing rhyodacite (Unit 20a). B. AFM plot of the Cahill Creek pluton, Mount Riordan stock and the garnet-bearing minor rhyodacite (Unit 20a).

In thin section the brown to green pleochroic hornblende phenocrysts are seen to contain abundant inclusions of plagioclase, quartz and pyrite. Mafic minerals make up between 6 and 15% by volume. Biotite forms fresh, stubby lathes up to 4 millimetres in diameter. The coarse plagioclase (An_{15-42}) is generally fresh and unzoned, but the orthoclase is altered and has marked optical zoning. The late, coarse quartz is weakly strained and comprises between 15 and 30% by volume. Accessory to trace amounts of sphene, zircon, epidote, carbonate, tremolite-actinolite, chlorite, apatite and ilmenite are also present.

On the summit of Mount Riordan, within the garnet skarn, are several small remnants of microdiorite (Unit 20g) that may represent strongly altered apophyses of the Mount Riordan stock. They contain 20 to 30% by volume amphibole, and are epidotized. Analysis of one less-altered sample (Sample No. HD 411; Appendix 11) suggests it is gabbroic in composition and alkalic (Figures 11 and 13).

The Mount Riordan stock is believed to be related to the Bromley batholith, either as a marginal phase or a satellitic body. A U-Pb date of 194.6±1.2 Ma on zircons from the stock (Appendix 1) is similar to the 193±1 Ma date obtained by Parrish and Monger (1992) from the batholith.

CAHILL CREEK PLUTON (Unit 12)

The Cahill Creek pluton outcrops as an irregularly shaped body that covers an area of at least 38 square kilometres (Figure 14). To the north and west it intrudes the Nicola Group and has several major sill and dike-like apophyses. One northwesterly striking apophysis, 2.5 kilometres long, is seen southwest of Nickel Plate mine, while a sill-like body farther south, strikes southwesterly, exceeds 8 kilometres in length and is partly controlled by the Cahill Creek fault zone. To the east the pluton intrudes and hornfelses rocks of the Apex Mountain Complex, while to the south it continues outside the mapsheet boundary and its full southern extent is unknown. Uranium-lead dating on zircons from the pluton (Appendix 1) give a mid-Jurassic age of 168.8±9 Ma.

The pluton consists largely of a pale grey to brownish pink, massive, coarse to medium-grained equigranular rock of mainly quartz monzodiorite and granodiorite composition; small amounts of mafic diorite are also present, particularly at the pluton margins. Outcrops are commonly well jointed and exhibit spheroidal weathering; locally the pluton contains rounded mafic xenoliths up to 30 centimetres wide (Plate 18). Whole rock and trace element analyses on seven samples are presented in Appendix 12; major oxide plots indicate that the Cahill Creek pluton is a sub-alkalic, calcalkaline intrusion (Figure 13) of largely quartz monzodiorite composition.

In thin section the main phase of these rocks contains between 50 and 70% feldspar, 20 to 30% quartz and 5 to 15% mafic minerals. The plagioclase is mostly andesine (An_{31-38}) although individual crystals range as low as An_{10} and as high as An_{50}; crystals are up to 4 millimetres long and they exhibit albite, carlsbad and pericline twinning. Compositional and optical zoning is seen in some of the plagioclase although it is not as marked or as common as in the Hedley intrusions. There are two generations of plagioclase; the earlier is represented by large, altered crystals with normal and oscillatory zoning while the later plagioclase is clear, fresh and well-twinned with no optical zoning. Some individual plagioclase crystals contain large, rounded, optically zoned calcic cores that are sericitized, surrounded by fresh, finely twinned sodic rims. Orthoclase

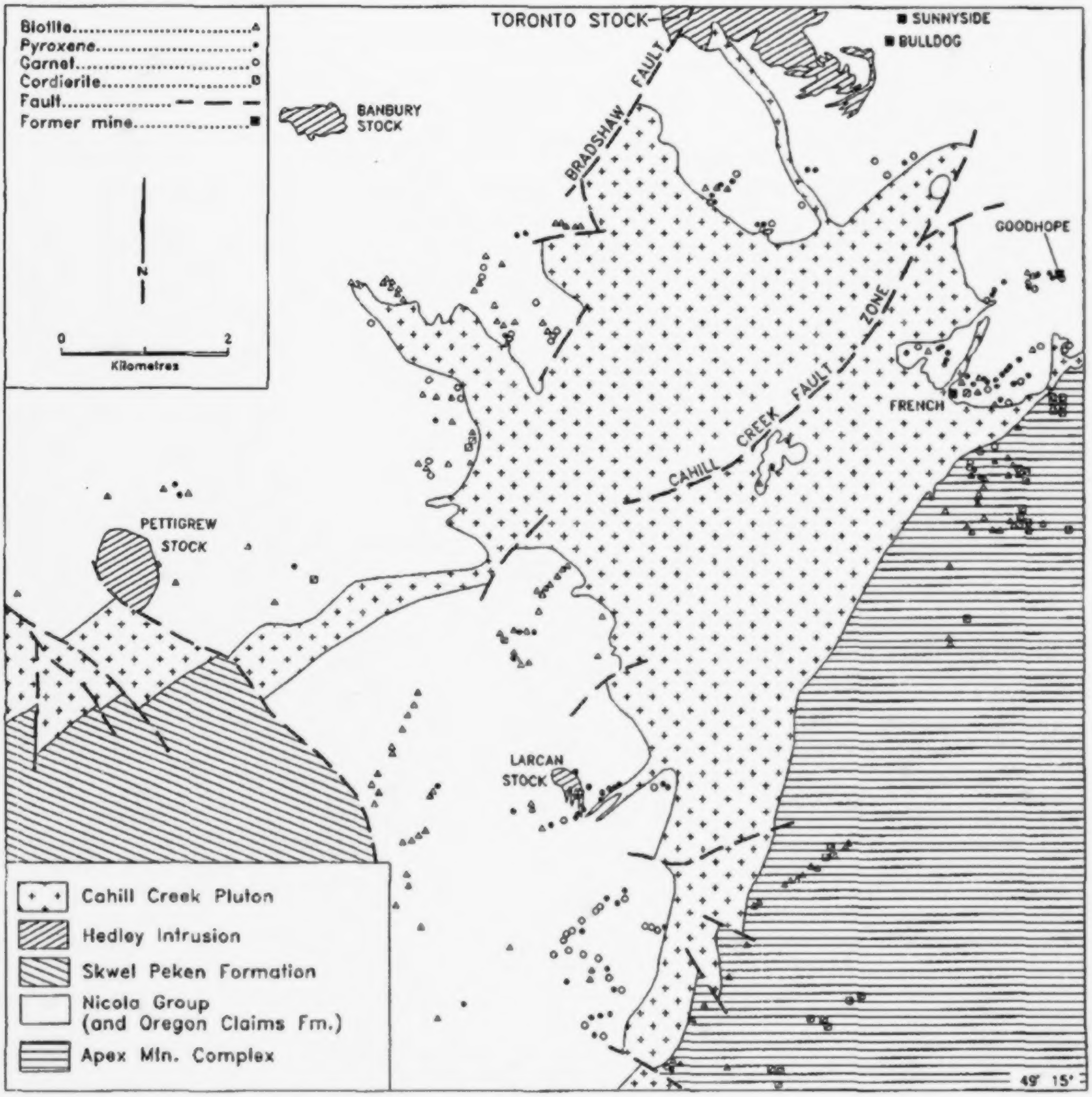
Biotite .... ▵
Pyroxene .... •
Garnet .... ○
Cordierite .... ▫
Fault .... — — —
Former mine .... ■
N
0
2
Kilometres
TORONTO STOCK
■ SUNNYSIDE
■ BULLDOG
BANBURY STOCK
BRADSHAW FAULT
GOODHOPE
CAHILL CREEK FAULT ZONE
FRENCH
PETTIGREW STOCK
LARCAN STOCK
Cahill Creek Pluton
Hedley Intrusion
Skwel Peken Formation
Nicola Group (and Oregon Claims Fm.)
Apex Mtn. Complex
49° 15'

Figure 14. Distribution of the Cahill Creek pluton and location of minerals in its thermal metamorphic aureole. *Note:* some of the garnet-pyroxene assemblages close to the Pettigrew and Larcan stocks may not be related to the Cahill Creek pluton.

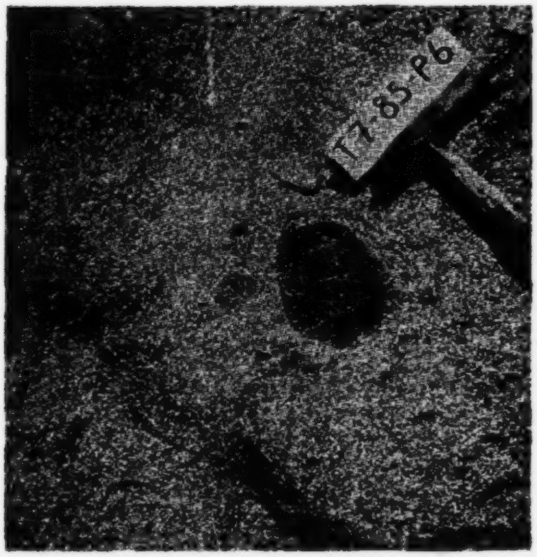

Plate 18. Cahill Creek pluton (Unit 12a). Quartz monzodiorite with rounded, partially assimilated xenoliths.

makes up between 15 and 25% by volume of the contained feldspar. Green to brown pleochroic hornblende contains inclusions of feldspar and sphene, and is partially altered to tremolite-actinolite and chlorite. The biotite forms laths up to 3 millimetres long. Accessory and trace minerals include apatite, carbonate, epidote, zircon, magnetite and pyrite.

The Cahill Creek pluton is surrounded by a thermal metamorphic aureole between 0.5 and 1.5 kilometres wide (Figure 14). In the Nicola Group this aureole is generally marked by silicification and development of red-brown biotite, as well as traces of garnet, pyroxene, magnetite, pyrrhotite and pyrite. In the Apex Mountain Complex, the aureole is wider and is characterized by biotite and cordierite. The rarity of cordierite in the thermally altered Nicola argillites and siltstones, and its abundance in similar lithologies in the Apex Mountain Complex, suggest the latter are more aluminous, or that the thermal metamorphism took place at a deeper level. In the French mine area, some of the hornfelsed Oregon Claims Formation argillites close to the Cahill Creek pluton contain small porphyroblasts of cordierite and pale pink almandine garnet. Likewise, cordierite and garnet occur in the package of rocks of unknown age (Unit 8f) adjacent to the western margin of the pluton south of the Similkameen valley. The presence of cordierite in this package and the Oregon Claims Formation at French mine is one supporting indication that both these rock units represent a westerly extension of the Apex Mountain Complex.

The margins of the pluton are highly irregular on outcrop scale; hornfelsed country rock adjacent to the intrusion is cut by numerous narrow, irregular and bifurcating dikes, sills and veinlets of granodiorite. There is no noticeable evidence of chilling along the contacts but the plutonic rocks are more silicious. Locally, the pluton is bordered by a late phase of silicious aplite (Unit 20b) that forms sills, dikes and irregular masses. Where the pluton cuts calcareous sediments, minor amounts of garnet-pyroxene skarn with sporadic pyrite and trace chalcopyrite are developed but are not auriferous. Skarn of this type is exposed on the steep, easterly facing slopes of Hedley Creek, 0.5 kilometre north of Hedley township, and in marble on the north side of Winters Creek, where there is also some weak malachite staining.

The Cahill Creek pluton was probably intruded at relatively shallow depth, and it is believed to be genetically related to the Skwel Peken Formation, the subvolcanic quartz porphyry intrusions (Unit 14) and the aplites (Unit 20b). The overall morphology of the pluton is uncertain. However, it probably represents a relatively thin, flat lying to gently west dipping sheet that was in part intruded along the contact between the Nicola Group and the Apex Mountain Complex. The eastern and lower margin is flat and more regular whereas most of the western and upper margin is irregular and its emplacement was partly controlled by fractures in the overlying Nicola Group. Cordierite is widespread in the hornfels adjacent to the eastern and deeper margin, whereas there is little sign of this mineral in Nicola rocks along the western and upper edge of the intrusive sheet.

LOOKOUT RIDGE PLUTON (Unit 13)

The extreme northern part of the map area, near Hedley Creek, is underlain by a poorly exposed intrusion that is characterized by its pink colour, equigranular to feldspar-porphyritic texture and quartz monzonitic to granodioritic composition. This intrusion, the Lookout Ridge pluton, was only briefly examined during this survey; it forms an elongate body that we believe to be an isolated satellite stock related to the larger Osprey Lake batholith farther north (Figure 2) Uranium-lead dating on zircons from the batholith gave a mid-Jurassic age of 166±1 Ma (Parrish and Monger, 1992). It is believed to be related to the same magmatic episode responsible for the Cahill Creek pluton, and was likewise associated with late, quartz-porphyritic felsic intrusions (Unit 20d) and the volcaniclastic rocks of the Skwel Peken Formation (Unit 15a). In the Hedley area the rocks of the Lookout Ridge pluton probably extend eastwards to the north shore of Nickel Plate Lake (Figure 38), although their precise contact with rocks of the Bromley batholith farther east and north is uncertain. In the Hedley Creek area, the pluton is bordered by a thin unit of coarse-grained mafic diorite and quartz diorite (Unit 12b) that probably represents a hybrid marginal phase.

The porphyritic quartz monzonite contains large phenocrysts of pink potassium feldspar up to 2 centimetres long. In thin section these rocks are seen to contain between 3 and 6% mafic minerals which include coarse, chloritized biotite and hornblende crystals up to 5 millimetres long. Abundant coarse perthite and microcline are intergrown with quartz. Trace to accessory minerals include carbonate, sericite, chlorite, ilmenite, leucoxene, pyrite and epidote.

The mafic marginal phase (Unit 12b) contains 40 to 60% altered hornblende with lesser amounts of biotite, plagioclase, epidote and chlorite, and trace amounts of quartz and potassium feldspar.

QUARTZ PORPHYRY (Unit 14)

Isolated dikes and sills of a distinctive suite of quartz porphyries are widespread throughout the district. Individual bodies, which are generally less than 5 metres thick, are seen cutting the Hedley, Whistle and Skwel Peken formations, as well as the Cahill Creek pluton. The largest sill is adjacent to the southwestern end of the Cahill Creek fault zone, southeast of Pettigrew Creek. This southwest-trending intrusion, which separates a major sill-like apophysis of the Cahill Creek pluton to the north from the Skwel Peken Formation to the south, reaches 250 metres in width and exceeds 4 kilometres in strike length. Uranium-lead analyses of zircons extracted from this body indicate a late-Jurassic age of 154.5 +8 −43 Ma (Appendix 1). Field and textural data, however, suggest these rocks may be related to the mid-Jurassic Skwel Peken Formation, and thus they may be older than the radiometric dating indicates. The quartz phenocrysts in the porphyries closely resemble quartz crystals in the nearby Skwel Peken tuffs (Unit 15a), and the sill is believed to have been a feeder to these volcaniclastic rocks. The porphyries are massive, pale pink to pale buff rocks that contain phenocrysts of glassy quartz, together with some coarse feldspar and rare biotite set in a fine-grained silicious matrix.

In thin section the groundmass is seen to consist of a fine intergrowth of quartz, plagioclase (An_{10-29}) and potassium feldspar crystals between 0.1 and 0.3 millimetre in length, that occasionally display granophyric textures. The rounded to subhedral quartz phenocrysts are generally clear and reach 5 millimetres in diameter. They are characterized by partial resorption which has resulted in long, delicate embayment features and thin, fine-grained reaction rims at the crystal margins (Plate 19). These rims contain rows of intergrown, elongate and radiating quartz and feldspar crystals. Phenocrysts of feldspar are less common; they include subhedral, tabular crystals of twinned oligoclase (An_{13-25}) up to 5 millimetres long, that are cracked and weakly altered. Coarse, subhedral to anhedral phenocrysts of microcline and perthite are also present; some rounded potassium feldspar crystals are overgrown by plagioclase rims. The rare biotite forms partially chloritized flakes up to 3 millimetres long. Trace minerals include zircon, ilmenite and magnetite.

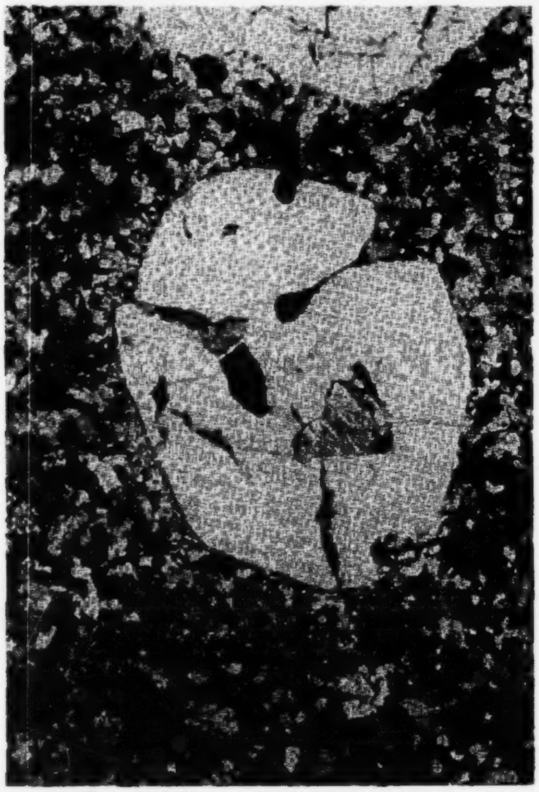

Plate 19. Quartz Porphyry (Unit 14). Photomicrograph (X polars) showing quartz phenocrysts with reaction rims and resorption embayments (field of view is 3 mm wide).

Plate 20. Garnet-bearing rhyodacite (Unit 20a). Photomicrograph (PPL) showing garnet phenocryst in a quartz-feldspar matrix. Microprobe analyses of this and other crystals are illustrated in Figures 15 and 16 (field of view is 2 mm wide).

VERDE CREEK STOCK (Unit 16)

Part of the Verde Creek stock (Dolmage 1934) extends into the western portion of the map area between Smith and Whistle creeks, where it covers an area of 3 square kilometres. It consists largely of fine to medium-grained, massive rocks that are commonly siliceous, leucocratic and of granite to quartz monzonite composition. The stock generally contains abundant pink potassium feldspar with less than 5% biotite; Preto (1972) records some hornblende-bearing phases to the west. Two K-Ar age dates on biotite from the stock farther west indicate an Early Cretaceous age of 98±4 and 101±4 Ma (Preto 1972). The stock is believed to be a high-level intrusion that was coeval with the Spences Bridge Group.

MINOR INTRUSIONS (Unit 20)

Various minor intrusions, ranging in composition from rhyodacite to andesite are exposed throughout the area, generally as isolated, narrow sills and dikes. One unique, garnet-bearing suite (Unit 20a) occurs as rare, thin (< 20 m) leucocratic units within the Skwel Peken Formation. However, it is uncertain whether it represents volcanic flows or intrusive sills and dikes, although we prefer the latter interpretation. In outcrop these are grey, massive and siliceous fine-grained rocks; only one contact, immediately south of Skwel-Kwel-Peken Ridge, was observed between them and tuffs of the Skwel Peken Formation. The contact is irregular and the adjacent intrusive rocks are very fine-grained and possibly chilled; they are also marked by a vague flow banding that trends northerly and dips moderately westwards. They contain very few ferromagnesian preferred minerals but locally they are weakly silicified and pyritic. Whole rock and trace element analyses of two samples from these garnet-bearing rocks are given in Appendix 13. Plots indicate that these rocks are calcalkaline and subalkalic (Figure 13), and of rhyodacite to dacite composition (Figure 10).

In thin section the rocks of Unit 20a are seen to be strongly altered. They are characterized by a fine-grained groundmass of abundant small quartz crystals intergrown with minute laths of aligned albitic plagioclase crystals and some altered orthoclase. Euhedral phenocrysts of orthoclase up to 3 millimetres long are present together with rare crystals of hornblende and remnant, corroded biotite. These phenocrysts are strongly altered and in some instances completely pseudomorphed by aggregates of sericite, biotite, quartz and chlorite. The dark red colour of the rare, isolated garnet crystals in Unit 20a distinguishes them from skarn-related garnets elsewhere in the district. They reach 3 millimetres in diameter but are usually smaller. In thin section they form anhedral crystals with irregular, corroded margins and thin reaction rims (Plate 20). They are commonly fractured, display no optical zoning and, in contrast to most of the skarn-related garnets, are completely isotropic. They often contain opaque inclusions, and occasionally occur as trails of small angular fragments that appear to have formed, during intrusion, by the mechanical breakup of larger phenocrysts.

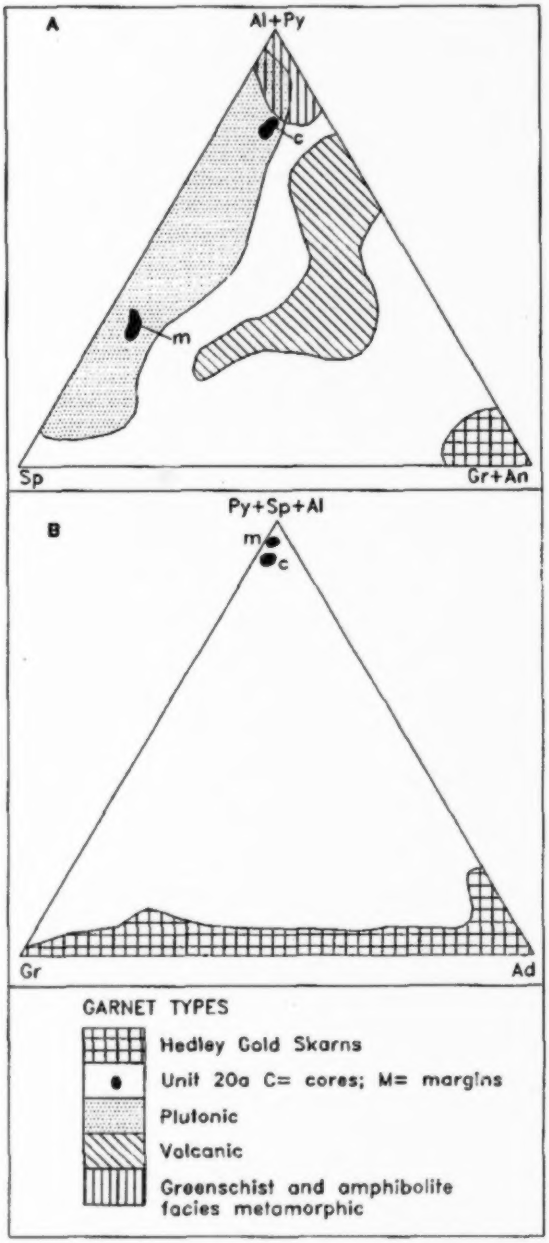

Figure 15. Composition of garnets from the Hedley gold skarns and garnet-bearing rhyodacite (Unit 20a) compared to garnets developed in plutonic, volcanic and regional metamorphic environments. A. End members; (Al + Py) = almandine + pyrope, (Sp) = spessartine, (Gr + An) = grossularite + andradite. Note different compositions for cores and margins of garnets in Unit 20a. B. End members; (Py + Sp + Al) = pyrope + spessartine + almandine, (Gr) = grossularite, (Ad) = andradite. Data for plutonic, volcanic and metamorphic garnets in Figure 15A from Oliver (1956), Troger (1959), Green and Ringwood (1968), Brown (1969), Fitton (1972), Bryant (1975), Fodor *et al.*, (1978), Vennum and Meyer (1979) and Andrew (1988).

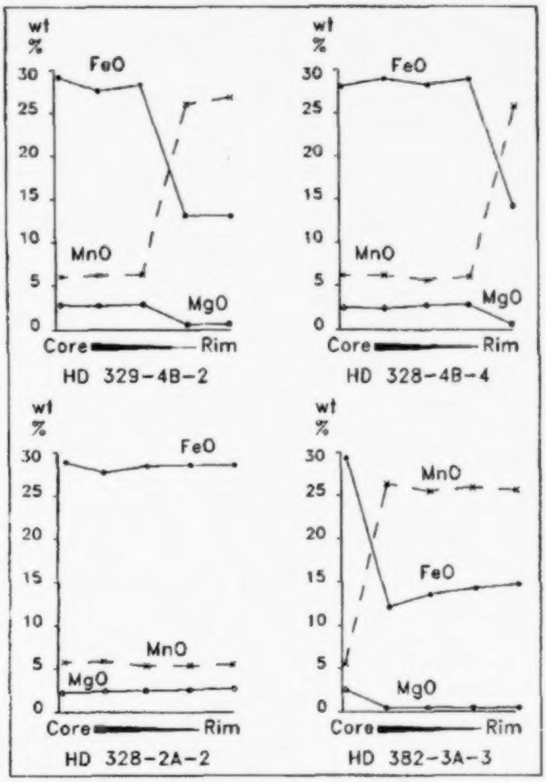

Figure 16. Compositional variation (in wt % MnO, MgO and total iron as FeO) across individual garnet crystals from garnet-bearing rhyodacite (Unit 20a). Microprobe analyses by G.E. Ray at The University of British Columbia.

Core-to-margin microprobe analyses of several garnet phenocrysts (Appendix 13C) indicate they are compositionally distinct from the skarn-related garnets (Figures 15 and 16). A few crystals show no compositional zoning and are almandine-rich throughout, but most are strongly zoned with iron and magnesium-rich (almandine) cores, and manganese-rich (spessartine) margins.

The resorbed margins of the garnet crystals suggest that they were not in equilibrium with the melt. There is insufficient data to determine their origin, although they are believed to have developed as magmatic phenocrysts at depth and were carried in the melt to a higher crustal level. This is supported by the mechanical fracturing and breakup of some crystals as well as a compositional plot of the microprobe analyses (Figure 15) which suggest the garnets have a plutonic origin.

Aplite (Unit 20b), which was originally described by Camsell (1910), is commonly found as a late phase of the Cahill Creek pluton. Locally, these rocks closely resemble the quartz porphyry (Unit 14), although they have been mapped as a separate unit. Aplite forms dikes and sills generally less than 10 metres wide, although rare, irregular masses up to 50 metres in outcrop width are seen. Most bodies were intruded along the presumed upper margin of the Cahill Creek pluton, but some cut the pluton or extend for short distances up into the Nicola Group. The aplites are leucocratic, light pink to pale reddish brown, silicious, massive rocks that are mostly equigranular although some weakly porphyritic varieties also occur. The phenocrysts include orthoclase, plagioclase and partially resorbed quartz with embayed margins. The fine-grained groundmass is an intergrowth of quartz, feldspar and minor sericite; Camsell (1910) reports the presence of fluxion structures in some of the aplites. Major element analyses on two samples of Unit 20b are presented in Appendix 14.

Several minor basaltic to andesitic intrusions (Unit 20c) have been mapped. One variety, which may correlate with the "andesites" of Camsell (1910), outcrops near the Nickel Plate deposit, and farther south and west, where it forms narrow, southerly trending dikes up to 3 metres wide. These dikes, which cut both the skarn alteration and the Cahill Creek pluton, are characterized by chilled margins and rounded to elongate carbonate-filled amygdules up to 2.5 millimetres long. In thin section this rock is seen to consist of abundant subparallel, flow-oriented laths of twinned plagioclase (An$_{29-48}$) up to 0.5 millimetre long. The minor brown and green hornblende is extensively chloritized, and the groundmass feldspars are intergrown with abundant fine-grained opaques. Trace to accessory amounts of sphene, rutile, epidote, ilmenite, apatite and clinozoisite also occur.

Another variety of late mafic dike cuts the Chuchuwayha Formation west of Hedley and forms north to northwest-trending bodies generally less than 2 metres wide. In thin section these rocks are observed to contain phenocrysts of euhedral augite up to 1.5 millimetres across, most of which are partially to completely pseudomorphed by chlorite. The groundmass mainly contains small, altered laths of plagioclase (An$_{10-35}$), intergrown with some augite, amphibole, epidote, carbonate and opaques. Trace amounts of apatite, clinozoisite, ilmenite and sericite are present. Extensive north to east-northeast-trending andesitic to dacitic dikes also cut the Banbury stock and its hornfelsic aureole (Figure 12).

Several leucocratic minor intrusions of granitic to quartz monzonitic composition (Unit 20d) occur throughout the area. One distinctive mass outcrops about 3 kilometres west-northwest of Skwel-Kwel-Peken Ridge where it forms an irregular body, 200 metres wide, that separates rocks of the Cahill Creek pluton from quartz porphyry (Unit 14). It comprises pink, coarse to medium-grained massive and leucocratic rocks that contain euhedral to subhedral phenocrysts of plagioclase and pink potassium feldspar up to 5 millimetres in length. Some biotite and phenocrysts of hornblende are also present, and locally the intrusion contains rounded xenoliths of hornfelsed metasedimentary rocks up to 15 centimetres in diameter. The intrusion is distinct because in places it closely resembles the Cahill Creek pluton while elsewhere it is intimately intermixed with irregular patches of quartz porphyry that are identical to Unit 14. Contacts between this quartz porphyry material and the phenocrystic quartz monzonite vary from diffuse to sharp; in places thin, deformed dikes of quartz porphyry cut the quartz monzonite. Thus, this quartz monzonite body is believed to indicate a close spatial and genetic relationship between the quartz porphyry suite (Unit 14) and the Cahill Creek pluton, and may represent an intermediate phase between the early, deeper level pluton, and the later, higher level porphyry.

Another distinctive minor granitic intrusion containing rounded quartz phenocrysts is exposed about 5 kilometres north-northwest of Nickel Plate Lake where it forms an irregular mass up to 400 metres wide. To the north, it intrudes a roof pendant of hornfelsed ash tuffs, while to the west, south and east it is in contact with the Bromley batholith and Lookout Ridge pluton. This granitic body is believed to represent a marginal phase of the Lookout Ridge pluton, and locally it is similar in mineralogy and texture to the quartz porphyry (Unit 14) and aplite (Unit 20b) associated with the Cahill Creek pluton.

STRUCTURAL EVOLUTION OF THE HEDLEY DISTRICT

INTRODUCTION

Two phases of folding are recognized in both the Apex Mountain Complex and the Nicola Group (designated f_1, f_2 and F_1, F_2 respectively), although the temporal relationship of the phases between one rock package and the other is unknown. However, the first and most intense deformation (f_1) identified in the complex predated the intrusion of the 168 Ma Cahill Creek pluton, as did the second (F_2) folding episode in the Nicola rocks. In addition, another and younger (post mid-Jurrassic) phase (F_3) has been recognized in the Skwel Peken Formation.

APEX MOUNTAIN COMPLEX

The two deformation phases identified in the Apex Mountain Complex produced some minor fold structures but no major folds have been recognized. The first (f_1) and most intense phase resulted in tight to isoclinal minor folds together with moderate to strong penetrative axial planar fabrics. A stereoplot of poles to bedding suggests that the f_1 deformation involved folding about subhorizontal axes and subvertical axial planes that strike approximately 020° (Figure 17A).

The second period of deformation (f_2) is only locally developed. It resulted in open to gentle folding of the bedding and f_1 cleavage. These folds have subvertical axial planes that strike northerly and are not associated with any penetrative planar fabrics.

NICOLA GROUP AND SKWEL PEKEN FORMATION

Nicola Group sedimentation in the Hedley district was controlled by a westerly dipping paleoslope with a rugged topography influenced by northerly trending active normal faults. These faults, which were related to the rifted eastern margin of the Nicola basin, subsequently influenced the emplacement of the Hedley intrusions and the development of their associated skarns. Later, they were the locus of recurrent movements and are now seen as the Chuchuwayha, Bradshaw and Cahill Creek faults which separate the four east-to-west sedimentary facies recognized in the Nicola rocks.

The late Carnian to late Norian conodont microfossils obtained from the Stemwinder Formation indicate it was deposited between approximately 208 and 230 Ma ago while those from the Chuchuwayha and Hedley formations indicate a narrower age range between approximately 216 and 223 Ma (Figure 6). The precise age of the Whistle Formation is uncertain due to the absence of microfossils. However, it stratigraphically overlies the Stemwinder, Hedley and French Mine formations suggesting that the arc volcanism responsible for the Whistle Formation occurred later than 208 Ma.

Nicola sedimentation was accompanied, or shortly followed, by the emplacement of the Hedley intrusions. Field and geochronometric data suggest they were intruded between 219 and 194 Ma (Late Triassic to Early Jurassic). It is uncertain whether they were intruded into wet, unconsolidated sediments, as suggested by Dawson *et al.* (1990a), or into consolidated rocks at a relatively high structural level, as preferred by the senior author. Lack of boiling or flaring features adjacent to sills at the Nickel Plate mine, similar to those described in the present-day Guaymas basin of western Mexico (Einsele, 1985), suggests the hostrocks were either consolidated, or that intrusion took place too deep in the sedimentary pile for boiling to occur.

The intrusion of the Hedley suite took place during, and was partially controlled by, the earliest period of folding (F_1) recognized in the Nicola Group. Some larger bodies, such as the Toronto stock, as well as many dikes at the Nickel Plate mine, were emplaced along easterly to southeasterly trending linear structures related to the F_1 deformation. These controlling structures may have originated as transform faults that were generated normal to the basin margin. The Hedley intrusion sill-dike swarms were preferentially developed around certain larger bodies, such as the Toronto stock, and were best developed in the thinly bedded packages such as the Chuchuwayha and Hedley formations.

The first phase of folding (F_1) seen in the Nicola Group did not produce large-scale structures and was only sporadically developed in the district. F_1 folds are best seen within the Nickel Plate deposit where their control of the gold-skarn orebodies makes them economically important (Billingsley and Hume, 1941). They have also been mapped in the vicinity of the Banbury stock but have not been recognized elsewhere in the district.

At Nickel Plate, the F_1 deformation produced tight to open flexure folds, some of the latter being merely gentle warps with wave lengths of 50 to 100 metres and amplitudes of 15 metres or less. The folds have west to northwest-striking, generally steeply inclined axial planes, and axes that plunge 20° to 40° northwest; no cleavage was generated during the F_1 event. Dolmage and Brown (1945) noted that some tight folds quickly die out along their axes while others form monoclinal structures with steeply inclined northern limbs that are occasionally overturned.

The sporadic development of F_1 minor folds, and their spatial and temporal relationship with the Hedley intrusions, suggests that they may not be the result of a regional tectonic regime. Instead, they were probably related to local stresses resulting from the forcible intrusion of the Hedley suite into the Nicola Group.

During the Early Jurassic, intrusion of the Bromley batholith and the Mount Riordan stock took place at approximately 194 Ma. The subsequent F_2 phase of deformation was the predominant structural event to overprint the Nicola rocks. It produced major and minor north-northeasterly striking, easterly overturned asymmetric folds (Figure 39, Sections 3-4 and 5-6), some of which have faulted hinge zones. Stereoplots of poles to bedding for Nicola rocks from various parts of the district are shown in Figure 17. These, and measurements of minor folds in the field, indicate that the F_2 folds are characterized by subhorizontal to moderately plunging axes and steep west-dipping axial planes that strike north-northeasterly. The anticlines tend to have gently inclined western limbs and steeply inclined eastern limbs.

Two major F_2 folds are recognized in the Nicola rocks across the district, the Hedley anticline in the west, and the western limb of the Good Hope syncline to the east. The western limb of the Hedley anticline is occupied by steeply dipping, westerly facing rocks of the Stemwinder and Chuchuwayha formations (Figure 17C). East of the Bradshaw fault and closer to the anticlinal crest, the Hedley and Whistle formations dip gently west (Figure 17E). These rocks, and the Stemwinder Formation farther west, contain numerous asymmetric minor F_2 folds that verge eastwards. The axial plane of the Hedley anticline lies close to the Cahill Creek fault zone (Figure 39, Section 3-4). Rocks of the Oregon Claims Formation are exposed in the core of the Hedley anticline; the eastern limb, east of Cahill and Sunset creeks, is a steeply dipping, overturned and east-facing succession of Whistle Creek tuffs (Figure 39, Sections 3-4 and 5-6). Farther east, structural relationships are less certain due to poor exposure and the later intrusion of the Cahill Creek pluton. However, the subhorizontal to gently northwest dipping rocks near the French and Good Hope mines (Figure 17F) probably lie close to the major Good Hope synformal closure.

The F_2 minor folds are widespread but relatively uncommon in the Nicola Group; these structures have axes that plunge up to 20° in either a north-northeast or south-southwest direction. Axial planar fabrics are rare except in some Stemwinder argillites where a poorly developed fracture and slaty cleavage is developed; the cleaved rocks exhibit a weak bedding-cleavage lineation. A stereo plot of poles to F_2 cleavages in the Stemwinder Formation (Figure 17G) indicates they strike north-northeast to northeast and are steeply dipping.

The F_2 event was accompanied by the development of west-dipping, reverse faults. These faults tend to be concentrated along hinges of the minor and major F_2 folds, and some, such as the Chuchuwayha, Bradshaw and Cahill Creek faults represent older synsedimentary growth faults that were reactivated during the F_2 event. The F_2 compressive movement was locally accompanied by the development of minor duplex structures as exposed in the Chuchuwayha Formation immediately west of Hedley.

Emplacement of the high-level Cahill Creek and Lookout Ridge plutons occurred after, or at the end of, the F_2 deformation and may have been related to superterrane collision and the mid-Jurassic orogeny that resulted in the formation of the Omineca Belt (Gabrielse and Yorath, 1989). The two plutons are believed to have been the magmatic sources of the subaerial to nonmarine, shallow-water Skwel Peken Formation volcaniclastic rocks.

The southern outlier of the Skwel Peken Formation appears to represent a large, gently northerly plunging syncline (Figure 39, Section 9-10) and a stereoplot of poles to bedding measurements in the inlier is given in Figure 17H. Locally, the layering and bedding are deformed by a set of F_3 minor open-flexure folds that strike north-northeast to northeast.

Uplift and erosion was followed by the unconformable deposition of the Early Cretaceous Spences Bridge Group. This involved subalkalic, calcalkaline volcanism and shallow-water to subaerial sedimentation, accompanied by the intrusion of the Verde Creek stock.

The youngest rocks in the area are represented by Middle Eocene sediments and volcanic flows of the Springbrook and Marron formations. East of the Hedley

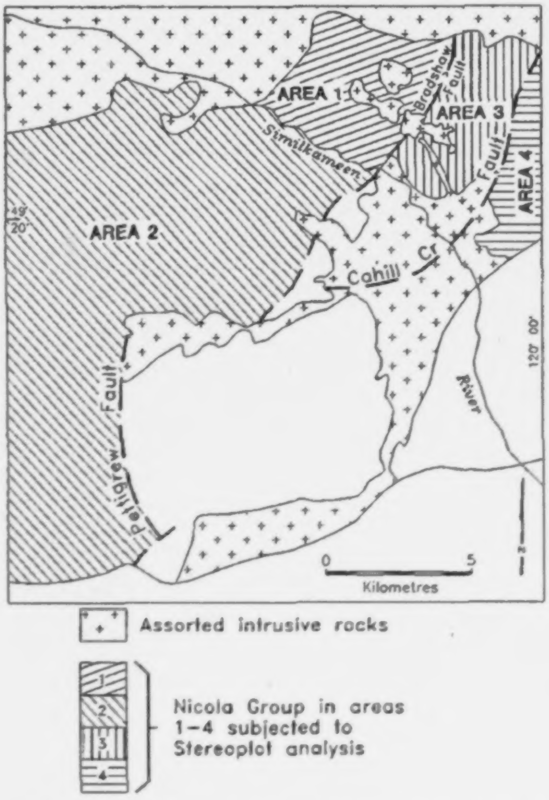

Figure 17. Location map of structural areas 1 to 4, and computer generated stereoplots (on Schmidt equal area nets; contour intervals are in % per 1% area): A. poles to bedding for the Apex Mountain Complex. B. poles to bedding for the Nicola Group in the entire Hedley district. C. poles to bedding for the Nicola Group in Area 1. D. poles to bedding for Nicola Group in Area 2. E. poles to bedding for Nicola Group in Area 3. F. poles to bedding for Nicola Group in Area 4. G. poles to fracture cleavage for Stemwinder Formation. H. poles to bedding for Skwel Peken Formation.

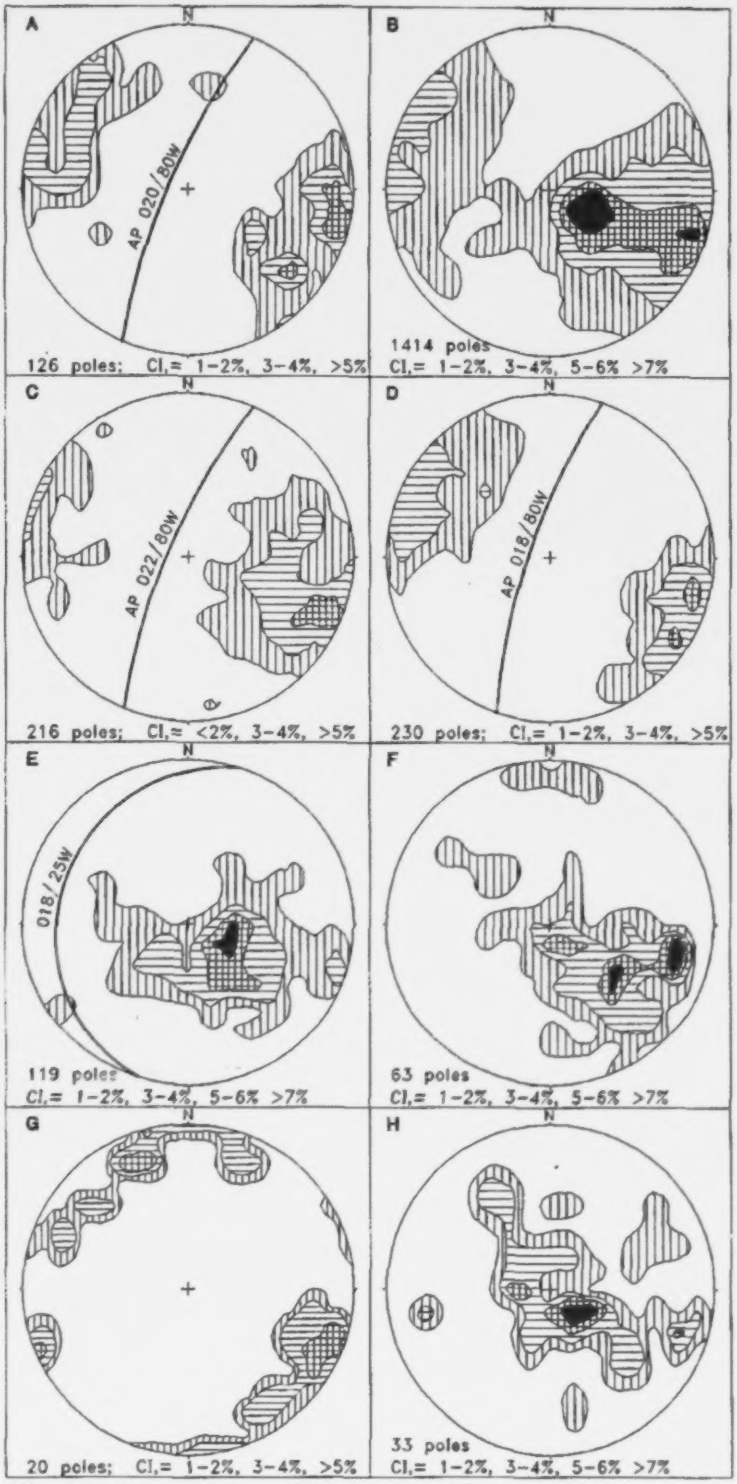

(CI= Contour Interval) (AP= Axial Plane)

Figure 17—*Continued*

district, major regional extensional faulting took place during the Eocene, resulting in the development of the westerly dipping Okanagan Lake crustal shear (Tempelman-Kluit and Parkinson, 1986). The Hedley district lies in the thin, upper plate that was subjected to an estimated 80 to 100 kilometres of westerly directed extensional movement, resulting in widespread listric normal faulting. No Eocene extensional faulting has been positively identified in the Hedley district. However, the faults responsible for the downdropping and subsequent preservation of the Skwel Peken Formation and Spences Bridge Group were possibly related to this Tertiary event.

Billingsley and Hume (1941) suggested that thrust faults were important at Hedley, and some minor evidence of thrusting was noted during this survey. Westerly dipping, easterly directed minor thrust structures were seen underground at the French and Nickel Plate mines. Also rocks of the Chuchuwayha Formation adjacent to the Bradshaw fault in Hedley Creek are separated from the underlying Oregon Claims Formation by a series of gently west dipping fractures that probably represent minor thrusts developed along what we believe to be the original unconformity. High-angle, east-directed reverse movements are inferred along the Chuchuwayha fault because conodonts indicate that rocks in the lowest part of the Stemwinder Formation are older (upper Carnian) than those in the structurally underlying Chuchuwayha Formation.

ECONOMIC GEOLOGY

INTRODUCTION

Gold has been the principal economic mineral in the Hedley district and it is found in both skarns and veins. Gold skarns, which are the most widespread and economically important, contain gold in intimate association with sulphide-bearing garnet-pyroxene-carbonate-scapolite alteration assemblages. They occur at the Nickel Plate, Canty, French and Good Hope mines, and at other occurrences such as the Peggy, Don and Speculator properties.

Gold-bearing veins are present at the Banbury, Gold Hill and Golden Zone properties, and two different types are recognized. One type, represented by the Banbury and Gold Hill mineralization, is related to, and coeval with, the skarn mineralization. It probably formed when fluids rich in carbon dioxide and silica, generated by skarn formation at depth, moved up fractures through unaltered rocks. It is characterized by gold and sulphides hosted in quartz-carbonate vein systems, some of which are associated with minor skarn wallrock alteration.

The second type of vein mineralization is seen at the Golden Zone mine approximately 8 kilometres north-northeast of the Nickel Plate mine. These gold-sulphide-bearing quartz veins are not associated with skarn and may be related to the intrusion of the Bromley batholith.

Skarn is exceedingly common throughout the Nicola Group in the Hedley district, particularly in carbonate-rich sections of the Hedley and French Mine formations. In many instances it apparently represents "reaction" skarn formed where intrusion-related contact metamorphism resulted in local metasomatic reaction between different lithologies. Such alteration overprints large parts of the French Mine Formation between the French and Good Hope mines but has little economic potential.

All of the economic skarns in the district are believed to represent "infiltration-type" alteration formed by metasomatism involving hydrothermal fluids related to magmatic intrusions. Economic skarns include two types: gold-skarns which are pyroxene dominant and associated with the Hedley intrusions, and the younger garnet-dominant skarns, such as the Mount Riordan garnet deposit, which contain some tungsten and copper but no gold. The latter are associated with the 194 Ma magmatism represented by the Bromley batholith and its related stocks. Gold skarns are by far the most widespread and important economically; the garnet-dominant skarns only occur in the eastern part of the district, and the largest, at Mount Riordan, is being evaluated as an industrial mineral deposit.

The intensity and amount of infiltration skarn developed throughout the district varies dramatically from the large alteration envelopes associated with the Nickel Plate gold and Mount Riordan garnet deposits, down to the smaller, narrower mineralized zones at the French, Canty and Good Hope gold mines. Barren, sulphide-poor infiltration skarn and associated Hedley intrusions are extremely common and widespread in the area, but economic gold skarns are rare. Even at the Nickel Plate deposit, where the hydrothermal system produced alteration up to 300 metres thick, the auriferous horizons are volumetrically small compared to the size of the skarn envelope which has an estimated volume of between 0.75 and 1.5 cubic kilometres.

Economic gold-skarn mineralization in the Hedley area is always developed close to altered Hedley intrusions but is almost wholly confined to the exoskarn; gold tends to be associated with abundant arsenopyrite and pyrrhotite, lesser amounts of pyrite and chalcopyrite, and traces of native bismuth, sphalerite and bismuth tellurides. Locally the endoskarn is cut by late veinlets of high-grade auriferous sulphides but these are rarely present in sufficient quantities to render the endoskarn economic. Ore-bearing skarn is characterized by a geochemical enrichment in Au, Ag, As, Te, Bi, Cu, Co, Sb and Zn. Anomalous Mo and W are found locally in some mineralized skarns. Gold mineralization is uncommon in the sulphide-poor garnet-pyroxene-carbonate skarn. However, there is no reliable visual method of distinguishing barren skarn from ore. At the Nickel Plate deposit for example, some zones of massive arsenopyrite are virtually barren, while in rare instances, sulphide-poor rocks are auriferous.

As well as the important local structural controls to mineralization, noted by Billingsley and Hume (1941) and Dolmage and Brown (1945), there are overall stratigraphic and lithological controls to the distribution of the skarns in the district. All of the large skarn envelopes and most of the economic gold mineralization are hosted by the carbonate-rich Hedley and French Mine formations, while the Oregon Claims, Whistle and Stemwinder formations are less favourable for skarn development. The emplacement of the Hedley intrusions and their associated skarns may have also been partly controlled by ancient growth structures such as the Bradshaw fault.

MAJOR SKARN DEPOSITS AND PROSPECTS

NICKEL PLATE AND HEDLEY MASCOT MINES (MINFILE 092H SE036, 038)

The Nickel Plate deposit, which is the largest gold skarn in Canada, was originally exploited by two different companies working the Nickel Plate and Hedley Mascot mines. The deposit has had a long history of geological investigation, and the following data are based partly on early studies by Camsell (1910), Warren and Cummings (1936), Billingsley and Hume (1941), Dolmage and Brown (1945) and Lee (1951), and partly on more recent work by the geological staff of Mascot Gold Mines Limited, (Simpson, 1987; Simpson and Ray, 1986), and on this study. In addition, fluid inclusion and geochemical studies of the deposit are described by Ettlinger (1990a) and Ettlinger *et al.* (1992).

TABLE 3
PRODUCTION FROM SKARN DEPOSITS — HEDLEY DISTRICT

Deposit	Ore milled (t)	Gold (kg)	Silver (kg)	Copper (t)	Grade (Au g/t)
Nickel Plate					
1904-1963[a] (Underground)	2 983 900	41 705	4 160	981	13.97
Nickel Plate* (Open pit)					
1987[b]	481 454	1512.4	832.4	0	3.14
1988[b]	879 645	2714.9	2955.7	0	3.08
1989[b]	1 065 026	2463.8	3246.0	0	2.31
1990[b]	1 141 255	2382.1	844.6	0	2.08
1991[b]	1 166 039	2842.7	677.7	0	2.43
Hedley Mascot (Underground)					
1936-1949[a,b]	619 022	7 248	1 707	871	11.70
Total	8 336 341	60 868.9	14 423.4	1 852	7.30
French					
1950-1955[a]	29 450	786	NA	NA	26.68
1957-1961[d]	48 158	817	66	NA	16.96
1982-1983[a]	4 438	26	135	20	5.86
Total	82 046	1629	201	20	19.85
Good Hope					
1946-1948[d]	4 241	89	NA	NA	20.98
1982[a]	6 874	77	119	0.6	11.20
Total	11 115	166	119	0.6	14.93
Canty					
1939-1941[a,c]	1 483	16	NA	NA	10.78
Grand total from skarn	**8 430 985**	**62 679.9**	**14 743.4**	**1872.6**	**7.43**

NA = Data not available

*Note: includes some open pit production from the Canty deposit.

Sources
(a) MINFILE
(b) Mineral Statistics, EMPR Mineral Policy Branch
(c) Rice (1947,1960)
(d) National Mineral Inventory - NMI 92H/8

The westerly dipping deposit was discovered in 1898 and mined in several underground operations until 1955; it produced approximately 48 953 kilograms of gold from 3.6 million tonnes of ore (Table 3). Mining resumed in April 1987 at a rate of 2450 tonnes of ore per day from an open pit (Plates 1 and 2). Ore reserves as of January 1989 were recalculated to be 5.07 million tonnes grading 3.0 grams gold per tonne (Corona Corporation, 1988 Annual Report). Between 1987 and 1991 approximately 11 915 kilograms of gold were produced from 4.7 million tonnes of ore (Table 3).

The gold deposit is hosted by the Hedley Formation where a discontinuous but extensive garnet-pyroxene-carbonate-scapolite skarn envelope is developed. This envelope, up to 300 metres thick and 4 square kilometres in area, lies around the eastern and northern ends of the Toronto stock and related swarms of sills and dikes (Figure 18). On surface, the main alteration zone is subcircular in shape and dips west. It is subparallel to, but locally crosscuts, the west-dipping hostrocks which consist of calcareous and tuffaceous siltstone, interbeds of impure limestone up to 40 metres thick, and minor amounts of bedded tuff, conglomerate and calcareous argillite.

Overall, the Nickel Plate skarn envelope has a similar strike to the host sediments although it generally has a slightly steeper dip than bedding in the east and more gentle dip in the west. In the vicinity of the old Hedley Mascot mine, where the skarn is probably at its thickest, it overprints the entire Hedley Formation and locally extends down into the underlying Oregon Claims Formation and up into the Whistle Formation. Farther west, the base of the skarn climbs back up the stratigraphy until, close to the Bradshaw fault, only the upper part of the Hedley Formation is overprinted. The skarn zone extends up to 1.5 kilometres north and northeast of the Toronto stock where it is developed within intensely folded Hedley Formation rocks. To the west and northwest, the main skarn envelope is truncated by the Bradshaw fault (Figure 18), while the northern margin of the skarn, which dips between 50° and 70° southwest, crosscuts the Hedley Formation at a high angle (Dolmage and Brown, 1945). To the northeast, the envelope is overlain by unaltered rocks of the Whistle Formation and its base is not exposed. The sharp, eastern boundary marks the lower skarn contact; here it dips west at 25° to 40° and is traceable on surface for approximately 1.5 kilometres. The southern boundary of the envelope is

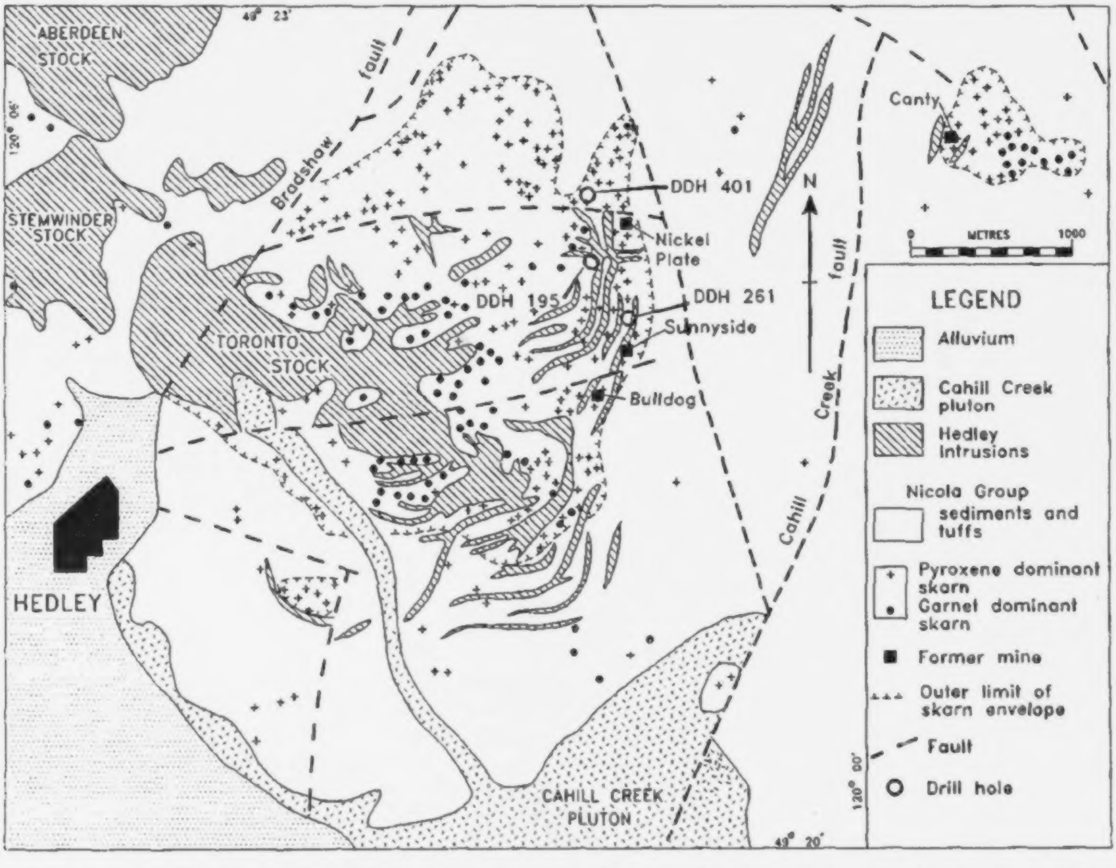
49° 23'
120° 05'
ABERDEEN STOCK
STEMWINDER STOCK
TORONTO STOCK
HEDLEY
Bradshaw fault
DDH 401
Nickel Plate
DDH 195
DDH 261
Sunnyside
Bulldog
Canty
N
fault
Cahill Creek
CAHILL CREEK PLUTON
METRES
0
1000
120° 00'
49° 20'
LEGEND
Alluvium
Cahill Creek pluton
Hedley intrusions
Nicola Group
sediments and tuffs
Pyroxene dominant skarn
Garnet dominant skarn
Former mine
Outer limit of skarn envelope
Fault
Drill hole

Figure 18. Outcrop distribution of the skarn envelopes surrounding the Nickel Plate and Canty deposits. *Note:* location of drill-holes illustrated in Figure 28.

more irregular and less precisely defined; it generally runs subparallel to, and within 200 metres of, the southern edge of the Toronto stock, but extensive, irregular patches of skarn alteration are developed in the Hedley formation up to 800 metres from the stock.

Economic mineralization outcrops along the northeast and eastern edges of the envelope, generally close to the base of the skarn. The principal Nickel Plate orebodies, worked downdip for over 900 metres, lie close to the steeply inclined northeast edge, while the Bulldog and the various Sunnyside orebodies were situated along the eastern margin of the skarn (Figure 18). No orebodies have been found adjacent to the skarn's southern margin.

Swarms of Hedley endoskarn diorite porphyry sills, 1 to 25 metres thick, locally make up 30% of the skarn-altered section. In addition, several diorite porphyry dikes have intruded west to northwest-trending fault zones, and the mineralization and alteration tend to follow these dikes.

The dominant episode of skarn development occurred during the F_1 folding event immediately after the emplacement of the Toronto stock and its related swarm of sills and dikes. The syntectonic nature of the intrusions is indicated by observations that some tightly (F_1) folded sediments are crosscut by sills that are also gently folded about the same F_1 axial planes. Most of the sills and dikes within the skarn envelope are bleached and altered. The Toronto stock is less altered and locally fresh at depth, but becomes progressively more overprinted with endoskarn alteration in its upper parts.

MINERALOGICAL AND GEOCHEMICAL VARIATIONS AT NICKEL PLATE.

Despite the large size and complexity of the Nickel Plate skarn, a vertical and concentric pattern of mineralogical zoning is recognized in the exoskarn envelope around the Toronto stock (Ray *et al.*, 1988; Ettlinger, 1990a). Three broad, mineralogically distinct, subhorizontal zones are identified; these are an upper, characteristically silicious zone, a middle zone of coarser grained pyroxene-garnet-carbonate skarn, and a lower zone of predominantly pyroxene skarn that also locally contains abundant carbonate, sulphides, scapolite and some gold.

The uppermost zone is up to 80 metres thick and forms a fine-grained silicious cap above the main skarn envelope. Early workers described these rocks as the "upper silicious beds"; some considered their silicious nature to be a sedimentary compositional feature, but Billingsley and Hume (1941) recognized it as epigenetic alteration. The alteration in this zone comprises a very fine grained intergrowth of mainly quartz and pyroxene, with lesser orthoclase, epidote, biotite and carbonate, and rare scapolite and plagioclase. Veins and vuggy masses of chalcedonic silica are locally abundant, and many outcrops have a cherty appearance. Garnet is uncommon and, when present, it generally occurs in thin (<1 cm) veinlets haloed by light green pyroxene, amphibole and chlorite. Thin (generally <10 cm), late veins of quartz and carbonate are also present. These silicious, altered rocks vary in colour from very pale grey, brown and green to green mottled with pink, depending on the proportions of pyroxene, epidote and orthoclase present. This silicious replacement alteration extends from the Hedley Formation up into the overlying Copperfield breccia, and despite the intense bleaching, the original bedding structures and fine sedimentary and tuffaceous textures are commonly clearly preserved.

The middle zone makes up the bulk of the alteration envelope and mainly comprises medium to course-grained pyroxene-garnet-carbonate skarn. The exoskarn in this zone typically consists of alternating pyroxene-rich and garnet-rich layers which reflect the original sedimentary bedding. Overall, pyroxene is more abundant than garnet; however, garnet in the exoskarn becomes more abundant and coarser grained, both locally toward individual sill margins and also westwards across the main envelope toward the Toronto stock. This is demonstrated both by surface mapping (Figure 18), and subsurface studies (Ettlinger, 1990a). Garnet-rich skarn is also preferentially developed in the more limy horizons, and massive garnetite often forms as a replacement of original limestone beds. Other less common minerals include wollastonite, scapolite, epidote and apatite with minor sphene. Locally, the garnet-pyroxene skarn contains silicious, altered remnants of bleached or dark argillite that have resisted much of the skarn overprinting.

The lowermost 50 to 100 metres of the envelope is a zone of pale green to grey, medium to fine-grained, massive to layered, pyroxene-carbonate skarn in which garnet is generally subordinate. This basal part of the skarn is also characterized by abundant scapolite, some chlorite, epidote and sericite, and the presence of the sulphide-rich, gold orebodies. Other minerals present include orthoclase, tremolite, plagioclase, wollastonite, prehnite, sphene, rutile and rare axinite.

The base of the skarn, particularly along its northern and southern margins, is irregular and characterized by prominent masses, clots and veins of calcite. The irregularity is partly due to the Hedley intrusion dikes; some dikes are flanked by zones of intense alteration that penetrate down into the unaltered sediments to form deep, narrow keels of skarn. These keels extend up to 70 metres beneath the general base of the skarn (Billingsley and Hume, 1941).

In the lowest part of the envelope, the skarn alteration is locally interrupted by patches of bleached, silicified, siltstone and marble, as well as remnant patches of dark, altered argillite. Passage from skarn into the underlying, unaltered sedimentary rocks is generally abrupt and may take place over a distance of 20 metres or less. Billingsley and Hume (1941) termed the transition between skarn and unaltered sediments the "marble line", and noted its economic importance because most ore deposits are located within 80 metres of this feature. Marble forms discontinuous bands from 2 to 20 metres thick that are interbedded with silicified siltstone and argillite, and remnant patches of unaltered limestone. In drill core, marble appears as a massive to weakly layered, pale grey to white coarse-grained rock that comprises between 70 and 95% calcite with lesser amounts of recrystallized quartz and rare remnant chert pebbles. Traces of wollastonite, scapolite, biotite, orthoclase, epidote, tremolite-actinolite, chlorite and opaque minerals are also present. The marble is locally cut by abundant late veins and segregations of calcite and quartz, some of which contain pyrrhotite, wollastonite and orthoclase.

Previous workers interpreted the marble at the marble line to be thermally metamorphosed limestone formed by heat from the overlying skarn. However, Wagner (1989) suggests that some of the calcite may result from carbonate metasomatism, when carbonate-saturated fluids were cooled or mixed with meteoric waters during the skarn-forming process. He notes that similar carbonate deposition is described by Torrey *et al.* (1986) at the Red Dome copper-gold skarn in Australia.

Significant geochemical and mineralogical variations are seen throughout the Nickel Plate deposit. Sulphides in the main Nickel Plate ore zone near the old Nickel Plate underground mine (Figure 18), in the northern part of the deposit, consist primarily of arsenopyrite with minor pyrrhotite and chalcopyrite. The Sunnyside ore zones in the central part of the deposit are strongly controlled by either sill-dike intersections or fold hinges. Although the sulphide mineralogy and textures resemble those in the Nickel Plate zone, pyrrhotite is more abundant. The skarn in the southern part of the deposit contains lenses and pods of massive to semimassive sulphide; it is noticeably richer in chalcopyrite and contains higher silver and zinc values. Chalcopyrite also increases westward towards the Toronto stock and the deeper levels of the deposit; a similar copper zoning is described in the Fortitude gold skarn in Nevada (Myers and Meinert, 1988; Myers, 1990) and the Crown Jewel deposit at Buckhorn Mountain in Washington State (Shannon *et al.*, 1990).

The Bulldog orebodies in the southern part of the Nickel Plate deposit are pyrrhotite and sphalerite rich; they occur at shallow depth but surface exposures are only weakly mineralized. In the area around the old Bulldog mine (Figure 18), electrum occurs in close association with chalcopyrite, pyrrhotite, sphalerite and native bismuth; it tends to be concentrated in microfractures within and around the sulphides.

A statistical study (Simpson, 1987) based on analyses of over 300 mineralized samples from various ore zones in the Nickel Plate deposit, showed the following correlation coefficients: Au:Bi, 0.94; Ag:Cu, 0.84; Bi:Co, 0.62; Au:Co, 0.58; Au:As, 0.46; Au:Ag, 0.28; and Au:Cu, 0.17. The strong positive correlation between gold and bismuth reflects the close association of native gold with hedleyite, while the moderate positive correlation between gold, cobalt and arsenic confirms the observed association of gold, arsenopyrite and gersdorffite. As no tetrahedrite is present, the high positive correlation between silver and copper may indicate that some silver occurs as a lattice constituent in the chalcopyrite. The gold and silver values are relatively independent of each other despite the presence of electrum, and there is generally a weak correlation between gold and copper. Gold/silver ratios in the Nickel Plate and Sunnyside zones are greater than 1 with silver averaging 2 ppm. By contrast, in the southern part of the deposit where electrum is present, the Au:Ag ratio is less than 1, with silver averaging 17 ppm.

Bismuth averages 20 ppm but may reach concentrations of several hundred parts per million in areas with higher gold contents. Nickel and cobalt values normally range from 100 to 200 ppm but both locally exceed 2%, and some outcrops contain abundant visible erythrite. Copper commonly exceeds 0.5% over intervals of several metres, particularly in the sulphide-rich South pit area and in the western, deeper levels of the deposit.

Secondary gold enrichment is present in some weathered, oxide-rich zones and along certain faults. The resulting red hematitic clay zones can carry gold grading over 34 grams per tonne.

SKARN MINERALOGY AT NICKEL PLATE.

The Nickel Plate skarn contains the following common gangue minerals: clinopyroxene, calcite, quartz, garnet, epidote, scapolite, potassium feldspar, wollastonite and chlorite. Other less common but locally abundant gangue minerals include biotite, clinozoisite, sericite, albitic plagioclase, apatite and tremolite-actinolite, with trace to rare amounts of axinite, idocrase, sphene and prehnite. Most of these minerals, including wollastonite, are found in both the endoskarn and exoskarn, although pyroxene and garnet are more abundant in the exoskarn and albitic plagioclase is locally common in the bleached endoskarn.

Arsenopyrite and pyrrhotite are the most common sulphides (Plate 21). Present in lesser amounts, but locally abundant, are pyrite, chalcopyrite and cadmium-rich sphalerite. Other less common to rare opaques include galena, native bismuth, gold, electrum, tetrahedrite, native copper, magnetite, bismuthinite, gersdorffite, marcasite, covellite, molybdenite, bismuth tellurides (hedleyite, tetradynite), cobaltite, erythrite, pyrargyrite, lollingite, breithauptite and maldonite (Au_2Bi).

MINERAL PARAGENESIS AT NICKEL PLATE

Numerous studies have been made of the paragenesis of the sulphide minerals (Camsell, 1910; Bostock, 1930; Warren and Cummings, 1936; Billingsley and Hume, 1941; Dolmage and Brown, 1945) but until this recent study and the work of Ettlinger (1990a), little had been done to determine the order of crystallization of the skarn gangue minerals. The results of these two recent studies are summarized in Figure 19, and the following stages of mineral deposition are recognized:

1. biotite, orthoclase, epidote, calcite and quartz.
2. clinopyroxene, orthoclase, calcite, quartz and minor wollastonite.
3. garnet, clinopyroxene, calcite and quartz with minor scapolite, albitic plagioclase and wollastonite.
4. sulphides (with gold and tellurides), scapolite, chlorite, epidote, orthoclase, calcite and quartz with minor sericite, axinite, idocrase and prehnite.
5. calcite, quartz, epidote, chlorite, sericite and prehnite.

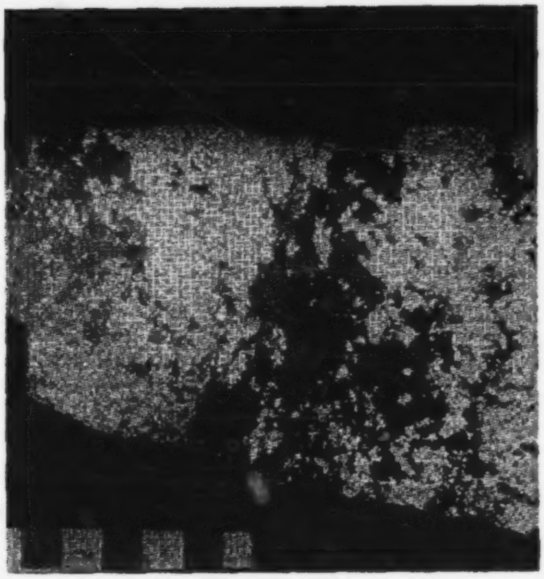

Plate 21. Nickel Plate deposit. Sulphide-rich ore with abundant arsenopyrite and pyrrhotite in a pyroxene gangue.

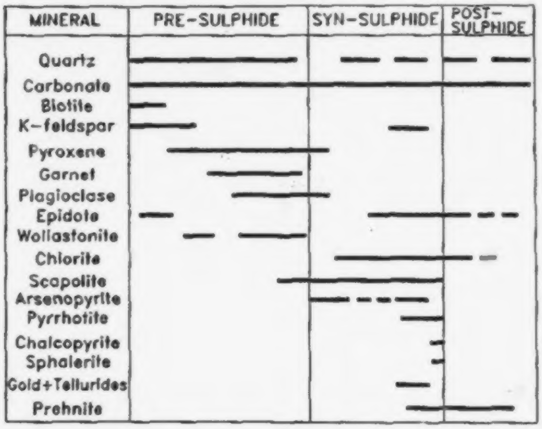

Figure 19. General paragenesis of skarn minerals in the Nickel Plate gold skarn.

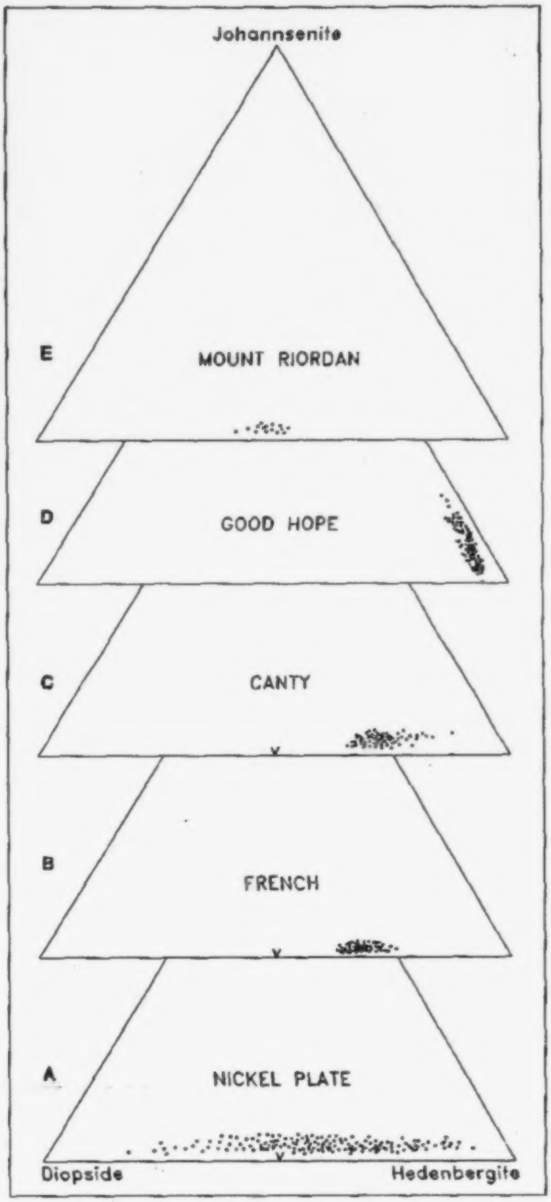

Figure 20. Composition of exoskarn pyroxenes in the Hedley skarns. A. Nickel Plate deposit (151 analyses). B. French deposit (52 analyses). C. Canty deposit (65 analyses). D. Good Hope deposit (42 analyses). E. Mount Riordan (15 analyses). Analyses by G.E. Ray and G.L. Dawson at The University of British Columbia, Vancouver, B.C.

Calcite and quartz crystallized throughout the entire period of skarn development. Biotite and orthoclase were the earliest minerals formed; their presence in Stage 1 may indicate that the magmatic skarn-forming fluids were originally potassium rich and that as the system evolved the fluids were later dominated by calcium derived from the sedimentary hostrocks. This early potassic alteration, first described at Nickel Plate by Ray *et al.* (1988), has now been noted at other gold skarns such as the Fortitude deposit in Nevada (Myers and Meinert, 1988). Biotite in the exoskarn is mostly preserved in remnant patches of silicious, purplish brown hornfels within the pyroxene-garnet skarn. This early hornfelsic biotite is often extremely fine grained and forms anhedral flakes and aggregates; it is commonly intergrown with quartz, epidote and minor carbonate. Biotite-rich hornfelsic alteration also locally overprints the Hedley sills where it tends to be coarser grained than in the sedimentary rocks; the original magmatic amphiboles and pyroxenes are rimmed and partially to completely replaced by randomly orientated flakes and masses of bright red biotite.

Clinopyroxene was the predominant mineral formed during Stage 2, but it continued to crystallize throughout Stage 3. The pyroxene commonly forms fine to medium-grained colourless to pale green, tabular to equigranular subhedral crystals that are disseminated throughout the skarn. Masses, bands and crosscutting veins of pyroxene are also seen.

Pyroxene enclosed within, or adjacent to, calcite commonly has euhedral faces. Crystals can be twinned and they vary from clear to clouded; the latter contain abundant very fine grained, dark inclusions. There is an overall decrease in size of the pyroxene (and garnet) crystals toward the margins of the skarn envelope. Light pink orthoclase commonly forms as a reaction product when pyroxene replaces biotite.

Two types of pyroxene are recognized. The most abundant is early and represented by widespread, disseminated to massive, fine to medium-grained pyroxene that in

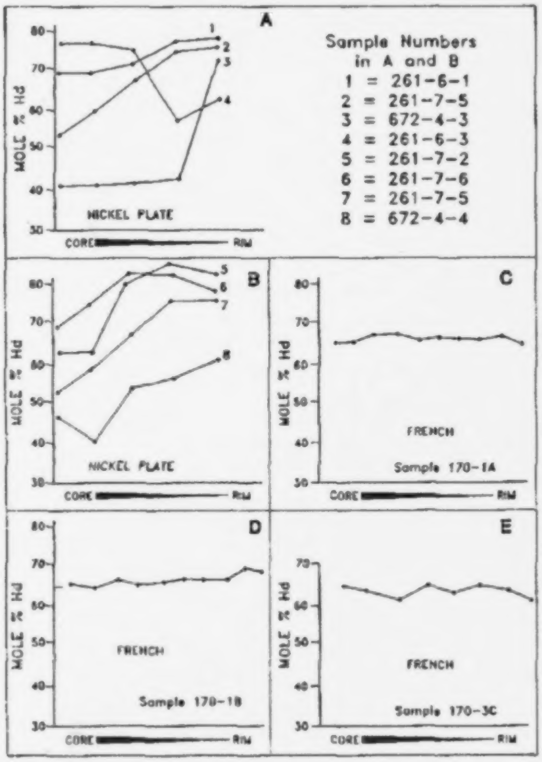

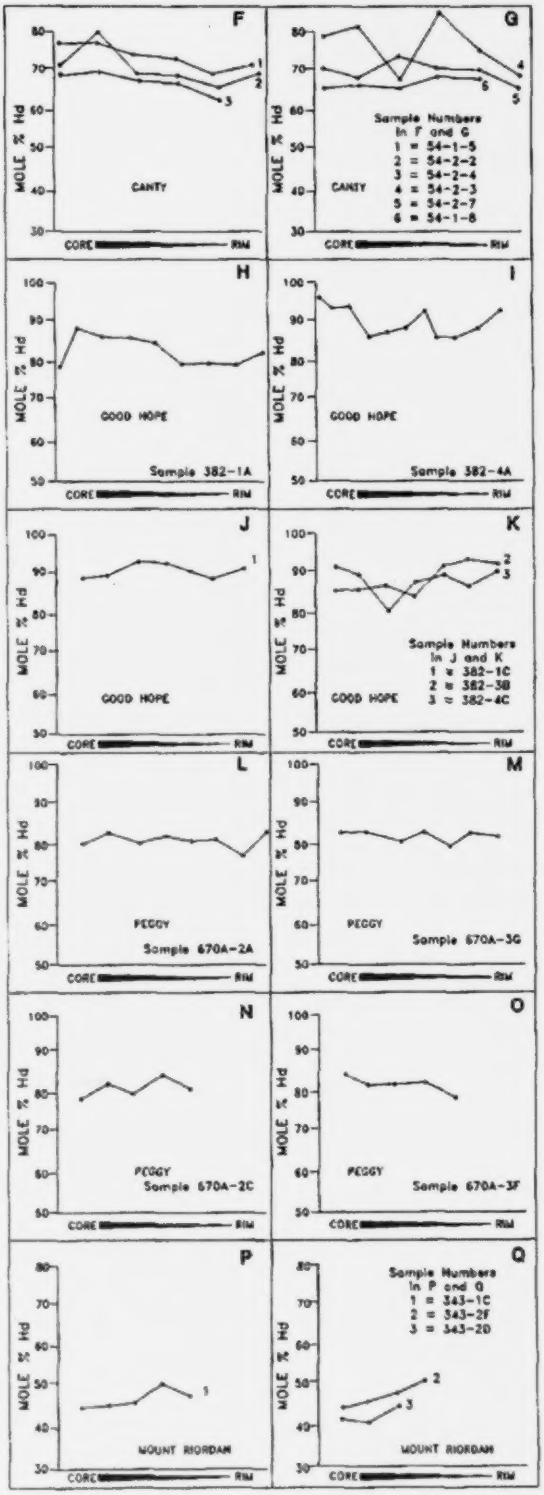

Figure 21. Composition variation (expressed as mole% hedenbergite) across individual exoskarn pyroxene crystals from the Hedley skarns. A and B. Nickel Plate deposit. C, D and E. French deposit. F and G. Canty deposit. H, I, J and K. Good Hope deposit. L, M, N and O. Peggy. P and Q. Mount Riordan.

outcrop varies in colour from light grey to medium green. The other type is later and darker coloured; it fills crosscutting fractures and forms masses and veins.

Pyroxenes at Nickel Plate and the other gold skarns in the Hedley district, generally contain less than 1.5 weight percent MnO, and range between Hd_{35} and Hd_{95} mole percent (Figure 20A). Figure 21 shows the results (listed in Appendix 15B) of microprobe traverses across pyroxenes collected from auriferous mineralized exoskarn at Nickel Plate. When present, compositional zoning in the pyroxene is variable; in most crystals the rims tend to be more hedenbergitic than the cores although less commonly the reverse pattern is seen (*e.g.*, sample 261-6-3, Figure 21A).

Garnet crystals are generally anhedral to subhedral but, like the pyroxenes, they are commonly euhedral adjacent to carbonate. Garnet varies from isolated crystals, up to 8 millimetres across, to large masses, clusters and bands of anhedral crystals. Fracture controlled veins of garnet also crosscut and replace pyroxene. Unlike the pyroxene veins which may cut unaltered country rock or biotite hornfels, the garnet veins are always enveloped by pyroxene, and are never in direct contact with unaltered hostrocks. Garnet also forms long wormy growths consisting of chains of crystals; these elongate growths represent a reaction phenomenon and are invariably developed between either carbonate and pyroxene or between carbonate and wollastonite. Bands of garnet commonly mimic sedimentary bedding.

Most garnets at Nickel Plate are a uniform brown colour although the euhedral garnets within, or adjacent to, carbonate are occasionally reddish pink or orange. In some outcrops the earliest garnet is a lighter brown colour and is replaced and crosscut by veins of darker brown garnet.

Garnet is mostly birefringent and sector twinned; however, some crystals have isotropic cores and birefringent margins (Plate 22). The cores of many crystals, both isotropic and birefringent, are often densely packed with small inclusions of carbonate, epidote and euhedral pyroxene, while the birefringent margins tend to be clear and have fewer inclusions (Plate 23). In some crystals the contrasting cores and rims are separated by a thin zone of carbonate; it is uncertain whether this marks a break between two stages of garnet growth or whether certain compositional zones in single generation garnets have been preferentially replaced by carbonate.

Like most of the skarn-related garnets throughout the Hedley district, those at Nickel Plate generally contain less than 1% MnO and range in composition from Ad_{20} to Ad_{80} mole percent (Figure 22A; Appendix 15A). Some of the small, wholly birefringent garnet crystals in mineralized skarn show no change in composition from core to rim (Figure 23A). However, most of these birefringent garnets tend to have andraditic cores and grossular margins (Figures 23B and C) although, in rare instances, the reverse is noted (Figure 23D).

In contrast to the small garnets, detailed microprobe traverses across the larger crystals with isotropic centres and birefringent edges reveal a consistent pattern of com-

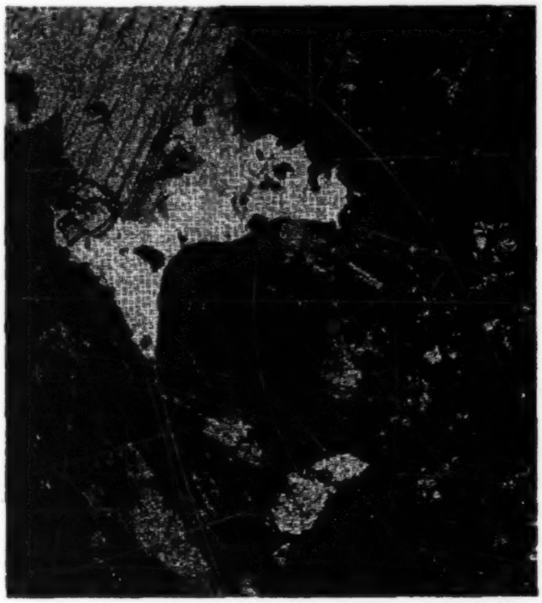

Plate 22. Nickel Plate deposit. Photomicrograph (X polars) showing subhedral exoskarn garnets with isotropic cores and birefringent margins (field of view is 2.5 mm wide).

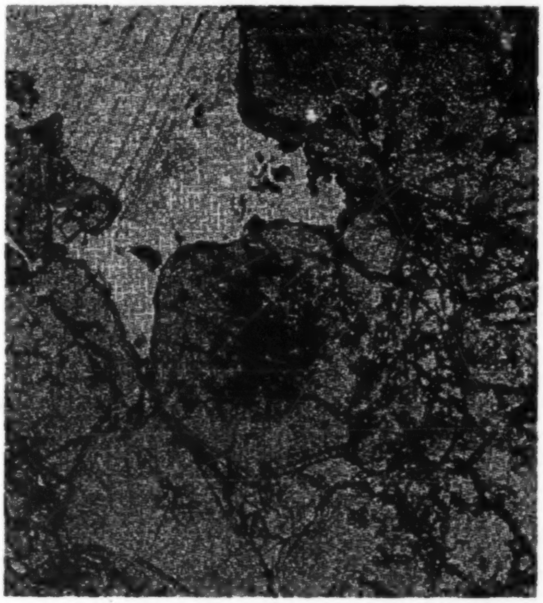

Plate 23. Nickel Plate deposit. Photomicrograph (PPL) of garnets seen in Plate 22. *Note* the isotropic cores contain abundant inclusions (field of view is 2.5 mm wide).

positional zoning. We believe these larger crystals have undergone longer periods of growth than the smaller, wholly birefringent garnets, and thus their compositions probably give a more complete chemical history of the evolving skarn system. The zoning in these large garnets, as illustrated by Figure 24, is marked by small core regions of intermediate composition (averaging Ad_{40}), that pass outwards into wider and more grossularitic zones averaging Ad_{25}. These in turn are overgrown by narrower zones of more andraditic garnet (Ad_{40-60}), although the thin, outermost rims of the crystals are commonly grossularitic. The composition of the crystal centres may be influenced by the chemistry of the original protolith, as suggested by Ettlinger and Ray (1989). The succeeding wide and uniform grossularitic zone probably reflects the chemistry of the skarn fluid responsible for the bulk of the prograde assemblages, while development of the andraditic margins may have coincided with the sulphide-gold mineralization. Crystallization of the wide grossularitic zones may have resulted from the reduced conditions prevailing in the skarn (*i.e.*, low Fe^{+3} inhibiting the production of andradite), whereas the andraditic margins may indicate that later, during deposition of the sulphides, the system became relatively more oxidized. The outermost grossularitic rim could be due to either the additional input of more reduced skarn fluids, a decrease in $X_{Fe\ total}$, or a change in X_{CO_2}, as described by Taylor and Liou (1978). It seems likely from the zoning patterns seen in Figures 23 B and C, that some of the smaller birefringent garnets only started to crystallized during the late andraditic phase seen in the larger crystals. This suggests that a more complete chemical history of a skarn can be obtained by microprobe studies on the larger garnets and pyroxenes rather than by analysing the smaller crystals.

White, fibrous wollastonite is present as bundles and radiating crystals in exoskarn, endoskarn and marble at the base of the envelope; some wollastonite predates, and is overgrown by, grossular garnet, while elsewhere a later episode of wollastonite replaces carbonate and garnet. Scapolite is widespread throughout the endoskarn, exoskarn and marbles, but it increases dramatically adjacent to and within orebodies where, in some thin sections, it makes up to 20% of the rock. It occurs as disseminated, subhedral, prismatic to tabular crystals up to 4 millimetres in length, as well as irregular crystalline masses and veins. Veins of scapolite cut sulphides, and sulphide veins crosscut massive scapolite, which emphasizes their close temporal, spatial and probably genetic relationship. While most of the scapolite was late and introduced during Stage 4, minor earlier scapolite occurs as small inclusions in pyroxene. In the upper parts of the envelope, large rounded cavities in the bleached and silicified Copperfield breccia are lined with coarse, euhedral crystals of white scapolite (identified by x-ray defraction as mizzonite) up to 1 centimetre long. These pre-skarn cavities, which reach 15 centimetres across, are believed to have formed by the dissolution and removal of some original cobbles in the conglomerate.

Microprobe analyses on scapolite from both barren and mineralized exoskarn at Nickel Plate were recently completed at the University of Western Ontario (Y. Pan,

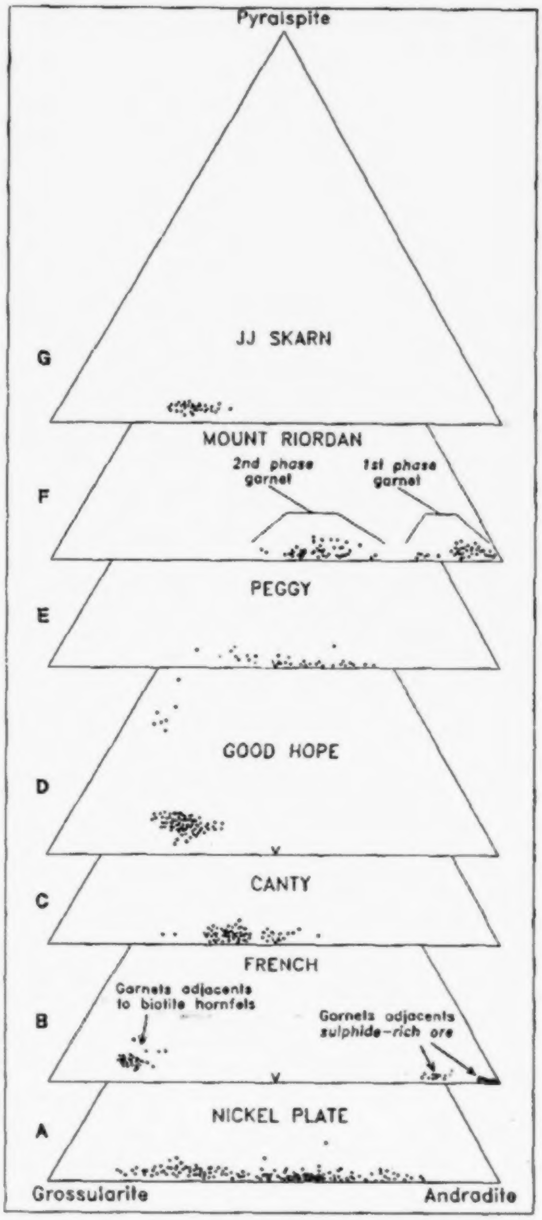

Figure 22. Composition of exoskarn garnets in the Hedley skarns. A. Nickel Plate deposit (145 analyses). B. French deposit (56 analyses). C. Canty deposit (60 analyses). D. Good Hope deposit (90 analyses). E. Peggy (30 analyses). F. Mount Riordan (74 analyses). G. JJ (35 analyses). Analyses by G.E. Ray and G.L. Dawson at The University of British Columbia, Vancouver, B.C.

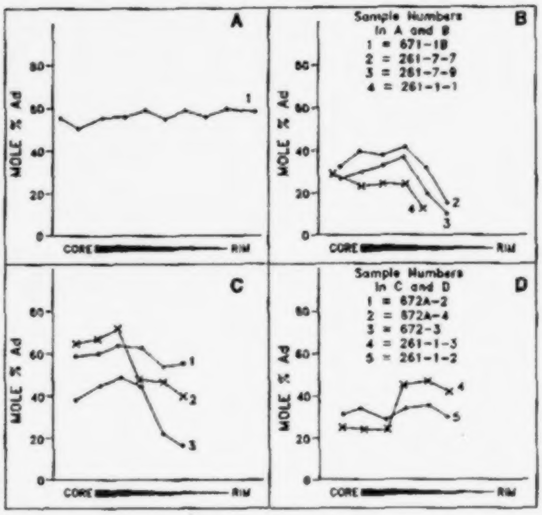

Figure 23. Compositional variation (expressed as mole% andradite) across various types of small birefringent exoskarn garnet crystals from the Nickel Plate deposit. A. Anhedral crystal. B. Vein or "wormy" garnet. C. Subhedral to anhedral crystals. D. Euhedral crystals.

written communication, 1993). These preliminary studies suggest there are no detectable chemical differences between scapolite in mineralized and barren skarn; the mineral contains between 9.6% and 13.1% CaO, and 6.2% and 8.2% Na_2O. In addition, they are chlorine rich, containing between 1.6% and 2.5% Cl.

Chlorite, like scapolite, is temporally and spatially related to the sulphides in the ore zones; it locally replaces and rims garnet and pyroxene, and in outcrop it forms black to very dark green veins and irregular clots. Some greenish brown tremolite also replaces garnet and to a lesser extent pyroxene in the ore zones. Generally however, the silicates in most parts of the Nickel Plate skarn are remarkably unaffected by retrograde alteration.

Epidote generally occurs as small disseminated, anhedral to subhedral crystals. Late veinlets of green epidote are also present, some of which are intimately associated with sulphide veins. Less commonly, epidote growing within carbonate forms coarse, euhedral crystals up to 5 millimetres long. Microprobe analyses of these large tabular crystals indicate they are calcic epidotes that show no evidence of manganese enrichment. However, Wagner, (1989) notes thin, pink rims on some epidote crystals, which he interprets as piedmontite overgrowths. Late prehnite in the skarn is seen as veinlets cutting sulphides, as small masses in the gangue matrix and as rims to some arsenopyrite and pyrrhotite crystals.

Studies of grain-boundary relationships suggest the following stages of opaque mineral growth in the ore:

1. barren arsenopyrite
2. arsenopyrite (with inclusions of gold, bismuth tellurides and cobaltite) and minor pyrrhotite.
3. pyrrhotite with minor chalcopyrite and sphalerite.

Thus, in relation to the sulphide paragenesis, gold was introduced relatively early in fluids that precipitated an arsenopyrite and scapolite-rich gangue (Ettlinger, 1990a).

Arsenopyrite occurs in both the exoskarn and endoskarn. It is the dominant sulphide in the ore and at least two generations are recognized (Camsell, 1910). The earliest is widely distributed throughout the skarn envelope and forms euhedral to subhedral, poikiloblastic crystals, irregular blebs, masses and veins that are often packed with small inclusions of carbonate, pyroxene, garnet, magnetite and unidentified iron-stained gangue minerals. The early generation of arsenopyrite does not contain gold, and neither does the disseminated arsenopyrite present in

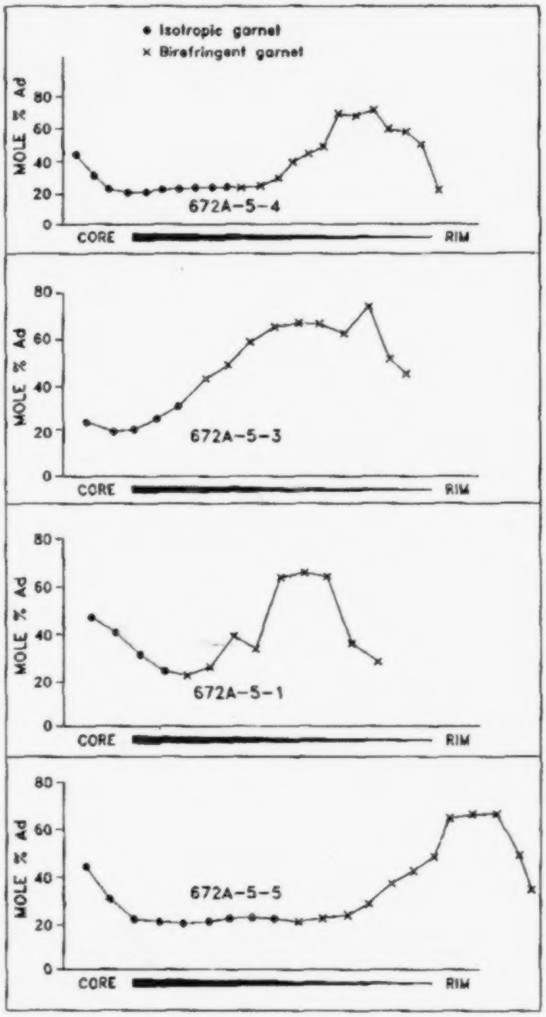

Figure 24. Compositional variation (expressed as mole% andradite) across large garnet crystals with isotropic cores and birefringent margins, Nickel Plate deposit.

many unaltered Hedley intrusions throughout the district. The subsequent generation of arsenopyrite produced anhedral to subhedral, twinned and striated crystals up to 1 centimetre long, as well as veins, massive pods, lenses and bands; the bands have preferentially replaced specific bedding lithologies in the exoskarn. This younger arsenopyrite is generally confined to the ore zones; it contains minute inclusions of gold, cobaltite, bismuth tellurides, and pyrrhotite as well as rare lollingite and gersdorffite. Camsell (1910) noted that in reflected light the early arsenopyrite is white and the later generation has a slight bluish tinge. The presence of both barren and auriferous arsenopyrite accounts for the extremely variable correlation between arsenic and gold throughout the Nickel Plate skarn envelope.

Native gold in the deposit occurs as minute blebs that are mainly but erratically distributed within second generation arsenopyrite. Gold inclusions reach up to 25 microns across but are more commonly less than 7 microns in diameter, and they are intimately associated with bismuth tellurides. Warren and Cummings (1936) reported that rare, larger grains of gold are also enclosed within some early pyrrhotite. Small particles of visible gold were present in the zone of supergene enrichment that originally capped the deposit.

Pyrrhotite is widespread and locally abundant (Plate 21). It mostly postdates the arsenopyrite although some is apparently coeval with the arsenopyrite and gold. It forms massive bands, and irregular blebs, and is often associated with chalcopyrite. Trace to moderate amounts of chalcopyrite are common and it becomes more plentiful in the deposit both westwards with depth towards the margin of the Toronto stock, and southwards. It forms microscopic veinlets, disseminations and bands as well as rims on arsenopyrite.

Pyrite is generally uncommon. It and sphalerite, are generally the youngest sulphides, although Bostock (1930) reported rare cubes of early pyrite as inclusions in pyrrhotite and chalcopyrite. Late pyrite is also present in veins and along fault planes. Sphalerite is generally rare but is more common in the southern parts of the deposit. It occurs as black blebs and isolated crystals in both the endoskarn and exoskarn, where it is associated with pyrrhotite, chalcopyrite and very rare molybdenite. Some sphalerite separates garnet-pyroxene from coarse white carbonate. In addition, small inclusions of sphalerite occur in pyrrhotite and, more rarely, chalcopyrite. Trace amounts of magnetite and ilmenite are present in the ore, and very rare occurrences of galena have been reported (Camsell, 1910).

ORE CONTROLS AT NICKEL PLATE

Studies on ore controls at Nickel Plate have been undertaken by Camsell (1910), Billingsley and Hume (1941), and Dolmage and Brown (1945), and more recently by Ettlinger (1990a). Much of the following section is a synopsis of this work.

Orebodies at Nickel Plate commonly have one or more of the following four controls:

- proximity to the marble line (the lower and outer margins of the skarn).
- proximity to igneous contacts or sill-dike intersections.
- proximity to suitable fold structures.
- The presence of cross-cutting fractures.

The gold-bearing sulphide zones normally form semiconformable, tabular bodies of variable size; there is both vein ore, where mineralization is largely fracture controlled and replacement ore where beds have been preferentially replaced by disseminated to massive sulphides. Orebodies may be hosted in any of the sedimentary lithologies at the mine provided they lie close to intrusive contacts or channelling fractures. There is a close relationship between sill density and ore development, particularly in the smaller orebodies along the base of the skarn.

Isolated sills are rarely associated with mineralization but places where sills bifurcate and converge, change direction, pinch and swell, or intersect dikes, are highly favourable for ore. The intensity of exoskarn alteration and mineralization is often greater above a sill than below it. However, the ore is not necessarily in direct footwall contact with the sill, but may be separated from it by a metre or more of gangue. The intensity of skarn alteration and the gold grade in the exoskarn tend to decline gradationally upwards from the sill contact; thus many orebodies have sharp footwall contacts and irregular, less well defined hangingwalls.

The controlling, northwest-plunging F_1 folds in the deposit are more abundant northeast of the Toronto stock. Ore is commonly found in the anticlinal hinges that formed structural traps The folds in the northern part of the deposit are more open, with vertical axial planes, while those farther south are tighter and either monoclinal or overturned to the north. The tight folds frequently die out over short distances up axis. Mineralization tends to be leaner on the southern, shallow-dipping limbs, and richer on the fold hinges or the northern, overturned and intensely fractured limbs. Some orebodies occur close to the dike-related keels of skarn that extend below the base of the envelope.

Camsell (1910) noted that where sills cut sediments at a high angle, the margins of the orebodies crosscut the bedding subparallel to the sills. The intensity of fracturing is also an important depositional control to the early skarn silicates and the subsequent gold-sulphide mineralization. Dolmage and Brown (1945) described three important, but locally impersistent sets of pre-ore fractures that trend either west, northwest or north; these fractures are probably related to the F_1 folding event. They noted that "narrow tongues" of fracture-controlled ore can be traced from one mineralized fold structure to another.

Orebodies close to the north margin of the skarn envelope differ in morphology from those along the eastern edge and the base of the skarn. To the north the Nickel Plate orebodies are large, persistent and have considerable lateral extent along bedding. Those at the eastern margin and base of the skarn are smaller and impersistent, but generally have higher gold grades; these are strongly con-

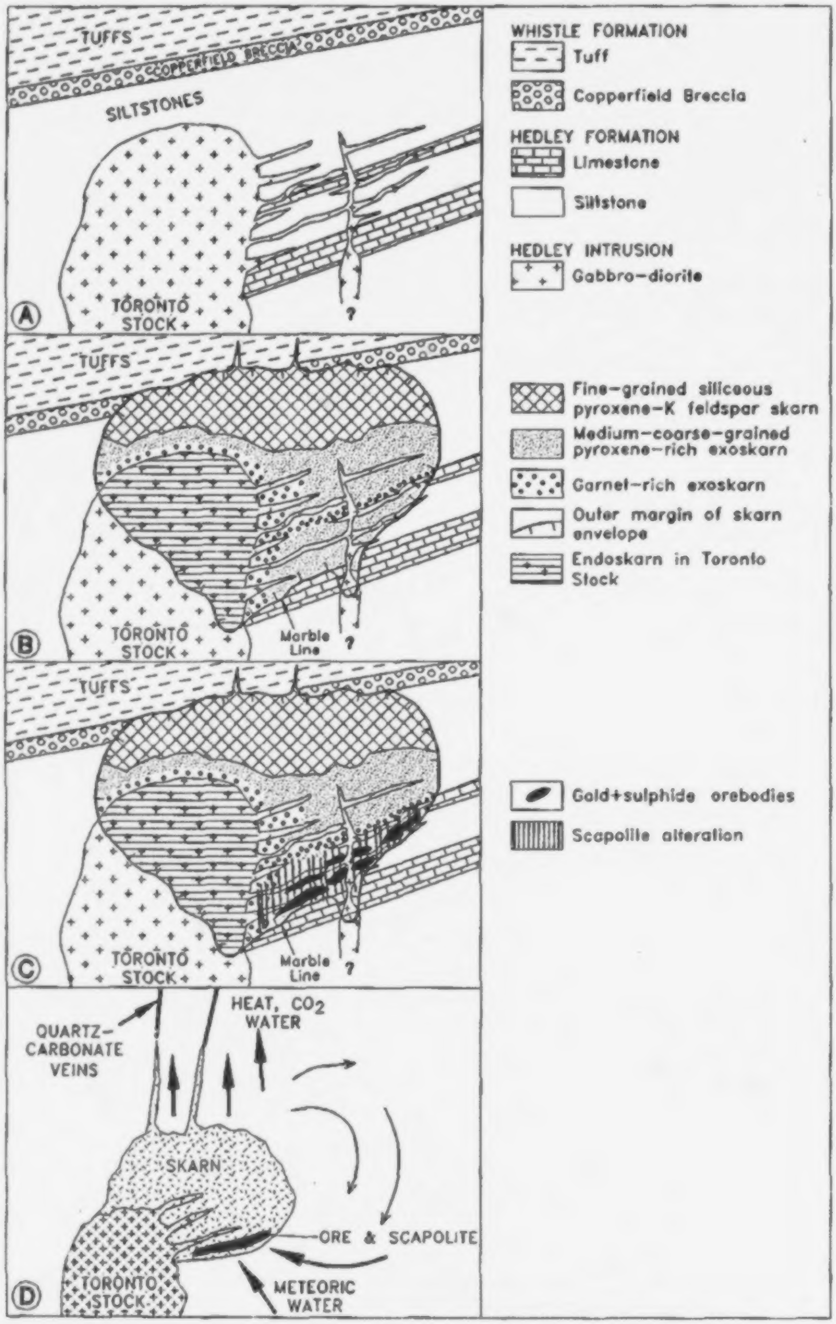
TUFFS
COPPERFIELD BRECCIA
SILTSTONES
TORONTO STOCK
A
B
C
D
Marble Line
?
QUARTZ-CARBONATE VEINS
HEAT, CO_2 WATER
SKARN
ORE & SCAPOLITE
METEORIC WATER
TORONTO STOCK
WHISTLE FORMATION
Tuff
Copperfield Breccia
HEDLEY FORMATION
Limestone
Siltstone
HEDLEY INTRUSION
Gabbro-diorite
Fine-grained siliceous pyroxene-K feldspar skarn
Medium-coarse-grained pyroxene-rich exoskarn
Garnet-rich exoskarn
Outer margin of skarn envelope
Endoskarn in Toronto Stock
Gold+sulphide orebodies
Scapolite alteration

Figure 25. Postulated development of the Nickel Plate skarn envelope (using our data and results of the study by Ettlinger, 1990a). A. Intrusion of the Toronto stock and associated sill-dike complex. B. Infiltration of hydrothermal fluids to produce a 300-metre-thick, pyroxene-dominant prograde skarn envelope with upper fine-grained siliceous zone. Coarser grained and garnet-dominant skarn developed adjacent to intrusions. C and D. Lower temperature deposition of sulphides, gold and scapolite close to the base of skarn envelope and formation of quartz-carbonate veins above the envelope. It is believed that development of a large thermal cell resulted in an influx of meteoric water into the base of the system which resulted in sulphide-gold-scapolite deposition.

trolled by dike-sill intersections and fold structures and mineralization does not extend far beyond these controlling features.

GENETIC MODEL FOR THE NICKEL PLATE DEPOSIT

A sequence outlining the postulated development of the Nickel Plate skarn envelope and the associated sulphide-gold mineralization is shown in Figure 25. Gold skarns are probably developed in the Hedley district for a number of reasons including:

- The presence of extensive permeable and reactive carbonate-bearing hostrocks suitable for exoskarn development. This is partly because the district was adjacent to the eastern margin of the Triassic Nicola basin where the deposition of carbonates was possible.
- The emplacement, into the reactive sedimentary rocks, of numerous iron-rich intrusions derived from oceanic crust and having a low oxidation state. The stocks were partly controlled by deep structures related to the rifted eastern margin of the Nicola basin, including some easterly striking transform faults, whereas the sill swarms were controlled by the presence of thinly bedded packages such as those in the Hedley Formation.

The Nickel Plate skarn is genetically related to the Toronto stock and its associated swarm of sills and dikes. Magmatic fluids, exsolved from the crystallizing intrusions, migrated upwards and outwards into the host sediments. Fluids were primarily channeled along bedding surfaces, folds and fractures, as well as along the margins of dikes and sills. As they permeated the country rock under pressure, pervasive replacement of the calcareous sediments by skarn gradually proceeded. This resulted in the complete overprinting of the upper parts of the Toronto stock and the adjacent sediments by a massive, subcircular calcsilicate envelope that extended up to 1.5 kilometres from the stock (Figure 25B). The exoskarn envelope reached 300 metres in thickness and involved the formation of an estimated 0.75 to 1.5 cubic kilometres of pyroxene-garnet skarn.

As the Nickel Plate skarn grew in size, a cap of reactive skarn and tactite characterized by fine-grained pyroxene-quartz-orthoclase assemblages developed in the upper part of the envelope (Figure 25B). Previous workers called this barren, upper part of the skarn "the upper silicious beds" (Billingsley and Hume, 1941; Dolmage and Brown, 1945). Carbonate and silica-rich fluids derived from the skarn system were probably driven, under high hydrostatic pressure, up fractures into the overlying country rocks to produce quartz-carbonate veins. No veins are seen above the Nickel Plate skarn because the rocks over the envelope have been removed by erosion. However, the Maple Leaf and Pine Knot veins and those at the Gold Hill and Hed prospects probably resulted from similar processes, indicating perhaps, the presence of skarn at depth.

Loss of heat and fluids above the skarn that accompanied the development of a large thermal convection cell, caused an influx of meteoric water from the country rocks into the base and sides of the envelope (Figure 25D). The reaction between the reduced magmatic skarn fluids and the more oxidized and cooler meteoric waters probably contributed to the precipitation of the sulphides, gold and scapolite close to the base of the envelope (Figure 25C and D).

Initially, the skarn fluids were possibly potassium rich, as suggested by the early growth of biotite and orthoclase. Later however, the system was influenced overwhelmingly by the presence of the calcareous host sediments, to produce massive amounts of calcsilicate.

Fluid inclusion studies (Ettlinger, 1990a; Ettlinger *et al.*, 1992) suggest that the bulk of the skarn silicates formed at temperatures of between 460° and 480°C while precipitation of the scapolite, sulphides and gold took place between 320° to 400°C. Ore mineral assemblages with native bismuth, arsenopyrite and high pyrrhotite/pyrite ratios indicate that the fluids responsible for the Hedley gold skarns were reducing. This conclusion is supported by the low Fe_2O_3/FeO ratios of the Hedley intrusions (Figure 11M) and the pyroxene and garnet compositions of the Hedley skarns (*see* Figure 33).

Microprobe data from the larger garnet crystals also suggest that the fluids present throughout much of the process of prograde skarn formation were reduced, resulting in the crystallization of wide zones of grossularite. The later overgrowth of andraditic garnet may indicate a more oxidized environment due to the influx of meteoric fluids.

The genetic model for the Nickel Plate suggests the following:

- Exploration for deposits similar to the Nickel Plate gold skarn should concentrate in areas along the rifted margins of island arc related basins. Favourable areas are marked by abrupt basin-edge facies changes, calcareous sediments and arc-related, iron-rich, porphyritic and reduced I-type dioritic intrusions.
- At Nickel Plate, the gold, sulphides and scapolite are concentrated in a narrow section close to the bottom and outer edges of the skarn envelope, while the remainder of the skarn tends to be barren (Figure 25). Thus, blind deposits overlain by barren skarn may be common. Because the upper and more silicious exoskarn is relatively impervious to geochemical dispersion, deep drilling with down-hole geophysics may be necessary to determine whether the base of the skarn is mineralized. In Saskatchewan, geobotanical sampling detected uranium orebodies beneath 150 metres of barren sandstone (Dunn, 1981) and similar techniques could perhaps determine whether buried deposits underlie barren exposures of skarn.

FRENCH MINE, (Oregon) (MINFILE 092HSE059)

The abandoned French mine is located approximately 5 kilometres south of the Nickel Plate mine (UTM 5467734 N, 716322 E; Figure 37). It has had a history of intermittent operation; consequently, production figures are uncertain. The British Columbia Geological Survey Branch MINFILE data and National Mineral

Inventory data suggest that between 1950 and 1983, the mine produced 1629 kilograms of gold, 201 kilograms of silver and 20 tonnes of copper from approximately 82 046 tonnes of ore milled (Table 3).

Ore was hosted by limestones, limestone breccias and calcareous, tuffaceous sediments of the French Mine Formation, close to their contact with the Cahill Creek pluton. It is believed to be related to several dioritic dikes and sills of the Hedley intrusions that cut the mine area. Skarn occupies the hinge zone of a faulted anticline, and extends down into the underlying Oregon Claims Formation. At least three sulphide-rich orebodies were discovered (Billingsley, 1936), and an overall increase in the copper/gold ratios is evident towards the lower parts of the deposit. The small, upper orebody had the highest gold grade (two grab samples taken by Billingsley averaged 28 grams gold per tonne) but had less copper and silver. The lowest and largest orebody reached up to 40 metres in length and 3 metres in thickness; six samples collected by Billingsley (1936) averaged 5.5 grams gold and 96 grams silver per tonne and 2.7% copper. Two sulphide-rich grab samples collected from the mine dump during this survey assayed up to 10% copper, 4.2 grams gold and 715 grams silver per tonne, and 0.5% bismuth, and also contained anomalous values of cobalt, antimony and arsenic (Appendix 24A). A good correlation exists between copper and silver, and a poor correlation is seen between copper and gold. Chip sampling along a 35-metre, gold-rich skarn section averaged 0.68% WO_3, with maximum values of 1.3% over 3 metres (Westervelt Engineering Ltd., unpublished report, January 12, 1978).

The French deposit is characterized by arsenopyrite, chalcopyrite, covellite, bornite and pyrrhotite with sporadic pyrite, coarse molybdenite and minor scheelite. Like Nickel Plate, the gold mainly occurs as minute inclusions in the arsenopyrite although, in the lower parts of the deposit, rare coarse visible gold and visible tellurides are present. Bornite forms irregular aggregates and is altered to covellite along microfractures. Chalcopyrite often rims bornite or is concentrated as grains along bornite-garnet contacts.

Skarn alteration is characterized by garnet, clinopyroxene and calcite, with variable amounts of twinned albitic plagioclase, wollastonite, clinozoisite, epidote, biotite, orthoclase, scapolite, tremolite-actinolite, chlorite, axinite and quartz. Mineralogical zoning is recognized on a local scale (Plates 24 and 25); an outer envelope of biotite hornfels passes inwards to a later, crosscutting garnet-pyroxene assemblage.

Two types of garnet are recognized. The youngest, which forms flesh coloured porphyroblasts often associated with cordierite, is most common where the lower

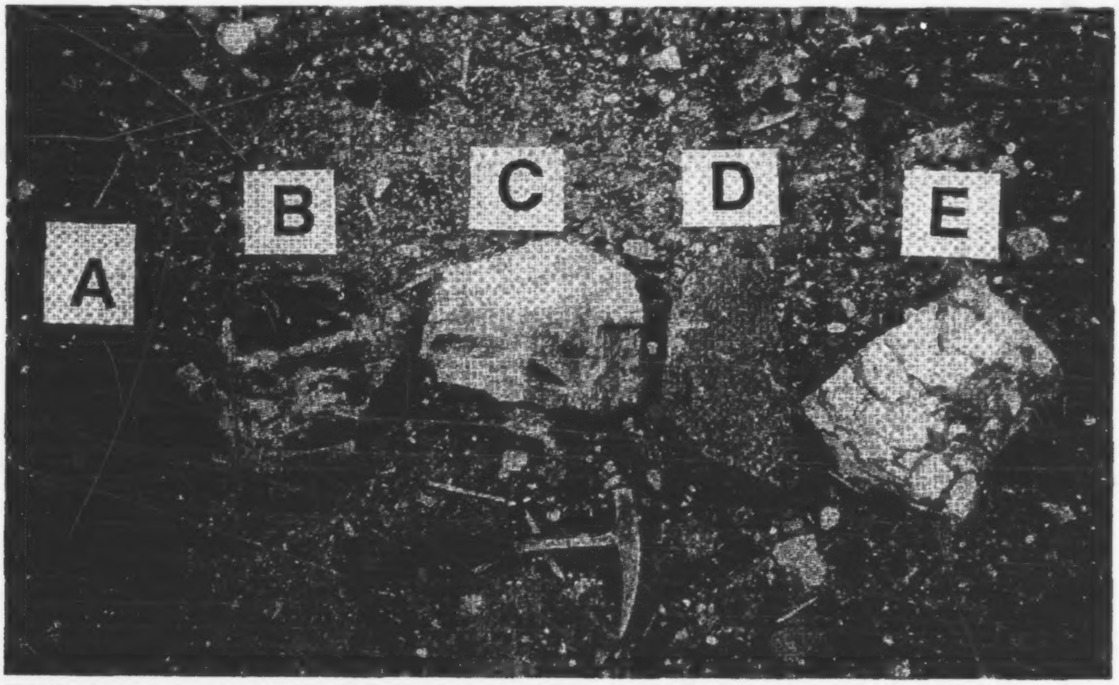

Plate 24. French deposit. Samples illustrating the various mineralogical zones associated with skarn alteration at the French mine (*see* Figures 35 and 36).
A: Massive, purple-brown biotite "hornfels" (Zone 4).
B: Massive biotite "hornfels" cut by veinlets of pyroxene-dominant skarn (Zone 2).
C: Pyroxene-dominant skarn (Zone 2) containing bands of light and dark green pyroxene.
D: Massive, dark brown garnet-dominant skarn (Zone 1).
E: Marble skarn breccia. Intensely skarn-altered limestone breccia comprising marble clasts in a dark brown garnet-dominant matrix.

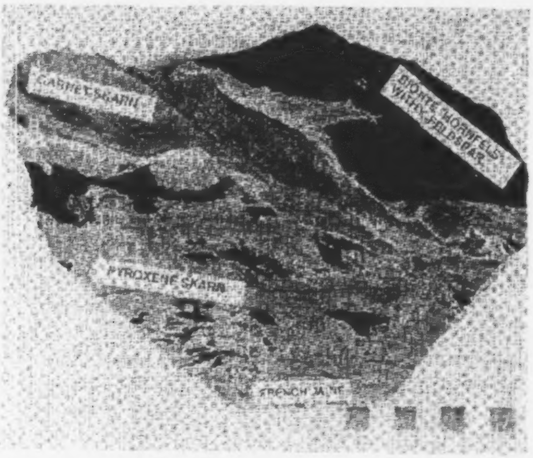

Plate 25. French deposit. Early biotite "hornfels" alteration (Zone 4) (*see* Figures 35 and 36) replaced in turn by clinopyroxene-rich (Zone 2) and garnet-rich (Zone 1) skarn. *Note* vein-like, cross cutting garnet as well as remnant patches of biotite alteration in pyroxene skarn; the latter are surrounded by thin, pink envelopes of orthoclase-rich alteration (Zone 3).

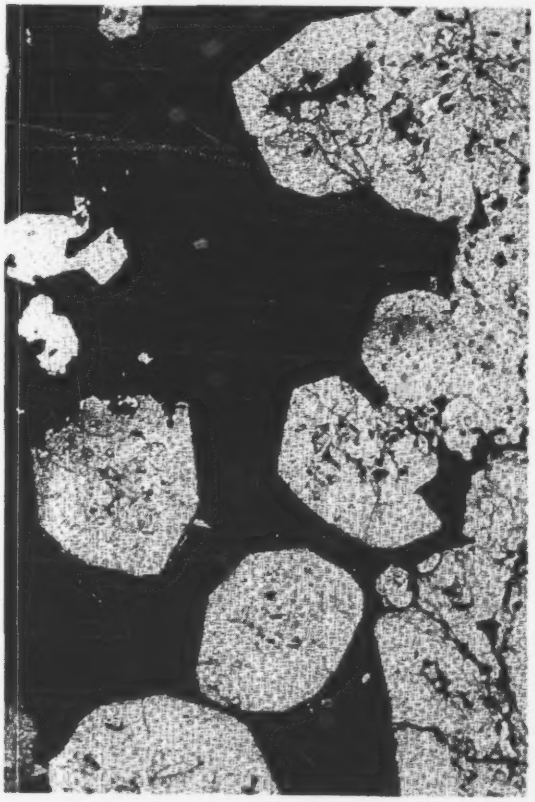

Plate 26. French deposit. Photomicrograph (PPL) of euhedral andraditic garnet enclosed by late chalcopyrite, pyrrhotite and arsenopyrite. Ore zone at French mine (field of view is 2.5 mm wide).

parts of the skarn overprint the Oregon Claims Formation argillites and siltstones; both the cordierite and garnet are believed to be related to thermal metamorphism by the nearby Cahill Creek pluton. The other, older type of garnet is related to skarn formation. Unlike the garnet crystals at Nickel Plate mine, which are commonly birefringent, skarn-related garnets at the French mine tend to be isotropic. They are generally brown and the form single, euhedral crystals (Plate 26), anhedral masses, stratiform bands and irregular or crossutting veins. They commonly contains abundant inclusions of pyroxene, and some are sparsely rimmed and veined with clinozoisite. Microprobe analyses (Figure 26; Appendix 18A)) indicate no systematic compositional zoning present in the crystals. However, the garnets present in the ore zone are strongly enriched in iron, ranging in composition from Ad_{80} to Ad_{100} mole percent; in some ore sections these euhedral andraditic garnets are entirely surrounded by late chalcopyrite (Plate 26). Garnets from veinlets that cut the early biotite-rich hornfels-like alteration in the unmineralized parts of the envelope range from Ad_{13} to Ad_{25} mole percent (Figures 22B and 26).

Pyroxene crystals generally contain less than 0.75% manganese (Figure 20B; Appendix 18B), and show little compositional zoning, commonly ranging from Hd_{63} to Hd_{67} mole percent (Figure 21). Some individual pyroxene crystals, like those in other gold skarns (Ettlinger and Ray, 1989) contain thin zones of aluminum enrichment.

The paragenesis and textures of the skarn minerals at the French mine are similar to those at the Nickel Plate deposit. Biotite and pink orthoclase were among the earliest minerals to develop, followed in turn by pyroxene, garnet, and then the sulphides, scapolite and gold. Extensive biotite overprinting affected some of the hornblende-porphyritic Hedley sills. Orthoclase commonly formed as a reaction product at the contact between the early biotite hornfels and the crosscutting veins of pyroxene. Locally the garnet-pyroxene-carbonate assemblages coexist with masses of finely twinned albitic plagioclase. Sulphides locally replace all skarn minerals except garnet; in some of the ore zones the euhedral andraditic garnets are entirely surrounded by massive sulphides (Plate 26). Minor prehnite rims some of the sulphide grains.

To summarize, the French mine represents the second largest gold skarn deposit in the district, although the volume of alteration and amount of gold production are considerably less than the Nickel Plate deposit. It shows many similarities to Nickel Plate in its mineralogy, geochemistry, and mineral paragenesis, including a local abundance of scapolite. Dissimilarities include the lack of Hedley sill swarms and a greater abundance of chalcopyrite and silver in parts of the deposit, as well as the presence of scheelite and molybdenite. Unlike Nickel Plate skarn, it is locally garnet dominant and the garnet tends to be isotropic.

CANTY MINE (Pittsburg, Boston, Greenwood) (MINFILE 092HSE064)

The Canty property is approximately 2 kilometres northeast of the Nickel Plate mine (UTM 5473628 N, 717538 E; Figure 37). Between 1939 and 1941 approximately 16 kilograms of gold were produced from 1483 tonnes of ore (Table 3).

The geology of the mine area is not well known due to poor exposure. Rice (1947, 1960) briefly described gold-arsenopyrite-rich mineralization in a faulted and folded zone of skarn-altered sedimentary rocks similar to those at the Nickel Plate mine. Our mapping however, shows that the area surrounding the Canty mine is underlain mostly by epidotized and skarn-altered andesitic ash and lapilli tuffs in the lower part of the Whistle Formation. It also indicates that the Canty deposit lies close to the western margin of an extensive, sporadically developed skarn zone (Figure 18). The eastern part of this zone is garnet-dominant whereas the western part, in the vicinity of the gold-sulphide mineralization, is dominated by pyroxene. This suggests that the magmatic source of the skarn lies to the east.

Drilling by Mascot Gold Mines Limited has demonstrated that the protolith of the skarn alteration is Whistle tuffs that are unusual in containing thin limestone-marble-siltstone units (J. Bellamy and R.G. Simpson, personal communications, 1989). Several skarn-altered and bleached hornblende-porphyritic Hedley sills are exposed at surface in the mine area, and these were intersected by drilling.

Underground development in 1939 exposed several ore shoots up to 21 metres long and 6 metres wide, controlled by a fracture zone along a fold hinge. Recent drilling has outlined reserves of approximately 328 000 tonnes grading 5.1 grams per tonne gold.

The ore tends to be more sulphide-rich than at Nickel Plate. Metallic minerals include arsenopyrite, pyrite, chalcopyrite, pyrrhotite and native bismuth. A mineralized grab sample from the mine dump assayed 34 grams per tonne gold, 0.6% cobalt and almost 29% arsenic (Appendix 24A); it also contained anomalous values of antimony and molybdenum.

Alteration assemblages include abundant clinopyroxene, calcite and scapolite, with lesser garnet, albitic plagioclase, potassium felspar, biotite and chlorite. The brown garnets, like those at the French mine, are commonly isotropic although small, birefringent crystals are locally numerous. They contain abundant fine inclusions and occasionally form irregular, wormy growths through the carbonate. Microprobe analyses indicate they, like other skarn garnets in the district, have a low manganese content (Figure 22C; Appendix 19A). However, there is very little compositional variation across individual garnet crystals (Figure 26C and D); 65 core-to-rim analyses on eight garnet crystals range from Ad_{29} to Ad_{53} mole percent, and average Ad_{41} mole percent.

Clinopyroxene forms small anhedral grains except where in contact with carbonate. It has a low manganese content (Figure 20C; Appendix 19B) and shows little consistent compositional zoning (Figure 21F and G). Sixty core-to-rim analyses on eleven crystals averaged Hd_{71} mole percent and range from Hd_{64} to Hd_{80} mole percent. As at the French mine, some rare pyroxene crystals contain thin zones of aluminum enrichment (Ettlinger and Ray, 1989).

GOOD HOPE MINE (MINFILE 092HSE060)

The Good Hope gold skarn is exposed 4 kilometres southeast of the Nickel Plate mine (Figure 37; UTM 5469293 N, 717689 E), within the same flat-lying stratigraphic package of marbles and metasedimentary rocks that hosts the French mine deposit. Intermittent open-pit mining in the 1940s and in 1982 reportedly resulted in the total production of 166 kilograms of gold, 119 kilograms of silver and 602 kilograms of copper from 11 115 tonnes of ore (Table 3).

At the mine, a marble unit of the French Mine Formation, 1 to 2 metres thick, overlies a 1 metre wide Hedley diorite sill; this in turn is underlain by altered tuffaceous sediments. Garnet-rich skarn is developed along the marble-sill contact. In addition, a sill and some small irregular bodies of Cahill Creek plutonic rocks occur in the vicinity of the deposit.

The ore zone is approximately 1 metre thick and up to 55 metres long (B.C. Minister of Mines Annual Report 1947, page A143). The ore consists of disseminated to massive arsenopyrite and pyrrhotite, with sporadic chalcopyrite and pyrite, and trace native bismuth, native gold, molybdenite, hedleyite, scheelite, and magnetite. The 1947 report states that small grains of gold were seen along crystal cleavages in pyroxene and coarse calcite, and that the deposit had an average grade of 21 grams per tonne gold. A mineralized grab sample collected during this survey assayed 94 grams per tonne gold and 0.47% bismuth, as well as containing anomalous antimony (Appendix 24A).

In some aspects the Good Hope skarn resembles the Nickel Plate system in being enriched in gold, arsenic and bismuth, yet it also shows some similarities to the gold-poor Mount Riordan skarn 8 kilometres to the northeast. These include sporadic presence of scheelite and magnetite, and the presence of coarse, euhedral, variably coloured garnet crystals. In contrast to the Nickel Plate skarn, which is pyroxene dominant, the skarns at Good Hope and Mount Riordan are garnet rich. This probably reflects different protoliths with pyroxene-dominant skarn forming in siltstones at Nickel Plate and garnet-dominant skarn at Good Hope and Mount Riordan forming in a massive limestone protolith. The garnets at Good Hope are mostly reddish brown, but some amber and dark brown to black varieties were noted. Like the garnets at Mount Riordan and unlike those at Nickel Plate and Canty, they can occur as subhedral to subhedral crystals.

Pyroxenes at Good Hope occur either as small inclusions within garnet and carbonate (Plate 27) or as large, tabular, optically twinned, euhedral crystals of hedenbergite that reach 15 centimetres in length.

A mineralogical zoning is recognized that differs from that seen in the other skarns in the district. Passage from the biotite-altered dioritic sills to massive marble is marked by the following zones:

1. intrusive sill (endoskarn).
2. fine to medium-grained clinopyroxene-dominant exoskarn.

3. garnet-dominant exoskarn.
4. very coarse hedenbergite-rich exoskarn with sulphides and gold.
5. jasperoid.
6. marble.

The garnets and pyroxenes at Good Hope are the only ones in the Hedley area that show some late alteration, being partially replaced by a dark green amphibole. Garnet forms as subhedral to euhedral crystals up to 1.5 centimetres in diameter that are markedly birefringent and sector twinned; rarely, crystals contain small isotropic cores, and some individual garnets have alternating zones of inclusion-rich and inclusion-free material. Many garnets are intensely fractured, and some of the garnet-rich skarn is cut by sub-vertical quartz-carbonate veins, up to 5 centimetres thick, that are rimmed with narrow alteration zones of black tremolite and chlorite.

Microprobe analyses of pyroxenes and garnets from the Good Hope mine show they are manganese-rich relative to those in other Hedley skarns (Figures 20D and 22D). Sixty-eight core-to-rim analyses on seven garnet crystals indicate they range from Ad_7 to Ad_{33} mole percent and average Ad_{25} mole percent, and representitive microprobe analyses are presented in Appendix 20A. Individual crystals show very little compositional variation, despite the presence of optical zoning (Figure 26); they usually contain less than 11 mole percent pyralspite (pyrope+almandine+spessartine) but some contain narrow growth zones of manganese enrichment marked by up to 45 mole percent pyralspite.

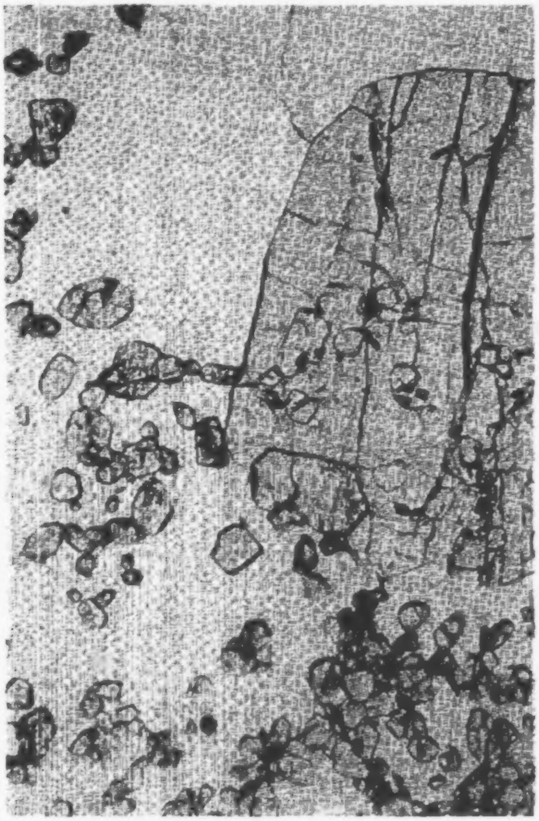
Plate 27. Good Hope deposit. Photomicrograph (PPL) of small, subhedral hedenbergitic pyroxene overgrown by a large garnet crystal and carbonate (field of view is 2.5 mm wide).

The pyroxenes at Good Hope are distinct, not only because some are coarse and tabular, but also due to their relatively high hedenbergite-johannsenite solid solution (Figure 20D), which is similar to the pyroxenes described in some tungsten skarns such as the Kagata deposit in Japan (Nakano, 1991). One hundred and one core-to-rim analyses across fifteen pyroxene crystals from Good Hope indicate they average Hd_{88} mole percent, and range from Hd_{79} to Hd_{95} mole percent, and up to Jo_{23} mole percent; representative microprobe analyses are presented in Appendix 20B. The pyroxenes generally exhibit little compositional zoning (Figure 21).

PEGGY (Hedley Amalgamated) (MINFILE 092HSE066)

The Peggy property is located close to the top of the southeastern ridge of Stemwinder Mountain, approximately 1.6 kilometres northwest of Hedley (Figure 37; UTM 5472804 N, 711850 E). The No. 1 and No. 2 level adits of the Hedley Amalgamated mine workings are on the southwest side of the ridge, at an elevation of approximately 1140 metres; these adits are 230 and 120 metres in length, respectively. Another working, the McKinnon adit is approximately 550 metres farther south-southwest and the short Rawhide and Cyclone exploration adits are on the northeast side of the ridge.

The Peggy - Hedley Amalgamated prospect was explored in the 1930s and the property is of historic interest because in 1937 it was the subject of a scandal involving charges of assay salting and stock fraud (Cruise and Griffiths 1987); a subsequent enquiry confirmed these charges.

The property lies close to the intrusive contact between the Stemwinder quartz diorite stock and steep, northwesterly dipping calcareous siltstones, argillites and thin limestones of the Chuchuwayha Formation. The sediments are also cut by several sills of altered Hedley diorite. The No. 1 adit follows the upper margin of a sill above which is developed a zone with massive sulphide mineralization; this zone reaches 1 metre in width and 67 metres in length. The No. 2 adit follows a fault zone which hosts some massive sulphides. Mineralization is both lithologically and structurally controlled and has been affected by faulting. It includes abundant arsenopyrite with pyrrhotite, marcasite, crystalline and botryoidal pyrite, and traces of chalcopyrite, covellite, sphalerite, ilmenite and magnetite. Several generations of pyrite are present and the chalcopyrite is rimmed and partially replaced by covellite. Sulphides are disseminated throughout the garnet-pyroxene exoskarn, although the richer, more massive mineralization is concentrated along fault zones. Some minor, narrow quartz veining is also present.

Twenty three channel samples from the Nos. 1 and 2 adits, totalling 12 metres in length, averaged 8.3 grams per tonne gold. The best sample returned values of 29 grams per tonne gold over 55 centimetres (B.C. Minister of Mines Annual Report 1947, page A150). Three grab samples of sulphide-rich material collected from the dump outside the Nos. 1 and 2 adits during this survey returned assays ranging up to 21 grams gold per tonne, 1.18% copper, and 0.76% arsenic (Appendix 24A); no anomalous bismuth or antimony values were recorded.

Gold at the Nos. 1 and 2 adits, together with tellurides, occurs as micron-sized inclusions within arsenopyrite (Webster, 1988); the arsenopyrite also contains pyrrhotite inclusions and Webster notes that gold tends to be more abundant where magnetite is more common. Gold also occurs interstitial to arsenopyrite in supergene enrichment zones containing goethite and maghemite (a strongly magnetic spinel of the magnetite series).

The Rawhide adit was driven along the contact between a thin, massive limestone bed and a Hedley sill. Mineralization at the contact is generally less than 1 metre thick and comprises arsenopyrite, pyrrhotite, chalcopyrite, minor pyrite and trace gold in a gangue of calcite, garnet, epidote and clinopyroxene. Mineralization at the McKinnon adit includes pyrrhotite, arsenopyrite and minor pyrite, with weak skarn alteration in a mafic Hedley intrusion. A mineralized grab sample from the dump outside the adit assayed 5.8 grams gold per tonne and 1.5% arsenic, and is enriched in cobalt (Appendix 24A). At the Cyclone adit, minor skarn alteration with arsenopyrite is developed in a limestone bed.

The mineralogy and textures of the skarns at the Nos. 1 and 2 adits closely resemble the Nickel Plate skarns; they are pyroxene dominant and the pyroxenes are generally fine grained and anhedral. Most of the garnets are brown and optically birefringent, but some contain small, irregular isotropic cores similar to those seen at the Nickel Plate deposit. Some crystals are weakly optically zoned and the abundant fine inclusions are preferentially concentrated in specific zones. Other minerals present include carbonate, quartz, scapolite, epidote, wollastonite, sericite, chlorite, orthoclase and prehnite. Despite some optical zoning, microprobe analyses indicates little compositional zoning in the garnets (Figure 26G).

Both the garnets and pyroxenes at the Hedley Amalgamated Nos. 1 and 2 adits have a low manganese content similar to those at Nickel Plate. Twenty-nine core-to-rim analyses on six garnet crystals indicate they average Ad_{53}

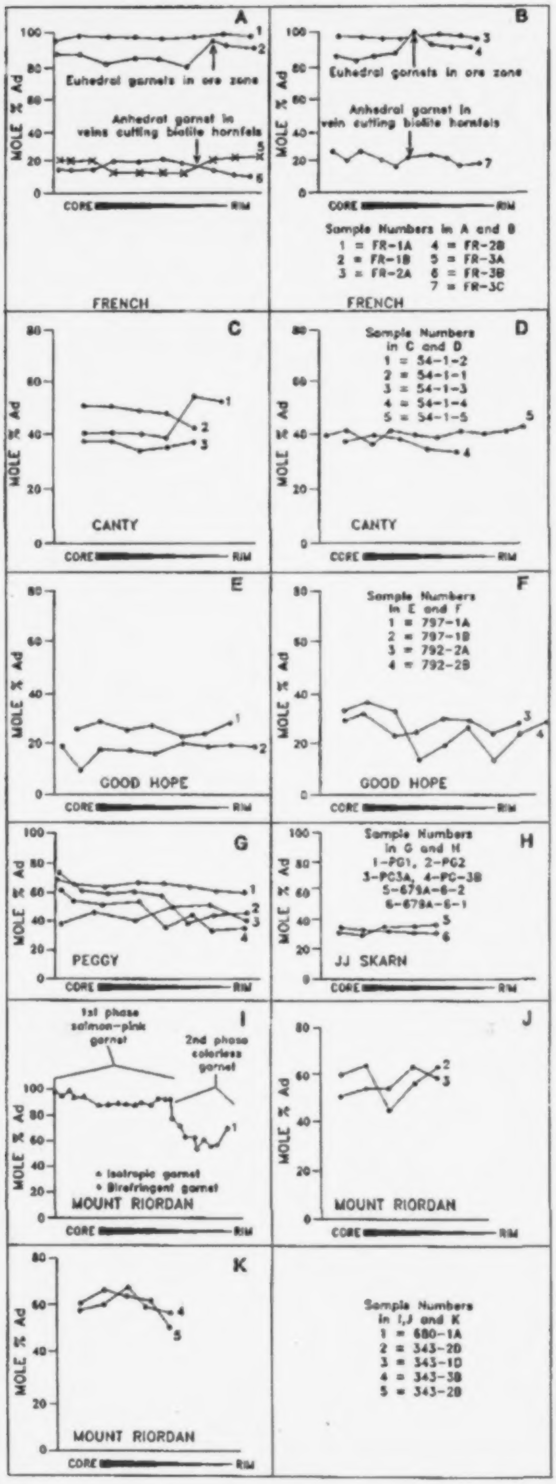

Figure 26. Compositional variation (expressed as mole% andradite) across individual garnet crystals from Hedley skarns. A and B. French deposit. Note differences between euhedral garnets in mineralized skarn and anhedral garnet veins in unmineralized biotite "hornfels". C and D.: Canty deposit. E and F. Good Hope deposit. G. Peggy. H. JJ skarn. I. Mount Riordan; large crystal with first phase isotropic cores and second phase birefringent margins. J and K. Mount Riordan: small crystals of birefringent, second phase garnet.

mole percent, and range from Ad_{30} to Ad_{70} mole percent. Thirty-eight analyses on seven pyroxene crystals show they range from Hd_{76} to Hd_{85}, and average Hd_{82} mole percent. Representative core-to-rim microprobe analyses of garnets and pyroxenes from the Peggy skarn are presented in Appendices 21A and B).

MOUNT RIORDAN (Shamrock, Billie Goat, Crystal Peak, Garnet, Polestar; MINFILE 082ESW102) AND PATRICIA (MINFILE 082ESW107)

The Mount Riordan and Patricia properties are located on Mount Riordan, approximately 7 kilometres east-northeast of the Nickel Plate mine (Figure 38) at UTM 5475011 N, 287347 E. They are associated with the Mount Riordan skarn which represents the largest garnet-dominant skarn in the Hedley district. The Shamrock, Billie Goat and Patricia prospects cover areas containing minor chalcopyrite and scheelite mineralization, while the Mount Riordan, Crystal Peak Garnet, and Polestar properties have recently been explored for their industrial garnet potential by Polestar Exploration Inc.

Apart from the skarn, which is widely exposed on the summit and flanks of Mount Riordan, rocks in the surrounding area are poorly exposed. The Mount Riordan stock (Unit 11) lies immediately northeast and east of the skarn while to the south, and presumably separated from the skarn by a fault, is the Apex Mountain Complex (Unit 1). The skarn is believed to be genetically related to the adjacent Mount Riordan stock, and the minor remnants of altered microgabbro in the skarn (Figure 27) possibly represent apophyses or dikes from the stock.

On and around Mount Riordan, the skarn reaches 900 metres in length and is exposed over a 0.3 square kilometre area (Figure 27), although discontinuous and small outcrops of skarn extend in a westerly direction for 1.5 kilometres.

Early exploration in the area was primarily concentrated on the sulphides and scheelite occurrences close to the summit of Mount Riordan; in the 1890s, several Crown-granted mineral claims were awarded. Bulk sampling of the sulphide showings took place in the 1950s, and McCammon (1954) described the scheelite-sulphide occurrences. However, relatively little exploration work was done until the 1980s. While conducting exploration drilling for gold east of Nickel Plate Lake, Canova Resources Ltd. intersected skarn up to 150 metres thick with minor lenses of unaltered sedimentary rocks (Shaw, 1985). The large size of this garnet-dominant skarn was revealed by geological mapping (Ray and Dawson, 1988; Ray *et al.*, 1988), and in 1989 Polestar Exploration Inc. acquired the property. Forty-one diamond-drill holes, totalling 1606 metres, were completed by Polestar to outline the size, continuity, and quality of the skarn as a potential source of industrial abrasive garnet. Within the main skarn, drilling outlined three high-grade zones – the North, West and South zones (Figure 27) that contain 60 to 100% garnet. The true thickness of these zones is unknown although drilling indicates they are at least 70 to 90 metres thick; one longer hole was stopped in garnet-rich skarn at a depth of 175 metres.

Details on the company's work together with the metallurgy, mineral processing, proposed production and physical properties of the garnet are given by Mathieu *et al.* (1991) and Grond *et al.* (1991). Drill-indicated reserves for the three zones total 40 million tonnes averaging 78% garnet. The proposed open pit area in the North zone contains 3.35 million tonnes with a slightly higher average grade of 81.3% garnet. An additional possible geological reserve of 60 million tonnes of high-grade garnet is calculated to be present.

Almost no original sedimentary structures are recognizable in the massive garnet skarn, although rare, sharply defined and gently dipping layers of different coloured garnet are present; these probably represent relict sedimentary bedding. In some outcrops the pale-coloured garnet matrix contains elongate "clasts" of dark brown garnet up to 1 metre long and 0.2 metre wide. These clasts have sharp boundaries and may represent remnant limestone breccia or conglomeratic textures similar to those seen elsewhere in parts of the unaltered French Mine Formation.

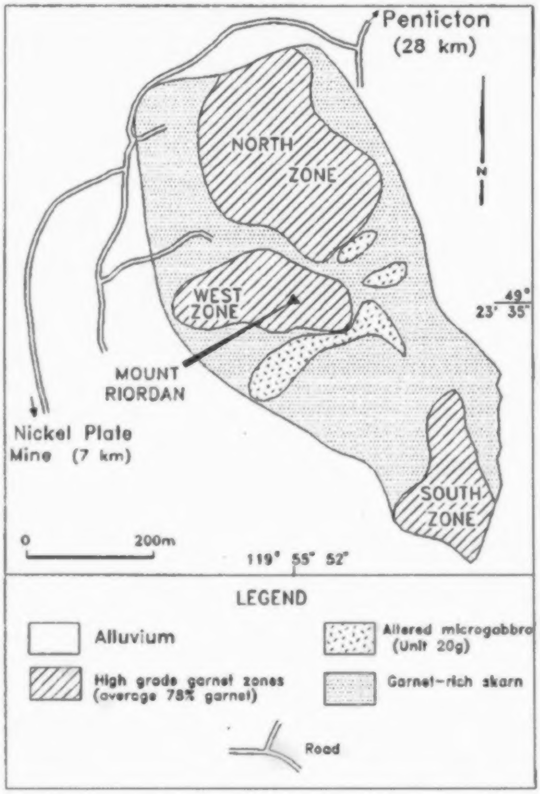

Figure 27. The Mount Riordan skarn showing location of the North, West and South zones of high-grade garnet. Data from Polestar Exploration Inc.

Apart from rare, thin horizons of gently dipping marble, the alteration to skarn is so intense that the protolith is uncertain. However, the general low titanium content of the Mount Riordan garnets (< 0.05 wt % TiO_2) suggests a limestone protolith, and we believe the skarn has replaced a massive unit of limestone that included some carbonate breccias; the French Mine Formation elsewhere in the district contains these lithologies and is considered to be the most likely host sequence for the deposit.

MINERALOGY OF THE MOUNT RIORDAN SKARN

Unlike many of the gold skarns in the district, neither garnet-pyroxene mineralogical zoning, early biotite-orthoclase assemblages nor scapolite alteration are seen at Mount Riordan. Throughout the skarn, garnet commonly makes up from 60 to 100% by volume of the rock with lesser amounts of pyroxene, actinolite, epidote, quartz and calcite.

Differences in grain size and colour of the garnets are noted in the three high-grade garnet zones (Mathieu *et al.* 1991). Garnets in the North and West zones (Figure 27) tend to be extremely variable in size and colour. Large garnets, up to 10 centimetres across and with prominent growth zonations, are enclosed in a matrix of smaller crystals. In hand specimen, the crystals in the North and West zones, vary in colour from green and yellow-green to black and brown. Pyroxene is the main accessory mineral in these zones where it averages 11% by volume (Grond *et al.*, 1991). Garnets in the South zone tend to be more uniform in size and colour, averaging 1 centimetre in diameter and generally orange-red in hand specimen. Retrograde alteration is more prevalent in the South zone where the pyroxene is replaced extensively by tremolite-actinolite, which forms up to 6% by volume.

Grond *et al.* (1991) note that the North zone averages just under 80% by volume garnet, 11% pyroxene, 2.5% quartz, 1.8% calcite and approximately 5% combined amphibole, epidote and sericite. Magnetite and sulphides generally make up less than 0.45% by volume. Other rare accessories in the deposit include plagioclase, orthoclase, sphene, apatite, chlorite, axinite, idocrase and wollastonite.

Locally, particularly near the summit of Mount Riordan, the skarn is cut by veins, up to 1 metre thick, of white quartz and coarsely crystalline calcite that contain sporadic scheelite. In some veins where the quartz and carbonate are intergrown, the quartz forms elongate, well-terminated crystals up to 3 centimetres long.

Thin section studies and electron microprobe analyses indicate that two chemically and optically distinct types of garnet are present, each representing different phases of crystal growth. The earliest phase is isotropic, and under plane polarized light is seen to be an optically zoned, salmon-pink garnet that contains inclusions of quartz and pyroxene. The second phase, which forms the bulk of the deposit and is more commonly birefringent, is represented by clear, euhedral to subhedral crystals that rarely contain inclusions and exhibit little or no optical or chemical zoning. In many of the larger crystals the early phase is preserved as dark, irregular and isotropic cores that are overgrown by colourless, birefringent, euhedral and sector-twinned second generation garnet (Plate 28).

Electron microprobe analyses indicate that the garnets, like those in most of the Hedley gold skarns, are grandites with a very low manganese content (Figure 22F; Appendix 22A). Analyses show the early pink garnets are andraditic and iron rich (averaging Ad_{90} mole percent) while the younger colourless garnets are more grossularitic and range from Ad_{45} to Ad_{65} mole percent (Figure 22F). The analytical results of microprobe traverses across a large, optically zoned crystal containing both the first and second phases of garnet are presented in Figure 26I while those across crystals containing only second phase material are plotted in Figures 26J and K. The zoning in Figure 26I, from andraditic centres to more grossularitic margins, is opposite to that seen in garnets at the Nickel Plate gold skarn (Figure 24).

Pyroxene is present either as inclusions within the first generation garnet (Plate 28) or as small discreet and clear crystals intergrown with garnet, quartz or calcite; it is commonly altered partially to amphibole and chlorite.

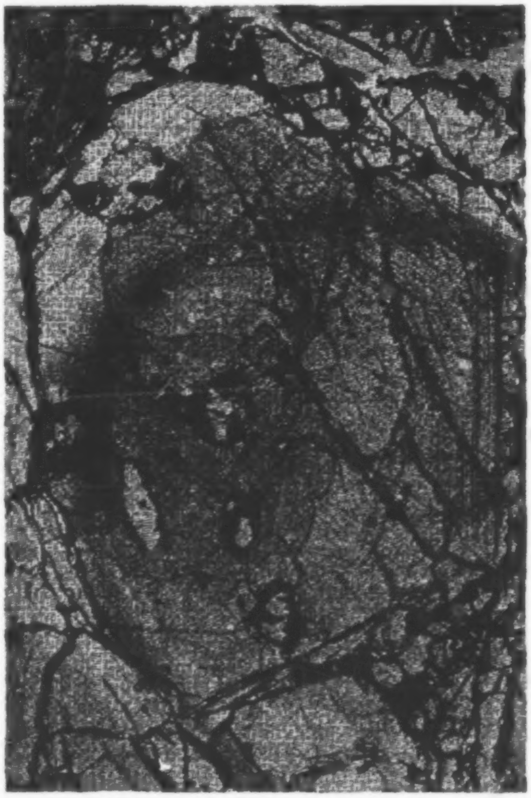

Plate 28. Mount Riordan skarn. Photomicrograph (PPL) of garnet with salmon-pink, isotropic cores and clear, isotropic margins. Results of a tracked microprobe analysis across these crystals are seen in Figure 26I (field of view is 2.5 mm wide).

Microprobe analyses indicate that the pyroxenes at Mount Riordan, like those in most of the gold skarns, contain less than 1.3 weight percent MnO (Appendix 22B). The pyroxene crystals show no marked optical or chemical zoning (Figure 21P and 21Q) and range from Hd_{41} to Hd_{51} mole percent (Figure 20E).

The massive garnet skarn is generally barren of sulphide and other opaque minerals but locally contains small, isolated pockets of magnetite intergrown with variable and minor amounts of pyrrhotite, pyrite, chalcopyrite, scheelite and trace bornite. Chalcopyrite commonly rims garnet, separating it from either massive pyrrhotite or coarse euhedral pyrite. Magnetite is locally abundant (up to 20% by volume), particularly in a short exploratory adit on the east side of the mountain and in the small westernmost isolated outcrop of garnet skarn. Scheelite, which shows no apparent spatial association with the sulphide minerals, is present in two forms. The more common, and paragenetically earliest, forms small crystals, generally less than 1 millimetre across, either sparsely disseminated or clustered in zones throughout the garnet skarn. The other, possibly later generation, occurs as coarse blebs, crystalline masses, and irregular veinlets up to 5 centimetres wide and 30 centimetres in length. This coarse scheelite is usually associated with quartz and calcite veins, and is best exposed in several old trenches close to the summit of the mountain. The scheelite in these workings is associated with minor powellite and axinite, and the sulphide minerals are extensively weathered to jarosite.

Analyses of sulphide and magnetite-rich grab samples are presented in Appendix 24B; values of up to 5% WO_3, 0.7% copper, 310 ppm molybdenum, 19 ppm Ag and 0.1% zinc were recorded. Gold contents are generally low although one magnetite-rich, pyrrhotite and chalcopyrite-bearing sample collected from the old exploratory adit southeast of Mount Riordan assayed 1.6 grams per tonne gold. Unlike the gold skarns, sulphide minerals at Mount Riordan are not enriched in arsenic, cobalt and bismuth.

MINOR SKARN OCCURRENCES

DON and SPECULATOR (MINFILE 092HSE051)

The Don and Speculator occurrences lie close to one another on the southern slopes of the ridge between Johns and Larcan creeks, approximately 4.5 kilometres east of Skwel-Kwel-Peken Ridge (UTM 5462610 N, 712767 E). They are hosted by northerly striking, steep westerly dipping calcareous siltstone and thick limestone and marble beds of the Hedley Formation, close to the western margin of the Cahill Creek pluton. The sedimentary rocks are intruded by several Hedley sills, and the whole package has been thermally overprinted by the nearby Cahill Creek pluton.

The Don showing, which is exposed in shallow trenches, is close to the pluton. Silicified and folded beds of marble contain minor amounts of arsenopyrite, pyrrhotite and chalcopyrite. Several large open cuts have been put down on the Speculator prospect. They expose strongly altered Hedley sills that carry variable quantities of pyrrhotite and traces of arsenopyrite. One fractured and faulted sill, 6 to 8 metres wide, is traceable along strike for about 100 metres. Massive to weakly disseminated mineralization is concentrated in the sill but is generally absent in the wallrocks; it includes pyrrhotite and arsenopyrite with variable amounts of pyrite and trace gold (up to 0.3 gram per tonne). The wallrocks are intensely bleached and silicified. They contain quartz, pyroxene, carbonate and trace garnet with minor pyrrhotite.

In 1987 and 1988, Chevron Minerals Ltd. drilled into skarn-altered rocks close to the Larcan stock approximately 1 kilometre west of the Speculator occurrence. This drilling was on property Chevron Minerals called "the Lost Horse claims" which should not be confused with the Lost Horse occurrence (MINFILE 092HSE050) 2.5 kilometres farther southwest at UTM 5461266 N, 709680 E. The area explored by Chevron Minerals is underlain by a swarm of southerly striking Hedley sills that are associated with extensive alteration and bleaching. This alteration is characterized by minor amounts of coarse pyroxene-garnet-scapolite-wollastonite-carbonate exoskarn alteration as well as purple-brown biotite alteration and silicious, fine-grained pyroxene-orthoclase-quartz assemblages that are mottled pink and green in colour. Alteration has been traced discontinuously for over 2.5 kilometres southwards from the Larcan stock to the south-facing slopes of the Paul Creek valley in Ashnola Indian Reserve No.10. Generally, the alteration zone overprints the Hedley Formation but locally, particularly to the south, it extends up into the Whistle Formation. Numerous old pits and trenches have been dug along this zone of alteration, particularly where pyrrhotite and arsenopyrite mineralization occurs. The drilling by Chevron Minerals intersected endoskarn and garnet-pyroxene exoskarn containing abundant scapolite with albitic plagioclase, tremolite, idocrase, pyrrhotite, pyrite and rare arsenopyrite and chalcopyrite (Duba *et al.*, 1988). Like Nickel Plate, the scapolite was late and associated with the sulphides. Late prehnite was also identified. Gold values are generally low; one sample from a trench assayed 5.4 grams gold per tonne, and values up to 1 gram gold per tonne were obtained in drill-core samples. The style of alteration in this area closely resembles the upper barren portion of the Nickel Plate envelope. Thus, this area has good economic potential because the westerly dipping zone of alteration may overlie gold-bearing mineralization developed close to the base of the skarn, similar to that at Nickel Plate.

DUFFY (MINFILE 092HSE063)

The Duffy occurrence was not examined during this survey; it reportedly lies north of the Toronto stock, close to but west of the Bradshaw fault at UTM 5473120 N, 713579 E. In the 1920s some exploration work consisting of open cuts and short tunnels and shafts was completed. Garnet-pyroxene skarn assemblages overprint a mixed sequence of pyroclastic and limy sedimentary rocks of the Chuchuwayha Formation that are intruded by sills of Hedley intrusions. Arsenopyrite and pyrrhotite replacements of limestone contain traces of gold, silver and copper. Five grab samples collected in 1926 had assays of 0.6 to 7.9 grams per tonne gold and trace to 1.16% copper (B.C. Minister of Mines Annual Report 1926, page A217).

FLORENCE (MINFILE 092HSE061)

The Florence prospect was not examined during this survey. It reportedly lies on the south side of Aberdeen Ridge, close to the Bradshaw fault, at approximately UTM 5473981 N, 713909 E. Mineralization is hosted by thin limestones, presumably belonging to the Chuchuwayha Formation, where they are intruded by Hedley gabbroic to dioritic sills. Some exploration tunnels have been driven on the property (Camsell, 1910) and the skarn mineralization includes arsenopyrite, pyrrhotite, rare chalcopyrite and sphalerite and some gold (B.C. Minister of Mines Annual Report 1916, page K206).

HEDLEY NORTH (South Corrall) (MINFILE 092HSE156)

The Hedley North prospect is reportedly situated about 3 kilometres east-southeast of Hedley at UTM 5470421 N, 715068 E, close to the northeast margin of the Cahill Creek pluton; Hedley Formation siltstone, conglomerate, limestone and some Hedley sills underlie the area. Exploration work includes trenching and one exploratory adit (Di Spirito *et al.*, 1986). Several skarn occurrences with garnet-pyroxene-carbonate-scapolite assemblages are present; they carry pyrrhotite and arsenopyrite with traces of pyrite, galena, sphalerite and chalcopyrite. MINFILE reports that at one occurrence, the South Corrall trench, a grab sample assayed 0.12 gram gold per tonne and 1.8% copper.

JJ (MINFILE 082ESW114)

The JJ occurrence is located approximately 2.5 kilometres northwest of Mount Riordan at UTM 5476051 N, 289713 E. It is hosted by superacrustal rocks that occupy a northeast-trending roof pendant within the Bromley batholith. This pendant is about 3.5 kilometres long; its northwest margin is intruded and hornfelsed by the batholith while its southeast contact is apparently faulted against deformed rocks of the Apex Mountain Complex. The pendant consists largely of hornfelsed, schistose and strongly foliated ash tuffs but it also contain thin beds of marble and conglomerate; these are cut by granodiorite and diorite dikes that are presumably related to the Bromley batholith. It is uncertain whether the metasedimentary rocks and tuffs belong to the Whistle or Oregon Claims Formation.

Disseminated pyrite and trace pyrrhotite, arsenopyrite and chalcopyrite are present in both the schistose sediments and the granodiorite; no gold is reported. Two sulphide-rich grab samples assayed less than 20 ppb gold and up to 280 ppm copper (Appendix 24A); one sample was moderately enriched in zinc (605 ppm) and arsenic (1200 ppm). Locally, extensive, coarse-grained garnet-epidote-wollastonite-pyroxene skarn and lesser amounts of massive garnet-rich skarn are developed in the marbles; much of this probably represents reactive rather than infiltration skarn. The brownish pink garnets form anhedral to euhedral crystals that are generally isotropic; they lack both inclusions and optical zoning. Microprobe analyses of individual garnets indicate very little variation in composition from core to rim (Figure 26H); they are grossularitic, have a low manganese content and range in composition from Ad$_{23}$ to Ad$_{34}$ mole percent (Figure 22G; Appendix 23).

KEL (MINFILE 92HSE090)

The Kel occurrence is located at the extreme southern edge of the map area, on Paul Creek (UTM 5457232 N, 712011 E). The area is poorly exposed and its geology not clearly understood. It appears to be mainly underlain by the Cahill Creek pluton which, in the vicinity of the occurrence, contains large screens of hornfelsed argillite and tuffaceous and calcareous sedimentary rocks; the latter presumably belong to the Whistle Formation. The screens are cut by numerous large granodiorite dikes from the surrounding Cahill Creek pluton. Fine-grained biotite hornfels and pyroxene-skarn alteration overprint both the metasedimentary rocks and the dikes Trenches expose exoskarn with arsenopyrite, pyrrhotite and minor pyrite. The sulphides occur as disseminations and stratiform masses up to 20 centimetres thick. A mineralized grab sample taken from one trench assayed 1.1 grams gold per tonne, 0.13% copper and 2.69% arsenic (Appendix 24A).

KINGSTON (MINFILE 092HSE062)

The Kingston prospect, with an exploratory adit and shaft, is located on the western slopes of Nickel Plate mountain, south of the Toronto stock, at UTM 5471817 N, 713919 E. The area is underlain by gently dipping calcareous and tuffaceous siltstones and limestone interbeds of the Hedley Formation which are cut by numerous Hedley gabbro and quartz diorite dikes and sills. Several areas of exoskarn alteration are developed adjacent to some intrusions, and Camsell (1910) noted two types of skarn mineralization, namely gold-rich and copper-rich. The latter is developed in altered limestones, principally on the Warhorse claim; it carries minor gold values with abundant pyrrhotite and variable amounts of chalcopyrite, arsenopyrite and galena. Camsell (1910) reported that "an average sample of the ore on the dump of the Warhorse will give about 6% copper." He also noted that this mineralization carries some of the highest silver values in the district (up to 350 g/t Ag): this reemphasises the strong association between copper and silver in the Hedley skarns. The gold-rich skarns are found mainly within 65 metres of intrusive contacts. Thin section examination of samples collected during this study indicates the presence of brown garnet, clinopyroxene, variable amounts of scapolite and trace apatite. Arsenopyrite and chalcopyrite with minor pyrrhotite are the principal sulphides.

Showings on the Metropolitan claim (which was not examined during this survey) contain both reddish and greenish coloured garnet with arsenopyrite, minor chalcopyrite and some surface oxidation with free, secondary gold (Camsell, 1910). The gold forms small thin flakes along microfractures cutting exoskarn.

LOST HORSE (MINFILE 92HSE050)

The Lost Horse occurrence is located about 1.9 kilometres southeast of Skwel-Kwel-Peken Ridge at UTM 5461266 N, 709680 E. The area surrounding the occurrence is underlain by strongly altered, fine and coarse-grained tuffaceous sediments of the Whistle Formation; less than 200 metres west of the showing these rocks are faulted against the Skwel Peken Formation. The Whistle rocks are folded, cut by narrow Hedley dikes and overprinted by patchy, fine-grained, pale green pyroxene and dark brown biotite hornfels. Minor coarse-grained garnet skarn is also present. Shallow trenches expose pale, fine-grained pyroxene alteration cut by veinlets of pyrrhotite, arsenopyrite and minor pyrite. Traces of silver and gold up to 0.4 gram gold per tonne are reported in mineralized grab samples (Rice, 1947).

SWEDEN (Boundary Zone, Galena Pit) (MINFILE 092HSE086)

Several prospects are known on the Sweden reverted Crown-granted claim (Lot 425), located about 1.6 kilometres east of Hedley (UTM 5470883 N, 713914 E). Past work includes trenching and sinking the 5-metre-deep Sweden shaft. The area is underlain by limestone and siltstone belonging to the upper part of the Hedley Formation as well as a small outlier of Copperfield breccia and Whistle Formation tuffs. The sedimentary rocks dip moderately north and are cut by numerous bleached Hedley sills. Locally, the country rocks are intensively bleached and altered to fine-grained pyroxene and biotite hornfels and coarse garnet-pyroxene-scapolite-carbonate skarn.

At the Sweden shaft the coarse garnet skarn contains massive pyrrhotite with traces of pyrite, arsenopyrite and chalcopyrite. These minerals are also seen in a trench east of the shaft, together with a zone of magnetite-rich skarn. About 175 metres northwest of the shaft, the Copperfield breccia is overprinted with fine-grained pyroxene-quartz-orthoclase-garnet-carbonate assemblages that contain minor amounts of pyrrhotite with traces of arsenopyrite, chalcopyrite, sphalerite, pyrite and galena.

RED MOUNTAIN (MINFILE 092HSE082)

The Red Mountain occurrence is exposed in trenches on a ridge north of Windfall canyon, approximately 1.75 kilometres west-southwest of Lookout Mountain (UTM 5473614 N, 714362 E). The area is underlain by Hedley Formation calcareous sedimentary rocks that are cut by several Hedley diorite dikes. The showing is hosted by garnet-pyroxene endoskarn and exoskarn, close to a southeast-striking fault. Mineralization consists of massive to disseminated pyrrhotite with minor arsenopyrite. Two grab samples collected during this survey returned low values of gold and copper (up to 0.49 g/t Au and 0.16% Cu) but have anomalous amounts of arsenic, antimony, bismuth and cobalt (Appendix 24A).

RED TOP (MINFILE 092HSE087)

The Red Top occurrence is located about 2.25 kilometres east of Hedley and 750 metres northwest of the Hedley North occurrence (UTM 5470946 N, 714694 E). Garnet-pyroxene-carbonate skarn is associated with narrow dikes and sills of porphyritic Hedley intrusion that crosscut thick limestones of the Hedley Formation. MINFILE reports the presence of arsenopyrite, pyrrhotite and trace chalcopyrite, with one grab sample assaying 0.5 gram per tonne gold and 0.65% arsenic.

ROLLO (Horsefly) (MINFILE 092HSE049)

Several prospects are located about 2.25 kilometres east-northeast of Hedley and 1.3 kilometres southwest of Nickel Plate Mountain (UTM 5471636 N, 714698 E); these have been extensively explored by drilling and trenching (Dolmage and Duffell, 1937). Folded and sheared calcareous sedimentary rocks of the Hedley Formation close, to the Toronto stock, are cut by numerous Hedley sills and dikes; intense garnet-pyroxene-scapolite-carbonate skarn alteration overprints both the sediments and intrusions. Mineralization and mineral textures are similar to those at the nearby Nickel Plate deposit; sulphides include disseminated to massive arsenopyrite and pyrrhotite with trace pyrite, chalcopyrite and sphalerite. Some secondary oxidation is present. Assays on four grab samples ranged between 19.8 and 61 grams gold per tonne (B.C. Minister of Mines Annual Report 1937, pages D11 to D14).

STAG FRACTION (Pickaxe Zone) (MINFILE 092HSE085)

The Pickaxe occurrence is hosted by skarn-altered Hedley Formation approximately 2 kilometres east-southeast of Hedley (UTM 5470585 N, 714283 E). Several pits expose massive pyrrhotite and arsenopyrite with traces of chalcopyrite. MINFILE reports that a grab sample of sulphide-rich material assayed 7.47 grams per tonne gold.

SUNNYSIDE (MINFILE 092HSE038)

The old Sunnyside underground mine (UTM 5472361 N, 715668 E), was originally recorded as a separate occurrence in MINFILE. However, its sulphide-rich gold-skarn mineralization forms part of the Nickel Plate orebody and it now lies within the Corona Corporation open pit mine.

TOUGH OAKS (MINFILE 082ESW143)

The Tough Oaks occurrence is situated on a ridgetop north of Broken Creek, about 6.5 kilometres north of Mount Riordan (UTM 5481632 N, 287403 E). It is hosted by hornfelsed and silicified ash tuffs within a roof pendant in the Bromley batholith; it is uncertain whether the tuffs belong to the Whistle, French Mine or Oregon Claims Formation. Workings include trenches and a short exploratory shaft. At the shaft, the tuffs are altered to skarn with coarse and fine-grained garnet-pyroxene assemblages and coarse, radiating wollastonite. Irregular quartz-feldspar veins are also present. Mineralization includes disseminated pyrrhotite and lesser pyrite with traces of chalcopyrite, scheelite and arsenopyrite. A grab sample from the shaft, collected during this survey, contained no gold.

Approximately 200 metres south-southwest of the Tough Oaks shaft are two pits that expose a coarse mafic diorite that probably represents a marginal phase of the Bromley batholith. The diorite is cut by pyrite stringers, and encloses xenoliths of garnet-pyroxene exoskarn containing disseminated pyrrhotite.

WINTERS GOLD (MINFILE 092HSE084)

The Winters Gold occurrence is located approximately 750 metres north of Winters Creek at UTM 5466665 N, 716382 E. It is hosted by sheared and hornfelsed rocks of the Apex Mountain Complex close to their contact with the Cahill Creek pluton. Minor amounts of skarn are present. Some shear zones are mineralized with sparsely disseminated pyrrhotite and pyrite with traces of chalcopyrite. Malachite staining is also found locally along this southeast margin of the Cahill Creek pluton and in the thick limestone-marble unit northwest of Winters Creek. MINFILE reports that a chip sample of a thin sulphide-rich shear assayed 0.9 gram per tonne gold and 0.14% copper.

UNNAMED SKARN OCCURRENCES

Three unnamed, weakly mineralized skarn occurrences warrant mention. Two of these have been explored by trenching north of Broken Creek, approximately 7.5 kilometres north of Mount Riordan. Both are hosted by massive marble that is presumed to belong to the French Mine Formation; the marbles are cut by Hedley sills. One occurrence is situated about 750 metres north of the Golden Oaks occurrence, while the other is a kilometre farther east (Figure 38). At both occurrences the coarse garnet-pyroxene skarn contains minor wollastonite together with sparse pyrrhotite and trace arsenopyrite.

The third unnamed mineralized skarn occurrence forms several small outcrops surrounded by till about 1 kilometre west of Mount Riordan; it may be a western outlier of the Mount Riordan garnet skarn. The occurrence includes massive brown, subhedral to euhedral garnet with minor epidote and clinopyroxene. Mineralization, which is similar to the Mount Riordan skarn, includes magnetite with lesser pyrrhotite and trace pyrite, chalcopyrite and scheelite. The pyrrhotite has annealed breccia textures, and the chalcopyrite commonly rims garnet, separating garnet from pyrrhotite. Two mineralized grab samples collected during this survey contained up to 0.45% copper and 700 ppb gold.

VEINS AND OTHER MINERAL PROSPECTS

BRADSHAW (MINFILE 092HSE154)

The Bradshaw occurrence was not visited during this survey. It is located north of Bradshaw Creek, and is hosted by Apex Mountain tuffs adjacent to minor granodiorite intrusions. Mineralization consists of disseminated pyrite and quartz. MINFILE reports that a pyrite-rich grab sample assayed 7.27 grams gold per tonne, 72 grams silver per tonne, 1% arsenic and 0.59% copper.

HEDLEY STAR (MINFILE 092HSE037)

The Hedley Star occurrence, which was not examined during this survey, is located on the northern slopes of Winters Creek. Disseminated sulphides are hosted both by hornfelsed Apex Mountain rocks and the nearby Cahill Creek pluton. MINFILE reports that a sample of chert and quartz adjacent to a granodiorite dike assayed 2.06 grams gold per tonne, 13.8 grams silver per tonne and more than 1% copper and arsenic.

GOLDEN OAKS (Wheelbarrow, Creek) (MINFILE 082ESW143)

The two Golden Oaks occurrences, which lie on the Tough Oaks property, are located just south of Broken Creek, about 7 kilometres north-northwest of Mount Riordan. The area is underlain by a large hornfelsed roof pendant, 3.7 kilometres long, within rocks of the Bromley batholith and Lookout Ridge pluton. The pendant consists largely of tuffs with minor marble and chert-pebble conglomerate; it is uncertain whether this sequence belongs to the Whistle, French Mine or Oregon Claims Formation.

At the Golden Oaks (Creek) occurrence, close to Broken Creek, hornfelsed bedded-ash tuffs are cut by a dioritic dike containing disseminated pyrite. A shallow pit exposes a zone 1 metre wide that contains numerous narrow quartz veins, generally less than 2 centimetres thick. MINFILE contains a report that the veins contain only low gold values with rare disseminations of arsenopyrite and some blebs of tetrahedrite.

The Golden Oaks (Wheelbarrow) occurrence is about 250 metres farther southwest at UTM 5481532 N, 284902 E. Hornfelsed, silicified tuffs are cut by narrow quartz stringers with pyrrhotite and rare arsenopyrite.

MINFILE contains a report that a grab sample assayed 3.9 grams per tonne gold. Old drill core left at the site includes unmineralized ash tuffs and Hedley-type porphyritic diorites, both of which are extensively hornfelsed and biotite rich.

GOLD HILL (MINFILE 092HSE054)

The Gold Hill prospect is south of the Similkameen River, about 5 kilometres west-southwest of Hedley (Figure 37). There are several trenches and short exploratory adits on the property. The area is underlain by andesitic ash and lapilli tuffs and minor tuffaceous sediments belonging to the lower part of the Whistle Formation. These are cut by dikes and sills of both fine-grained equigranular and coarse hornblende-porphyritic Hedley intrusions. The mineralization shows some similarities to that in the Maple Leaf and Pine Knot veins which outcrop 1250 metres to the northeast. At the Gold Hill occurrence, tuff beds adjacent to one porphyritic diorite body are hornfelsed and eratically overprinted with early carbonate-pyroxene-garnet skarn alteration that contains pyrrhotite and traces of pyrite and chalcopyrite. Fault zones, along both the intrusive contacts and within the diorite body, have controlled a northwest-trending, irregular carbonate vein up to 60 metres long and 15 metres wide. On surface this vein consists largely of coarsely crystalline white to pale buff carbonate, together with minor quartz and some disseminated pyrite cubes. However, waste dumps in front of short adits driven on the vein contain abundant vuggy quartz-vein material that is similar in appearance to the Maple Leaf and Pine Knot veins. This quartz-rich material contains ma[illegible] blebs of coarse pyrite with traces of arsenopyrite, [illegible]ite, black sphalerite and galena. Macdonald ([illegible]) sample of gossan from the dum[illegible] per tonne gold and 0.48% arsenic. [illegible]inantly massive pyrite assayed 4.3 gram[illegible]nd 0.64% arsenic.

Plate 29. Gold Hill property. Angular clasts of hornfelsed and weakly skarn-altered tuffaceous wallrock surrounded by a carbonate matrix close to the margin of a mineralized carbonate vein.

Locally, the carbonate vein margins are densely packed with elongate, interlocking, sharply angular brecciated fragments of hornfelsed and skarn-altered wallrock up to 15 centimetres long (Plate 29). The clasts are rimmed with two generations of carbonate, an early, brown-coloured, possibly ankeritic carbonate, and a later phase of white crystalline calcite that was apparently coeval with the injection of the main carbonate-quartz vein. The sequence of events at the Gold Hill property appears to have been as follows: (1) intrusion of the diorite body accompanied by biotite hornfelsing and silicification of the country rock, (2) weak skarn alteration with the introduction of some sulphides, (3) fault brecciation, (4) minor ankerite precipitation, and (5) formation of the carbonate-quartz-sulphide vein accompanied by further brecciation.

GOLDEN ZONE (MINFILE 82ESW42)

The Golden Zone property is located about 5.5 kilometres south-southeast of Nickel Plate Lake (UTM 5480779 N, 283183 E). Between 1905 and 1983 at least four episodes of drilling and underground exploration took place on the property. In 1908 a small mill was built but it only operated for a short time; two shafts and two exploration adits were completed. In the 1980s a program of soil and rock-chip sampling was conducted together with airborne magnetic and VLF-EM surveys (Peto, 1983).

The property lies close to the western edge of a large roof pendant of possible Whistle Formation tuffaceous rocks (Unit 8a), in a poorly exposed area. The pendant, which is largely surrounded by the Bromley batholith, is cut by various minor bodies of fine and coarse-grained granitic rock. Contacts between the batholith and the pendant are generally north striking but highly irregular.

Exploration has concentrated on two steep, southerly dipping and east-striking veins. These largely comprise white to vitreous quartz that is locally crystalline, drusy or ribbon banded. The southern vein is less than 40 metres long and is wholly confined to the granitic rocks; one of the two shafts (B shaft) was sunk on this vein (B.C. Minister of Mines Annual Report 1937, page D15). The other vein is longer and has been more extensively explored. It is up to 1.3 metres thick on surface but underground reaches 2 metres in width. The vein is offset locally by north-striking faults, but can be traced eastwards for 360 metres from granitic rocks into hornfelsed tuffs, silicious siltstone and impure limestone. The character of the vein changes laterally. Where it cuts granitic rocks it tends to be narrow and regular, with drusy, ribbon-banded to coxcomb milky quartz. Farther east, in the sedimentary rocks, it becomes highly variable in width and irregular in form; locally it splits into numerous veins and quartz stringers, and becomes sulphide-rich. This vein was the main target of the A shaft. The veins contain, and are haloed by, zones of fine-grained sulphides up to 3.5 metres wide. Mineralization, which occurs as masses, stringers, aggregates and platy smears along fault planes, includes pyrite, arsenopyrite and traces of chalcopyrite, sphalerite, gold, silver and jamesonite. The character of this vein changes across the area and with depth (B.C. Minister of Mines Annual Report 1937, pages D15-16; Peto, 1983). To the west, in the granitic rocks, it contains more sphalerite and less gold, but may carry up to 300 grams silver per tonne. Farther east, in the sedimentary rocks, pyrite and arsenopyrite are more abundant on surface (but not at depth) and the gold values are higher.

Gold values throughout the two quartz veins are generally low but some spectacular assays have been recorded, particularly from sulphide-rich samples in the eastern part of the vein system. A sample rich in arsenopyrite and pyrite assayed 66 grams per tonne gold and over 300 grams per tonne silver (B.C. Minister of Mines Annual Report 1937, page D16). Peto (1983), using dump samples and various geochemical data from other sources, estimated the average grades for the various rock types to be as follows: quartz vein – 0.27 grams gold and 74 grams per tonne silver over 1.3 metres; sulphide pods – 8 grams gold and 75 grams per tonne silver over 1.5 metres; fault gouge – 9 grams gold and 13 grams per tonne silver over 0.3 metre. The tailings averaged 1.2 grams gold and 3 grams per tonne silver, and percussion-drill hole intersections averaged 1 gram gold and 45 grams per tonne silver over 6.7 metres.

A grab sample of pyrite-arsenopyrite-bearing quartz from the dump collected during this survey assayed 23 grams per tonne gold, 100 grams per tonne silver, 25.6% arsenic, and 286 and 420 ppm antimony and bismuth, respectively (Appendix 24A).

HED (MINFILE 92HSE138)

The Hed prospect is located on the south side of the Similkameen River approximately 1400 metres west of the Maple Leaf and Pine Knot veins (UTM 5470776 N, 707146 E). It is hosted by argillites and tuffaceous siltstones of the Whistle Formation which are cut by thin sills of Hedley diorite. Two of three drill holes intersected a brecciated quartz-carbonate vein with an intercept thickness of up to 15 metres (Macdonald, 1977). The textures and mineralogy of this subvertical, north-northeast striking vein resemble those in the Gold Hill vein 800 metres to the south. The margins of the vein tend to contain angular, brecciated fragments of wallrock argillite, some of which are skarn-altered. Mineralization consists of disseminated to coarse grained and massive pyrite with minor black sphalerite, arsenopyrite and traces of chalcopyrite. Gold values in the quartz-carbonate-suphide breccia are generally low; Macdonald (1977) reports that the highest values are 6.39 grams gold per tonne over an intercept of 0.6 metre.

IOTA (Islay B)
(MINFILE 092HSE119)

The Iota property is located at an elevation of approximately 1400 metres, on the northwest side of Stemwinder Mountain (UTM 5475078 N, 70976 E). It is underlain by north-striking, steeply east-dipping calcareous argillites, siltstone and thin impure limestones of the Stemwinder Formation. These sedimentary rocks are extensively hornfelsed by the Bromley batholith which crops out approximately 350 metres farther west. A thin, deeply weathered mineralized zone, up to 0.3 metre wide, follows an east-northeast-trending fault, and is traceable for 40 metres. The zone is marked by brecciation, silicification and black, graphitic quartz. Sulphides include schistose galena, partially altered to anglesite, with lesser argentite and sphalerite. Past exploration work includes driving a short adit and a 10 metres-deep shaft. A 32-tonne bulk sample, shipped to the Trail smelter in 1947, yielded 62 grams of gold, 17.8 kilograms of silver, 1652 kilograms of lead and 256 kilograms of zinc (B.C. Minister of Mines Annual Report 1947, pages A147-A147).

ILE (MINFILE 92HSE108)

The Ile occurrence, which was not visited during this survey, is located on Smith Creek at UTM 5471618 N, 702256 E. Mineralization is reported to be disseminated pyrite with minor chalcopyrite and sphalerite (Geology, Exploration and Mining in British Columbia 1972, page 124). The area is underlain by tuffs and tuffaceous sediments of the Whistle Formation. No gold values are reported.

MAPLE LEAF AND PINE KNOT (Banbury)
(MINFILE 092HSE046)

These veins are is located south of the Similkameen River about 4 kilometres west of Hedley (Figure 37). The showings were discovered in 1900 and during the next ten years several exploratory open-cuts, adits and crosscuts were driven along the gold and sulphide-bearing Maple Leaf and Pine Knot quartz veins. In 1936, after further underground exploration, a 50-ton per day mill was installed to mill the Maple Leaf ore; the mill operated from January to May 1937 and produced approximately 29.4 kilograms of gold, 13.3 kilograms of silver, 846 kilograms of copper and 891 kilograms of lead from 5897 tonnes of ore (Table 4).

In 1978, Banbury Gold Mines Ltd. acquired the property. Its work included drilling the Maple Leaf and Pine Knot veins as well as some newly discovered areas of disseminated mineralization in the Banbury stock. In 1982, a further 4.1 kilograms of gold were recovered from approximately 1179 tonnes of ore. In 1984 geological reserves were estimated to be approximately 220 000 tonnes grading 9.4 grams gold per tonne.

The property is underlain by northerly striking, steeply dipping sediments and tuffs that are intruded by the Banbury stock. Detailed mapping by M.R. Sanford (Figure 12) indicates that the stock intrudes Stemwinder Formation argillites and Whistle Formation tuffs as well as the Copperfield breccia. It is surrounded by a thermal aureole (Figure 12) and comprises a northern leucocratic quartz diorite suite and a southern mafic suite. The stock has irregular contacts that interfinger with the bedded country rock; it and the surrounding aureole are cut by several, irregular, northerly trending fracture zones. These fractures include steep and gently dipping sets, some of which contain quartz-carbonate veins, the most prominent of which are the steeply dipping Maple Leaf and Pine Knot veins (Figure 12).

Individual veins are up to 3.3 metres thick and exceed 100 metres in length; they contain mainly glassy to white to pale pink strained quartz with lesser amounts of coarse carbonate and arsenopyrite, pyrrhotite, pyrite, sphalerite, chalcopyrite and trace galena. The arsenopyrite can be exceedingly fine and the pyrite coarsely euhedral. Gold is generally associated with the sulphides. Visible gold is more common in the deeper parts of the veins, and the highest gold values tend to be where the veins cut the hornfelsic aureole, approximately 30 to 100 metres from the margin of the stock. Sphalerite is sometimes abundant in the Pine Knot vein and tends to be less common in the Maple Leaf. Locally, the veins are sheared, vuggy and contain angular brecciated clasts of chloritic, silicified country rock. Some veins have sheared or faulted margins and locally the contacts are marked by thin halos of sericite-rich alteration. The sheared quartz veins that crosscut the hornfelsic aureole are locally surrounded by an envelope of "zebra rock", 1 metre-wide, consisting of many thin, subparallel carbonate veins between 2 and 6 millimetres thick, spaced 1 to 2 centimetres apart. Minor amounts of garnet-pyroxene skarn also overprint the intrusive and sedimentary wallrocks immediately adjacent to the Maple Leaf and Pine Knot veins. In addition, the leucocratic Banbury stock is locally overprinted by small irregular patches of garnet-pyroxene endoskarn containing pyrite and pyrrhotite. Pendants and xenoliths of sedimentary rock in the stock also tend to be altered to skarn, which is associated with narrow quartz stringers.

TABLE 4
PRODUCTION FROM VEINS — HEDLEY DISTRICT

Vein	Ore milled (t)	Gold (kg)	Silver (kg)	Copper (kg)	Lead (kg)
Maple Leaf; Pine Knot 1937	5 897	29.4	13.3	846	891
1982 (Banbury Mines Ltd.)	1 179	4.1	NA	NA	NA
Total	7 076	33.5	13.3	846	891

Some vein contacts are intruded by parallel, late and generally narrow andesitic dikes that carry disseminated pyrite and pyrrhotite, but no gold.

Drilling by Banbury Gold Mines Ltd. in quartz diorite of the Banbury stock revealed areas of pervasive carbonate alteration, together with disseminated pyrite and impersistent zones of low-grade gold mineralization. The best intersection graded 4 grams per tonne gold over 40 metres (M.R. Sanford, personal communication, 1989).

MISSION (Flint)
(MINFILE 092HSE052)

The Mission-Flint prospect is south of the Similkameen River, on the upper reaches of Jameson Creek (UTM 5467752 N, 710431 E). Exploration in the 1930s included extensive trenching and sinking two short shafts (B.C. Minister of Mines Annual Report 1936, pages D11-D12). The area is underlain by calcareous siltstone, argillite and lapilli tuff of uncertain age. These rocks are intruded by a large, northwesterly trending tongue of biotite granodiorite from the Cahill Creek pluton. In this vicinity the pluton contains screens and small pendants of mafic intrusive rocks and hornfelsed sedimentary country rocks. Mineralization is fracture controlled and hosted by altered granodiorite of the Cahill Creek pluton, close to its margin.

Three mineralized fractures are known; the largest of these, the "Barnes zone" trends north-northeasterly and is 240 metres long and up to 4.5 metres wide. Two shorter and less well mineralized fractures, the "Winkler and Walker zones" strike northeast and appear to be splays from the Barnes zone. The altered zones contain quartz, sericite, kaolinite, chlorite, carbonate and epidote. Mineralization, which is wholly confined to the granodiorite, includes abundant arsenopyrite and pyrite with variable amounts of chalcopyrite, dark brown sphalerite and traces of tetrahedrite. Sulphides occur as bands and masses, locally with lesser amounts of white quartz. Low gold values, ranging between 1.4 and 2.7 grams gold per tonne are reported (B.C. Minister of Mines Annual Report 1936, page D12), although one sphalerite-rich sample assayed 6.8 grams gold per tonne. One arsenopyrite-rich sample collected during this survey returned 3.3 grams gold and 370 grams silver per tonne, as well as 0.18% lead, 2.85% zinc and 19% arsenic (Appendix 24A). The sample was also enriched in bismuth (205 ppm) and antimony (620 ppm).

PATSY NO. 1
(MINFILE 092HSE047)

The Patsy No. 1 workings are located on the south side of the Similkameen River, close to its confluence with Whistle Creek (UTM 5472288 N, 706648 E). Several exploratory open cuts, short adits and shafts were driven on the property in the 1920s (B.C. Minister of Mines Annual Report 1927, page C240). The area is underlain by north-striking and steeply dipping Whistle Formation argillites and tuffs which are intruded by several Hedley dioritic sills. Fractures and shears in the sediments are filled with irregular, discontinuous veins, generally less than 10 centimetres wide, that quickly pinch out when they pass into the diorite sills. Veins contain quartz with minor carbonate and erratic pyrite, pyrrhotite, arsenopyrite, sphalerite and chalcopyrite.

The largest vein reaches a width of 20 centimetres; it is seen in the No. 1 adit and strikes north-northeast and dips northwest. A subparallel shear zone, 10 centimetres wide, is exposed in the No. 2 adit. MINFILE reports that a sample from the No. 2 adit assayed 3.4 grams gold per tonne, although grab samples containing up to 83 grams gold per tonne are recorded from the property. However, the mineralized veins and fractures lack continuity.

PATSY NO. 2 (MINFILE 092HSE048)

The Patsy No. 2 property is located in the Whistle Creek valley about 2.5 kilometres south-southwest of the Patsy No.1 prospect at UTM 5470177 N, 705408 E. The area is underlain by graphitic argillites, tuffs and thin impure limestone beds that are tentatively assigned to the Whistle Formation. Past exploration work includes diamond drilling, several short shafts and at least three exploratory adits, one of which is 196 metres long (Hedley, 1937).

Erratic mineralization is found in at least five irregular shear zones that reach 1.8 metres in width. These shears trend subparallel to bedding, and may be related to the Whistle Creek fault that passes just west of the prospect. The veins contain pyrite and arsenopyrite in a gangue of quartz and minor calcite. Hedley reports erratic gold values up to 30 grams gold per tonne. A grab sample of pyrite-arsenopyrite-bearing vein material collected during this survey assayed 5 grams gold per tonne as well as 95 ppm antimony and 14.7% arsenic (Appendix 24A).

SNOWSTORM (MINFILE 092HSE053)

The Snowstorm occurrence, which was not examined during this survey, is located south of the Similkameen River, close to the Hed showing (UTM 5471102 N, 705877 E). The area is poorly exposed but a shallow exploratory shaft was sunk on an oxidised fracture zone containing arsenopyrite, pyrite and carbonate. Grab samples assayed between 2.3 and 17 grams gold per tonne gold (Rice, 1947).

TORONTO (Galena) (MINFILE 092HSE065)

The Toronto occurrence, which was not visited during this survey, is located immediately west of Hedley Creek, approximately 1100 metres northeast of Stemwinder Mountain (UTM 5475372 N, 711270 E). The area is underlain by calcareous siltstone, argillite and thin limestone beds of the Stemwinder Formation; these are intruded by a variety of minor igneous bodies including dioritic Hedley intrusions and granitic rocks related to the Bromley batholith and Lookout Ridge pluton. Exploration work has included trenching and sinking a shallow shaft. The sedimentary rocks are cut by quartz veinlets that contain pyrite with minor chalcopyrite and galena. Nearby, a granodiorite body is cut by two sparsely mineralized, easterly trending quartz veins up to 1.5 metres wide. Gold assays from the veinlets and veins are low (B.C. Minister of Mines Annual Report 1936, page D12; Rice 1947).

VICTORIA (MINFILE 092HSE058)

The Victoria occurrence, which was not visited during this survey, lies just east of Winters Creek at UTM 5466130 N, 717899 E. Exploration has included driving three adits, the longest of which extends 58 metres (B.C. Minister of Mines Annual Report 1936, page D12). A steeply dipping quartz vein, up to 0.6 metre wide, cuts argillites and quartzites of the Apex Mountain Complex. The vein contains vitreous, crystalline quartz with erratic arsenopyrite, pyrite, pyrrhotite and chalcopyrite; locally sulphides form up to 50% of the vein. Seams and patches of chloritic material are also present. A chip sample across a quartz vein, 0.6 metre wide, assayed 9.5 grams gold and 10 grams silver per tonne, and a grab sample rich in arsenopyrite contained 10 grams gold per tonne (B.C. Minister of Mines Annual Report 1936, page D12).

OTHER MINERAL RESOURCES

HEDLEY TAILINGS (MINFILE 92HSE144)

Old tailings from past underground mining activity are contained in four dumps close to Hedley township. Candorado Mines Ltd.'s "old" and "new" piles, situated immediately south of Hedley, are the result of mining at the Nickel Plate mine; they contain an estimated 1.5 million tonnes with a drill-indicated grade of 1.41 grams gold per tonne. The Nos. 1 and 2 piles are north of Hedley and come from the Mascot mine operations. Sumac Ventures Inc. report reserves of 453 500 tonnes grading 1.71 grams gold per tonne.

CHANGES IN GEOCHEMISTRY AND OXIDATION STATE IN THE GOLD SKARNS

INTRODUCTION

An attempt has been made to determine the geochemical and oxidation changes that occur when skarn alteration overprints both the Hedley intrusions and the sedimentary rocks. Samples of unaltered Hedley diorite were collected from the Stemwinder stock and from various Hedley sills and dikes throughout the district. For comparison, endoskarn samples of sills and dikes were taken mainly from three drill holes, numbers 195, 261 and 401, at the Nickel Plate mine. The locations of the holes in relation to the Nickel Plate skarn envelope are shown on Figure 18, while the lithologies and variable skarn alteration encountered, together with the sample location down each drill hole are illustrated by Figure 28. The holes intersected moderately to intensely skarn-altered sediments and tuffs interlayered with numerous sills of endoskarn Hedley intrusion. Hole 401 was collared outside the open-pit perimeter and intersected barren, generally fine-grained pyroxene-rich skarn. Holes 195 and 261 were collared within the open-pit area and cut ore-grade skarn mineralization forming part of the Nickel Plate deposit.

Exoskarn samples were taken from the same three drillholes. Comparative samples of unaltered limestone, argillite and siltstone were collected from the Hedley, Chuchuwayha and Stemwinder formations from throughout the district.

The major and trace element analytical results from the unaltered diorite are presented in Appendix 9; those for endoskarn are given in Appendices 10, 16 and 17. In addition, CIPW norms of the unaltered Hedley intrusions have been published by Ray *et al.* (1988). The lithogeochemical data for the unaltered Nicola Group sedimentary rocks are given in Appendix 4, and data for the exoskarn intersected in the drill holes in Appendices 16 and 17. In addition, analyses of marble samples collected from various drillholes at Nickel Plate are given in Appendix 4C. Comparative mean values for the major elements for the unaltered sedimentary rocks and Hedley intrusions, and the skarn samples from the drill holes are presented in Tables 5A and 5B.

It should be noted that the apparent chemical changes discussed below are based on normalized values and no allowance has been made for any volume changes, as described by Gresens (1967), that may have occurred during the metasomatic process. This is because of discrepancies between some of the calculated volume changes and the geological evidence. A mass balance study (Wagner, 1989), using some of the samples listed in Appendices 9, 10, 16 and 17, indicates relatively minor volume increases in the endoskarn of between 3 and 21%, with the greatest changes occurring in the more altered endoskarn adjacent to the ore zones. However, Wagner also concluded that alteration of the sedimentary rocks at Nickel Plate resulted in volume losses averaging 29 to 33% for the argillites, 67% for the siltstones, and 89% for the limestones. Such large volume decreases in the siltstones for example, which make up the dominant part of the stratigraphic section at the mine, are incompatible with the geological evidence: an absence of stylolite pressure-solution surfaces in the marble units at the base of the Nickel Plate skarn, the lack of disruption or collapse brecciation features, and the perfect preservation of delicate sedimentary structures in the exoskarn. Isocon plots of the Nickel Plate data, constructed using a method described by Grant (1986), indicate that volume changes of 20% could explain variations in such elements as Si and Al. However, changes in excess of 200% (which we consider unreasonable) would be required to account for the variations in Fe, K and Na. Thus, we believe that the progressive changes in the Fe, K and Na contents of the Hedley intrusions and sedimentary rocks during skarn overprinting are largely the result of metasomatism rather than volume changes.

CHANGES IN THE ENDOSKARN.

Data presented in Table 5A and Appendices 9, 10, 16 and 17 indicate that many major elements, including calcium, aluminum and titanium show little or no variation between the unaltered and skarn-altered Hedley intrusions. However, attainment of intense endoskarn alteration, as present in holes 261 and 195, is accompanied by overall losses in iron, and variable gains in silica and potassium (Figure 29), as well as increases in the K_2O/Na_2O ratios (Table 5A). These changes mark the destruction of the igneous ferromagnesian minerals and their replacement by biotite, orthoclase, quartz and magnesium-rich clinopyroxene.

Initiation of endoskarn overprinting in the outer parts of the envelope, as seen in hole 401, is accompanied by a minor loss of iron, although the main losses take place after the onset of intense alteration (Figure 30). However, initial skarn development is marked by an immediate and dramatic reduction in the Fe_2O_3/FeO ratios in endoskarn compared to unaltered Hedley intrusions. This change in oxidation state suggests that the skarn-forming fluids at Nickel Plate were extremely reducing. More intense endoskarn alteration in mineralized holes 195 and 261 is accompanied by no further changes in oxidation state although major losses in iron did occur during this stage (Figure 30; Table 5A).

CHANGES IN THE EXOSKARN

Comparing the geochemistry of the unaltered sedimentary hostrocks and the Nickel Plate exoskarn is more difficult than similar comparisons in the intrusive rocks. This is due to the varied lithology and chemistry of the Hedley Formation siltstones and limestones, and the

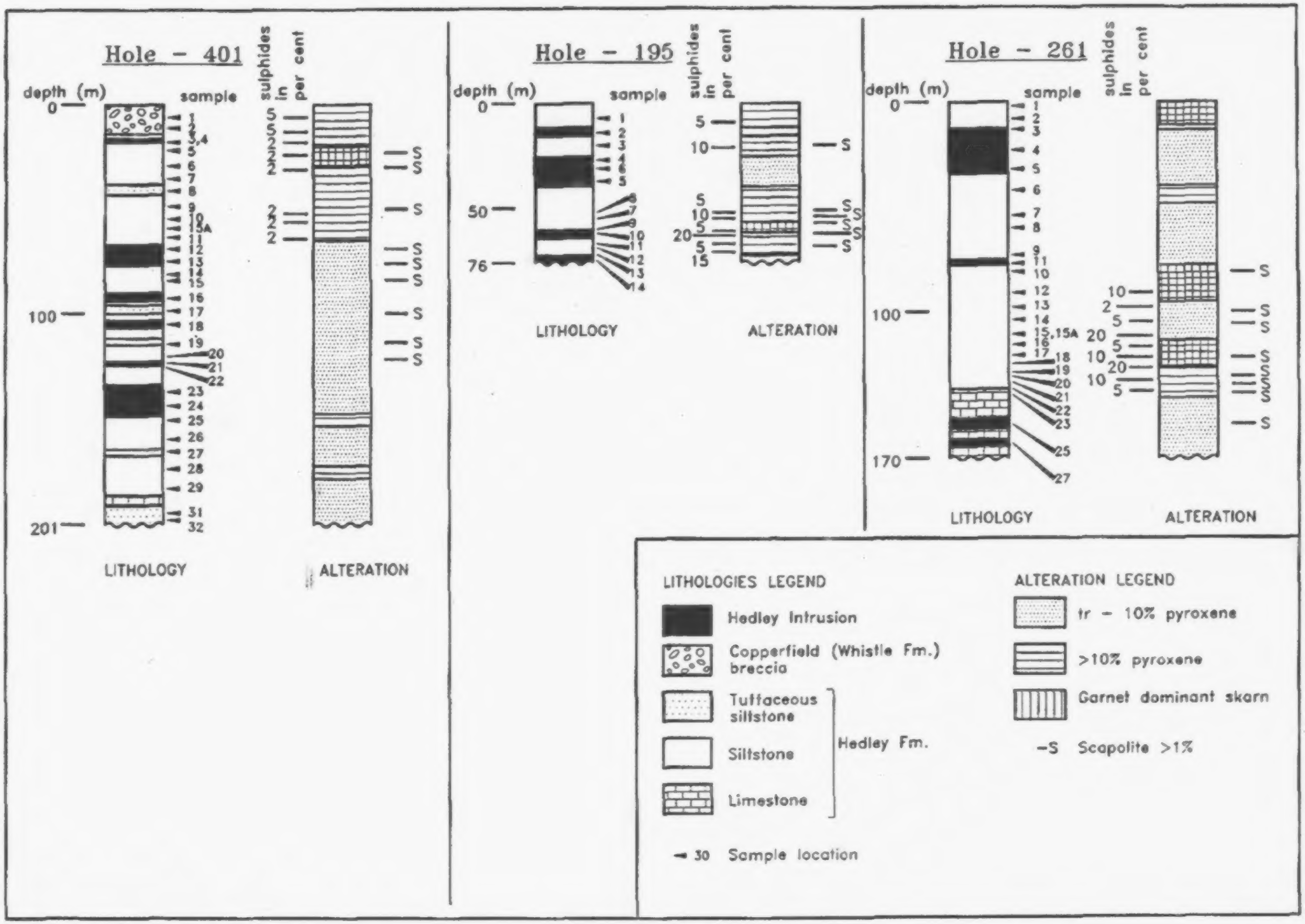
Hole - 401
depth (m)
sample
sulphides in per cent
0
100
201
LITHOLOGY
ALTERATION
Hole - 195
50
76
Hole - 261
170
S
LITHOLOGIES LEGEND
Hedley Intrusion
Copperfield (Whistle Fm.) breccia
Tuffaceous siltstone
Siltstone
Limestone
Hedley Fm.
30 Sample location
ALTERATION LEGEND
tr - 10% pyroxene
>10% pyroxene
Garnet dominant skarn
-S Scapolite >1%

Figure 28. Lithologies and skarn alteration in drill holes 401, 261 and 195 that intersect various parts of the Nickel Plate skarn envelope (*see* Figure 18). Hole 401 intersected barren skarn and holes 261 and 195 intersected economic gold ore. *Note:* locations of geochemical samples from drill-core (*see* Appendices 16 and 17 for analytical results).

TABLE 5A

COMPARATIVE CHEMISTRY OF THE UNALTERED HEDLEY INTRUSIONS AND MODERATELY AND INTENSELY ALTERED ENDOSKARN

Element	Unaltered Hedley Intrusions	Moderately altered endoskarn DDH401	Strongly altered endoskarn DDHs 195 and 261
SiO_2	54.82	52.45	58.79
TiO_2	0.66	0.71	0.52
Al_2O_3	18.59	17.16	17.05
Fe_2O_3	1.28	0.27	0.24
FeO	5.81	5.75	2.89
Fe_2O_3T	7.74	6.66	3.45
MnO	0.14	0.11	0.07
MgO	3.82	4.76	3.10
CaO	8.40	9.82	8.70
Na_2O	3.21	2.92	3.61
K2O	1.43	2.54	3.33
P_2O_5	0.18	0.19	0.14
LOI	1.31	1.53	1.01
Fe_2O_3/FeO	0.23	0.05	0.08
K_2O/Na_2O	0.44	1.01	1.19
No. of samples	27	9	12

Major oxide values in percent; Fe_2O_3T = total iron as Fe_2O_3.

TABLE 5B

COMPARATIVE CHEMISTRY OF THE UNALTERED NICOLA GROUP SEDIMENTARY ROCKS AND MODERATELY AND INTENSELY ALTERED EXOSKARN

Element	Unaltered Limestone	Unaltered Siltstone	Moderately altered exoskarn	Strongly altered exoskarn
			DDH401	DDHs 195 and 261
SiO2	8.11	57.3	55.01	42.50
TiO2	0.03	0.35	0.55	0.26
Al2O3	.80	6.29	12.45	5.34
Fe2O3	0.00	0.78	0.2	3.35
FeO	0.27	1.56	4.16	9.08
Fe2O3T	0.29	2.50	4.79	13.44
MnO	0.11	0.09	0.10	0.44
MgO	1.37	2.56	3.91	2.79
CaO	49.02	18.48	12.27	26.28
Na2O	0.09	1.14	1.72	0.16
K2O	0.15	1.17	3.76	1.24
P2O5	0.09	0.21	0.21	0.31
LOI	37.19	9.64	3.63	6.53
Fe2O3/FeO	0.41	0.50	0.05	0.21*
K2O/Na2O	1.67	1.03	2.19	37.24
No. of samples	5	6	23	28

Major oxide values in percent; Fe_2O_3T = total iron as Fe_2O_3;
*the mean Fe_2O_3/FeO ratio excludes the five uppermost and oxidized samples in DDH 261.

TABLE 5C

MAJOR ELEMENT ANALYSES OF BIOTITE "HORNFELS" ALTERED OREGON CLAIMS FORMATION TUFFS — FRENCH MINE

Element	HD798*
SiO_2	60.03
TiO_2	0.96
Al_2O_3	17.57
Fe_2O_3T	7.96
MnO	0.08
MgO	3.19
CaO	1.84
Na_2O	0.07
K_2O	5.92
P_2O_5	0.49
LOI	0.76
Total	98.87

Values in percent; Fe_2O_3T = total iron as Fe_2O_3.
* Purple-brown, silicious ("hornfelsic") mafic crystal tuff overprinted with pervasive, fine-grained biotite and lesser orthoclase alteration. Collected from the footwall tuffs at French mine.

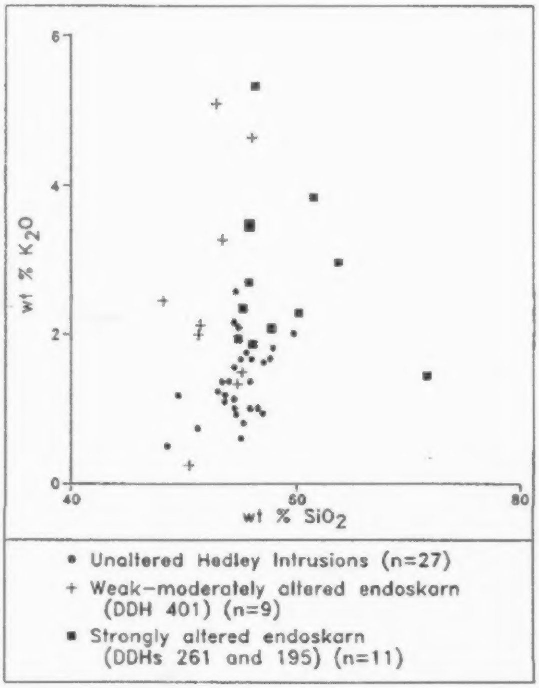

Figure 29. Plot of K_2O vs. SiO_2 illustrating that endoskarn alteration at Nickel Plate is accompanied by an increase in potassium.

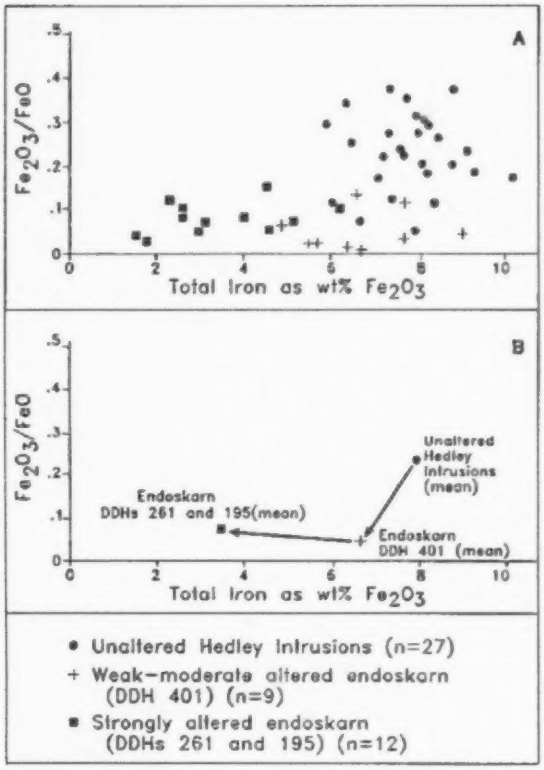

Figure 30. A. Plot of Fe_2O_3/FeO vs. total iron demonstrating that increasing endoskarn alteration at Nickel Plate is accompanied by decreasing ferric/ferrous ratios and a progressive fall in the total iron content. B. Plot of Fe_2O_3/FeO vs. total iron using mean values for the unaltered Hedley intrusions, weak to moderately altered endoskarn (DDH 401) and strongly altered endoskarn (DDHs 261 and 195) samples shown in Figure 30A.

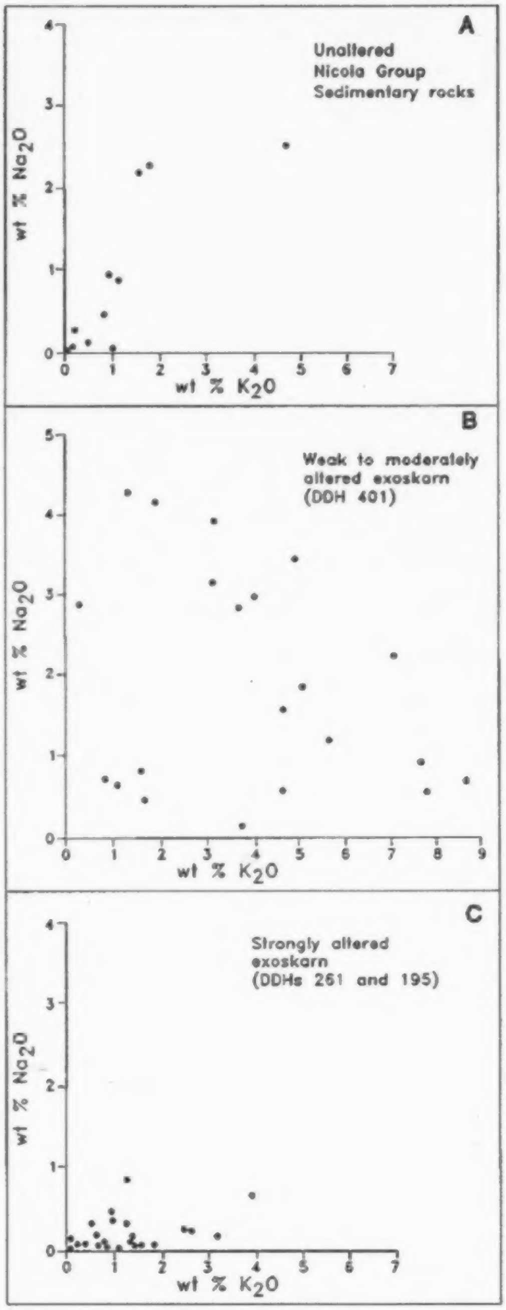

Figure 31. Na_2O vs. K_2O plots of: A. Unaltered Nicola Group sedimentary rocks. B. Weak to moderately altered exoskarn at Nickel Plate. C. Strongly altered exoskarn at Nickel Plate. *Note:* increases of sodium and potassium in the weak to moderately altered exoskarn and decrease in these elements in the strongly altered exoskarn.

uncertain nature of the protolith in the more extremely altered exoskarn samples. However, the majority of the pyroxene-dominant exoskarn samples in the drillholes represent siltstones, whereas the thin garnet-dominant horizons were probably originally limestones.

Intense skarn overprinting of the siltstones results in overall losses of silica and sodium, gains of iron, and increased K_2O/Na_2O ratios (Table 5B). Alkalis show an increase in the weakly altered exoskarn (Figure 31B) reflecting the initial crystallization of albite, orthoclase and biotite during incipient skarn alteration. With more intense alteration, the albite and much of the orthoclase and biotite were destroyed, leading to a loss of sodium and potassium in the exoskarn (Figure 31C).

Increases in iron in the exoskarn took place immediately after the onset of alteration and continued during the later, more intense overprinting (Figure 32). As in the

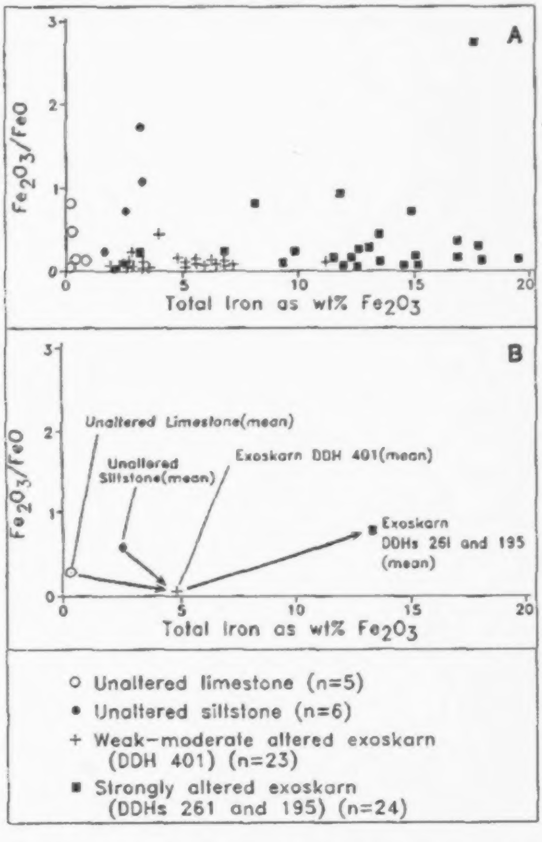

Figure 32. A. Plot of Fe_2O_3/FeO vs. total iron illustrating that increasing exoskarn overprinting at Nickel Plate is accompanied by a progressive increase of iron. B. Plot of Fe_2O_3/FeO vs. total iron using mean values for the unaltered Nicola Group sedimentary rocks, weak to moderately altered exoskarn and strongly altered exoskarn samples shown in Figure 32A.

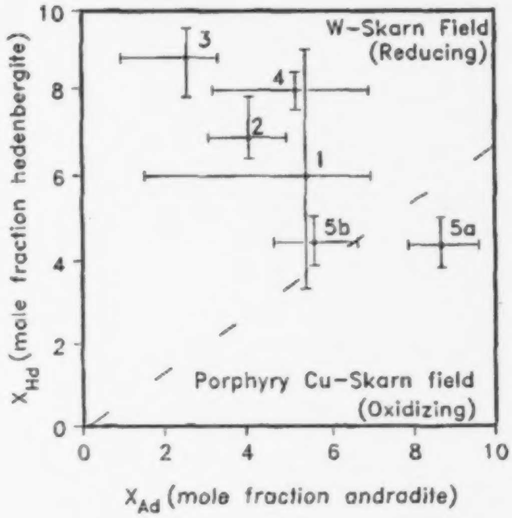

Figure 33. Plot of mole fraction hedenbergite vs. mole fraction andradite of the Hedley skarns. Fields for reduced tungsten skarns and oxidized porphyry-copper related skarns after Einaudi (1982). *Note:* the reduced state of the Hedley gold skarns and the relatively oxidized state of the first phase of the Mount Riordan skarn. Bar lines show range of X Hd and X Ad values; centre dots = mean values. 1 = Nickel Plate. 2 = Canty. 3 = Good Hope. 4 = French. 5a = Mount Riordan using first phase garnet. 5b = Mount Riordan using second phase garnet.

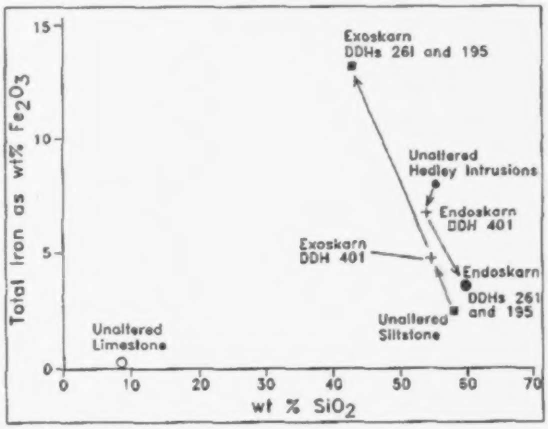

Figure 34. Plot (using mean values) of total iron vs. SiO_2 showing overall loss of iron and gain of silica in the Nickel Plate endoskarn with increasing alteration and corresponding gain of iron and loss of silica in the exoskarn (compared to unaltered Nicola Group siltstones). *Note:* geochemistry of the unaltered Nicola limestone and siltstone samples are listed in Appendix 4; skarn samples are from drill holes 195, 261 and 401 at Nickel Plate; *see* Figure 18.

endoskarn, the first appearance of alteration in the siltstones was accompanied by a decrease in Fe_2O_3/FeO ratios (Figure 32; Table 5B).

CONCLUSIONS

Compared to the unaltered plutonic rocks associated with Fe, Cu, Zn-Pb, W, and Sn skarn deposits, the unaltered Hedley intrusions have the lowest Fe_2O_3/FeO ratios (Figure 11M) which suggests that they were in a highly reduced state, although they represent relatively high-level intrusions. There are also a number of features that suggest the fluids responsible for the Hedley gold skarns were strongly reduced; these include the iron-rich composition of the early biotite (Ettlinger, 1990a), high pyrrhotite/pyrite ratios in the ore and the presence of arsenopyrite and native bismuth. Garnet and pyroxene compositions (Figure 33) also indicate reduced conditions prevailed in all of the Hedley gold skarn deposits. This contrasts with the more oxidising environment that probably existed during the first phase of garnet growth in the Mount Riordan skarn (Figure 33). Plots of Fe_2O_3/FeO versus total iron (Figures 30 and 32) also illustrate the progressive reduction in oxidation state that accompanied increasing skarn overprinting at Nickel Plate.

Intense alteration is also accompanied by a sharp drop in the iron content of the endoskarn and a corresponding increase of iron in the adjacent exoskarn (Figure 34). It is likely that the magmatic pyroxene and hornblende in the Hedley intrusions, which were destroyed during alteration, were the source of much of the iron in the exoskarn. These minerals may also have been the source of some of the gold.

MINERALOGICAL ZONING IN THE GOLD SKARNS

Skarn-related alteration envelopes containing pyroxene-garnet assemblages with variable amounts of carbonate, quartz, orthoclase, plagioclase, wollastonite, biotite, epidote, scapolite and chlorite are widespread and common in Nicola Group rocks throughout the Hedley district. The intensity, extent and texture of the skarns vary considerably. Alteration effects range from narrow veinlets or irregular patches only centimetres or metres in diameter, up to large alteration envelopes such as those associated with the Nickel Plate, French, Good Hope and Canty deposits. Mineral assemblages are generally fine grained in the smaller patches of alteration and in the outer parts of the larger envelopes. However, on an outcrop scale, there is a consistent concentric zoning of exoskarn gangue mineralogy that resembles, in part, the skarn-related mineralogical patterns described at other contact metasomatic deposits in the Canadian Cordillera (Dick, 1980; Dick and Hodgson, 1982).

Exoskarn alteration initially developed either adjacent to Hedley intrusion sills or some distance from the source intrusions where fractures channelled the hydrothermal fluids into carbonate-bearing sediments. Passage from the inner, intensely altered and coarser grained exoskarn core to the outer, unaltered country rock is marked by up to four concentric zones (Figure 35). These zones vary from a few millimetres to many tens of metres in width. In areas of weak alteration some of the inner zones may be absent, and only one or two of the outer alteration zones are developed. If present, the core (Zone 1) contains either pinkish brown massive garnetite or isolated clusters and veins of garnet (Plate 25) that crosscut lesser amounts of coarse clinopyroxene and quartz. This garnet-rich core passes outwards to a wider, green, clinopyroxene-rich zone (Zone 2) that may also contain quartz and epidote. Contacts between Zones 1 and 2 are generally sharp, with veinlets of garnet-rich Zone 1 alteration penetrating and replacing the Zone 2 envelope. In some outcrops, Zone 2 is divisible into an inner subzone of dark green and probably iron-rich pyroxene, and an outer subzone containing lighter green pyroxene that is commonly fine grained. Zone 2 may pass outwards to a narrow, pink-coloured section (Zone 3) containing orthoclase and quartz with rare chlorite and amphibole. Where present, this zone is generally no more than a few centimetres wide; it probably represents a reaction phenomenon from the replacement of the outer biotite-rich zone by clinopyroxene alteration (Plate 25).

The outermost alteration zone (Zone 4) in these small skarns is of variable thickness and comprises a dark purplish brown, siliceous, massive and fine-grained biotite-rich zone that resembles a hornfels (Plates 24 and 25). Thin section studies show it contains an intimate intergrowth of very small, decussate biotite and quartz with variable amounts of epidote, chlorite, orthoclase and clinozoisite. Contacts between this outermost envelope and the unaltered country rocks are either regular and diffuse, or sharp and highly irregular with veinlets and small apophyses of hornfels-like alteration penetrating the country rocks. The outer hornfels-like zone is frequently cut by veinlets and pods of pyroxene (Plate 24), some of which have garnetiferous cores and orthoclase-rich margins. The veinlets are mostly irregular, but some appear to have been controlled by pre-existing, intersecting sets of microfractures. In many cases, these pyroxene veinlets extend from Zone 2, through Zone 4 into unaltered country rock. Where this occurs, pyroxene is stable in direct contact with the country rock, but garnet, if present, is always separated from unaltered rocks by pyroxene.

The pattern of skarn zoning observed in many outcrops has led to the recognition of a sequence of skarn development (Figure 36). Small-scale skarn development generally begins with the formation of the purple-brown, silicious biotite-rich alteration (Zone 4), that has a hornfelsic appearance; it is commonly preserved as thin irregular zones, often along channelways such as bedding planes or fractures (Figure 36A), or as larger pervasive patches. This alteration is not a contact isochemical hornfels related to the Hedley intrusions but rather represents the initial stage of the skarn-forming metasomatic process. Potassic metasomatism at this early stage is suggested by the analysis of the biotite "hornfels" altered Oregon Claims Formation tuffs in the footwall of the French mine (Table 5C). The unaltered Oregon Claims tuffs contain <1.5% potassium (Appendix 3A) whereas the sample overprinted with the purple-brown biotite alteration at the French mine contains 5.92%. Locally, the Hedley intrusions are also affected by this pervasive biotite-rich alteration which emphasizes its postmagmatic, rather than synmagmatic character.

As the skarn-forming fluids passed through the sedimentary hostrock, the biotite-rich aureoles grew in size, and Zone 2 clinopyroxene-rich alteration then started to develop in the core, usually adjacent to the controlling fractures (Figure 36B). With time, the area of this clinopyroxene alteration also grew, and development of Zone 1 garnet-rich alteration then began. The garnetiferous alteration, which also expanded steadily outwards with time, generally initiated in the cores of pre-existing pyroxene veins and zones, either along fractures or as reaction rims adjacent to original carbonate beds (Figure 36C).

When the Zone 4 aureoles reached a certain diameter, which in some outcrops was less than 20 metres, their development apparently slowed or stopped. However, both the garnetiferous and pyroxene-rich alteration zones often continued growing until they completely replaced the biotite-rich aureoles (Figure 36D). This replacement was accompanied by the formation of an intervening thin reaction zone of Zone 3 orthoclase-rich alteration.

The larger skarn envelopes, such as those surrounding the Nickel Plate deposit, in contrast to the outcrop-sized skarns, have no peripheral biotitic aureoles, because

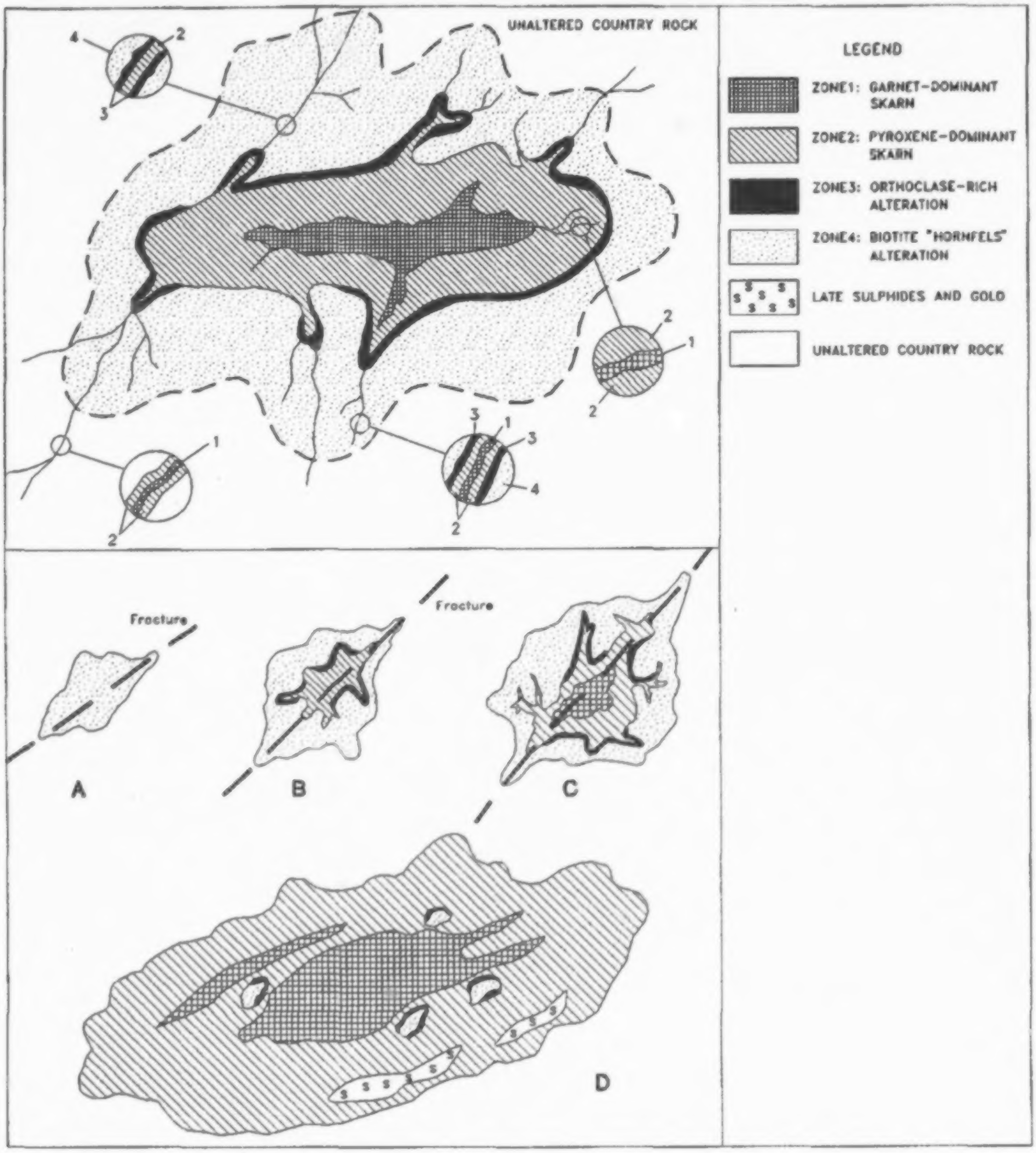
UNALTERED COUNTRY ROCK
LEGEND
ZONE1: GARNET-DOMINANT SKARN
ZONE2: PYROXENE-DOMINANT SKARN
ZONE3: ORTHOCLASE-RICH ALTERATION
ZONE4: BIOTITE "HORNFELS" ALTERATION
LATE SULPHIDES AND GOLD
UNALTERED COUNTRY ROCK
1
2
3
4
Fracture
Fracture
A
B
C
D
S

Figure 35. (Top) Idealized mineralogical zoning associated with small-scale exoskarn alteration in the Hedley district. Enlarged circles show various types of veinlets that may develop. *Note:* Zone 3 (orthoclase-rich) alteration only develops adjacent to Zone 4 (biotite "hornfels") alteration. Where garnet-rich (Zone 1) veinlets penetrate unaltered country rock, they are invariably haloed by pyroxene (Zone 2) alteration.

Figure 36. (Bottom) Temporal sequence of exoskarn formation at Hedley; A. Development of Zone 4 biotite "hornfels" alteration, along controlling fracture or dike margin. B. Continued growth of biotite-rich alteration accompanied by development of Zone 2 pyroxene skarn; local reaction of Zone 3 orthoclase-rich alteration forms where the pyroxene replaces biotite-rich zone. C. Cessation of biotite-rich Zone 4 alteration and initiation of inner core of Zone 1 garnet-dominant skarn. This is accompanied by continuing growth of the pyroxene-rich zone which steadily overprints the outer biotite-rich alteration. D. Continued growth of pyroxene and garnet skarn leading to almost complete destruction of the outer biotite-rich zone. Biotite-rich Zone 4 alteration is commonly only preserved as small remnants within the large pyroxene skarn envelope. Introduction of sulphides, scapolite and gold occurs late during this stage. Diameter of skarn in Figures 36A to 36C is generally less than 20 metres, whereas in Figure 36D the skarn may be up to 2 kilometres wide.

these were largely overgrown by the expanding pyroxene-rich assemblages. Consequently, the margins of the larger skarns comprise fine-grained pyroxene-rich alteration zones that are in sharp contact with the unaltered hostrocks. Where overprinting is incomplete, these wide pyroxene-rich envelopes contain small, irregularly distributed remnants of the earlier biotite and orthoclase-rich alteration assemblages (Figure 36D; Plate 25).

TABLE 6
COMPARISON OF THE NICKEL PLATE AND MOUNT RIORDAN SKARNS

	Nickel Plate	**Mt. Riordan**
Host formation and age	Upper Triassic Hedley Fm.	?Upper Triassic French Mine Fm?
Hostrock lithology	Predominantly siltstone, minor limestone	?Massive limestone and carbonate breccia?
Associated intrusive rocks	Hedley intrusions (gabbro, diorite)	Mount Riordan stock (granodiorite, gabbro)
Age of intrusions	Post 219 and pre 194 Ma (Late Triassic - Early Jurassic)	194.6 ± 1.2 Ma (Early Jurassic)
Initial $^{87}Sr/^{86}Sr$ of intrusions	0.7038*	0.7044*
Skarn mineralogy	Banded, clinopyroxene-dominant skarn with sulphides and scapolite. Garnets generally anhedral and brown coloured. No scheelite present.	Massive, garnet-dominant skarn. Coarse, euhedral garnets with highly variable colour. Generally low sulphide content. Minor pyroxene, actinolite, epidote. Scheelite present.
Opaque minerals	Pyrrhotite, arsenopyrite, minor chalcopyrite and rare pyrite	Magnetite, pyrrhotite, pyrite, minor chalcopyrite.
Degree of skarn alteration	Original sedimentary bedding commonly preserved in skarn.	Virtually no primary structures preserved.
Approximate exposed area of skarn	4 km^2	0.3 km^2
Maximum thickness of skarn	300 m	At least 175 m
Geochemistry of mineralization	Anomalous Au,As,Cu,Co,Bi,Te,Ag,Sb	Anomalous Cu,W,Ag,Mo
Garnet composition	Low manganese (< 0.5% MnO) *Grossularitic cores, andraditic margins* Ad_{15-80}	Low manganese (< 1.0 % MnO *Andraditic cores, grossularitic margins* Ad_{45-98}
Pyroxene composition	Low manganese (< 1.0% MnO) Hd_{40-95}	Low manganese (<1.3 % MnO) Hd_{41-51}

* R.L.Armstrong, personal communication, 1989.

CONCLUSIONS

The main conclusions of this study are:

- The Hedley district straddles the eastern tectonic edge of the Late Triassic Nicola back-arc basin. Its geology provides an insight into how rifting controlled the basin margin, the easterly derived sedimentation, and development of several economically important sedimentary facies in the Nicola Group.
- A stratigraphic succession is recognized in the Nicola Group. The succession includes one distinct marker horizon, the Copperfield breccia, that provides dramatic evidence of Late Triassic syntectonic sedimentation. The breccia represents a chaotic gravity-slide deposit of carbonate reefal debris that was probably derived from a shallow-marine, carbonate platform that originally lay immediately east of Hedley. Similar megabreccias could be expected to mark the proximity to the eastern boundary of the Nicola basin elsewhere in British Columbia.
- The Nicola Group is overlain by the newly recognized Skwel Peken Formation, comprising a succession of Middle Jurassic andesitic to dacitic tuffs that were laid down in a subaerial to shallow-water environment. The formation is associated with some minor rhyodacitic flows or intrusions that contain igneous garnet phenocrysts. It is believed to be the first Middle Jurassic supracrustal assemblage recognized in south-central British Columbia, and was probably related to the emplacement of the 168 Ma Lookout Ridge and Cahill Creek plutons.
- The district contains gold skarn deposits (Nickel Plate, French, Canty and Good Hope) as well as the Mount Riordan (Crystal Peak) garnet skarn which has industrial mineral potential. The latter is associated with the 194 Ma Mount Riordan stock whereas the gold skarns are genetically related to the slightly older Hedley intrusions.
- The Hedley intrusions, in comparison with other plutons related to iron, copper, tungsten, zinc-lead, molybdenum and tin skarns are the least differentiated; this chemistry reflects their derivation from primitive oceanic crust in an island arc environment.
- Nickel Plate, French, Canty and Good Hope represent type examples of reduced gold skarn deposits. Their alteration is characterized by an initial phase of potassium-rich metasomatism that predated development of the extensive hedenbergitic pyroxene-garnet skarn. The presence of this early metasomatism, although volumetrically insignificant, may be a favourable indicator for similar gold skarn deposits elsewhere.
- During gold skarn development, destruction of igneous ferromagnesian minerals and a lowering of the iron content of the endoskarn were matched correspondingly by an increase of iron in the exoskarn. This suggests that the ferromagnesian minerals in the Hedley intrusions were the source of the iron enrichment in the exoskarn and ore zones, and may also be the source of the gold. Onset of skarn alteration was accompanied by a sharp decline in the Fe_2O_3/FeO ratios in both the endoskarn and exoskarn which indicates that the hydrothermal fluids were strongly reduced.
- The Hedley geology suggests that rifted margins of back-arc basins are favourable environments for the development of reduced gold skarns. These areas contain deep structures that can channel arc-related, iron-rich and reduced plutonic magmas up into aprons of reactive calcareous sedimentary rocks.

REFERENCES

Alberti, G.K.B. (1987): Zur palaobiogeographischen Verbreitung unter und mitteldevonischer Dacryoconarida (Tentaculiten). *Courier Forschungs — Institut Senckenberg,* Volume 92, pages 161-176.

Andrew, K.P.E. (1988): Geology and Genesis of the Wolf Precious Metal Epithermal Prospect and the Capoose Base and Precious Metal Porphyry-style Prospect, Capoose Bay Area, Central British Columbia; unpublished M Sc. thesis, *The University of British Columbia,* 334 pages.

Billingsley, P. (1936): Report on the Oregon Prospect, Hedley, B.C.; unpublished report, 3 pages.

Billingsley, P. and Hume, C.G. (1941): The Ore Deposits of Nickel Plate Mountain, Hedley, B.C.; *Canadian Institute of Mining and Metallurgy,* Bulletin, Volume 44, pages 524-590.

Bischoff, G.C.O. (1978): Internal Structures of Conulariid Tests and their Functional Significance, with Special Reference to Circonulariina N. Suborder; *Senckenbergiana lethaea,* Volume 59, pages 275-327.

Bostock, H.S. (1930): Geology and Ore Deposits of Nickel Plate Mountain, Hedley, B.C.; *Geological Survey of Canada,* Summary Report, 1929, Part A, pages 198A-252A.

Bostock, H.S. (1940a): Map of the Hedley Area; *Geological Survey of Canada,* Map 568A.

Bostock, H.S. (1940b): Map of the Wolfe Creek Area; *Geological Survey of Canada,* Map 569A.

Bostock, H.S. (1941a): Okanagan Falls, British Columbia; *Geological Survey of Canada,* Map 627A.

Bostock, H.S. (1941b): Olalla, British Columbia; *Geological Survey of Canada,* Map 628A.

Bouma, A.H. (1962): *Sedimentology of some Flysch Deposits; Elsevier Scientific Publishing Company,* Amsterdam, 168 pages.

Brown, E.H. (1969): Some Zoned Garnets from the Greenschist Facies; *The American Mineralogist,* Volume 54, pages 1662-1677.

Bryant, V.Y. (1975): A Study of the Occurrence of Garnet in Silicious Igneous Rocks of the Mt. Pilchuck Area, Snohomish County, Washington; unpublished M.Sc. thesis. *University of Washington,* Seattle, 31 pages.

Camsell, C. (1910): Geology and Ore Deposits of the Hedley Mining District, B.C.; *Geological Survey of Canada,* Memoir 2.

Carr, J.M. (1968): Geology of Brenda Lake Area; B.C. Minister of Mines and Petroleum Resources Annual Report 1967, *B.C. Ministry of Energy, Mines and Petroleum Resources,* pages 183-212.

Chlupac, I. and Oliver, W.A. (1989): Decision on the Lochkovian-Pragian Boundary Stratotype (Lower Devonian); *Episodes,* Volume 12(2), pages 109-113.

Church, B.N. (1973): Geology of the White Lake Basin; *B.C. Ministry of Energy, Mines and Petroleum Resources,* Bulletin 61, 120 pages.

Church, B.N. (1975): Quantitative Classification and Chemical Composition of Common Volcanic Rocks; *Geological Society of America,* Bulletin 86, pages 257-263.

Cruise, D. and Griffiths, A. (1987): Fleecing the Lamb – The Inside Story of the Vancouver Stock Exchange; *Douglas and McIntyre,* Vancouver/Toronto, 277 pages.

Dawson, G.M.(1879): Preliminary Report on the Physical and Geological Features of the Southern Portion of the Interior of British Columbia; *Geological Survey of Canada,* Report of Progress 1877-78, pages 1B-187B.

Dawson, G.L., Godwin, C.I., Ray, G.E., Bordin, D. and Hammack, J. (1990a): Geology of the Goodhope-French Mine Area, South-central British Columbia; *in* Geological Fieldwork 1989, *B.C. Ministry of Energy, Mines and Petroleum Resources,* Paper 1990-1.

Dawson, G.L., Godwin, C.I. and Ray, G.E. (1990b): Gold Skarn Mineralization Associated with a Sediment-Sill Complex, French Mine, South-central B.C.; *Geological Association of Canada — Mineralogical Association of Canada,* Program with Abstracts, Volume 15, page A30, Annual Meeting, May 16-18, Vancouver, B.C.

Dick, L.A. (1980): A Comparative Study of the Geology, Mineralogy and Conditions of Formation of Contact Metasomatic Mineral Deposits in the North-eastern Canadian Cordillera; unpublished Ph.D. thesis, *Queen's University,* 471 pages.

Dick, L.A. and Hodgson, C.J. (1982): The Mactung W-Cu(Zn) Contact Metasomatic and Related Deposits of the North-eastern Canadian Cordillera; *Economic Geology,* Volume 77, pages 845-867.

Di Spirito, F., Hulme, N. and Laird, B. (1986): Reconnaissance Surveys on the Hedley Project; *B.C. Ministry of Energy, Mines and Petroleum Resources,* Assessment Report 14879.

Dolmage, V.(1934): Geology and Ore Deposits of Copper Mountain, British Columbia; *Geological Survey of Canada,* Memoir 171.

Dolmage, V. and Duffell, S. (1937): Reports on the Trethewey Syndicate Operation, Hedley, B.C.; unpublished report, 20 pages.

Dolmage, V. and Brown, C.E. (1945): Contact Metamorphism at Nickel Plate Mountain, Hedley, B.C.; *Canadian Institute of Mining and Metallurgy,* Bulletin, Volume 48.

Drysdale, C.W. (1914): Geology of the Thompson River Valley below Kamloops Lake, British Columbia; *Geological Survey of Canada,* Summary Report 1912.

Duba, D., McAllister, S.G. and Getsinger, J.S. (1988): Geological, Geochemical and Diamond Drilling Report on the Similkameen Property, Montello Option, Lost Horse 1-4, Lost Horse A-B.; *B.C. Ministry of Energy, Mines and Petroleum Resources,* Assessment Report 18233.

Dunn, C.E.(1981): The Biogeochemical Expression of a Deeply Buried Uranium Deposit in Saskatchewan, Canada; *Journal of Geochemical Exploration,* Volume 15, pages 437-452.

Einsele, G. (1985): Basaltic Sill-Sediment Complexes in Young Spreading Centers: Genesis And Significance; *Geology,* Volume 13, pages 249-252.

Einaudi, M.T. (1982): General Features and Origin of Skarns Associated with Porphyry Copper Plutons, Southwestern North America; *in* Advances in Geology of the Porphyry Copper Deposits, Southwestern U.S., Titley, S.R., Editor, *University of Arizona Press,* pages 185-209.

Ettlinger, A.D. (1990a): A Geological Analysis of Gold Skarns and Precious-Metal-Enriched Iron and Copper Skarns in British Columbia, Canada; unpublished Ph.D thesis, *Washington State University,* Pullman, 246 pages.

Ettlinger, A.D. (1990b): Skarn Evolution and Hydrothermal Fluid Characteristics in the Nickel Plate Deposit, Hedley, B.C.; *Geological Association of Canada — Mineralogical Association of Canada,* Program with Abstracts, Annual meeting, Vancouver, May 16-18, Volume 15, page A37.

Ettlinger, A.D. and Ray, G.E. (1988): Gold-enriched Skarn Deposits of British Columbia; *in* Geological Fieldwork 1987, *B.C. Ministry of Energy, Mines and Petroleum Resources,* Paper 1988-1, pages 263-279.

Ettlinger, A.D. and Ray, G.E. (1989): Precious Metal Enriched Skarns in British Columbia: An Overview and Geological Study; *B.C. Ministry of Energy, Mines and Petroleum Resources,* Paper 1989-3, 128 pages.

Ettlinger, A.D., Meinert, L.D. and Ray, G.E. (1992): Skarn Evolution and Hydrothermal Fluid Characteristics in the Nickel Plate Deposit, Hedley District, British Columbia; *Economic Geology,* Volume 87, pages 1541-1565.

Fitton, J.G. (1972): The Genetic Significance of Almandine-Pyrope Phenocrysts in the Calc-alkaline Borrowdale Volcanic Group, Northern England; *Contributions to Mineralogy and Petrology*, Volume 36, pages 231-248.

Floyd, pages.A. and Winchester, J.A. (1978): Identification and Discrimination of Altered and Metamorphosed Volcanic Rocks Using Immobile Elements; *Chemical Geology*, Volume 21, pages 291-306.

Fodor, R.V., Stoddard, E.F. and Burt, E.R. (1978): Origin of Spessartine-rich Garnet in Meta-rhyolite, Carolina Slate Belt; *Southeastern Geology*, Volume 22, pages 103-114.

Gabrielse, H. and Yorath, C.J. (1989): DNAG # 4. The Cordilleran Orogeny in Canada; *Geoscience Canada*, Volume 16, No. 2, pages 67-83.

Grant, J.A. (1986): The Isocon Diagram — A Simple Solution to Gresens' Equation for Metasomatic Alteration; *Economic Geology*, Volume 81, pages 1976-1982.

Green, T.H. and Ringwood, A.E. (1968): Origin of Garnet Phenocrysts in Calk-alkaline Rocks; *Contributions to Mineralogy and Petrology*, Volume 18, pages 163-174.

Gresens, R.L. (1967): Composition-Volume Relationships of Metasomatism; *Chemical Geology*, Volume 2, pages 47-65.

Grond, H.C., Wolfe, R., Montgomery, J.H. and Giroux, G.H. (1991): A Massive Skarn-hosted Andradite Deposit near Penticton, British Columbia; *in* Industrial Minerals of Alberta and British Columbia, Canada, Hora, Z.D., Hamilton, W.N., Grant, B. and Kelly, P.D., Editors, *B.C. Ministry of Energy, Mines and Petroleum Resources*, Open File 1991-23, pages 131-133.

Hedley, M.S. (1937): Report on the Property of Hedley Sterling Gold Mines Ltd.; *B.C. Ministry of Energy, Mines and Petroleum Resources*, Property File, unpublished report, 15 pages.

Hedley, M.S. (1939): Report on the Danger to the Townsite of Hedley from Falls of Rock; *B.C. Ministry of Energy, Mines and Petroleum Resources*, Property File, unpublished report, 14 pages.

Hine, A.C., Locker, S.D., Tedesco, L.P., Mullins, H.T., Hallock, P., Belknap, D.F., Gonzales, J.L., Neumann, A.C. and Snyder, S.W. (1992): Megabreccia Shedding from Modern, Low-relief Carbonate Platforms, Nicaraguan Rise; *Geological Society of America*, Volume 104, pages 928-943.

Irvine, T.N. and Baragar, W.R.A. (1971): A Guide to the Chemical Classification of the Common Volcanic Rocks; *Canadian Journal of Earth Sciences*, Volume 8, pages 523-547.

Lardeux, H. (1969): Les Tentaculites d'Europe Occidentale et d'Afrique du Nord; Cahiers de Paleontologie, *Centre National de la Recherche Scientifique*, Paris, 238 pages.

Lütke, F. (1985): Devonian Tentalulites from Nevada (U.S.A); *Courier Forschungs — Institut Senckenberg*, Volume 75, pages 197-226.

Lee, J.W. (1951): The Geology of Nickel Plate Mountain, B.C. unpublished Ph.D. thesis, *Stanford University*.

Little, H.W. (1961): Geology of the Kettle River (West Half), British Columbia; *Geological Survey of Canada*, Map 15-1961, scale 1:253 440.

Ludvigsen, R. (1972): Late Devonian Dacryoconarid Tentaculites, Northern Yukon Territory; *Canadian Journal of Earth Sciences*, Volume 9, pages 297-318.

MacDonald, G.A. (1968): Composition and Origin of Hawaiian Lavas; *Geological Society of America*, Memoir 116, pages 477-522.

Macdonald, C.C. (1977): Geology, Geochemistry and Diamond Drilling of the Hed Claims; *B.C. Ministry of Energy, Mines and Petroleum Resources*, Assessment Report 6060.

Mason, D.R. (1978): Evolution of Porphyry Copper Mineralization in an Oceanic Island Arc: Panama – A Discussion, *Economic Geology*, Volume 73, pages 982-985.

Mathieu, G.I., Boisclair, M.R. and Wolfe, R. (1991): Geology, Mineralogy and Processing of Mount Riordan Garnet Ores; *in* Industrial Minerals of Alberta and British Columbia, Canada, Hora, Z.D., Hamilton, W.N., Grant, B. and Kelly, P.D., Editors, *B.C. Ministry of Energy, Mines and Petroleum Resources*, Open File 1991-23, pages 135-145.

McCammon, J.W. (1954): Tungsten-copper, Billie Goat, Shamrock, etc.; *in* Report of the Minister of Mines 1953, *B.C. Ministry of Energy, Mines and Petroleum Resources*, pages A107-A108.

Meinert, L.D. (1983): Variability of Skarn Deposits; Guides to Exploration; *in* Revolution in the Earth Sciences – Advances in the Past Half-Century; Boardman, S.J., Editor, *Kendall/Hunt Publishing Company*, pages 301-316.

Milford, J.C. (1984): Geology of the Apex Mountain Group, North and East of the Similkameen River, South-central British Columbia; unpublished M.Sc. thesis, *The University of British Columbia*, 108 pages.

Monger, J.W.H. (1989): Geology of Hope and Ashcroft Map Areas, British Columbia; *Geological Survey of Canada*, Map 42-1989.

Mortimer, N. (1986): Late Triassic, Arc-related, Potassic Igneous Rocks in the North American Cordillera; *Geology*, Volume14, pages 1035-1038.

Mortimer, N. (1987): The Nicola Group: Late Triassic and Early Jurassic Subduction-related Volcanism in British Columbia; *Canadian Journal of Earth Sciences*, Volume 24, pages 2521-2536.

Myers, G.L. and Meinert, L.D. (1988): Zonation of the Copper Canyon-Fortitude Gold Skarn System; *Geological Society of America*, Abstracts with Program, Volume 20, No. 7, page A93.

Myers, G.L. (1990): Alteration Zonation of the Fortitude Gold Skarn Deposit, Lander County, Nevada; *Mining Engineering*, April 1990, pages 360-368.

Nakano, T. (1991): An Antipathetic Relation between the Hedenbergite and Johannsenite Components in Skarn Clinopyroxene from Kagata Tungsten Deposit, Central Japan; *Canadian Mineralogist*, Volume 29, pages 427-434.

Oliver, R.L. (1956): The Origin of Garnets in the Borrowdale Volcanic Series and Associated Rocks, English Lake District; *Geology Magazine*, Volume 93, pages 121-139.

Parrish, R.R. and Monger, J.W.H. (1992): New U-Pb Dates from Southwestern British Columbia; *in* Radiogenic Age and Isotope Studies: Report 5, *Geological Survey of Canada*, Paper 91-2, pages 87-108.

Pearce, J.A. (1975): Basalt Geochemistry Used to Investigate Past Tectonic Environments on Cyprus; *Tectonophysics*, Volume 25, pages 41-67.

Pearce, J.A. and Cann, J.R. (1973): Tectonic Setting of Basic Volcanic Rocks Determined Using Trace Element Analyses; *Earth and Planetary Science Letters*, Volume 19, pages 290-300.

Peto, P. (1973a): Petrochemical Study of the Similkameen Batholith, British Columbia; *Geological Society of America*, Volume 84, pages 3977-3984.

Peto, P. (1973b): Potassium-Argon Ages of Igneous Rocks from the Area Near Hedley, Southern British Columbia; *Canadian Journal of Earth Sciences*, Volume 10, pages 1357-1359.

Peto, P. (1983): Geological, Geochemical and Geophysical Report on the Golden Zone Property; *B.C. Ministry of Energy, Mines and Petroleum Resources*, Assessment Report 11514.

Peto, P. and Armstrong, R.L. (1976): Strontium Isotope Study of the Composite Batholith Between Princeton and Okanagan Lake; *Canadian Journal of Earth Sciences*, Volume 13, pages 1577-1583.

Preto, V.A. (1972): Geology of Copper Mountain; *B.C. Ministry of Energy, Mines and Petroleum Resources*, Bulletin 59, 87 pages.

Preto, V.A. (1979): Geology of the Nicola Group Between Merrit and Princeton, *B.C. Ministry of Energy, Mines and Petroleum Resources*, Bulletin 69, 90 pages.

Preto, V.A., Osatenko, M.J., McMillan, W.J. and Armstrong, R.L. (1979): Isotopic Dates and Strontium Isotopic Ratios for Plutonic and Volcanic Rocks in the Quesnel Trough and Nicola Belt, South-central British Columbia; *Canadian Journal of Earth Sciences*, Volume 16, No. 9, pages 1658-1672.

Ray, G.E and Dawson, G.L. (1987): Geology and Mineral Occurrences in the Hedley Gold Camp; *B.C. Ministry of Energy, Mines and Petroleum Resources*, Open File 1987-10.

Ray, G.E. and Dawson, G.L. (1988): Geology and Mineral Occurrences in the Hedley Gold Camp; *B.C. Ministry of Energy, Mines and Petroleum Resources*, Open File 1988-6.

Ray, G.E., Simpson, R., Wilkinson, W. and Thomas, P. (1986): Preliminary Report on the Hedley Mapping Project; *in* Geological Fieldwork 1985, *B.C. Ministry of Energy, Mines and Petroleum Resources*, Paper 1986-1, pages 101-105.

Ray, G.E., Dawson, G.L. and Simpson, R. (1987): The Geology and Controls of Skarn Mineralization in the Hedley Gold Camp, Southern British Columbia; *in* Geological Fieldwork 1986, *B.C. Ministry of Energy, Mines and Petroleum Resources*, Paper 1987-1, pages 65-79.

Ray, G.E., Dawson, G.L. and Simpson, R. (1988): Geology, Geochemistry and Metallogenic Zoning in the Hedley Gold Skarn Camp; *in* Geological Fieldwork 1987, *B.C. Ministry of Energy, Mines and Petroleum Resources*, Paper 1988-1, pages 59-80.

Ray, G.E., Grond, H.C., Dawson, G.L. and Webster, I.C.L. (1992): The Mount Riordan (Crystal Peak) Garnet Skarn, Hedley District, Southern British Columbia; *Economic Geology*, Volume 87, pages 1862-1876

Ray, G.E., Webster, I.C.L., Dawson, G.L. and Ettlinger, A.D. (1993): A Geological Overview of the Hedley Gold Skarn District, Southern British Columbia; *in* Geological Fieldwork 1992, Grant, B. and Newell, J.M., Editors, *B.C. Ministry of Energy, Mines and Petroleum Resources*, Paper 1993-1, pages 269-279.

Read,P.B. and Okulitch, A.V. (1977): The Triassic Unconformity of South-central British Columbia; *Canadian Journal of Earth Sciences*, Volume 14, pages 1127-1145.

Rice, H.M.A. (1947): Geology and Mineral Deposits of the Princeton Map-area, B.C.; *Geological Survey of Canada*, Memoir 243.

Rice, H.M.A. (1960): Geology and Mineral Deposits of the Princeton Map-area, British Columbia; *Geological Survey of Canada*, Memoir 243, 136 pages.

Roddick, J.C., Farrar, E. and Procyshyn, E.L. (1972): Potassium-Argon Ages of Igneous Rocks from the area near Hedley, Southern B.C.; *Canadian Journal of Earth Sciences*, Volume 9, pages 1632-1639.

Shannon, J.R., Drinkard, M.J., Herald, C.E. and Miller, R.E. (1990): Geology of the Crown Jewel Deposit (Buckhorn Mtn) Gold Skarn, Okanogan County, Washington; *Geological Association of Canada — Mineralogical Association of Canada Annual Meeting*, Vancouver, Abstracts, Volume 15, page A120.

Shaw, D.A. (1985): Geological Report for Canova Resources Ltd. on the Lake Claims; *B.C. Ministry of Energy, Mines and Petroleum Resources*, Assessment Report 14549.

Simpson, R.G. (1987): Geology of the Nickel Plate Gold Deposit; *Mascot Gold Mines Ltd.*, unpublished report, September 15.

Simpson, R.G. and Ray, G.E. (1986): Nickel Plate Gold Mine; *Canadian Institute of Mining and Metallurgy*, District 6 Meeting, Paper 30, page 19, Victoria, British Columbia, October.

Soregaroli, A.E. and Whitford, D.F. (1976): Brenda; *in* Porphyry Deposits of the Canadian Cordillera, Sutherland Brown, A., Editor, *Canadian Institute of Mining and Metallurgy*, Special Volume 15, pages 186-194.

Tempelman-Kluit, D. and Parkinson, D. (1986): Extension Across the Eocene Okanagan Crustal Shear in Southern British Columbia; *Geology*, Volume 14, pages 318-321.

Taylor, B.E. and Liou, J.G. (1978): The Low-temperature Stability of Andradite in C-O-H Fluids; *American Mineralogist*, Volume 63, pages 378-393.

Thorkelson D.J. and Rouse G.E. (1989): Revised Stratigraphic Nomenclature and Age Determinations for Mid-Cretaceous Volcanic Rocks in Southwestern British Columbia; *Canadian Journal of Earth Sciences*, Volume 26, pages 2016-2031.

Torrey, C.E. Karjalainen, H., Joyce, P.J., Erceg, M. and Stevens, M. (1986): Geology and Mineralization of the Red Dome (Mungana) Gold Skarn Deposit, North Queensland, Australia; *in* Proceedings of Gold 86 – An International Symposium on the Geology of Gold, Macdonald A.J., Editor, *Gold 86*, Toronto, pages 504-517.

Troger, E. (1959): Die Granatgruppe: Beziehungen Zwischen Mineralchemismus und Gesteinsart; *Neues Jahrbuch fur Mineralogie*, Volume 93, pages 1-44.

Vennum, W.R. and Meyer, C.E. (1979): Plutonic Garnets from the Werner Batholith, Lassiter Coast, Antarctic Peninsula; *American Mineralogist*, Volume 64, pages 268-273.

Wagner, D.W. (1989): Mass Balance Relationships and their Influence on the Mineralization of the Auriferous Skarns Of the Nickel Plate Mine, Hedley, British Columbia; unpublished B.Sc.thesis, *University of Waterloo*, 77 pages.

Warren, H.V. and Cummings, J.M. (1936): Mineralogy at the Nickel Plate Mine; *The Miner*, Volume 9, pages 27-28.

Warren, H.V. and Peacock, M.A. (1945): Hedleyite, a New Bismuth Telluride from British Columbia, with notes on Wehrlite and some Bismuth-Tellurium Alloys; *University of Toronto*, Geological Series, No. 49, pages 55-69.

Webster, I.C.L. (1988): Skarn and Ore Mineralogy at the Hedley Amalgamated Mine, Hedley, British Columbia; *Brock University*, unpublished B.Sc. thesis, 39 pages.

Wheeler, J.O., Brookfield, A.J., Gabrielse, H., Monger, J.W.H., Tipper, H.W. and Woodsworth, G.J. (1991): Terrane Map of the Canadian Cordillera; *Geological Survey of Canada*, Open File 1713A.

Winchell, H.V. (1902): Report on the Nickel Plate Gold Mine; *B.C. Ministry of Energy, Mines and Petroleum Resources*, Property File, unpublished report, 17 pages.

Winchester, J.A. and Floyd, P.A. (1977): Geological Discrimination of Different Magma Series and their Differentiation Products Using Immobile Elements; *Chemical Geology*, Volume 20, pages 325-343.

APPENDICES

APPENDIX 1A

U-Pb ZIRCON GEOCHRONOLOGY OF THE HEDLEY AREA

Janet E. Gabites, Geochronology Laboratory,
Department of Geological Sciences, U.B.C.,
Vancouver, B.C., Canada V6T 1Z4

Uranium-lead zircon ages were determined for five samples of intrusive and volcanic rocks from the Hedley area. The ages obtained have been used to help define the timing of geological events in the region. The analyses are plotted on concordia diagrams in Appendix Figures 1B-1G, and data are presented in Appendix Table 1. The interpreted ages are summarized in Appendix Table 2.

ANALYTICAL METHODS

Zircon concentrates are split into fractions of varying grain size and magnetic susceptibility, and hand picked to 100% purity. Concordance is improved by air abrasion techniques (Krogh, 1982). Chemical dissolution and mass spectrometry are modified from procedures described by Parrish and Krogh (1987), and employ a mixed ^{205}Pb-^{233}U-^{235}U spike. Zircons were dissolved in small-volume teflon capsules contained in a large Parr bomb (Parrish, 1987). Both U and Pb were eluted into the same beaker and loaded and analysed sequentially on the same Re filament with silica gel and phosphoric acid. The mass spectrometer used is a V.G. Micromass 54R with a Daly collector to improve the quality of measurement of low-intensity ^{204}Pb signals. Errors in U-Pb ages were obtained by individually propagating all calibration and measurement uncertainties through the entire age calculation and summing the individual contributions to the total variance (Roddick, 1987). The decay constants used for the age calculation are those recommended by the IUGS Subcommission on Geochronology (Steiger and Jäger, 1977). Concordia intercepts are based on a modified version of the York (1969) regression model in which calculated concordia ages are multiplied by the square root of the MSWD (Parrish and Krogh, 1987). Errors reported for the raw U-Pb data are one sigma; those for final ages and shown on concordia plots are two sigma (95% confidence limits).

INTERPRETATION OF ANALYSES

a) HD 80, Cahill Creek pluton (Unit 12) (Appendix 1B).

The four fractions analysed lie on a least squares regression line through zero with an upper intercept of 168.8±9.3 Ma (Middle Jurassic). This is the best estimate of the age of the rock. A lower limit on the age is given by the ^{206}Pb/^{238}U age, 162.6±1.4 Ma, for the abraded coarse non-magnetic fraction b), which yields the oldest Pb-U ages and overlaps concordia. The other three fractions have lost lead. There is no evidence for inherited old zircon in this sample.

b) HD 271, quartz feldspar dacite crystal tuff, Skwel Peken Formation (Unit 15) (Appendix 1C).

Three fractions were analysed from this sample. The interpreted age of the rock is the upper intercept of this isochron passing through zero and fractions b) and c). This gives a maximum date of 187±9 Ma, which suggests that the unit is Early to Middle Jurassic age. The non-magnetic fraction a) gives a ^{207}Pb/^{206}Pb age of 284 Ma, indicating the presence of an inherited zircon component of Paleozoic or older age, and strong post-crystallisation lead loss.

c) HD 81, Stemwinder stock, Hedley Intrusions (Unit 9) (Appendix 1D).

The result obtained from four fractions is inconclusive due to combined lead loss and inheritance of old zircon No regression is possible. If the rock is Triassic or younger, a three stage lead evolution is implied by the old ^{207}Pb/^{206}Pb ages. The age of the intrusion is most likely to be between 175±0.6 Ma (the youngest ^{206}Pb/^{238}U age) and 219±11 Ma (the ^{207}Pb/^{206}Pb age of the most concordant fraction). The age of the inherited zircon is Paleozoic or older.

d) HD 273, mafic phase of Banbury stock, Hedley Intrusions (Unit 9) (Appendix 1E).

The interpretation of the age of this rock based on the five fractions is complicated by combined lead loss and inheritance of old zircon. The best estimate of the age at 215.4 4 Ma is given by the upper intercept of a least squares regression passing through zero and the two non-magnetic fractions, a) and b), which are closest to concordia. Two fine magnetic fractions, d) and e), plot below concordia and thus indicate inheritance of Cambrian or older zircon as well as lead loss.

e) HD 406, granodiorite, Mount Riordan stock (Unit 11) (Appendix 1F).

The two fractions analysed define an isochron with a lower intercept of 194.6±1.2 Ma. The fractions contain inherited old zircon with an average age of 1719±138 Ma.

f) HD 272, Quartz Porphyry (Unit 14) (Appendix 1G).

The four fractions analysed indicate inheritance of zircon of Paleozoic or older age. The lower intercept of a three point least squares regression line gives the best estimate of the age of the rock, 154.5 + 8/ - 43 Ma. The average age of inherited old zircons in fractions a), c), and d) is 391 Ma with a very large associated error. Fraction b) plots below concordia, indicating the presence of an inherited zircon component and strong post-crystallisation lead loss.

SUMMARY

The two oldest plutonic rocks are the Stemwinder (HD 81) and Banbury stocks (HD 273) of the Hedley Intrusions. The Late Triassic maximum dates obtained here suggest inheritance of Paleozoic or older zircons. The details of this inherited zircon component are not well defined. It could be assimilated detrital zircon of a variety of ages, or zircon picked up from lower crust, also with a range of ages. Single ion-probe analyses of these fractions and of Hedley area sedimentary rocks would be needed to proceed further in clarification of this inheritance. The three plutons represent the Nicola - Guichon - Coldwater volcanic-intrusive episode (217 to 210 Ma), in the Hedley area.

The Mount Riordan stock (HD 406) is Early Jurassic and younger than the Hedley Intrusions. This suggests that there are skarns of two different ages in the district. The gold skarns are related to the older Hedley Intrusions, and the Mount Riordan garnet skarn is associated with the younger Mount Riordan stock.

The youngest plutonic suites dated during this study are represented by the Cahill Creek pluton (HD 80) and the Quartz Porphyry (HD 272). These are believed to be part of the Late to Middle Jurassic Oliver - Osprey Lake - Eagle phase of plutonism. Field evidence suggests that the Skwel Peken Formation is related to this intrusive episode, although the dating on the sample HD 271 gives an older age of 187±9 Ma. This apparent discrepancy may reflect different cooling rates for the intrusive and extrusive rocks.

REFERENCES CITED

Krogh, T. E., 1982, Improved accuracy of U-Pb zircon ages by the creation of more concordant systems using an air abrasion technique: Geochimica et Cosmochimica Acta, v. 46, p. 637-649.

Ludwig, K. R., 1980, Calculation of uncertainties of U-Pb isotope data: Earth and Planetary Science Letters, v. 46, p. 212-220.

Parrish, R. R., 1987, An improved micro-capsule for zircon dissolution in U-Pb geochronology: Chemical Geology, Isotope Geoscience Section, v. 66, p. 99-102.

Parrish, R. R. and Krogh, T. E., 1987, Synthesis and purification of ^{205}Pb for U-Pb geochronology: Chemical Geology, Isotope Geoscience Section, v. 66, p. 103-110.

Roddick, J. C., 1987, Generalized numerical error analysis with applications to geochronology and thermodynamics. Geochimica et Cosmochimica Acta, v. 51, p. 2129-2135.

Stacey, J. S. and Kramers, J. D., 1975, Approximation of terrestrial lead isotope evolution by a two-stage model: Earth and Planetary Science Letters, v. 26, p. 207-221.

Steiger, R. H. and Jäger, E., 1977, Subcommission on Geochronology: Convention on the use of decay constants in geo- and cosmochronology: Earth and Planetary Science Letters, v. 36, p. 359-362.

York, D., 1969, Least-squares fitting of a straight line with correlated errors: Earth and Planetary Science Letters, v. 5, p. 320-324.

APPENDIX 1A (TABLE 1)
U-Pb ZIRCON DATA FROM SAMPLES IN THE HEDLEY AREA

Fraction^{1,2} Magnetic & size split	wt mg	U^3 ppm	Pb^3 ppm	^{207}Pb	^{208}Pb ^{206}Pb=100	^{204}Pb	$^{206}Pb/^{204}Pb$ Measured^4 Blank Pb, pg^3	$^{206}Pb/^{238}U$ ratio^5 Date±1σ	$^{207}Pb/^{235}U$ ratio^5 Date±1σ	$^{207}Pb/^{206}Pb$ ratio^5 Date±1σ
HD 80	**Cahill Creek Pluton**									
a NM 2A/1° -149+74 μ	3.2	513	11.6	5.2916	11.879	0.0193	4056 120	0.02238 (.268) 142.7±0.4	0.1546 (2.91) 145.9±3.9	0.05008 (2.91) 198.8±65
b NM2A/1° abr -149+74 μ	4.8	404	10.5	5.1414	12.454	0.0132	5018 200	0.02554 (.861) 162.6±1.4	0.1742 (.746) 163.1±1.4	0.04947 (.344) 170.2±8.0
c NM 2A/1° abr -74+44 μ	2.5	546	12.8	5.1534	12.377	0.0149	5871 37	0.02311 (.865) 147.3±1.3	0.1572 (.954) 148.2±1.3	0.04934 (.324) 164.1±7.6
d M 2A/3° -74+44 μ	3.2	785	18.4	8.0147	19.172	0.2051	478 120	0.02060 (.388) 131.4±0.5	0.1420 (1.26) 134.9±1.6	0.05002 (1.12) 195.7±26.4
HD 271	**Crystal tuff (Skwel Peken Formation)**									
a NM2A/1° abr -149+74 μ	0.4	229	5.1	5.569	9.9861	0.0253	1538 50	0.02227 (.988) 142.0±1.4	0.1596 (.501) 150.3±0.7	0.05198 (.981) 284.3±22
b NM2A/1° abr -149+74 μ fragments	0.2	283	8.1	7.696	16.179	0.1842	260 200	0.02593 (.232) 165.0±0.4	0.1783 (1.18) 166.6±1.8	0.04989 (1.12) 189.9±26.5
c M1.5A/3° -74+44 μ	0.4	372	9.5	6.1330	13.591	0.0782	1055 37	0.02445 (.245) 155.7±0.4	0.1680 (.416) 157.7±0.6	0.04984 (.241) 187.5±5.6
HD 81	**Stemwinder Stock**									
a NM2A/3° -149+74 μ	2.0	440	12.6	5.4758	14.398	0.0204	3515 120	0.02758 (.253) 175.4±0.5	0.1969 (.406) 182.5±0.7	0.05177 (.309) 275.3±6.9
b M2A/0.5° -149+74 μ	0.4	421	13.4	6.6426	18.137	0.1035	600 200	0.02898 (.276) 184.2±0.5	0.2047 (.830) 189.1±1.5	0.05124 (.761) 251.7±17.5
c M2A/0.5° -74+44 μ	0.4	893	27.6	6.6251	19.910	0.1072	721 200	0.02778 (.324) 176.6±0.6	0.1935 (.413) 179.6±0.7	0.05051 (.238) 218.6±5.4
d M2A/3° -74+44 μ	1.6	879	26.1	5.7486	17.400	0.0426	2099 120	0.02782 (.360) 176.9±0.6	0.1965 (.509) 182.2±0.8	0.05124 (.351) 251.5±8.2
HD 273	**Banbury Stock**									
a NM2A/1° -149+74 μ	0.4	1174	34.9	5.2106	15.771	0.0114	2794 200	0.02847 (.211) 181.0±0.4	0.1980 (.252) 183.4±0.4	0.05043 (.119) 214.9±2.9
b NM2A/1° -74+44 μ	2.0	926	27.0	5.2167	14.171	0.0110	5774 200	0.02833 (.318) 180.1±0.6	0.1975 (.354) 183.0±0.6	0.05056 (.138) 220.6±3.2
c M2A/1° abr -149+74 μ	0.4	1203	36.5	7.1229	20.172	0.0036	664 37	0.02695 (1.56) 171.4±2.6	0.1855 (1.87) 172.7±3.0	0.04991 (1.14) 191.0±26.6
d M2A/1° -74+44 μ	1.0	1524	39.0	5.9840	16.611	0.0568	1521 200	0.02387 (.167) 152.1±0.2	0.1696 (.177) 159.0±0.3	0.05150 (.078) 263.4±1.6
e M2A/1° abr -74+44 μ	0.4	1124	31.7	5.6641	15.889	0.0262	3173 37	0.02678 (.637) 170.4±1.0	0.1950 (1.23) 180.9±2.0	0.05281 (.663) 320.5±15
HD 406	***Mount Riordan Stock***									
a NM2A/1° abr +74 μ	0.9	191	6.4	6.5872	12.063	0.0817	1078 37	0.03274 (.275) 207.7±0.6	0.2435 (.411) 221.2±0.8	0.05392 (.204) 367.8±4.7
b M1.5A/3° abr -74+44 μ	0.4	250	8.5	7.6780	14.735	0.1742	517 37	0.03127 (.256) 198.5±0.5	0.2209 (.498) 202.6±0.9	0.05123 (.351) 251.1±7.9
HD 272	**Quartz Porphyry**									
a NM2A/1° -149+74 μ	3.9	1097	31.7	6.6546	14.330	0.1131	854 200	0.02717 (1.104) 172.8±1.9	0.1870 (1.12) 174.1±1.8	0.04992 (.521) 191.3±12.0
b NM2A/1° abr -149+74 μ	1.6	1042	26.3	6.7361	14.023	0.1075	865 200	0.02381 (.504) 151.7±0.8	0.1694 (.531) 158.9±0.8	0.05159 (.019) 267.9±4.4
c M2A/1° -74+44 μ	2.1	1567	44.3	7.9137	17.335	0.2006	484 200	0.02523 (.515) 160.6±0.6	0.1727 (.679) 161.8±1.0	0.04965 (.403) 178.7±9.2
d M2A/1° abr -74+44 μ	2.1	1251	31.3	5.9025	12.516	0.0689	1417 37	0.02425 (.619) 154.5±0.9	0.1641 (.670) 154.2±1.0	0.04907 (.245) 151.0±5.8

Analyses by P. Van der Heyden, D. Murphy, and J. Gabites, 1987 to 1990.

IUGS conventional decay constants (Steiger and Jäger, 1977) are: $^{238}U\lambda=1.55125\times10^{-10}a^{-1}$, $^{235}U\lambda=9.8485\times10^{-10}a^{-1}$, $^{238}U/^{235}U=137.88$ atom ratio.

1. Column one gives the label used in the Figures.
2. Zircon fractions are labelled according to magnetic susceptibility and size in microns. NM = non-magnetic at given amperes on magnetic separator, M = magnetic. Side slope is given in degrees. Abr = air abraded. The size (-74+44) indicates zircons pass through 74 micron sieve but not the 44 micron sieve.
3. U and Pb concentrations are corrected for blank U and Pb. Isotopic composition of laboratory Pb blank is 206:207:208:204 = 17.75:15.50:37.30:1.00 (before 1990), 18.16:15.614:38.283:1.00 (after 1990), based on ongoing analyses of total procedural blanks. The 1990 total procedural blank is 37 ± 5 pg; larger values have been used for fractions run before 1990. Laboratory U blank is 6 ± 0.5 pg, based on total procedural blanks.
4. Common Pb is assumed to be Stacey and Kramers (1975) model Pb of 190 ± 80 Ma age.
5. Uncertainties in the isotopic ratios are one sigma.

APPENDIX 1A (TABLE 2)
U-Pb DATA REGRESSION AND INTERPRETED AGES

Sample Number	n	MSWD	Lower concordia intercept (Ma ± 2σ)	Upper concordia intercept (Ma ± 2σ)	Interpreted Age (Ma ± 2σ)
HD 80	5	0.76	0[1]	168.8 ± 9	168.8 ± 9 max
HD 271	4	18.54	0[1]	187 ± 9	187 ± 9 max
HD 81	4		minimum 175 ± 0.6[2]	maximum 219 ± 11[3]	between limits
HD 273	3	0.54	0[1]	215.4 ± 4	215.4 ± 4 max
HD 406	2	0	194.6 ± 1.5	1719.3 ± 138	194.6 ± 1.2
HD 272	3	2.36	154.5 +8/-43	391 +266/-214	154.5 +8/-43

1. Calculation forced through zero, n includes zero point.
2. ^{206}Pb/^{238}U age.
3. ^{207}Pb/^{206}Pb age from most concordant fraction.
4. Data regression is by the methods of Ludwig (1980)
5. MSWD = mean square of weighted deviate

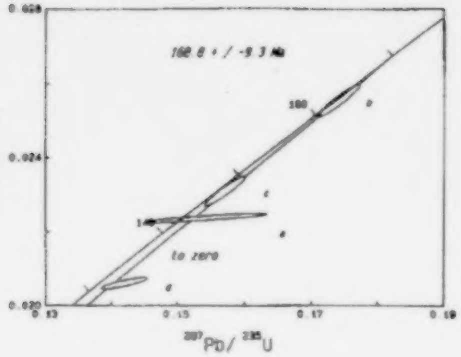

Appendix 1B:
HD 80 (Cahill Creek pluton)

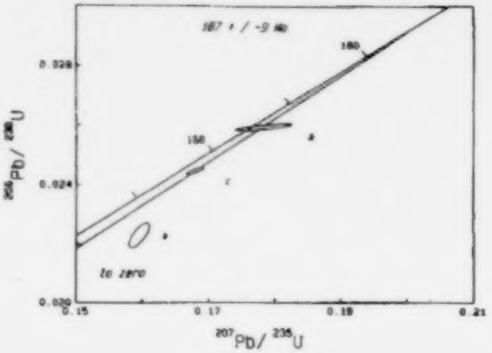

Appendix 1C:
HD 271 (Skwel Peken Formation)

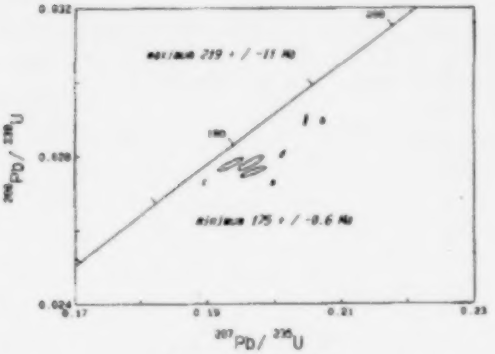

Appendix 1D:
HD 81 (Stemwinder stock)

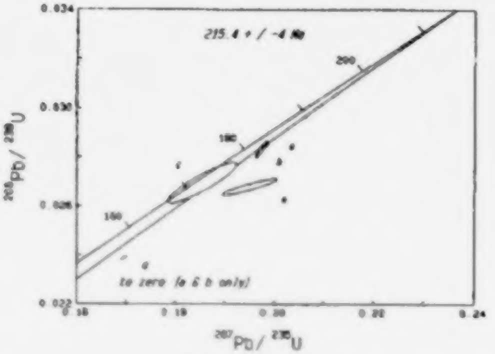

Appendix 1E:
HD 273 (Banbury stock)

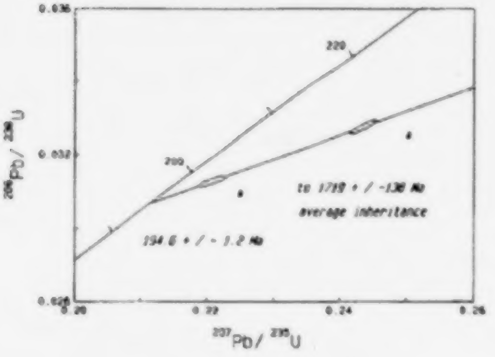

Appendix 1F:
HD 406 (Mount Riordan stock)

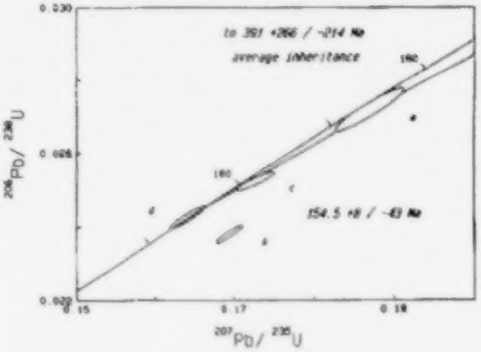

Appendix 1G:
HD 272 (Quartz Porphyry)

Error elipses are 2 sigma.

APPENDIX 2A
REPORT ON CONODONTS AND OTHER MICROFOSSILS COLLECTED DURING THIS STUDY
BY M.J. ORCHARD
GEOLOGICAL SURVEY OF CANADA

Summary of microfossils whose locations are shown in Figure 37

No. in Fig.37	Lithology	*Fossil Type	Age	GSC Location	**Collector
F1	1m thick limestone - Chuchuwayha Fm	C	Early Norian	C-103723	GER
F2	2m thick limestone - Chuchuwayha Fm	C	late Early Norian	C-103722	GER
F3	0.25m thick limestone - Chuchuwayha Fm	C	Early Norian	C-143397	GER
F4	0.6m diameter limestone clast, Copperfield breccia	C	Carnian	C-103300	GER
F5	Chert pebble - Coppperfield breccia	R	Permian	-	FC
F6	Limestone clast - Copperfield breccia	C	late Early Norian	C-103724	GER
F7	Tuffuceous limestone - Stemwinder Fm	C	Early Norian	C-103739	GER
F8	Limestone bed at top of Stemwinder Fm	C	Late Norian	C-103725	GER
F9	Limestone bed - Stemwinder Fm	C	Late Carnian	C-103727	GER
F10	Thin limestone at top of Stemwinder Fm	C	Middle to Late Norian	C-143399	GER
F11	Thin limestone - Stemwinder Fm	C	Late Carnian	C-103726	GER
F12	2m thick limestone - Stemwinder Fm	C	Carnian	C-103728	GER
F13	Thin limestones in argillites - Stemwinder Fm	C	Early Norian	C-103729	GER
F14	Limestone clast, Copperfield breccia	C	Late Carnian	C-143398	GER
F15	Limestone bed - Hedley Fm	C	Probable Early Norian	C-103732	GER
F16	0.3m thick limestone - Stemwinder Fm	C	late Early Norian	C-103735	GER
F17	Limestone - Hedley Fm	C	Early Norian	C-103746	GER
F18	Massive limestone - Hedley Fm	C	Early Norian	C-103736	GER
F19	Massive limestone - Hedley Fm	C	Early Norian	C-103737	GER
F20	0.2m thick limestone - Hedley Fm	C	Early Norian	C-103750	GER
F21	Massive limestone - Hedley Fm	C	Early Norian	C-102996	DTK
F22	Limestone clast - Copperfield breccia	S	Probable Upper Triassic	C-143201	GER
F23	Limestone boulder in conglomerate-Apex Mt. Complex	T	mid Early to early Late Devonian	C-153760	GER
F24	Limestone boulder in conglomerate-Apex Mt. Complex	T	mid Early to early Late Devonian	C-153761	GER
F25	Limestone boulder in conglomerate-Apex Mt. Complax	T	mid Early to early Late Devonian	C-153762	GER
F26	Marble - Apex Mountain Complex	I	Phanerozoic	C-103299	GER
F27	0.6m thick limestone boulder - Copperfield breccia	I	Phanerozoic	C-143400	GER

* C = Conodont R = Radiolarian T = Nowakiid tentacilites I = Ichthyoliths S = Shelly fossil
**GER = G.E. Ray FC = F. Cordey DTK = D. Tempelman-Kluit

Details of individual microfossil samples (collected by G.E. Ray)

1. COPPERFIELD BRECCIA

GSC Loc. No: **C-103300** **NTS**: Hope, 92H
Fld. No: 85HD-45
Collector: G.E. Ray
GEOGR - Lat./Long.:
UTM: Zone 10; 707900E, 5470500N.
Description: 4.5 km WSW of Hedley.
STRAT - Rock Unit: Nicola Group, Copperfield Breccia
Description: Carbonate: a 0.6 m diameter limestone clast containing crinoid stems within the breccia.

PALEO - Fossils: conodonts, ichthyoliths, spicules
Conodont taxa: **CAI:** 5
Metapolygnathus ex gr. polygnathiformis (Budurov & Stefanov 1965) (3)
Neogondolella? sp. (1)
AGE - Late Triassic, Carnian.

GSC Loc. No: **C-103724** **NTS**: Hope, 92H
Fld. No: 85HD-48
Collector: G.E. Ray
GEOGR - *Lat./Long.:*
UTM: Zone 10; 707800E, 5470400N.
Description: S side of Similkameen valley, 4.5 km WSW of Hedley.
STRAT - Rock Unit: Nicola Group, Copperfield Breccia
Description: *Carbonate: from a limestone boulder within* the Copperfield Breccia; the limestone is a black, fine grained, massive rock with abundant bivalve fossils.
PALEO - Fossils: conodonts
Conodont taxa: ***CAI:*** 5
Epigondolella triangularis (Budurov 1972) (3)
AGE - Late Triassic, late Early Norian, *triangularis* Zone

GSC Loc. No: **C-143398** **NTS**: Hope, 92H
Fld. No: 85HD-47
Collector: G.E. Ray
GEOGR - Lat./Long.:
UTM: *Zone 10; 707800E, 5470410N.*
Description: 4.5 km WSW of Hedley.
STRAT - Rock Unit: Nicola Group, Copperfield Breccia.
Description: Carbonate: a light grey coarse crystalline limestone boulder within the breccia
***PALEO* - Fossils:** *conodonts, ichthyoliths, shell fragments*
Conodont taxa: **CAI:** 5 - 5.5
Metapolygnathus sp. cf. *M. samueli* Orchard 1991 (1)
Metapolygnathus nodosus (Hayashi 1968) (1)
AGE - Late Triassic, Late Carnian.

GSC Loc. No: **C-143400** **NTS**: Hope, 92H
Fld. No: 85HD-46
Collector: G.E. Ray
GEOGR - Lat./Long.:
UTM: Zone 10; 707800E, 5470410N.
Description: 4.5 km WSW of Hedley.
STRAT - Rock Unit: Nicola Group, Copperfield Breccia
Description: *Carbonate: 0.6 m diameter massive grey* limestone clast within the breccia.
PALEO - Fossils: ichthyoliths
AGE - Phanerozoic

GSC Loc. No: **C-103732** **NTS**: Hope, 92H
Fld. No: 86HD-T06
Collector: G.E. Ray
GEOGR - **Lat./Long.:**
UTM: Zone 10; 713570E, 5470270N.
Description: 1.5 km SE of Hedley; 2950' elevation.
STRAT - **Rock Unit:** Nicola Group, Hedley Formation.

Description: Carbonate: a 0.5-1.0 m thick limestone bed.
PALEO - **Fossils:** conodonts
Conodont taxa: **CAI:** 6.5 - 7
Epigondolella sp. (3)
AGE - Late Triassic, probably Early Norian.

GSC Loc. No: **C-103736** **NTS**: Hope, 92H
Fld. No: 86HD-T18
Collector: G.E. Ray
GEOGR - **Lat./Long.:**
UTM: Zone 10; 714810E, 5471500N.
Description: 2.5 km E of Hedley; 5250' elevation.
STRAT - **Rock Unit:** Nicola Group, Hedley Formation
Description: Carbonate: a massive to weakly bedded limestone.
PALEO - **Fossils:** conodonts, ichthyoliths
Conodont taxa: **CAI:** 5.5 - 6
Epigondolella quadrata Orchard 1991 (4)
Epigondolella triangularis (Budurov 1972) (4)
AGE - Late Triassic, Early Norian, *triangularis* Zone

GSC Loc. No: **C-103737** **NTS**: Hope, 92H
Fld. No: 86HD-T20
Collector: G.E. Ray
GEOGR - **Lat./Long.:**
UTM: Zone 10; 714350E, 5471165N.
Description: 2.0 km E of Hedley; 4550' elevation.
STRAT - **Rock Unit:** Nicola Group, Hedley Formation
Description: Carbonate: a massive bedded limestone.
PALEO - **Fossils:** conodonts, ichthyoliths
Conodont taxa: **CAI:** 6
Epigondolella sp. indet. (1)
AGE - Late Triassic, Early? Norian.

GSC Loc. No: **C-103746** **NTS**: Hope, 92H
Fld. No: 86HD-260
Collector: G.E. Ray
GEOGR - **Lat./Long.:**
UTM: Zone 10; 715030E, 5471350N.
Description: 2.5 km E of Hedley; 5250' elevation.
STRAT - **Rock Unit:** Nicola Group, Hedley Formation.
Description: Carbonate: a grey limestone.
PALEO - **Fossils:** conodonts, ichthyoliths
Conodont taxa: **CAI:** 5
Epigondolella quadrata Orchard 1991 (4)
AGE - Late Triassic, Early Norian.

GSC Loc. No: **C-103750** **NTS**: Hope, 92H
Fld. No: 86HD-305
Collector: G.E. Ray
GEOGR - **Lat./Long.:**
UTM: Zone 10; 715710E, 5473300N.
Description: 4 km NE of Hedley; 5700' elevation.
STRAT - **Rock Unit:** Nicola Group, Hedley Formation
Description: Carbonate: a 0.20 m thick limestone bed.
PALEO - **Fossils:** conodonts, sponge spicules
Conodont taxa: **CAI:** 5.5 - 6.5
Epigondolella quadrata Orchard 1991 (6)
Epigondolella triangularis (Budurov 1972) (11)

Metapolygnathus spp. (2)
AGE - Late Triassic, Early Norian, *triangularis* Zone
Remarks: Metapolygnathids may be derived.

3. *CHUCHUWAYHA FORMATION*

GSC Loc. No: **C-103722** **NTS**: Hope, 92H
Fld. No: 85HD-19
Collector: G.E. Ray
GEOGR - **Lat./Long.:**
UTM: Zone 10; 711150E, 5472520N.
Description: 1.75 km NW of Hedley.
STRAT - **Rock Unit:** Nicola Group, Chuchuwayha Formation
Description: *Carbonate: grey, thin bedded limestone.*
PALEO - **Fossils:** conodonts
Conodont taxa: **CAI:** 5
ramiform elements (8)
Epigondolella triangularis (Budurov 1972) (45)
AGE - Late Triassic, late Early Norian, *triangularis* Zone

GSC Loc. No: **C-103723** **NTS**: Hope, 92H
Fld. No: 85HD-20
Collector: G.E. Ray
GEOGR - **Lat./Long.:**
UTM: Zone 10; 711202E, 5472811N.
***Description:** 2 km NW of Hedley.*
STRAT - **Rock Unit:** Nicola Group, Chuchuwayha Formation
Description: Carbonate: a 1 m thick bed of black-grey massive coarse grained limestone interbedded with argillites and tuffs.
PALEO - **Fossils:** conodonts
Conodont taxa: **CAI:** 5
ramiform elements (1)
Epigondolella sp. cf. *triangularis* (Budurov 1972) (3)
AGE - Late Triassic, Early Norian.

GSC Loc. No: **C-143397** **NTS**: Hope, 92H
Fld. No: 85HD-12
Collector: G.E. Ray
GEOGR - **Lat./Long.:**
UTM: Zone 10; 711200E, 5471770N.
Description: 1 km NW of Hedley.
STRAT - **Rock Unit:** Nicola Group, Chuchuwayha Formation
Description: Carbonate: 0.23 m thick limestone bed.
PALEO - **Fossils:** conodonts, sponge spicules
Conodont taxa: **CAI:** 5
Epigondolella quadrata Orchard 1991 (1)
AGE - Late Triassic, Early Norian.

4. STEMWINDER FORMATION

GSC Loc. No: **C-103725** **NTS**: Hope, 92H
Fld. No: 85HD-49
Collector: G.E. Ray
GEOGR - **Lat./Long.:**
UTM: Zone 10; 707900E, 5470250N.
Description: 4.5 km WSW of Hedley.
STRAT - **Rock Unit:** Nicola Group, Stemwinder Formation
Description: Carbonate: from an undisturbed, bedded limestone horizon close to the stratigraphic top of the Stemwinder Formation, immediately beneath the Copperfield Breccia.
PALEO - **Fossils:** conodonts
Conodont taxa: **CAI:** 5 - 5.5
ramiform elements (50)
Epigondolella bidentata Mosher 1968 (5)
Neogondolella steinbergensis (Mosher 1968) (25)
AGE - Late Triassic, Late Norian, *bidentata* Zone

GSC Loc. No: **C-103726** **NTS**: Hope, 92H
Fld. No: 85HD-56
Collector: G.E. Ray
GEOGR - **Lat./Long.:**
UTM: Zone 10; 708830E, 5469510N.
Description: 4 km SW of Hedley.
STRAT - **Rock Unit:** Nicola Group, Stemwinder Formation
Description: Carbonate: from a thin bedded, black-grey limestone which is interbedded with minor black limey siltstones.
PALEO - **Fossils:** conodonts
Conodont taxa: **CAI:** 5
Metapolygnathus sp. cf. *M. communisti* Hayashi 1968 (2)
AGE - Late Triassic, Late Carnian, ?*communisti* Zone

GSC Loc. No: C-103727 **NTS**: Hope, 92H
Fld. No: 85HD-57
Collector: G.E. Ray
GEOGR - **Lat./Long.:**
UTM: Zone 10; 709500E, 5469695N.
Description: 3 km SW of Hedley.
STRAT - **Rock Unit:** Nicola Group, Stemwinder Formation
Description: Carbonate: a thin bed of black limestone within the limey argillite sequence.
PALEO - **Fossils:** conodonts
Conodont taxa: **CAI:** 5 - 5.5
Metapolygnathus nodosus (Hayashi 1968) (4)
AGE - Late Triassic, Late Carnian.

GSC Loc. No: C-103728 **NTS**: Hope, 92H
Fld. No: 85HD-8
Collector: G.E. Ray
GEOGR - **Lat./Long.:**
UTM: Zone 10; 710370E, 5471480N.
Description: 2 km W of Hedley, close to No. 3 Highway, station number 84.
STRAT - **Rock Unit:** Nicola Group, Stemwinder Formation
Description: Carbonate: a 1-2 m thick black limestone bed.
PALEO - **Fossils:** conodonts
Conodont taxa: **CAI:** 5
Metapolygnathus sp. (1)
AGE - Late Triassic, Carnian.

GSC Loc. No: C-103729 **NTS**: Hope, 92H
Fld. No: 85HD-28
Collector: G.E. Ray
GEOGR - **Lat./Long.:**
UTM: Zone 10; 709180E, 5471995N.
Description: 3 km W of Hedley, close to No. 3 Highway.
STRAT - **Rock Unit:** Nicola Group, Stemwinder Formation
Description: Carbonate: from a thin (< 1 m) limestone bed within the black argillte sequence.
PALEO - **Fossils:** conodonts
Conodont taxa: **CAI:** 5
?*Epigondolella quadrata* Orchard 1991 (1)
ramiform elements (1)
Metapolygnathus primitius (Mosher 1970) (2)
AGE - Late Triassic, Early Norian

GSC Loc. No: C-103735 **NTS**: Hope, 92H
Fld. No: 86HD-T12
Collector: G.E. Ray
GEOGR - **Lat./Long.:**
UTM: Zone 10; 708950E, 5472750N.
Description: 4.5 km WNW of Hedley; 2400' elevation.
STRAT - **Rock Unit:** Nicola Group, Stemwinder Formation
Description: Carbonate: a 0.3 m thick limestone bed.
PALEO - **Fossils:** conodonts, ichthyoliths
Conodont taxa: **CAI:** 5 - 5.5
ramiform elements (2)
Epigondolella sp. cf. *E. transitia* Orchard 1991 (4)
Epigondolella sp. cf. *E. carinata* Orchard 1991 (2)
Epigondolella triangularis (Budurov 1972) (45)
Neogondolella sp. cf. *N. steinbergensis* (Mosher 1968) (2)
Neogondolella navicula Huckriede 1958 (3)
AGE - Late Triassic, late Early Norian.

GSC Loc. No: C-103739 **NTS**: Hope, 92H
Fld. No: 86HD-T35
Collector: G.E. Ray
GEOGR - **Lat./Long.:**
UTM: Zone 10; 708230E, 5466075N.
Description: 5 km SSW of Hedley; 5500' elevation.
STRAT - **Rock Unit:** Nicola Group, Stemwinder Formation
Description: Carbonate: a tuffaceous limestone.
PALEO - **Fossils:** conodonts
Conodont taxa: **CAI:** 5 - 5.5
Epigondolella triangularis (Budurov 1972) (4)
Metapolygnathus? sp. (1)
AGE - Late Triassic, Early Norian, *triangularis* Zone
Remarks: Metapolygnathid may be derived.

GSC Loc. No: C-143399 **NTS**: Hope, 92H
Fld. No: 85HD-51
Collector: G.E. Ray
GEOGR - **Lat./Long.:**
UTM: Zone 10; 708000E, 5469540N.
Description: 4.5 km WSW of Hedley.
STRAT - **Rock Unit:** Nicola Group, Stemwinder Formation
Description: Carbonate: a 0.3 - 0.6 m thick limestone bed within the black argillite sequence.
PALEO - **Fossils:** conodonts, ichthyoliths, sponge spicules, shell fragments
Conodont taxa: **CAI:** 5
Epigondolella sp. (1)
AGE - Late Triassic, Middle-Late Norian.

---

5. APEX MOUNTAIN COMPLEX

GSC Loc. No: C-153760 **NTS**: Hope, 92H
Fld. No: 87GER-HD-651
Collector: G.E. Ray
GEOGR - **Lat./Long.:**
UTM: Zone 10; 717950E, 5462220N.
Description: Between Shoemaker and Bradshaw creeks.
STRAT - **Rock Unit:** Apex Mountain Complex.
Description: Limestone boulder from a carbonate conglomerate.
PALEO - **Fossils:** tubes, inarticulate brachiopods, ?tentaculitids
AGE - Cambrian-Devonian.

GSC Loc. No: C-153761 **NTS**: Hope, 92H
Fld. No: 87GER-HD-652
Collector: G.E. Ray
GEOGR - **Lat./Long.:**
UTM: Zone 10; 717950E, 5462220N.
Description: Between Shoemaker and Bradshaw creeks.
STRAT - **Rock Unit:** Apex Mountain Complex.
Description: Limestone boulder from a carbonate conglomerate.
PALEO - **Fossils:** ?tentaculitids
AGE - Cambrian-Devonian.

GSC Loc. No: C-153762 **NTS**: Hope, 92H
Fld. No: 87GER-HD-653
Collector: G.E. Ray
GEOGR - **Lat./Long.:**
UTM: Zone 10; 717950E, 5462220N.
Description: Between Shoemaker and Bradshaw Creeks.
STRAT - **Rock Unit:** Apex Mountain Complex.
Description: Composite sample of several *limestone boulders from a carbonate conglomerate.*
PALEO - **Fossils:** tubes, inarticulate brachiopods, ?tentaculitids
AGE - Cambrian-Devonian.
Remarks: Prosh reports tentaculite, ?microconulariid, and bactritid fragments of mid Early - early Late Devonian age: "quite possibly Pragian".

GSC Loc. No: C-103299 **NTS**: Hope, 92H
Fld. No: 86HD-186
Collector: G.E. Ray
GEOGR - **Lat./Long.:**
UTM: Zone 10; 714400E, 5461550N.
Description: 4100' elevation.
STRAT - **Rock Unit:** Apex Mountain Group.
Description: Carbonate: marble.
PALEO - **Fossils:** ichthyoliths
AGE - Phanerozoic

SUMMARY

Carbonate samples from the Nicola Group at Hedley commonly yield conodont fauna, as indicated by this collection, as well as others made by M.J. Orchard, J.W.H. Monger, and D. Templeman Kluit of the GSC.

Of the collection made by G.E. Ray, five samples from the Hedley Formation are definitely or probably of Early Norian age, the larger of them belonging to the *triangularis* Zone of late Early Norian age. There is some suggestion of the slightly older, *quadrata* Zone in these faunas.

The three conodont collections from the Chuchuwayha Formation are demonstrably co-eval with those from the Hedley Formation, and represent the same interval of middle to late Early Norian time.

The eight conodont collections from the Stemwinder Formation clearly span a much greater part of Late Triassic time than the former units. Several samples are Carnian, or in some cases more specifically late Carnian in age. Several other faunas collectively span the entire Lower Norian, and at least one is Late Norian, *bidentata* Zone in age. The Middle Norian is not definitely represented, which is commonly the case elsewhere within the Nicola Group (sensu lato) of Quesnel Terrane.

Four conodont (and one ichthyolith) collections from clasts of the Copperfield Breccia are dated as both late Early Norian triangularis Zone, and (Late) Carnian. Whereas the former may have been derived from any of the underlying formations, the only known source for the Carnian clast is the Stemwinder Formation.

In summary, the conodont data suggests that the Chuchuwayha and Hedley formations (at least the sampled carbonate!) are confined to the upper half of the Early Norian. This may represent a maximum 'transgression' of the 'Stemwinder Formation sea' (or at least a carbonate maxima). The latter formation, having accumulated for some time before and after the Early Norian, may lie at a depocenter for the Hedley area. Emplacement of the Copperfield Breccia must have been a major event downcutting through Norian strata to incorporate Carnian clasts from the Stemwinder, or it may have taken place on an irregular seafloor where faulting had previously exposed older strata. The fact that the breccia contains clasts within clasts suggests that reworking had occurs prior to the final accumulation.

APPENDIX 2B
REPORT BY E.C. PROSH DESCRIBING MICROFOSSILS IN LIMESTONE SAMPLES FROM THE THE APEX MOUNTAIN COMPLEX

Paleontological Report
GSC Sample C-153762 (87HD 653)

March 30, 1990

Report of E.C. Prosh

Penticton Map Area
Zone 10 717950E, 5462220N
49°16'32.8", 120°0012.7"
Apex Mountain Complex

Three principal categories of fossils (excluding indeterminate miscellanea) are present in sample C-153762. These can be definitively or tentatively identified as follows:

#24-26 (top row) - Nowakiid (tentaculite) fragments.

middle rows - ? "micronulariid" (Circoconulariina) fragments (very tentative).

#53-55 (bottom row) - bactritid cephalopod fragments (tentative).

Rationale:

Nowakiids - Samples 24, 25, 26 are nowakiid (dacryoconarid) tentaculites based on the following criteria: thin, tapering (cylindrical) shell, diameter *ca.* 0.5 mm; acute, regularly spaced transverse rings; fine longitudinal ribbing (perpendicular to rings). This latter criterion, longitudinal ribbing, is the most diagnostic, tentaculite-specific feature that distinguishes these samples from other small conoidal fossils (*e.g.* hyolithellids).

The character of the rings, ribs, and overall dimensions indicate placement in the Family Nowakiidae, and hence a conservative age estimate (family duration) of, generally speaking, mid-Early Devonian (Pragian) to early Late Devonian (Frasnian).

Speculatively, a more precise age estimate can be offered, based on comparison of the nowakiid fragments to known species. Two major caveats apply: the taxonomically critical proximal ends of the tentaculites are missing, and without these identification cannot be definitive; there is no established dacryoconarid zonation outside of Europe, and nearly nothing known from North America.

That stated, I would suggest that the fragments in question belong to *Nowakia acuaria* (s.s.), a rather diagnostic Pragian (mid-Early Devonian) index fossil. Comparison of available measurements on C-153762 specimens versus type measurements (after Lardeux, 1969) is (C-153762/Lardeux types): ring spacing, per unit shell width, medial region - 5 / 5-6; longitudinal rib spacing, medial region, # ribs per shell half-circumference - 16-20 / 15-16; diameter, mm - 0.5-0.6 / within pre-apertural range; growth angle, degrees (approx.) - ca. 10 / 10-13.

Younger nowakiids are in general more ornate, with better developed or organized ring styles, and more advanced patterns of growth. A *N. acuaria* assignment is therefore plausible.

While it is imprudent at best to attempt tentaculite biostratigraphy in the absence of anything approaching a North American scheme, *Nowakia acuaria* is perhaps the most widely distributed and best documented of all tentaculites. Its known distribution is virtually worldwide (cf. Alberti, 1987; Chlupac and Oliver, 1989), and has been recorded from Yukon-Alaska (Ludvigsen, 1972), Nevada (as aff.?, Lutke, 1985), throughout Asia, from Australia, and elsewhere.

Middle rows (numerous, coarsely-corrugated, quasi-circular x-section fragments) - These are most enigmatic, no one who looked at them (Nowlan, McCracken, Bolton) had much of a clue. My best guess, a long-shot, would be with an obscure suborder of conulariids, SO. Circonulariina Bischoff, 1978 (see attached). To my (limited) knowledge these "micronulariids" have not been studied other than the once by Bischoff (1978). The size, cross section (?), ornament and (especially composition (phosphatic) seem compatible. With so little study, biostratigraphy is near meaningless, but the range cited for Bischoff's Australian material, Silurian to earliest Devonian, is basically compatible (and indeed Conulata s.s. ranges throughout the Devonian).

#53, 54, 55 (bottom) - Poorly preserved, but the thickness, suggestion of an elliptical or subcircular cross-section, and possible hint of evenly-spaced, sinusoidal septal traces, suggest to me immature bactritid cephalopods (consistent with this pelagic assemblage). Again, a basically Siluro-Devonian group, with something of an apogee in the Early Devonian.

BIOSTRATIGRPAHIC SUMMARY:
mid-Early to early Late Devonian (Pragian to Frasnian). Quite possibly Pragian.

NOTE ON FOSSIL COMPOSITION: I presume this collection was recovered from heavy residue after dissolution for conodonts, the conclusion being that the fossil fragments are phosphatic. The presumed bactritid fragments indeed appear phosphatized, and the phosphatic appearance of the questionable circonulariid fragments is or course compatible with a conulariid assignment. However, I am unaware of any examples of phosphatized tentaculites (original composition calcareous, most probably aragonite), and my guess is the specimens here are silicified, despite their dark coloration. (I have often found silicified fossils in heavy residues, entrained by heavy minerals). If they are silicified (and I am by no means certain they are), then it might be worthwhile examining the light residues for more. Furthermore, if any tentaculites are present in their unaltered calcareous state, then careful examination of fresh broken surfaces might reveal them (Godfrey Nowlan described the host as "calcareous nodules").

APPENDIX 2C
REPORT BY E.T. TOZER ON MEGAFOSSIL IN LIMESTONE BOULDER: COPPERFIELD BRECCIA

Report on a Triassic fossil from Stemwinder Provincial Park, near Hedley, B.C. (NTS 92H), submitted by G. Ray, B.C. Geological Survey, Victoria.

Field No. 86 284

Triassic or older. Stemwinder Park, 3.5 km west of Hedley. UTM 5, 471, 200 m N, 708,200 m E.

Geological Survey of Canada,
Ottawa Paleontology Section,
November 24, 1987

Report Tr5 1987 ETT

The relevant parts of any manuscript prepared for publication that paraphrase or quote from this report should be referred to the Ottawa Paleontology Section for possible revision.

GSC C-143201
Palaeocardita sp.
Age: Probably Late Triassic.

(signed) E.T. Tozer

APPENDIX 3A
MAJOR ELEMENT GEOCHEMICAL ANALYSES OF OREGON CLAIMS FORMATION TUFFS (Unit 2)

Field No.	SiO2	TiO2	Al2O3	Fe2O3*	MnO	MgO	CaO	Na2O	K2O	P2O5	FeO	Fe2O3	Fe2O3/ FeO	LOI	SUM
HD313	50.07	0.75	16.96	9.66	0.18	5.53	7.69	5.71	1.04	0.24	7.41	1.49	0.20	1.36	99.19
HD346	51.60	0.79	14.47	10.57	0.22	5.85	11.54	2.16	1.31	0.28	8.21	1.51	0.18	0.72	99.51

Major element values in percent; Fe2O3 = total iron as Fe2O3*
Sum excludes FeO and Fe2O3

APPENDIX 3B
TRACE ELEMENT GEOCHEMICAL ANALYSES OF OREGON CLAIMS FORMATION TUFFS (Unit 2)

Field No.	Cu	Pb	Zn	Co	Cr	Ni	As	Ba	Sr	Rb	Y	Zr	Nb	Ta	Th	V	Sc	La	Ce	Cs
HD313	42	16	98	22	50	19	5	899	NA	16	17	58	2	<4	10	NA	NA	NA	NA	NA
HD346	57	24	137	30	78	25	8	986	573	23	23	57	2	<4	8	362	32	26	31	8

All values in ppm; N A = element not analysed

APPENDIX 4A

UNALTERED LIMESTONES IN THE HEDLEY, CHUCHUWAYHA AND STEMWINDER FORMATIONS (Units 5 and 6)

Field No.	SiO2	TiO2	Al2O3	Fe2O3*	MnO	MgO	CaO	Na2O	K2O	K2O/ Na2O	P2O5	FeO	Fe2O3	Fe2O3/ FeO	LOI	SUM
HD542	13.47	0.06	1.49	0.73	0.35	1.99	44.84	0.12	0.44	3.67	0.09	0.59	0.07	0.12	35.92	99.50
HD549	4.26	0.01	0.48	0.14	0.02	0.97	52.48	0.05	0.06	1.20	0.07	0.09	0.04	0.44	41.47	100.01
HD550	6.83	0.01	0.51	0.10	0.02	0.76	50.82	0.03	0.07	2.33	0.07	0.05	0.04	0.80	40.74	99.96
HD551	1.74	0.01	0.26	0.06	0.02	2.08	52.84	0.03	0.01	0.33	0.09	0.05	0.00	0.00	42.31	99.45
HD285	14.27	0.04	1.27	0.41	0.12	1.07	44.13	0.23	0.16	0.70	0.13	0.33	0.04	0.12	37.19	99.02
Average	8.11	0.03	0.80	0.29	0.11	1.37	49.02	0.09	0.15	1.65	0.09	0.22	0.04	0.30	39.53	99.59
Stdev	5.56	0.02	0.54	0.28	0.14	0.61	4.22	0.09	0.17	1.36	0.02	0.24	0.02	0.33	2.80	0.41
Max	14.27	0.06	1.49	0.73	0.35	2.08	52.84	0.23	0.44	3.67	0.13	0.59	0.07	0.80	42.31	100.01
Min	1.74	0.01	0.26	0.06	0.02	0.76	44.13	0.03	0.01	0.33	0.07	0.05	0.00	0.00	35.92	99.02

APPENDIX 4B

UNALTERED SILTSTONES AND ARGILLITE FROM THE CHUCHUWAYHA AND STEMWINDER FORMATIONS (Units 5 and 6)

Field No.	SiO2	TiO2	Al2O3	Fe2O3*	MnO	MgO	CaO	Na2O	K2O	K2O/ Na2O	P2O5	FeO	Fe2O3	Fe2O3/ FeO	LOI	SUM
HD541	35.38	0.11	2.92	2.07	0.24	3.86	29.74	0.84	0.92	1.10	0.13	1.85	0.01	0.01	24.16	100.37
HD545	64.74	0.30	5.78	2.42	0.04	1.18	17.63	0.91	0.98	1.08	0.20	2.03	0.16	0.08	5.63	99.81
HD546	57.05	0.31	4.98	2.56	0.10	1.07	25.74	0.90	1.03	1.14	0.32	1.40	1.00	0.71	6.18	100.24
HD547	41.95	0.15	3.43	1.63	0.11	1.25	33.97	0.49	0.77	1.57	0.43	1.22	0.27	0.22	16.04	100.22
HD543	74.46	0.62	10.26	3.15	0.01	1.86	1.91	2.23	1.59	0.71	0.08	1.12	1.91	1.71	3.07	99.24
HD544	74.24	0.62	10.35	3.18	0.02	2.16	1.87	2.28	1.70	0.75	0.08	1.46	1.56	1.07	2.76	99.26
Average	57.97	0.35	6.29	2.50	0.09	1.90	18.48	1.28	1.17	1.06	0.21	1.51	0.82	0.63	9.64	99.86
Stdev	16.43	0.22	3.28	0.61	0.09	1.05	13.93	0.77	0.38	0.31	0.14	0.36	0.80	0.67	8.61	0.51
Max	74.46	0.62	10.35	3.18	0.24	3.86	33.97	2.28	1.70	1.57	0.43	2.03	1.91	1.71	24.16	100.37
Min	35.38	0.11	2.92	1.63	0.01	1.07	1.87	0.49	0.77	0.71	0.08	1.12	0.01	0.01	2.76	99.24

APPENDIX 4C

MARBLES IN THE HEDLEY FORMATION (Unit 4) (TAKEN FROM DRILL HOLES 73, 261 AND 401, NICKEL PLATE DEPOSIT)

Field No.	SiO2	TiO2	Al2O3	Fe2O3*	MnO	MgO	CaO	Na2O	K2O	CO2	P2O5	FeO	Fe2O3	Fe2O3/ FeO	LOI	SUM
73.31	27.33	0.18	4.54	2.03	0.06	1.97	37.67	1.10	0.70	22.29	0.19	1.64	0.22	0.13	22.10	97.87
73.33	3.96	0.02	0.33	0.24	0.01	0.95	52.77	0.03	0.13	41.40	0.06	0.26	0.00	0.00	35.72	99.90
73.31	32.08	0.19	4.80	2.39	0.07	2.26	36.15	1.12	0.71	19.71	0.21	2.03	0.15	0.07	19.88	99.86
261.23	32.57	0.17	3.32	2.88	0.14	2.01	39.64	0.01	1.37	17.01	0.26	2.29	0.35	0.15	15.65	97.76
261.24	28.39	0.08	1.91	1.20	0.07	1.17	45.67	0.01	0.93	21.00	0.21	0.74	0.38	0.51	20.55	99.98
261.26	12.55	0.08	1.60	1.47	0.09	1.08	49.39	0.01	0.49	32.29	0.14	1.24	0.10	0.08	30.62	99.05
261.28	30.55	0.10	2.26	1.91	0.12	2.17	44.15	0.01	0.31	18.49	0.12	1.66	0.08	0.05	17.79	99.37
261.29	4.29	0.04	0.20	0.42	0.06	1.22	54.08	0.01	0.01	38.77	0.05	0.29	0.10	0.34	40.84	101.17
401.30	20.15	0.10	3.09	0.93	0.06	2.95	42.28	0.29	0.30	28.71	0.00	0.64	0.22	0.34	28.70	98.85
Average	27.33	0.18	4.54	2.03	0.06	1.97	37.67	1.10	0.70	22.29	0.19	1.64	0.22	0.13	22.10	97.87
Stdev	11.64	0.06	1.65	0.89	0.04	0.68	6.43	0.47	0.43	9.08	0.09	0.75	0.14	0.21	8.66	1.08
Max 0	32.57	0.19	4.80	2.88	0.14	2.95	54.08	1.12	1.37	41.40	0.26	2.29	0.38	0.51	40.84	101.17
Min 0	3.96	0.02	0.20	0.24	0.01	0.95	36.15	0.01	0.01	17.01	0.00	0.26	0.00	0.00	15.65	97.76

Major element values in percent. Fe2O3 = total iron as Fe2O3. Sum excludes Fe2O3, FeO and CO2.*

APPENDIX 5 .

MAJOR AND TRACE ELEMENT GEOCHEMICAL ANALYSES OF THE WHISTLE FORMATION TUFFS (Unit 7)

Field No.	SiO2	TiO2	Al2O3	Fe2O3*	MnO	MgO	CaO	Na2O	K2O	P2O5	Fe2O3	FeO	Fe2O3/ FeO	LOI	SUM	Cu	Pb	Zn	Co	Ni	Cr	As	Ba	Sr	Rb	Y	Zr	Nb	Th
HD522	45.56	0.79	16.62	10.11	0.21	4.67	10.91	2.80	2.05	0.26	1.62	7.70	0.21	5.55	99.53	120	23	90	32	23	25	7	1067	720	40	19	46	1	2
HD523	50.29	0.77	17.86	9.00	0.18	3.85	8.00	4.16	1.16	0.16	1.53	6.77	0.23	3.81	99.24	69	7	90	23	8	16	6	715	482	24	19	48	1	11
HD524	48.85	0.38	11.14	4.34	0.10	2.54	16.93	1.60	1.29	0.27	NA	NA	-	11.83	99.27	52	5	73	15	19	31	5	1020	671	28	24	50	4	11
HD525	55.89	0.66	15.38	7.04	0.16	3.58	7.04	3.91	1.52	0.30	1.09	5.39	0.20	4.52	100.00	104	5	90	22	29	66	5	1391	569	31	26	80	7	1
HD526	49.55	0.94	15.72	10.34	0.19	5.57	6.86	3.51	2.21	0.27	2.17	7.41	0.29	4.47	99.63	103	5	103	33	44	136	6	2136	704	38	23	64	1	5
HD521	48.27	0.72	15.51	10.94	0.19	8.51	11.88	2.04	0.53	0.14	2.21	7.91	0.28	1.20	99.93	65	20	94	40	87	296	5	281	439	10	14	28	1	2

Major element values in percent, trace element values in ppm. FeO3 = total iron as Fe2O3. Sum excludes Fe2O3 and FeO.*

APPENDIX 6

MAJOR AND TRACE ELEMENT GEOCHEMICAL ANALYSES OF SKWEL PEKEN FORMATION TUFFS (Unit 15)

LOWER MEMBER

Field No.	SiO2	TiO2	Al2O3	Fe2O3*	MnO	MgO	CaO	Na2O	K2O	P2O5	CO2	FeO	LOI	SUM	Cu	Pb	Zn	Co	Ni	As	Ba	Sr	Rb	Y	Zr	Nb	Th	Cr
HD151	62.51	0.51	18.14	5.33	0.10	0.69	3.93	3.73	1.39	0.16	0.34	1.56	1.62	98.11	18	16	105	28	6	3	937	632	33	19	110	2	22	NA
HD152	62.45	0.49	19.15	3.60	0.12	0.55	3.88	4.72	1.59	0.17	0.41	2.42	1.06	97.78	12	16	72	28	6	2	946	596	24	23	133	3	22	NA
HD171	62.77	0.54	18.61	5.06	0.11	0.93	4.71	3.73	1.49	0.15	0.21	2.27	0.98	99.08	14	13	83	37	7	2	926	532	30	22	113	4	26	NA
HD172	65.21	0.48	18.17	5.30	0.11	0.89	4.17	3.65	1.40	0.14	0.14	2.49	1.03	100.55	9	13	74	24	4	1	1028	543	30	17	93	3	24	NA
HD173	64.99	0.49	18.13	4.28	0.13	0.94	3.95	3.79	1.57	0.15	0.41	3.20	1.52	99.94	6	12	73	24	6	2	1211	538	34	17	106	4	20	NA
HD309	62.08	0.47	17.25	5.13	0.14	1.44	5.74	4.02	1.47	0.12	NA	NA	1.16	99.02	5	11	87	20	6	0	987	489	20	16	96	3	21	NA
HD332	62.17	0.55	17.17	5.61	0.17	2.07	5.85	3.96	1.51	0.17	NA	NA	0.91	100.14	4	16	90	17	<3	8	1100	556	22	22	118	9	11	NA
HD333	60.64	0.62	17.41	5.84	0.15	2.37	6.04	3.58	2.07	0.18	NA	NA	0.76	99.66	5	17	101	11	<3	12	1023	610	34	27	111	10	5	NA

UPPER MEMBER

Field No.	SiO2	TiO2	Al2O3	Fe2O3*	MnO	MgO	CaO	Na2O	K2O	P2O5	CO2	FeO	LOI	SUM	Cu	Pb	Zn	Co	Ni	As	Ba	Sr	Rb	Y	Zr	Nb	Th	Cr
HD527	61.11	0.65	17.16	6.69	0.12	1.46	5.82	3.21	1.78	0.17	NA	NA	1.68	99.85	26	36	75	14	NA	2	1070	391	29	23	121	4	NA	14
HD528	60.67	0.63	16.00	6.71	0.12	2.32	5.18	3.15	1.96	0.16	NA	NA	2.04	98.94	36	15	77	14	NA	3	1041	362	41	21	116	1	NA	12
HD529	59.03	0.65	16.48	6.95	0.19	2.40	5.58	3.12	2.02	0.17	NA	NA	2.47	99.06	38	18	83	14	NA	3	925	333	47	30	123	15	NA	28
HD530	58.56	0.75	17.18	7.73	0.17	2.58	6.39	3.25	1.94	0.18	NA	NA	0.75	99.48	20	14	93	16	NA	2	655	359	40	24	105	2	NA	6
HD531	60.69	0.61	17.18	6.93	0.17	2.38	5.65	3.45	1.90	0.16	NA	NA	1.04	100.16	12	20	99	12	NA	3	911	371	29	22	103	5	NA	19
HD532	60.80	0.58	16.83	6.45	0.19	2.37	5.93	3.53	1.92	0.16	NA	NA	1.26	100.02	25	17	88	12	NA	5	872	363	37	26	113	12	NA	28

Major elements in percent; trace element values in ppm. Fe2O3 = total iron as Fe2O3. Sum excludes Fe2O3, FeO and CO2. NA = element not analysed.*

APPENDIX 7

MAJOR AND TRACE ELEMENT GEOCHEMICAL ANALYSES OF SPENCES BRIDGE GROUP ROCKS (Unit 17)

Field No.	SiO2	TiO2	Al2O3	Fe2O3*	MnO	MgO	CaO	Na2O	K2O	P2O5	LOI	Sum	Cu	Pb	Zn	Cr	As	Ba	Sr	Rb	Y	Zr	Nb
HD424	71.89	0.35	14.96	2.05	0.05	0.40	1.17	4.44	4.05	0.05	0.87	100.28	3	16	41	16	28	1385	194	91	34	282	17
HD299	69.10	0.43	14.87	4.34	0.11	0.55	1.65	4.55	3.01	0.07	1.06	99.74	5	14	96	18	1	1163	221	56	46	257	13
HD700	55.65	1.02	18.03	8.65	0.15	2.70	6.49	3.43	1.15	0.20	2.76	100.23	19	10	104	15	3	454	452	15	38	137	11
HD701	54.50	0.87	17.19	8.98	0.16	3.28	7.36	3.38	0.97	0.17	0.80	97.66	20	8	106	11	1	512	412	8	25	103	3
HD702	55.64	0.91	17.22	9.28	0.17	3.91	7.36	3.28	0.90	0.17	0.88	99.72	13	10	101	40	1	434	452	9	46	257	13

Footnote: *Major element values in percent*
Trace element values in ppm
Fe2O3 = total iron as Fe2O3*

APPENDIX 8

MAJOR AND TRACE ELEMENT GEOCHEMICAL ANALYSES OF THE MARRON FORMATION VOLCANICS (Unit 19)

Field No.	SiO2	TiO2	Al2O3	Fe2O3*	MnO	MgO	CaO	Na2O	K2O	P2O5	LOI	Sum	Cu	Pb	Zn	Co	As	Ba	Sr	Rb	Y	Zr	Nb
HD510	53.65	0.97	15.05	7.55	0.11	4.66	8.58	3.52	2.45	0.55	2.46	99.55	61	32	108	28	6	1550	2031	35	20	147	3
HD511	56.73	0.89	15.20	7.04	0.16	3.87	6.18	3.99	2.43	0.52	3.07	100.08	38	16	98	29	2	1629	1757	34	18	165	1

Footnote: *Major element values in percent*
Trace element values in ppm
Fe2O3 = total iron as Fe2O3*

APPENDIX 9

MAJOR AND TRACE ELEMENT GEOCHEMISTRY OF UNALTERED HEDLEY INTRUSIONS, (Unit 9) HEDLEY DISTRICT

Sample No.	**HD50**	**HD52**	**HD60**	**HD62**	**HD64**	**HD65**	**HD66**	**HD67**	**HD68**	**HD69**	**HD70**	**HD71**	**HD72**	**HD73**	**HD60A**
Body type	sill	sill	stock	stock	stock	stock	stock	stock	stock	stock	stock	stock	stock	stock	stock
SiO2	55.01	54.29	56.81	54.08	52.94	59.48	53.27	50.82	59.46	54.27	49.13	55.92	54.85	57.68	57.24
TiO2	0.79	0.83	0.60	0.68	0.65	0.53	0.72	0.65	0.51	0.64	0.80	0.58	0.65	0.67	0.62
Al2O3	19.00	19.53	17.50	18.35	19.89	17.86	19.02	20.24	17.99	19.33	20.18	18.41	18.72	18.60	18.01
Fe2O3*	9.25	8.11	7.03	8.77	7.93	6.41	8.75	8.39	5.83	7.66	9.07	7.27	8.08	7.91	7.13
MnO	0.17	0.15	0.12	0.17	0.15	0.11	0.16	0.17	0.13	0.17	0.16	0.14	0.15	0.15	0.13
MgO	4.29	3.24	3.81	4.03	4.04	2.51	3.93	4.18	2.88	3.27	5.09	3.13	3.54	3.10	3.86
CaO	9.00	9.16	7.98	9.25	10.15	6.66	9.12	10.30	7.24	9.19	11.46	8.14	8.73	8.23	8.04
Na2O	2.69	3.12	3.03	2.91	3.40	3.28	3.10	2.90	3.72	3.20	2.55	3.22	3.06	3.22	3.04
K2O	0.83	0.93	1.64	1.11	1.24	2.00	1.35	0.75	2.01	1.55	1.17	1.66	1.65	1.80	1.65
P2O5	0.23	0.26	0.15	0.16	0.19	0.14	0.17	0.20	0.15	0.20	0.18	0.17	0.18	0.21	0.15
S	0.01	0.02	0.01	0.12	0.02	0.01	0.08	0.02	0.02	0.01	0.21	0.01	0.04	0.04	0.01
CO2	0.48	0.35	0.28	0.14	0.42	0.28	0.41	0.35	0.35	0.48	0.42	0.14	0.21	0.28	0.29
LOI	1.68	1.25	0.97	1.03	1.10	1.00	1.32	1.24	0.87	1.12	1.51	1.26	1.17	1.26	0.96
SUM	102.94	100.87	99.64	100.54	101.68	99.98	100.91	99.84	100.79	100.60	101.30	99.90	100.78	102.83	100.83
FeO	7.19	6.29	5.48	5.93	5.75	4.72	6.69	6.12	4.15	5.23	6.76	5.26	5.72	5.58	5.36
Fe2O3	1.26	1.12	0.94	2.18	1.54	1.16	1.32	1.59	1.22	1.85	1.56	1.42	1.72	1.71	1.17
Fe2O3/FeO	0.18	0.18	0.17	0.37	0.27	0.25	0.20	0.26	0.29	0.35	0.23	0.27	0.30	0.31	0.22
K2O/Na2O	0.31	0.30	0.54	0.38	0.36	0.61	0.44	0.26	0.54	0.48	0.46	0.52	0.54	0.56	0.54
Au	<5	21	6	49	5	22	9	16	15	19	11	6	8	5	10
Ba	940	962	974	1160	862	1307	1300	918	606	1141	1232	1088	40	1014	977
Ce	15	20	32	19	16	20	16	14	19	26	15	20	18	21	30
Co	34	30	36	37	37	35	32	32	30	29	30	31	31	31	27
Cr	36	11	40	20	2	4	20	11	13	3	9	12	20	73	52
Cs	2	<1	2	2	1	1	<1	2	<1	<1	2	1	1	<1	2
F	350	350	350	370	440	370	410	350	330	370	330	350	340	380	350
La	7	9	10	9	8	9	8	6	9	7	7	9	9	11	9
Nb	<3	<3	<3	<3	<3	<3	<3	<3	<3	<3	<3	<3	<3	<3	<3
Ni	10	7	16	12	4	4	2	4	7	4	3	6	4	3	3
Rb	5	3	39	41	22	17	29	22	18	22	21	35	39	26	38
Sc	43	38	20	61	55	41	39	22	24	21	26	58	35	45	21
Sr	575	614	484	438	546	810	333	494	653	540	520	466	708	519	486
Th	29	23	30	24	25	28	23	32	23	25	19	35	23	27	27
U	<2	<2	<2	<2	<2	<2	<2	<2	<2	<2	<2	<2	<2	<2	<2
V	217	127	157	250	165	144	189	161	120	222	254	176	145	310	270
Y	12	14	17	10	12	13	18	14	12	19	15	13	12	12	10
Zr	48	55	73	64	52	47	81	53	40	54	50	44	66	56	71

Appendix 9 (Continued)

Sample No.	**HD73A**	**HD156**	**HD157**	**HD158**	**HD159**	**HD161**	**HD162**	**HD163**	**HD164**	**HD218**	**HD767**	**HD334**	**Mean**	**Max.**	**Min.**	**Stdev.**
Body type	stock	sill	sill	sill	stock	stock	stock	sill	sill	sill	sill	sill	-	-	-	-
SiO2	55.38	54.83	55.56	53.33	55.61	54.12	53.36	54.13	56.38	54.31	53.68	54.25	54.82	59.48	49.13	2.23
TiO2	0.66	0.67	0.66	0.56	0.61	0.65	0.68	0.62	0.58	0.61	1.04	0.65	0.66	1.04	0.51	0.11
Al2O3	18.61	18.81	18.71	19.24	18.38	18.22	18.57	17.55	18.37	18.29	16.72	17.92	18.59	20.24	16.72	0.81
Fe2O3*	8.05	7.98	7.53	8.19	7.35	8.32	7.31	6.64	6.29	6.01	10.11	7.59	7.74	10.11	5.83	1.01
MnO	0.15	0.14	0.16	0.14	0.12	0.14	0.12	0.09	0.10	0.07	0.17	0.16	0.14	0.17	0.07	0.03
MgO	3.06	4.83	4.16	4.45	3.69	4.10	4.23	3.99	3.41	3.83	4.84	3.71	3.82	5.09	2.51	0.62
CaO	8.00	8.00	7.13	9.47	8.12	8.32	8.32	6.48	7.10	7.45	8.00	7.83	8.40	11.46	6.48	1.14
Na2O	3.21	3.20	3.28	2.77	2.91	2.72	2.77	4.79	4.06	3.34	3.26	3.87	3.21	4.79	2.55	0.47
K2O	1.78	0.64	1.37	1.17	1.00	1.01	1.10	2.13	1.01	2.08	1.36	2.54	1.43	2.54	0.64	0.48
P2O5	0.21	0.14	0.17	0.17	0.15	0.16	0.16	0.16	0.17	0.18	0.20	0.19	0.18	0.26	0.14	0.03
S	0.01	0.03	0.04	0.03	0.17	0.32	1.80	0.52	0.46	1.10	0.22	0.08	0.20	1.80	0.01	0.40
CO2	0.29	0.35	0.49	0.07	0.14	0.14	0.07	0.28	0.07	0.62	0.41	0.00	0.29	0.62	0.00	0.15
LOI	1.15	1.42	1.82	1.36	1.35	1.11	2.69	1.75	1.28	2.43	0.56	0.62	1.31	2.69	0.56	0.47
SUM	100.26	100.66	100.55	100.85	99.29	98.87	99.31	98.33	98.75	98.60	99.94	99.33	100.30	102.94	98.33	1.14
FeO	6.15	6.90	5.62	5.83	5.97	6.82	4.94	5.62	4.34	4.90	7.90	5.69	5.81	7.90	4.15	0.86
Fe2O3	1.22	0.31	1.28	1.71	0.72	0.74	1.82	0.39	1.47	0.56	1.33	1.27	1.28	2.18	0.31	0.45
Fe2O3/FeO	0.20	0.04	0.23	0.29	0.12	0.11	0.37	0.07	0.34	0.11	0.17	0.22	0.23	0.37	0.04	0.09
K2O/Na2O	0.55	0.20	0.42	0.42	0.34	0.37	0.40	0.44	0.25	0.62	0.42	0.66	0.44	0.66	0.20	0.12
Au	30	20	<5	22	17	<5	<5	27	30	<5	20	20	15	49	<5	11
Ba	1113	756	811	854	652	653	1040	1441	1022	1520	1070	978	979	1520	40	293
Ce	35	15	22	16	19	18	29	14	32	24	44	49	23	49	14	9
Co	28	41	33	35	32	37	38	29	30	29	24	37	32	41	24	4
Cr	6	44	16	23	8	20	18	17	9	17	19	39	21	73	2	17
Cs	<1	2	1	1	<1	<1	<1	2	1	1	1	1	1	2	<1	1
F	370	370	490	440	350	380	391	330	440	372	340	340	372	490	330	40
La	11	8	9	15	7	8	12	7	7	5	10	12	9	15	5	2
Nb	<3	<3	<3	<3	<3	<3	<3	<3	<3	<3	<3	<3	<3	<3	<3	0
Ni	2	25	9	13	8	11	11	9	10	8	2	22	8	25	2	6
Rb	28	14	32	28	30	23	32	50	30	50	29	22	28	50	3	11
Sc	19	28	25	50	42	39	21	41	32	25	27	21	34	61	19	13
Sr	541	841	667	636	654	679	819	920	837	676	391	678	612	920	333	148
Th	30	25	22	16	25	18	23	21	22	17	8	15	24	35	8	6
U	<2	<2	<2	<2	<2	<2	3	<2	<2	<2	-	7	1	7	<2	1
V	190	224	327	152	207	201	220	178	155	102	329	223	201	329	102	61
Y	17	11	14	13	13	13	14	14	12	14	23	15	14	23	10	3
Zr	76	53	59	51	67	60	59	59	63	59	83	65	60	83	40	11

N.B., half the value of the detection limit (e.g., 1.5 for <3) was used for calculating Mean and Stdev. Fe2O3 = total iron as Fe2O3. Sum excludes S and CO2*

Major element values in percent; trace element values in ppm; except Au in ppb

APPENDIX 10A
MAJOR ELEMENT GEOCHEMISTRY OF THE TORONTO STOCK AND OTHER SKARN-ALTERED HEDLEY INTRUSIONS (Unit 9)

Field No.	SiO2	TiO2	Al2O3	Fe2O3*	MnO	MgO	CaO	Na2O	K2O	P2O5	CO2	FeO	Fe2O3	Fe2O3/ FeO	LOI	SUM
HD 84	59.79	0.50	15.68	4.97	0.14	3.04	11.43	3.73	1.07	0.13	0.21	3.83	0.75	0.20	0.45	100.80
HD 85	61.87	0.55	18.16	3.76	0.04	2.41	7.63	3.62	2.28	0.15	0.22	2.82	0.65	0.23	0.65	100.97
HD130	54.01	0.68	18.39	8.74	0.15	4.44	8.93	2.66	1.21	0.19	0.83	7.25	0.75	0.10	1.44	100.82
HD131	54.60	0.66	18.79	8.32	0.13	4.18	8.14	2.81	1.53	0.20	0.42	7.18	0.41	0.06	1.25	100.59
HD720	56.65	0.42	16.66	4.00	0.15	3.06	9.09	3.03	4.82	0.14	0.33	3.30	0.36	0.11	0.70	98.72
HD722	55.32	0.63	18.00	5.54	0.07	3.94	8.84	3.71	2.26	0.18	0.72	3.80	1.34	0.35	1.27	99.76
HD335	55.13	0.66	18.91	2.32	0.10	3.64	11.98	4.00	1.99	0.20	0.20	0.00	2.31	0.00	0.83	99.77
average	56.77	0.59	17.80	5.38	0.11	3.53	9.43	3.37	2.17	0.17	0.42	4.03	0.94	0.15	0.94	100.20
std dev	2.95	0.10	1.19	2.38	0.04	0.72	1.64	0.52	1.27	0.03	0.26	2.54	0.68	0.12	0.38	0.82
max	61.87	0.68	18.91	8.74	0.15	4.44	11.98	4.00	4.82	0.20	0.83	7.25	2.31	0.35	1.44	100.97
min	54.01	0.42	15.68	2.32	0.04	2.41	7.63	2.66	1.07	0.13	0.20	0.00	0.36	0.00	0.45	98.72

APPENDIX 10B
TRACE ELEMENT GEOCHEMISTRY OF THE TORONTO STOCK AND OTHER SKARN ALTERED HEDLEY INTRUSIONS (Unit 9)

Field No.	Au	Cu	Pb	Zn	Co	Ni	As	Sb	Ba	Sr	Rb	Y	Zr	Nb	U	Th
HD84	<30	29	17	78	10	7	12	12	1112	568	27	15	76	1	3	22
HD85	48	25	20	88	35	6	10	10	1820	594	37	17	95	2	3	27
HD130	<30	33	17	79	37	13	20	3	821	627	34	16	64	1	2	29
HD131	<30	26	10	79	37	4	17	2	1193	619	50	16	60	1	4	30
HD720	33	13	20	67	8	10	140	18	2292	942	116	17	72	11	27	4
HD722	36	184	19	55	19	8	190	4	1180	934	46	21	65	2	16	13
HD335	<30	31	14	61	7	9	20	3	1571	671	37	30	86	1	19	5

APPENDIX 10C
MAJOR ELEMENT ANALYSES OF SILICIFIED HEDLEY INTRUSIONS (Unit 9)

Field No.	SiO2	TiO2	Al2O3	Fe2O3*	MnO	MgO	CaO	Na2O	K2O	P2O5	CO2	FeO	Fe2O3	LOI	SUM
HD61	60.45	0.46	17.12	5.72	0.12	2.55	6.41	3.48	1.67	0.13	0.41	4.16	1.13	1.37	99.35
HD63	62.71	0.36	18.24	3.31	0.07	1.94	6.71	3.68	2.03	0.11	0.35	2.39	0.67	0.66	99.71
HD155	60.37	0.46	18.01	5.62	0.12	2.66	6.03	3.37	2.13	0.14	0.42	3.98	1.23	2.07	100.98
HD160	60.47	0.43	18.34	4.46	0.07	2.29	6.03	4.51	0.96	0.14	0.62	3.48	0.63	1.37	99.07
HD160A	60.56	0.43	18.22	4.39	0.07	2.21	6.06	4.49	0.99	0.14	0.68	3.84	0.15	1.37	98.93

APPENDIX 10D
TRACE ELEMENT ANALYSES OF SILICIFIED HEDLEY INTRUSIONS (Unit 9)

Field No.	Au	Ag	Cu	Pb	Zn	Co	Ni	Mo	Cr	Hg	As	Sb	Ba	Sr	Bi	Te	Rb	Y	Zr	Nb	U	Th
HD61	10	<10	16	9	65	35	7	<3	39	25	10	1	1425	508	<3	<5	33	13	74	<3	<2	34
HD63	10	<10	4	5	25	36	4	<3	25	<10	8	10	1403	588	<3	<5	25	10	60	<3	3	31
HD155	20	<10	7	13	60	27	8	<3	18	<10	25	1	1348	825	8	<5	51	9	71	<3	<2	15
HD160	10	<10	8	13	53	28	10	<3	19	<10	8	1	944	809	5	<5	25	10	65	<3	2	24
HD160A	23	<10	6	13	54	30	10	<3	17	<10	7	1	936	806	8	<5	22	9	67	<3	<2	23

Footnote: *Major element values in percent*
Fe2O3 = total iron as Fe2O3*
Sum excludes FeO, Fe2O3 and CO2.

Trace element values in ppm,
except Au and Hg in ppb

APPENDIX 11A

MAJOR ELEMENT GEOCHEMISTRY OF THE MOUNT RIORDAN STOCK (Unit 11)

Field No.	SiO2	TiO2	Al2O3	Fe2O3*	MnO	MgO	CaO	Na2O	K2O	P2O5	FeO	Fe2O3/ FeO	Fe2O3	LOI	SUM
HD406	63.72	0.48	16.88	5.51	0.09	2.23	5.31	3.53	1.56	0.12	3.15	0.64	2.03	0.75	100.18
HD409	51.29	0.79	17.41	8.36	0.27	3.05	13.11	2.69	1.60	0.17	3.29	1.43	4.72	1.30	100.04
HD411	49.15	0.93	17.89	10.16	0.20	4.64	10.24	3.66	1.66	0.19	5.90	0.62	3.65	1.10	99.83
HD381	64.02	0.48	16.60	5.53	0.10	2.15	5.25	3.15	2.09	0.11	3.05	0.71	2.16	0.72	100.20

APPENDIX 11B

TRACE ELEMENT GEOCHEMISTRY OF THE MOUNT RIORDAN STOCK (Unit 11)

Field No.	Au	Cu	Pb	Zn	Co	Ni	As	Ba	Sr	Rb	Y	Zr	Nb	Th	V	Sc	La	Ce	Cs	Yb
HD406	<20	20	10	61	NA	5	1	812	385	55	21	96	5	2	115	11	30	44	1	5
HD409	90	17	8	59	NA	5	12	463	770	32	32	103	1	4	249	29	25	43	6	5
HD411	<20	59	8	133	NA	5	7	692	479	13	29	78	2	5	357	31	19	36	7	2
HD381	<20	12	7	44	11	8	3	1360	353	56	20	98	7	2	120	11	18	43	2	5

Footnote: *Major element values in percent*
Trace element values in ppm, except Au in ppb
Fe2O3 = total iron as Fe2O3*
Sum excludes FeO, and Fe2O3
NA = element not analysed.

APPENDIX 12A
MAJOR ELEMENT GEOCHEMISTRY OF THE CAHILL CREEK PLUTON (Unit 12)

Field No.	SiO_2	TiO_2	Al_2O_3	$Fe_2O_3^*$	MnO	MgO	CaO	Na_2O	K_2O	P_2O_5	CO_2	FeO	Fe_2O_3	Fe_2O_3/FeO	LOI	SUM
HD77	61.29	0.66	18.34	5.46	0.11	1.83	4.81	4.39	2.44	0.13	0.51	2.92	2.24	0.77	0.99	100.45
HD78	61.13	0.65	18.17	5.34	0.12	1.84	4.86	4.39	2.48	0.13	0.36	3.15	1.86	0.59	0.79	99.90
HD79	60.00	0.71	18.12	5.70	0.13	2.09	5.24	4.26	2.43	0.17	0.51	3.32	2.03	0.61	1.08	99.93
HD80	60.54	0.66	18.67	5.23	0.11	1.80	4.96	4.25	2.59	0.10	0.36	3.10	1.81	0.58	0.80	99.71
HD717	64.72	0.50	16.33	4.80	0.11	1.56	3.95	3.80	2.87	0.13	0.46	2.62	1.91	0.73	1.35	100.12
HD514-15	63.82	0.50	18.06	4.06	0.08	1.08	3.85	4.32	2.89	0.12	0.46	2.62	4.05	1.55	1.31	100.09
HD514-60	63.01	0.53	17.80	4.32	0.09	1.25	4.01	4.35	2.89	0.13	0.37	1.46	4.31	2.95	1.53	99.91
Average	62.07	0.60	17.93	4.99	0.11	1.64	4.53	4.25	2.66	0.13	0.43	2.74	2.60	1.11	1.12	100.02
Stdev	1.78	0.09	0.75	0.61	0.02	0.36	0.57	0.21	0.22	0.02	0.07	0.62	1.09	0.88	0.28	0.23
Max	64.72	0.71	18.67	5.70	0.13	2.09	5.24	4.39	2.89	0.17	0.51	3.32	4.31	2.95	1.53	100.45
Min	60.00	0.50	16.33	4.06	0.08	1.08	3.85	3.80	2.43	0.10	0.36	1.46	1.81	0.58	0.79	99.71

Footnote: *Major element values in percent*
$Fe_2O_3^*$ = total iron as Fe_2O_3
Sum excludes FeO, Fe_2O_3 and CO_2

APPENDIX 12B
TRACE ELEMENT GEOCHEMISTRY OF THE CAHILL CREEK PLUTON (Unit 12)

Field No.	Cu	Pb	Zn	Co	Ni	Ba	Sr	Rb	Y	Zr	Nb	Th
HD77	11	5	53	33	48	1297	432	57	21	209	1	20
HD78	15	5	27	29	4	1333	421	61	25	217	4	23
HD79	6	12	66	30	1	1319	423	56	24	218	1	23
HD80	20	14	50	26	5	1390	425	49	22	216	1	26
HD717	6	15	65	8	3	1510	329	73	22	172	6	13
HD514-15	10	17	47	7	3	1345	367	66	20	201	2	22
HD514-60	8	9	46	9	2	1121	433	47	23	199	1	21

Footnote: *Trace elements values in ppm*

APPENDIX 13A

MAJOR ELEMENT ANALYSES OF GARNET-BEARING INTRUSIONS (UNIT 20a)

Field No.	SiO2	TiO2	Al2O3	Fe2O3*	MnO	MgO	CaO	Na2O	K2O	P2O5	CO2	FeO	LOI	SUM
HD150	72.33	0.09	14.46	1.79	0.12	0.26	1.34	3.28	2.59	0.05	0.21	1.14	1.09	97.40
HD154	69.75	0.09	14.12	1.95	0.12	0.22	1.11	3.76	3.25	0.17	0.28	1.14	1.07	95.61

Footnote: *Major element values in percent*
Fe2O3 = total iron as Fe2O3*
Sum excludes CO2 and FeO

APPENDIX 13B

TRACE ELEMENT ANALYSES OF GARNET-BEARING INTRUSIONS (UNIT 20a)

Field No.	Cu	Pb	Zn	Co	Ni	Ba	Sr	Rb	Y	Zr	Nb	Th
HD150	2	18	85	24	4	1283	252	52	13	91	3	26
HD154	2	13	78	21	<3	1790	243	61	11	92	5	24

Footnote: Trace element values in ppm

APPENDIX 13C
CORE-TO-RIM MICROPROBE ANALYSES OF MAGMATIC GARNET CRYSTALS: Unit 20a
(see Figure 16)

HD 329-4B-2

	Core				*Rim*
	1	*2*	*3*	*4*	*5*
SiO2	36.31	36.51	36.35	35.97	35.62
TiO2	0.28	0.20	0.24	0.05	0.04
Al2O3	20.23	20.14	20.17	20.23	20.07
Fe2O3	0.62	0.76	0.89	0.14	0.36
MgO	2.72	2.66	2.78	0.15	0.17
CaO	3.22	3.26	3.33	2.25	2.20
MnO	6.21	6.14	6.14	25.90	26.22
FeO	29.29	28.94	29.41	13.66	13.71
Total	98.88	98.61	99.31	98.35	98.39
	Cations				
Si	5.9373	5.9754	5.9262	5.9976	5.9592
Ti	0.0344	0.0249	0.0288	0.0058	0.0052
Al	3.8994	3.8844	3.8755	3.9762	3.9577
Fe+3	0.0763	0.0934	0.1089	0.0179	0.0456
Mg	0.6632	0.6480	0.6755	0.0370	0.0422
Ca	0.5643	0.5721	0.5809	0.4026	0.3918
Mn	0.8604	0.8516	0.8476	3.6581	3.7144
Fe+2	4.0051	3.9610	4.0095	1.9045	1.9180
Total	16.041	16.011	16.053	15.999	16.034
	Mole %				
AD	2.39	2.70	3.11	0.54	1.20
GR	6.56	6.56	6.14	6.12	5.21
PY	10.92	10.77	11.08	0.62	0.69
SP	14.17	14.15	13.90	60.98	61.26
AL	65.96	65.82	65.77	31.75	31.63

HD 328-4B-3

	Core				*Rim*
	1	*2*	*3*	*4*	*5*
SiO2	36.58	36.33	36.67	36.72	36.38
TiO2	0.24	0.21	0.25	0.30	0.09
Al2O3	20.11	20.11	20.29	20.24	20.45
Fe2O3	0.90	0.85	0.72	0.84	0.14
MgO	2.75	2.79	2.80	2.83	0.26
CaO	3.19	3.40	3.38	3.40	2.24
MnO	6.11	6.07	5.78	5.79	25.69
FeO	29.19	28.97	29.37	29.47	14.49
Total	99.07	98.73	99.26	99.59	99.74
	Cations				
Si	5.9650	5.9453	5.9601	5.9534	5.9602
Ti	0.0299	0.0254	0.0299	0.0367	0.0043
Al	3.8646	3.8788	3.8871	3.8669	3.9864
Fe+3	0.1099	0.1052	0.0886	0.1026	0.0176
Mg	0.6677	0.6802	0.6783	0.6847	0.0629
Ca	0.5571	0.5954	0.5889	0.5898	0.3973
Mn	0.8433	0.8415	0.7960	0.7954	3.6002
Fe+2	3.9803	3.9655	3.9933	3.9355	2.0045
Total	16.018	16.037	16.022	16.025	16.033
	Mole %				
AD	3.18	2.98	2.65	3.09	0.5
GR	5.76	6.59	6.81	6.3	6.01
PY	11.07	11.21	11.23	11.33	1.04
SP	13.98	13.87	13.18	13.16	59.39
AL	66.00	65.36	66.13	66.11	33.06

HD 328-4B-4

	Core				*Rim*
	1	*2*	*3*	*4*	*5*
SiO2	36.7	36.18	36.48	36.34	35.8
TiO2	0.22	0.22	0.33	0.25	0.08
A12O:	20.17	20.17	20.06	20.23	20.14
Fe2O3	0.67	0.47	0.68	0.71	0.23
MgO	2.67	2.67	2.78	2.82	0.16
CaO	3.32	3.08	3.28	3.4	2.05
MnO	6.45	6.02	5.82	6.05	25.95
Fe0	28.25	29.1	28.92	29.18	13.98
Total	98.45	97.91	98.35	98.98	98.39
	Cations				
Si	6.0014	5.9633	5.9786	5.933	5.9793
Ti	0.027	0.0277	0.0403	0.0304	0.0104
Al	3.8875	3.9191	3.8769	3.8934	3.964
Fe+3	0.0621	0.0583	0.0835	0.0877	0.0391
Mg	0.6504	0.6548	0.6796	0.6857	0.6837
Ca	0.5817	0.5447	0.5769	0.5952	0.5952
Mn	0.8929	0.8407	0.808	0.8364	0.8364
Fe+2	3.8637	4.0117	3.9659	3.9841	3.9841
Total	15.987	16.02	16.005	16.046	16.046
	Mole %				
AD	2.47	1.86	2.7	2.61	0.88
GR	7.00	6.89	6.5	6.87	5.11
PY	10.89	10.85	11.31	11.27	0.67
SP	14.95	13.93	13.45	.13.75	60.94
AL	64.69	66.47	66.03	65.49	32.4

HD 328-1A-1

	Core				*Rim*
	1	*2*	*3*	*4*	*5*
SiO2	36.72	37.00	36.62	36.6	36.6
TiO2	0.26	0.21	0.23	0.24	0.27
Al2O3	20.25	20.52	20.22	20.19	20.24
Fe2O3	0.59	0.51	0.58	0.66	0.7
MgO	2.77	2.7	2.74	2.83	2.78
CaO	3.07	3.02	2.97	3.36	3.36
MnO	6.31	6.53	6.12	5.7	6.06
FeO	28.73	29.18	29.00	28.88	29.01
Total	98.7	99.67	98.48	98.46	99.02
	Cations				
Si	5.9914	5.9851	5.9907	5.9854	5.9633
Ti	0.0314	0.0254	0.0282	0.0289	0.0327
Al	3.8941	3.9130	3.8993	3.8902	3.8864
Fe+3	0.0780	0.0621	0.0714	0.0809	0.0855
Mg	0.6746	0.6498	0.6689	0.6887	0.6744
Ca	0.5365	0.5241	0.5205	0.5878	0.5864
Mn	0.8724	0.8951	0.8486	0.7888	0.8366
Fe+2	3.9204	3.9472	3.9680	3.9495	3.9530
Total	15.994	16.002	15.996	16.000	16.018
	Mole %				
AD	2.3	1.93	2.21	2.46	2.61
GR	6.35	6.55	6.2	7.05	6.78
PY	11.27	10.83	11.17	11.48	11.18
SP	14.58	14.92	14.17	13.15	13.87
AL	65.5	65.78	66.25	65.85	65.55

Appendix 13C (Continued)

HD 328-1A-2

	Core				*Rim*
	1	*2*	*3*	*4*	*5*
SiO2	36.71	36.6	36.73	35.83	36.16
TiO2	0.16	0.24	0.18	0.12	0.21
Al2O3	0.54	0.67	0.62	0.33	0
Fe2O3	20.45	20.23	20.31	20.2	20.48
MgO	29.14	29.21	29.00	13.83	14.57
CaO	2.72	2.7	2.77	0.14	0.22
MnO	3.09	3.36	3.33	2.1	1.71
FeO	6.42	5.8	5.83	26.65	25.64
Total	99.23	98.81	98.77	99.20	98.99
	Cations				
Si	5.9695	5.9737	5.9876	5.9506	5.9892
Ti	0.0194	0.0291	0.0221	0.0146	0.0259
Al	3.9191	3.8914	3.9020	3.9534	3.9974
Fe+3	0.0660	0.0821	0.0762	0.0414	0.0000
Mg	0.6597	0.6574	0.6731	0.0348	0.0548
Ca	0.5381	0.5874	0.5818	0.3744	0.3039
Mn	0.8837	0.8023	0.8053	3.7481	3.5968
Fe+2	3.9629	3.9870	3.9532	1.9202	2.0181
Total	16.019	16.011	16.001	16.038	15.986
	Mole %				
AD	1.93	2.48	2.24	1.24	0.89
GR	6.79	6.99	7.24	4.78	4.45
PY	10.94	10.93	11.22	0.57	0.92
SP	14.65	13.34	13.42	61.76	60.37
AL	65.69	66.26	65.89	81.64	33.87

HD 328-2A-3

	Core				*Rim*
	1	*2*	*3*	*4*	*5*
SiO2	36.28	36.52	36.91	36.54	36.38
TiO2	0.2	0.24	0.22	0.28	0.26
Al2O3	0.51	0.72	0.94	0.82	0.8
Fe2O3	20.34	20.11	20.12	20.09	20.04
MgO	29.12	28.38	29.14	29.27	29.22
CaO	2.8	2.74	2.78	2.83	2.77
MnO	3.31	3.39	3.32	3.27	3.35
FeO	6.1	6.23	5.62	5.65	5.56
Total	98.66	98.33	99.05	98.75	98.38
	Cations				
Si	5.9386	5.9836	6.0009	5.9685	5.9657
Ti	0.0251	0.0291	0.0264	0.0346	0.0317
Al	3.9232	3.8826	3.8557	3.8683	3.8736
Fe+3	0.0625	0.0887	0.1148	0.1003	0.0987
Mg	0.6819	0.6694	0.6745	0.6888	0.6782
Ca	0.5801	0.5955	0.5789	0.5728	0.5883
Mn	0.8461	0.8640	0.7736	0.7811	0.7727
Fe+2	3.9860	3.8887	3.9627	3.9983	4.0075
Total	16.043	16.002	15.988	16.013	16.016
	Mole %				
AD	1.91	2.65	3.28	3.02	2.93
GR	7.38	6.98	6.15	6.16	6.51
PY	11.22	11.16	11.29	11.44	11.25
SP	13.92	14.4	12.95	12.97	12.82
AL	65.57	64.81	66.33	66.42	66.49

HD 328-2A-2

	Core				*Rim*
	1	*2*	*3*	*4*	*5*
SiO2	36.5	36.39	36.46	36.48	35.84
TiO2	0.26	0.24	0.28	0.25	0.07
Al2O3	0.78	0.55	0.72	0.34	0.2
Fe2O3	20.19	20.25	20.3	20.32	20.21
MgO	29.00	28.77	29.27	28.71	12.46
CaO	2.67	2.74	2.83	2.69	0.14
MnO	3.4	3.4	3.36	3.42	2.42
FeO	6.32	6.16	6.22	5.9	27.15
Total	99.12	98.50	99.44	98.11	98.49
	Cations				
Si	5.9514	5.9587	5.9282	5.9834	5.9758
Ti	0.0316	0.0301	0.0345	0.0389	0.0086
Al	3.8799	3.9075	3.8897	3.9276	3.9707
Fe+3	0.0957	0.0683	0.0879	0.0418	0.0251
Mg	0.6493	0.6678	0.6863	0.6581	0.0335
Ca	0.5935	0.5963	0.5861	0.6011	0.4315
Mn	0.8731	0.8539	0.8559	0.8196	3.8350
Fe+2	3.9544	3.9407	3.9798	3.9386	1.7375
Total	16.029	16.023	16.048	16.001	16.018
	Mole %				
AD	2.84	2.14	2.68	1.51	0.75
GR	6.65	7.43	6.61	8.2	6.32
PY	10.73	11.06	11.27	10.97	0.56
SP	14.43	14.14	14.06	13.66	63.57
AL	65.35	65.24	65.38	65.65	28.8

HD 382-3A-3

	Core				*Rim*
	1	*2*	*3*	*4*	*5*
SiO2	36.55	36.06	35.68	36.32	35.64
TiO2	0.24	0.06	0.07	0.21	0.15
Al2O3	0.88	0.35	0.16	0.4	0.14
Fe2O3	20.07	20.23	20.11	20.12	20.14
MgO	29.07	12.9	13.64	14.35	14.71
CaO	2.82	0.13	0.17	0.18	0.19
MnO	3.3	2.46	2.25	1.86	1.8
FeO	5.76	26.88	25.84	25.92	25.63
Total	98.69	99.07	97.92	99.36	98.4
	Cations				
Si	5.9734	5.9795	5.9820	6.0036	5.8614
Ti	0.0294	0.0074	0.0091	0.0260	0.0189
Al	3.8653	3.9530	3.9733	3.9201	3.9696
Fe+3	0.1079	0.0434	0.0206	0.0502	0.0179
Mg	0.6864	0.0310	0.0429	0.0444	0.0479
Ca	0.5779	0.4970	0.4033	0.3293	0.8218
Mn	0.7918	3.7749	3.6690	3.6283	3.6314
Fe+2	3.9734	1.7889	1.9117	1.9838	2.0570
Total	16.011	16.015	16.012	15.985	16.426
	Mole%				
AD	3.13	1.19	0.65	1.65	0.73
GR	6.18	5.99	5.96	3.6	4.41
PY	11.41	0.51	0.71	0.74	0.79
SP	13.24	62.63	60.93	60.78	60.06
AL	66.04	29.68	31.75	33.22	34.02

Appendix 13C (Continued)

HD 328-3A-2

	Core				Rim
	1	2	3	4	5
SiO2	36.52	36.64	36.78	36.71	36.6
TiO2	0.24	0.32	0.35	0.27	0.18
Al2O3	0.41	0.74	0.89	0.49	0.73
Fe2O3	20.35	20.27	20.23	20.27	20.26
MgO	28.98	29.69	29.46	29.17	29.37
CaO	2.79	2.86	2.79	2.76	2.77
MnO	3.26	3.25	3.34	3.36	3.44
FeO	5.9	5.71	6.08	5.42	5.55
Total	98.45	99.48	99.92	98.45	98.9
	Cations				
Si	5.9744	5.9488	5.9495	5.9968	5.9676
Ti	0.0294	0.0390	0.0425	0.0335	0.0226
Al	3.9229	3.8782	3.8559	3.9028	3.8931
Fe+3	0.0501	0.0898	0.1081	0.0606	0.0890
Mg	0.6791	0.6909	0.6730	0.6713	0.6738
Ca	0.5715	0.5651	0.5785	0.5877	0.6001
Mn	0.8179	0.7851	0.8332	0.7496	0.7670
Fe+2	3.9644	4.0313	3.9853	3.9856	4.0056
Total	16.010	16.028	16.026	15.988	16.019
	Mole %				
AD	1.69	2.81	3.32	2.03	2.55
GR	7.52	6.15	5.83	7.47	7.17
PY	11.29	11.42	11.13	11.24	11.17
SP	13.6	12.98	13.78	12.55	12.71
AL	65.91	66.64	65.93	66.71	66.39

HD 328-5A-1

	Core				Rim
	1	2	3	4	5
SiO2	36.63	36.68	36.57	35.8	36.18
TiO2	0.26	0.24	0.25	0.18	0.18
Al2O3	0.58	0.9	0.58	0.46	0.07
Fe2O3	20.25	20.11	20.37	20.04	20.32
MgO	28.88	28.89	28.85	14.09	14.54
CaO	2.75	2.72	2.64	0.17	0.22
MnO	3.23	3.28	3.40	2.13	1.72
FeO	6.06	6.24	6.62	26.2	25.85
Total	98.64	99.06	99.28	99.07	99.08
	Cations				
Si	5.9831	**	5.9506	5.9536	**
Ti	0.0319	**	0.0302	0.0222	**
Al	3.8976	**	3.9070	3.9277	**
Fe+3	0.0707	**	0.0704	0.0560	**
Mg	0.6706	**	0.6409	0.0419	**
Ca	0.5649	**	0.5930	0.3792	**
Mn	0.8379	**	0.9124	3.6900	**
Fe+2	3.9442	**	3.9260	1.9587	**
Total	16.001	**	16.031	16.031	**
	Mole %				
AD	2.25	3.2	2.19	1.77	0.57
GR	6.85	6.02	7.3	4.28	4.32
PY	11.18	10.99	10.59	0.69	0.91
SP	13.97	14.31	15.07	60.93	60.56
AL	65.75	65.47	64.85	32.34	33.64

***Cation data not available due to printer malfunction.*

HD 328-5A-2

	Core				Rim
	1	2	3	4	5
SiO2	36.4	36.53	36.56	36.59	35.91
TiO2	0.23	0.23	0.22	0.27	0.17
Al2O3	20.35	20.38	19.33	20.28	20.15
Fe2O3	0.5	0.41	1.17	0.77	0.23
MgO	2.73	2.76	2.71	2.68	0.14
CaO	3.18	3.14	3.25	3.55	1.9
MnO	5.98	5.65	5.44	5.69	25.98
FeO	29.52	29.54	27.27	29.67	14.33
Total	98.89	98.64	95.95	99.5	98.81
	Cations				
Si	5.9458	5.9701	6.0985	5.9451	5.9770
Ti	0.0286	0.0279	0.0279	0.0328	0.0213
Al	3.9189	3.9251	3.8002	3.8823	3.9526
Fe+3	0.0614	0.0506	0.1419	0.0935	0.0289
Mg	0.6635	0.6713	0.6739	0.6481	0.0354
Ca	0.5561	0.5494	0.5808	0.6182	0.3385
Mn	0.8277	0.7822	0.7684	0.7828	3.6627
Fe+2	4.0335	4.0377	3.8033	4.0315	1.9946
Total	16.036	16.014	15.900	16.034	16.011
	Mole %				
AD	1.94	1.68	4.23	2.8	1.04
GR	6.95	7.17	5.48	7.07	4.37
PY	10.94	11.15	11.6	10.69	0.59
SP	13.65	12.98	13.23	12.91	60.86
AL	66.52	67.03	65.46	66.52	33.14

HD 328-5A-3

	Core				Rim
	1	2	3	4	5
SiO2	36.57	36.52	36.74	35.92	35.76
TiO2	0.2	0.26	0.3	0.06	0.15
Al2O3	20.34	20.08	19.91	20.26	20.25
Fe2O3	0.5	0.91	1.02	0.09	0
MgO	2.75	2.78	2.73	0.12	0.21
CaO	3.13	3.27	3.25	2.48	1.66
MnO	6.25	6.26	5.75	26.85	25.36
FeO	28.92	28.88	28.93	12.52	14.95
Total	98.66	98.96	98.63	98.3	98.34
	Cations				
Si	5.9741	5.9610	6.0028	5.9907	5.9757
Ti	0.0250	0.0314	0.0366	0.0077	0.0191
Al	3.9160	3.8623	3.8334	3.9827	3.9888
Fe+3	0.0620	0.1115	0.1253	0.0108	0.0000
Mg	0.6701	0.6755	0.6658	0.0304	0.0516
Ca	0.5482	0.5716	0.5688	0.4427	0.2974
Mn	0.8653	0.8658	0.7962	3.7939	3.5886
Fe+2	3.9513	3.9417	3.9523	1.7459	2.0897
Total	16.012	16.021	15.981	16.005	16.011
	Mole %				
AD	1.92	3.24	3.71	0.38	0.28
GR	6.94	5.92	5.47	6.91	4.47
PY	11.13	11.19	11.17	0.51	0.86
SP	14.37	14.35	13.36	63.14	59.65
AL	65.64	65.31	66.3	29.06	34.74

AD = andradite

GR = grossularite

PY = pyrope

SP = spessartine

AL = almandine

Major element values in percent

APPENDIX 14

MAJOR ELEMENT ANALYSES OF "APLITE" (Unit 20b)

Field No.	SiO2	TiO2	Al2O3	Fe2O3*	MnO	MgO	CaO	Na2O	K2O	P2O5	CO2	FeO	Fe2O3	Fe2O3/FeO	LOI	SUM
HD514-14	76.81	0.08	12.85	0.68	0.01	0.01	0.60	3.31	4.66	0.01	0.12	0.37	0.68	1.84	0.84	99.86
HD514-40	77.20	0.09	12.70	0.27	0.00	0.01	0.90	2.99	5.05	0.00	0.10	0.14	0.27	1.93	0.86	100.07

Footnote: *Major element values in percent*
Fe2O3 = total iron as Fe2O3*
Sum excludes CO2, FeO and Fe2O3

APPENDIX 15A

REPRESENTATIVE CORE TO RIM MICROPROBE ANALYSES OF EXOSKARN GARNETS: NICKEL PLATE DEPOSIT (see Figure 24)

HD 672A-5-1 (Large garnet with isotropic core and birefringent margin)

	Core												*Rim*
	1	*2*	*3*	*4*	*5*	*6*	*7*	*8*	*9*	*10*	*11*	*12*	*13*
SiO2	36.76	36.97	37.87	37.84	36.88	37.72	37.22	35.76	36.46	36.21	36.19	37.69	37.38
TiO2	0.85	0.47	0.03	0.19	0.41	0.12	0.29	0.50	0.17	0.04	0.03	0.24	0.67
Al2O3	10.56	12.16	14.49	16.14	16.19	15.84	12.79	13.58	7.37	7.32	6.98	13.58	15.04
Fe2O3	15.55	13.78	11.15	8.51	7.78	8.96	13.09	11.13	20.73	20.80	21.44	12.16	9.49
MgO	0.08	0.07	0.09	0.08	0.09	0.09	0.06	0.06	0.04	0.12	0.04	0.03	0.00
CaO	34.52	35.05	35.22	35.01	34.51	35.16	34.60	33.11	33.78	33.87	34.26	35.05	35.43
MnO	0.41	0.41	0.40	0.50	0.56	0.52	0.47	0.43	0.33	0.26	0.23	0.50	0.33
FeO	0.19	0.27	0.42	0.99	1.51	0.68	0.76	3.07	0.25	0.23	0.01	0.37	0.60
Total	98.93	99.18	99.66	99.26	97.92	99.09	99.27	97.63	99.13	98.73	99.17	99.61	98.93
Cations													
Si	5.9358	5.9170	5.9589	5.9368	5.8764	5.9343	5.9382	5.8254	5.9792	5.9676	5.9521	5.9585	5.9091
Ti	0.1028	0.0571	0.0031	0.0218	0.0488	0.0143	0.0344	0.0609	0.0204	0.0047	0.0031	0.0290	0.0796
Al	2.0102	2.2947	2.6861	2.9949	3.0400	2.9379	2.4042	2.6066	1.4236	1.4225	1.3533	2.5299	2.8030
Fe+3	1.8898	1.6604	1.3196	1.0048	0.9333	1.0609	1.5713	1.3645	2.5583	2.5795	2.6538	1.4471	1.1287
Mg	0.0192	0.0173	0.0217	0.0182	0.0222	0.0199	0.0130	0.0146	0.0106	0.0029	0.0100	0.0066	0.0000
Ca	5.9720	6.0114	5.9375	5.8460	5.8911	5.9265	5.9137	5.7788	5.9366	5.9819	6.0365	5.9369	6.0011
Mn	0.0563	0.0550	0.0533	0.0657	0.0756	0.0692	0.0632	0.0597	0.0459	0.0357	0.0313	0.0664	0.0440
Fe+2	0.0253	0.0356	0.0550	0.1296	0.2009	0.0891	0.1016	0.4176	0.0348	0.0319	0.0009	0.0435	0.0799
Total	16.0114	16.0484	16.0352	16.0465	16.0882	16.0520	16.0396	16.1281	16.0094	16.0267	16.0412	16.0240	16.0454
Mole %													
AD	48.70	41.77	32.68	25.09	23.44	26.32	39.33	33.71	64.10	64.03	65.55	36.36	29.04
GR	49.63	56.45	65.18	71.40	71.71	70.76	57.74	58.40	34.38	34.81	33.75	61.61	68.92
PY	0.32	0.28	0.36	0.30	0.36	0.33	0.21	0.23	0.18	0.05	0.16	0.11	0.00
SP	0.94	0.90	0.88	1.08	1.23	1.13	1.04	0.96	0.76	0.59	0.52	1.10	0.72
AL	0.42	0.58	0.91	2.13	3.26	1.46	1.67	6.70	0.58	0.53	0.01	0.82	1.31

NOTE = 1 - 4 = isotropic garnet 5 - 13 = birefringent garnet

Appendix 15A (Continued)

HD 261-7-2B (Vein garnet)

	Core								*Rim*
	1	*2*	*3*	*4*	*5*	*6*	*7.00*	*8*	*9*
SiO2	35.44	35.43	35.65	35.47	35.37	35.48	34.83	34.87	34.98
TiO2	0.06	0.07	0.01	0.06	0.05	0.05	0.00	0.06	0.03
Al2O3	9.95	9.26	9.15	8.99	8.82	8.62	7.50	9.77	7.31
Cr2O3	0.00	0.00	0.00	0.00	0.05	0.01	0.02	0.03	0.01
Fe2O3	18.96	20.08	19.83	20.06	20.56	20.91	22.83	20.15	23.15
MgO	0.04	0.03	0.02	0.02	0.02	0.03	0.03	0.01	0.04
CaO	34.03	33.93	33.91	33.76	33.76	33.64	33.55	33.43	33.71
MnO	0.30	0.24	0.27	0.25	0.22	0.22	0.23	0.30	0.23
FeO	0.00	0.00	0.00	0.00	0.00	0.00	0.00	0.00	0.00
Na2O	0.01	0.00	0.01	0.02	0.00	0.01	0.01	0.00	0.01
Total	98.79	99.04	98.85	98.63	98.85	98.97	99.00	98.62	99.47
	Cations								
Si	1.4490	1.4512	1.4602	1.4577	1.4531	1.4564	1.4421	1.4335	1.4431
Ti	0.0018	0.0000	0.0002	0.0019	0.0015	0.0014	0.0000	0.0017	0.0009
Al	0.4794	0.4468	0.4420	0.4357	0.4270	0.4172	0.3660	0.4733	0.3555
Cr	0.0001	0.0000	0.0000	0.0000	0.0015	0.0003	0.0005	0.0009	0.0002
Fe+3	0.5834	0.6188	0.6113	0.6203	0.6355	0.6458	0.7114	0.6232	0.7186
Mg	0.0023	0.0016	0.0011	0.0010	0.0014	0.0021	0.0020	0.0006	0.0022
Ca	1.4910	1.4892	1.4884	1.4864	1.4860	1.4792	1.4884	1.4723	1.4899
Mn	0.0105	0.0084	0.0095	0.0087	0.0075	0.0078	0.0082	0.0105	0.0080
Fe+2	0.0000	0.0000	0.0000	0.0000	0.0000	0.0000	0.0000	0.0000	0.0000
Na	0.0007	0.0000	0.0005	0.0015	0.0000	0.0005	0.0006	0.0000	0.0007
Total	4.0181	4.0160	4.0132	4.0131	4.0135	4.0108	4.0192	4.0161	4.0192

Appendix 15A (Continued)

HD 261-7-4A **(Anhedral garnet)**

	Core							*Rim*
	1	*2*	*3*	*4*	*5*	*6*	*7*	*8*
SiO2	36.13	36.20	36.43	36.69	36.67	36.47	36.31	36.82
TiO2	0.03	0.06	0.02	0.03	0.04	0.05	0.01	0.00
Al2O3	8.46	8.79	9.43	9.78	9.15	8.77	8.73	8.54
Fe2O3	19.38	18.83	18.13	17.56	18.93	18.93	18.93	19.47
MgO	0.03	0.02	0.02	0.02	0.03	0.02	0.01	0.00
CaO	34.778	34.57	34.74	34.72	34.51	34.47	34.69	34.41
MnO	0.26	0.25	0.28	0.23	0.12	0.26	0.18	0.30
FeO	0.11	0.3	0.47	0.21	0.04	0.24	0.03	0.26
Total	99.178	99.02	99.52	99.24	99.49	99.21	98.89	99.8
	Cations							
Si	5.9087	5.9173	5.9117	5.9453	5.9696	5.9437	5.935	5.9689
Ti	0.0042	0.0072	0.0025	0.004	0.0054	0.0064	0.0036	0.0000
Al	1.631	1.6942	1.8027	0.8672	1.7553	1.6844	1.6821	1.6321
Fe+3	2.3847	2.3162	2.2142	2.1406	2.2454	2.3210	2.3284	2.3747
Mg	0.0063	0.0053	0.0047	0.0041	0.0063	0.0057	0.0027	0.0001
Ca	6.094	6.054	6.0396	6.0266	6.0197	6.0181	6.0764	5.9756
Mn	0.0355	0.0351	0.0379	0.0314	0.0169	0.0358	0.0243	0.0406
Fe+2	0.0149	0.0409	0.0642	0.0278	0.0059	0.0322	0.0037	0.0355
Total	16.0793	16.0703	16.0774	16.0469	16.0246	16.0472	16.0562	16.0276

HD 672A-5-4 (Large garnet with isotropic core and birefringent margin)

	Core																						*Rim*
	1	*2*	*3*	*4*	*5*	*6*	*7*	*8*	*9*	*10*	*11*	*12*	*13*	*14*	*15*	*16*	*17*	*18*	*19*	*20*	*21*	*22*	*23*
SiO2	36.36	36.72	37.24	36.44	37.12	36.95	37.41	37.52	37.33	37.41	37.15	37.36	37.39	37.33	36.96	36.90	36.26	36.33	36.12	36.34	36.58	37.01	38.43
TiO2	0.51	0.06	0.18	0.11	0.17	0.24	0.45	0.38	0.20	0.28	0.18	0.14	0.10	0.15	0.30	0.49	0.09	0.05	0.01	0.00	0.47	0.33	0.10
Al2O3	11.37	14.38	16.38	16.74	16.84	16.51	16.58	16.57	16.84	16.78	16.74	16.65	15.39	13.42	12.15	10.65	7.25	7.32	6.61	8.88	9.42	10.91	18.12
Fe2O3	14.16	10.39	7.64	7.15	6.91	7.28	7.27	7.45	7.23	7.24	7.52	7.64	9.54	12.36	13.75	15.83	20.86	20.97	22.04	18.39	17.60	15.53	5.79
MgO	0.07	0.07	0.13	0.10	0.11	0.13	0.09	0.13	0.11	0.11	0.08	0.10	0.08	0.06	0.06	0.07	0.02	0.03	0.00	0.05	0.03	0.03	0.02
CaO	33.60	34.31	34.39	34.77	34.37	34.54	34.94	35.02	35.07	34.89	35.28	35.07	34.87	34.78	34.45	34.39	34.01	34.02	34.03	31.14	34.45	34.53	34.89
MnO	0.48	0.39	0.57	0.67	0.65	0.52	0.41	0.59	0.54	0.53	0.54	0.46	0.58	0.48	0.38	0.46	0.12	0.21	0.30	0.22	0.24	0.27	0.59
FeO	0.55	0.61	0.99	1.03	1.06	0.91	0.36	0.72	0.95	1.03	1.23	1.18	0.98	0.72	0.46	0.31	0.11	0.42	0.36	3.53	0.40	0.12	1.24
Total	97.1	96.9	97.5	97.01	97.2	97.1	97.5	98.4	98.3	98.3	98.7	98.6	98.9	99.3	98.5	99.1	98.7	99.4	99.5	98.6	99.2	98.7	99.2
Mole %																							
AD	44.48	31.23	22.86	21.02	20.65	21.89	22.12	22.48	21.33	21.56	21.90	22.34	27.95	36.69	41.85	48.67	64.46	64.07	67.23	56.74	54.13	47.70	16.99
GR	52.89	66.27	73.21	74.94	75.17	74.48	74.75	74.37	75.03	74.62	74.05	73.78	68.36	60.44	56.02	49.31	34.90	34.37	31.27	34.46	44.29	51.30	78.99
PY	0.28	0.26	0.51	0.37	0.44	0.50	0.37	0.51	0.43	0.43	0.29	0.37	0.29	0.25	0.23	0.28	0.10	0.13	0.01	0.19	0.13	0.12	0.07
SP	1.10	0.89	1.26	1.45	1.44	1.16	0.89	1.07	1.18	1.17	1.16	0.99	1.27	1.07	0.86	1.03	0.28	0.48	0.68	0.52	0.54	0.62	1.28
AL	1.25	1.35	2.17	2.21	2.30	1.98	1.87	1.57	2.03	2.22	2.61	2.52	2.12	1.57	1.03	0.70	0.26	0.95	0.81	8.09	0.90	0.27	2.67

1 - 10 = isotropic garnet
11 - 23 = birefringent garnet
major element values in percent

AD = andradite	*GR = grossularite*	*PY = pyrope*
SP = spessartine	*AL = almandine*	

APPENDIX 15B
REPRESENTATIVE CORE-TO-RIM MICROPROBE ANALYSES OF EXOSKARN CLINOPYROXENES: NICKEL PLATE DEPOSIT
(see Figures 21A and B)

HD 261-7-2

	Core				*Rim*
	1	2	3	4	5
SiO2	48.65	48.55	49.16	48.21	48.00
TiO2	0.00	0.05	0.00	0.00	0.01
Al2O3	0.13	0.14	0.17	0.19	0.18
Cr2O3	0.00	0.00	0.00	0.00	0.00
Fe2O3	2.46	2.83	2.10	3.69	2.99
MgO	4.53	4.85	5.58	5.16	3.98
CaO	22.90	22.76	23.20	23.08	23.12
MnO	0.92	0.75	0.61	0.83	0.56
FeO	18.67	18.15	18.14	17.55	19.85
Na2O	0.25	0.30	0.08	0.11	0.06
Total	98.51	98.38	99.04	98.82	98.75
	Cations				
Si	1.9692	1.9639	1.9674	1.9434	1.9517
Ti	0.0000	0.0015	0.0000	0.0000	0.0000
Al	0.0060	0.0068	0.0080	0.0092	0.0088
Cr	0.0000	0.0000	0.0000	0.0000	0.0000
Fe+3	0.0750	0.0862	0.0632	0.1120	0.0916
Mg	0.2736	0.2921	0.3326	0.3105	0.2414
Ca	0.9933	0.9862	0.9949	0.9966	1.0072
Mn	0.0315	0.0256	0.0208	0.0283	0.0192
Fe+2	0.6319	0.6140	0.6072	0.5916	0.6751
Na	0.0194	0.0237	0.0060	0.0083	0.0047
Total	3.9999	4.0000	4.0001	3.9999	3.9997

HD 261-7-5A

	Core									*Rim*
	1	2	3	4	5	6	7	8	9	10
SiO2	47.92	48.39	47.18	48.48	48.58	48.39	48.64	47.18	48.35	48.17
TiO2	0.00	0.00	0.00	0.00	0.03	0.00	0.02	0.01	0.00	0.02
Al2O3	0.21	0.12	0.22	0.28	0.14	0.14	0.10	0.35	0.18	0.19
Cr2O3	0.00	0.04	0.02	0.04	0.01	0.03	0.00	0.02	0.00	0.00
Fe2O3	2.20	3.12	3.29	2.59	3.30	3.03	2.17	4.35	2.56	3.43
MgO	3.67	4.98	4.26	5.42	5.69	5.55	5.41	5.67	5.00	5.18
CaO	22.76	23.04	22.77	23.22	23.37	23.22	23.04	23.14	22.98	23.26
MnO	0.29	0.84	0.70	0.69	0.66	0.65	0.70	0.60	0.70	0.65
FeO	20.95	17.83	18.62	17.61	17.01	17.28	18.04	15.79	18.49	17.67
Na2O	0.08	0.17	0.07	1.05	0.07	0.06	0.06	0.06	0.05	0.05
Total	98.08	98.53	97.13	99.38	98.86	98.35	98.18	97.17	98.31	98.62
	Cations									
Si	1.9640	1.9557	1.9226	1.9555	1.9488	1.9526	1.9661	1.9264	1.9588	1.9449
Ti	0.0001	0.0000	0.0000	0.0000	0.0008	0.0000	0.0006	0.0005	0.0000	0.0005
Al	0.0103	0.0059	0.0588	0.0134	0.0065	0.0067	0.0050	0.0169	0.0086	0.0092
Cr	0.0000	0.0012	0.0006	0.0012	0.0002	0.0008	0.0001	0.0007	0.0000	0.0000
Fe+3	0.0677	0.0949	0.1008	0.0786	0.0997	0.0921	0.0661	0.1338	0.0782	0.1042
Mg	0.2239	0.2999	0.2587	0.3260	0.3405	0.3337	0.3258	0.3449	0.3022	0.3119
Ca	0.9993	0.9978	0.9941	1.0033	1.0045	1.0039	0.9980	1.0121	0.9976	1.0064
Mn	0.0101	0.0289	0.0241	0.0236	0.0223	0.0222	0.0240	0.0207	0.0238	0.0221
Fe+2	0.7182	0.6027	0.6346	0.5941	0.5709	0.5831	0.6097	0.5390	0.6266	0.5967
Na	0.0063	0.0132	0.0055	0.0042	0.0057	0.0048	0.0046	0.0051	0.0043	0.0041
Total	4.0000	4.0000	4.0000	4.0000	4.0000	4.0000	4.0000	4.0000	4.0000	4.0000

HD 261-6-1

	Core				*Rim*
	1	2	3	4	5
SiO2	49.63	49.75	49.35	49.27	49.21
TiO2	0.00	0.02	0.00	0.00	0.01
Al2O3	0.14	0.14	0.14	0.14	0.14
Fe2O3	0.22	0.50	0.00	0.00	0.00
MgO	4.89	4.63	4.15	3.41	3.32
CaO	22.58	22.93	22.49	22.57	22.58
MnO	0.75	0.77	0.77	0.86	0.81
FeO	20.39	19.99	20.85	22.38	22.43
Na2O	0.15	0.24	0.19	0.06	0.08
Total	98.75	98.97	97.94	98.69	98.58
	Cations				
Si	1.9992	1.9978	2.0075	2.0036	2.0041
Ti	0.0000	0.0060	0.0000	0.0000	0.0020
Al	0.0065	0.0064	0.0066	0.0065	0.0069
Fe+3	0.0066	0.0151	0.0000	0.0000	0.0000
Mg	0.2933	0.2774	0.2515	0.2067	0.2015
Ca	0.9702	0.9867	0.9802	0.9833	0.9850
Mn	0.0257	0.0263	0.0268	0.0297	0.0278
Fe+2	0.6869	0.6713	0.7094	0.7610	0.7638
Na	0.0115	0.0183	0.0147	0.0044	0.0059
Total	4.0000	4.0000	3.9966	3.9953	3.9952

HD 261-6-2

	Core				*Rim*
	1	2	3	4	5
SiO2	49.18	49.19	49.01	49.06	49.35
TiO2	0.02	0.00	0.00	0.04	0.00
Al2O3	0.18	0.19	0.14	0.15	0.16
Fe2O3	0.25	0.20	0.08	0.13	0.30
MgO	3.56	3.52	3.57	3.54	3.52
CaO	23.11	22.73	22.81	23.05	22.91
MnO	0.86	0.92	0.67	0.82	0.75
FeO	21.73	21.98	21.93	21.68	22.18
Na2O	0.06	0.11	0.09	0.08	0.10
Total	98.95	98.84	98.30	98.55	99.27
	Cations				
Si	1.9935	1.9967	1.9989	1.9960	1.9954
Ti	0.0007	0.0000	0.0000	0.0013	0.0000
Al	0.0088	0.0089	0.0067	0.0074	0.0078
Fe+3	0.0076	0.0062	0.0024	0.0040	0.0091
Mg	0.2149	0.2129	0.2170	0.2148	0.2120
Ca	1.0035	0.9887	0.9968	1.0046	0.9924
Mn	0.0294	0.0317	0.0231	0.0282	0.0255
Fe+2	0.7365	0.7461	0.7481	0.7377	0.7500
Na	0.0050	0.0086	0.0070	0.0060	0.0077
Total	4.0000	4.0000	4.0000	4.0000	4.0000

Major element values in percent

APPENDIX 16A

MAJOR AND TRACE ELEMENT ANALYSES OF EXOSKARN SAMPLES COLLECTED FROM DDH 401: NICKEL PLATE DEPOSIT

Sample No.	401.01	401.02	401.05	401.06	401.07	401.08	401.09	401.10	401.15A	401.11	401.14	401.15	401.17	401.19	401.20	401.22	401.25	401.26	401.27	401.28	401.29	401.31	401.32	Mean	Stdev.
Depth (m)	6.60	12.20	22.60	29.30	33.40	41.50	48.80	54.90	55.06	63.40	81.10	85.30	99.10	114.60	120.70	126.25	150.90	160.30	166.40	175.28	183.50	196.60	200.90	-	-
SiO2	47.27	58.17	56.59	57.97	53.68	55.75	55.97	53.45	55.03	56.56	55.28	56.83	51.04	59.19	63.42	42.02	63.95	59.20	44.77	60.54	50.80	61.06	46.68	55.01	5.73
TiO2	0.51	0.57	0.66	0.63	0.55	0.58	0.54	0.47	0.73	0.66	0.67	0.74	0.68	0.87	0.86	0.23	0.33	0.90	0.20	0.25	0.32	0.41	0.28	0.53	0.21
Al2O3	8.77	16.06	17.04	16.18	13.21	13.82	14.38	14.41	17.30	17.75	18.00	17.23	16.81	12.62	13.06	4.59	6.12	17.53	4.89	4.99	6.41	8.66	6.17	12.45	4.91
Fe2O3*	11.14	2.56	6.35	5.42	3.53	5.49	5.79	5.11	3.34	2.69	4.80	3.26	6.52	7.12	6.65	2.77	3.29	6.42	1.84	2.21	2.77	5.15	3.88	4.79	2.14
MnO	0.20	0.08	0.13	0.08	0.18	0.13	0.12	0.12	0.06	0.07	0.07	0.07	0.11	0.08	0.07	0.19	0.12	0.12	0.06	0.06	0.05	0.09	0.10	0.10	0.04
MgO	6.60	3.46	3.33	3.98	4.17	3.48	2.94	3.08	4.55	2.76	4.89	4.27	5.85	4.05	3.30	3.80	3.20	2.15	2.59	3.85	2.71	3.57	7.50	3.91	1.27
CaO	17.92	6.91	7.26	6.59	11.52	10.25	8.69	10.42	10.00	8.48	9.57	10.27	14.91	6.03	4.16	27.62	11.24	4.44	27.73	15.91	18.02	9.50	24.21	12.27	6.82
Na2O	0.48	2.19	3.91	4.12	1.18	0.51	0.61	0.87	2.96	3.43	4.24	2.85	2.89	1.54	1.80	0.53	0.12	3.14	0.71	0.65	0.81	0.55	0.48	1.76	1.37
K2O	3.18	7.11	3.14	1.90	5.66	7.72	8.60	7.63	4.00	4.97	1.28	3.76	0.23	4.67	5.05	1.04	3.82	3.11	0.85	1.04	1.54	4.63	1.62	3.76	2.43
K2O/Na2O	6.63	3.25	0.80	0.46	4.80	15.14	14.10	8.77	1.35	1.45	0.30	1.32	0.08	3.03	2.81	1.96	31.83	0.99	1.20	1.60	1.90	8.42	3.38	5.02	7.18
P2O5	0.13	0.30	0.24	0.28	0.30	0.32	0.34	0.32	0.32	0.38	0.00	0.00	0.00	0.21	0.00	0.17	0.35	0.29	0.00	0.29	0.35	0.34	0.00	0.21	0.14
FeO	9.46	2.29	5.25	4.44	4.80	4.70	5.02	4.30	3.00	2.34	3.87	2.72	5.80	6.23	5.51	2.15	2.93	5.58	1.60	1.93	2.43	4.57	2.58	4.06	1.84
Fe2O3	0.63	0.02	0.54	0.49	0.22	0.27	0.21	0.53	0.01	0.20	0.50	0.24	0.07	0.20	0.53	0.38	0.03	0.22	0.06	0.07	0.07	0.07	1.01	0.28	0.25
Fe2O3/FeO	0.07	0.01	0.10	0.11	0.05	0.06	0.04	0.08	0.00	0.09	0.13	0.09	0.01	0.03	0.10	0.18	0.01	0.04	0.04	0.04	0.03	0.02	0.39	0.07	0.08
LOI	0.96	0.78	1.47	1.88	0.05	0.00	0.56	1.81	0.96	1.34	0.82	0.99	1.86	1.46	1.52	14.38	4.43	0.88	15.89	8.35	12.50	3.19	7.31	3.63	4.72
Sum	96.96	98.19	100.12	99.03	96.05	98.00	98.54	97.73	99.25	99.09	99.63	100.27	100.90	97.84	99.89	97.34	96.97	98.58	99.53	98.05	96.88	97.15	98.23	98.46	1.26
Au	92	45	90	103	64	33	<10	23	80	<10	<10	112	139	33	50	130	40	10	82	80	78	113	10	62	42
Ag	<10	<10	<10	<10	<10	<10	<10	<10	<10	<10	<10	21	<10	<10	<10	46	<10	<10	<10	<10	<10	<10	10	8	9
Cu	580	24	93	104	22	46	230	180	56	64	46	63	580	260	270	380	155	10	60	46	67	290	550	180	184
Pb	30	23	33	10	12	12	18	28	13	28	14	15	46	14	25	34	35	13	56	28	40	38	20	24	12
Zn	120	71	269	82	135	72	88	79	63	93	61	59	360	70	57	362	95	106	124	46	78	67	100	114	91
Co	26	21	29	40	27	23	28	21	16	36	20	17	33	31	30	12	15	20	8	15	13	19	13	22	8
Ni	18	14	16	22	29	45	30	28	11	9	18	14	78	85	55	26	41	3	30	31	72	35	48	33	22
Cr	47	17	19	40	47	48	40	23	36	32	26	32	53	90	90	26	57	<10	27	56	131	48	68	44	30
As	11.9	48.0	3.2	20.0	22.0	35.3	4.7	4.7	28.4	28.4	23.0	21.5	14.6	19.0	32.2	29.9	30.0	7.8	19.2	12.4	20.0	50.0	286.0	34	56
Sb	2.6	2.6	2.1	2.3	2.6	3.5	1.5	2.7	3.5	4.4	1.7	3.0	3.9	<5	1.8	10.0	5.0	4.1	3.4	6.1	5.3	4.6	4.0	4	2
Ba	1820	5109	1706	960	2477	4395	5729	5797	2432	1617	759	2631	115	2728	2751	669	1907	1503	954	1082	774	2668	1028	2138	1683
Sr	387	673	700	790	548	665	654	717	860	569	975	932	860	453	498	255	301	408	665	418	825	319	384	560	236
Rb	72	132	63	45	135	160	173	154	79	114	23	78	11	92	88	30	79	68	27	21	46	121	45	81	48
Y	19	21	20	24	23	22	21	20	27	19	22	30	17	15	29	19	31	31	18	21	34	24	26	23	5
Zr	72	102	77	92	88	85	84	80	86	73	60	89	52	71	137	61	73	153	55	58	78	67	75	81	24
Nb	<3	<3	<3	<3	<3	<3	<3	<3	<3	<3	<3	<3	<3	<3	8	4	<3	7	<3	<3	<3	<3	3	2	2
U	6	4	<2	2	1	<2	<2	5	4	3	11	9	11	<2	6	3	3	<2	<2	<2	2	7	8	4	3
Th	30	27	19	25	12	18	17	20	26	21	25	25	24	20	29	28	32	27	26	22	16	26	27	24	3

Note: half the detection limit (e.g., 1.5 for <3) was used for calculating the mean and standard deviations.Fe2O3 = total iron as Fe2O3; Sum excludes FeO and Fe2O3.*
Major element values in percent; trace element values in ppm, except Au in ppb

APPENDIX 16B
MAJOR AND TRACE ELEMENT ANALYSES OF ENDOSKARN SAMPLES COLLECTED FROM DDH 401: NICKEL PLATE DEPOSIT

Sample No.	401.03	401.04	401.12	401.13	401.16	401.18	401.21	401.23	401.24	**Mean**	**Stdev.**
Depth (m)	16.80	17.70	68.90	75.00	93.00	105.20	123.70	137.20	145.10	-	-
SiO2	53.36	51.17	47.99	50.40	52.57	55.88	51.18	54.89	54.58	52.45	2.51
TiO2	0.73	0.63	1.02	0.90	0.61	0.60	0.65	0.62	0.63	0.71	0.15
Al2O3	15.21	17.09	18.15	16.12	15.94	16.83	17.96	18.51	18.61	17.16	1.23
Fe2O3*	5.69	6.57	8.97	4.85	7.66	5.52	6.69	6.37	7.66	6.66	1.27
MnO	0.16	0.12	0.11	0.14	0.06	0.07	0.09	0.09	0.11	0.11	0.03
MgO	4.75	6.36	4.70	6.25	3.57	3.82	4.35	4.54	4.49	4.76	0.96
CaO	13.58	10.20	9.72	15.70	8.25	7.11	8.54	7.74	7.52	9.82	2.96
Na2O	1.87	3.38	2.70	2.79	2.05	2.52	3.87	3.99	3.11	2.92	0.74
K2O	3.30	2.14	2.43	0.30	5.11	4.65	2.12	1.48	1.36	2.54	1.56
K2O/Na2O	1.76	0.63	0.90	0.11	2.49	1.85	0.55	0.37	0.44	1.01	0.82
P2O5	0.12	0.05	0.27	0.27	0.27	0.23	0.15	0.17	0.17	0.19	0.08
CO2	0.14	0.07	0.14	0.43	0.63	0.14	0.14	0.56	0.21	0.27	0.21
FeO	5.02	5.31	7.77	4.16	6.70	4.87	6.01	5.66	6.29	5.75	1.08
Fe2O3	0.11	0.67	0.33	0.23	0.21	0.11	0.01	0.08	0.67	0.27	0.25
Fe2O3/Feo	0.02	0.13	0.04	0.06	0.03	0.02	0.00	0.01	0.11	0.05	0.05
LOI	0.72	1.58	2.26	1.50	2.00	1.25	2.01	1.21	1.22	1.53	0.49
Sum	99.49	99.29	98.32	99.22	98.09	98.48	97.61	99.61	99.46	98.84	0.73
Au	62	83	<10	56	126	44	38	114	<10	59	43
Ag	<10	<10	<10	<10	<10	<10	<10	<10	<10	5	-
Cu	106	220	102	52	98	230	490	43	44	154	144
Pb	21	24	15	45	31	15	31	14	5	22	12
Zn	123	126	75	143	124	57	147	59	63	102	38
Co	27	28	32	21	31	26	25	27	27	27	3
Ni	19	38	29	19	11	10	11	12	10	18	10
Cr	73	105	59	57	28	16	33	26	33	48	28
Hg	<10	<10	<10	<10	<10	<10	<10	<10	<10	5	-
As	13.3	660.0	12.4	9.3	9.3	66.0	8.2	44.4	16.9	93	213
Sb	2.9	2.1	3.6	3.5	1.7	2.6	2.5	2.1	1.5	3	1
Ba	1944	803	1544	146	3203	3039	1520	941	623	1529	1052
Sr	579	612	605	1068	642	596	868	688	578	693	167
Rb	64	76	78	11	102	102	54	1282	34	200	407
Y	18	15	19	23	24	22	17	107	15	29	29
Zr	71	55	55	60	94	81	59	314	63	95	83
Nb	<3	<3	<3	<3	<3	<3	<3	7	<3	2	2
U	<2	2	<2	9	7	1	1	<2	2	3	3
Th	21	19	26	28	30	21	25	87	33	32	21

***Note:** half the value of the detection limit (e.g., 1.5 for <3) was used for calculating the mean and standard deviations.*

Fe2O3 = total iron as Fe2O3. Sum excludes CO2, FeO and Fe2O3*

Major element values in percent

Trace element values in ppm, except Au and Hg in ppb

APPENDIX 17A

MAJOR AND TRACE ELEMENT ANALYSES OF EXOSKARN SAMPLES COLLECTED FROM DDh's 195 AND 261: NICKEL PLATE DEPOSIT

Sample No.	261.01	261.02	261.06	261.07	261.08	261.09	261.10	261.12	261.13	261.14	261.15	261.15A	261.16	261.17	261.18
Depth (m)	2.70	7.90	42.70	54.60	61.00	73.20	81.10	90.20	97.50	103.60	111.60	111.80	115.80	121.90	125.00
SiO2	38.10	36.66	41.61	36.42	35.06	46.28	34.14	43.23	45.36	46.86	33.82	33.38	35.99	36.44	47.90
TiO2	0.27	0.13	0.57	0.16	0.18	0.17	0.33	0.36	0.20	0.37	0.11	0.12	0.26	0.20	0.26
Al2O3	8.03	9.26	5.71	7.16	7.63	2.77	3.99	7.19	3.65	4.19	2.23	1.99	6.91	3.66	5.42
Fe2O3*	17.46	14.88	16.79	17.53	15.27	12.20	11.90	17.64	17.85	19.42	13.43	15.02	14.60	12.71	13.41
MnO	0.37	0.32	0.60	0.27	0.29	0.47	0.48	0.61	0.76	0.74	0.46	0.47	0.35	0.40	0.35
MgO	1.31	0.44	2.36	0.77	0.84	1.94	2.02	2.13	3.88	4.12	1.57	1.55	2.20	1.55	2.40
CaO	32.43	33.73	28.61	34.20	34.27	27.04	31.83	26.13	23.94	22.75	26.89	27.13	21.83	27.20	20.52
Na2O	0.06	0.05	0.04	0.01	0.01	0.01	0.41	0.06	0.14	0.31	0.01	0.01	0.22	0.01	0.27
K2O	0.05	0.80	0.02	0.33	0.71	0.64	0.93	1.27	0.60	0.45	0.81	0.61	2.47	1.80	1.26
P2O5	0.31	0.13	0.08	0.11	0.13	0.25	0.21	1.07	0.30	0.23	0.41	0.39	0.08	0.30	0.28
FeO	4.56	2.34	11.55	2.39	3.05	10.18	10.24	13.08	15.10	16.34	11.44	13.10	12.87	9.47	11.54
Fe2O3	12.39	12.28	3.95	14.87	11.88	0.89	0.52	3.10	1.07	1.26	0.72	0.46	0.30	2.19	0.59
Fe2O3/FeO	2.72	5.25	0.34	6.22	3.90	0.09	0.05	0.24	0.07	0.08	0.06	0.04	0.02	0.23	0.05
LOI	2.80	4.67	4.42	4.09	5.84	9.14	14.05	1.28	2.26	0.95	19.51	17.85	13.92	14.53	6.29
Sum	101.19	101.07	100.81	101.05	100.23	100.91	100.29	100.97	98.94	100.39	99.25	98.00	98.83	98.80	98.36
K2O/Na2O	0.83	16.00	0.50	33.00	71.00	64.00	2.27	21.17	4.29	1.45	81.00	61.00	11.23	180.00	4.67
Au	710	330	34	34	57	34	22	300	135	350	71	320	130	330	300
Ag	<10	<10	<10	<10	<10	<10	<10	<10	<10	<10	<10	<10	<10	<10	<10
Cu	9	5	5	12	8	7	4	68	30	50	59	71	66	2400	92
Pb	3	5	3	<3	4	3	10	3	7	21	8	6	8	<3	7
Zn	69	41	187	43	39	91	111	97	167	149	60	63	64	141	52
Co	14	14	11	8	8	10	8	16	14	20	9	12	10	19	19
Ni	11	10	21	4	6	21	14	16	25	35	33	37	30	46	34
Cr	69	<25	<25	<25	27	92	69	72	78	56	42	49	29	91	89
As	<10	126	<10	<10	<10	<10	<10	108	<10	241	20	25	20	132	78
Sb	<10	<10	<10	<10	<10	<10	<10	<10	<10	15	<10	<10	<10	10	12
Ba	<100	242	<100	188	324	<100	405	1248	398	242	<100	<100	507	1132	117
Sr	55	124	115	79	145	209	388	209	189	347	500	520	431	352	531
Rb	9	26	19	18	30	49	32	53	27	21	28	32	70	48	43
Y	10	12	29	5	12	10	26	25	5	29	11	7	20	14	7
Zr	43	24	138	24	32	42	70	69	41	101	22	24	91	40	50
Nb	<3	<3	<3	<3	<3	<3	<3	<3	<3	<3	<3	<3	<3	<3	<3
U	1	<2	<2	<2	<2	<2	<2	<2	<2	3	<2	<2	<2	<2	<2
Th	24	16	19	16	25	18	18	17	19	23	24	25	25	19	31

Appendix 17A (Continued)

Sample No.	261.19	261.20	261.21	261.22	261.23	195.01	195.03	195.07	195.08	195.09	195.11	195.12	195.13	Mean	Stdev.
Depth (m)	127.40	129.50	131.70	137.20	140.20	9.10	21.30	56.40	53.90	61.00	68.90	72.20	75.30	-	-
SiO2	44.46	36.67	48.82	39.84	32.57	53.22	66.04	48.93	44.50	41.92	46.44	42.94	52.51	42.50	7.55
TiO2	0.41	0.27	0.22	0.41	0.17	0.28	0.38	0.15	0.31	0.30	0.19	0.24	0.26	0.26	0.11
Al2O3	6.39	5.15	4.64	6.39	3.32	3.89	7.52	3.01	6.10	7.60	3.77	6.47	5.42	5.34	1.94
Fe2O3*	16.97	9.84	6.72	8.13	2.88	12.53	9.36	14.89	13.33	11.78	12.99	14.96	11.82	13.44	3.69
MnO	0.35	0.35	0.22	0.22	0.14	0.58	0.26	0.71	0.59	0.50	0.59	0.48	0.48	0.44	0.16
MgO	2.91	2.67	1.53	3.46	2.01	5.03	2.36	5.77	3.27	3.35	6.03	4.04	6.73	2.79	1.62
CaO	16.44	27.16	22.51	23.71	39.64	22.18	9.18	25.30	27.12	31.31	27.27	25.05	20.50	26.28	6.08
Na2O	0.21	0.01	0.01	0.12	0.01	0.30	0.62	0.13	0.22	0.10	0.21	0.12	0.83	0.16	0.20
K2O	2.54	1.10	1.50	3.09	1.37	1.01	3.90	1.34	0.98	1.20	1.35	1.32	1.25	1.24	0.87
P2O5	0.26	0.43	0.36	0.32	0.26	0.31	0.31	0.42	0.34	0.40	0.38	0.26	0.23	0.31	0.18
FeO	13.69	7.57	5.22	4.26	2.29	11.15	8.09	12.17	8.89	5.92	9.53	8.31	10.00	9.08	4.02
Fe2O3	1.76	1.43	0.92	3.40	0.34	0.14	0.37	1.36	3.45	5.20	2.40	5.72	0.71	3.35	4.24
Fe2O3/FeO	0.13	0.19	0.18	0.80	0.15	0.01	0.05	0.11	0.39	0.88	0.25	0.69	0.07	0.21*	0.25*
LOI	7.36	10.55	7.86	11.25	15.65	0.26	0.29	0.00	3.27	1.96	1.48	2.12	0.07	6.53	5.96
Sum	98.30	94.20	94.39	96.94	98.02	99.59	100.22	99.86	100.03	100.42	100.70	98.00	100.10	99.28	1.82
K2O/Na2O	12.10	110.00	150.00	25.75	137.00	3.37	6.29	10.31	4.45	12.00	6.43	11.00	1.51	37.24	50.78
Au	300	2400	2220	700	68	42	73	4126	33706	10463	14733	86654	365	5679.00	17319.00
Ag	<10	<10	<10	<10	<10	<0.5	<0.5	<0.5	2.0	0.8	1.0	2.0	0.5	4.00	2.00
Cu	490	180	27	130	26	15	55	6	4	64	14	90	189	149.00	452.00
Pb	3	9	33	9	6	12	49	8	8	6	5	20	15	10.00	10.00
Zn	67	134	41	44	54	206	128	218	173	121	176	118	163	108.00	56.00
Co	19	82	71	50	8	7	34	72	610	113	405	767	52	89.00	187.00
Ni	35	99	40	25	38	-	-	-	-	-	-	-	-	29.00	20.00
Cr	64	81	92	53	58	-	-	-	-	-	-	-	-	57.00	27.00
As	255	2400	2700	7500	1500	19	170	3000	1000	6700	7000	33200	1300	2412.00	6431.00
Sb	10	16	18	<10	<10	4	3	41	2	28	20	10	5	9.00	9.00
Ba	384	421	769	2850	788	-	-	-	-	-	-	-	-	513.00	653.00
Sr	504	720	444	826	798	-	-	-	-	-	-	-	-	374.00	235.00
Rb	87	9	19	50	23	-	-	-	-	-	-	-	-	35.00	20.00
Y	10	36	15	22	11	-	-	-	-	-	-	-	-	16.00	9.00
Zr	51	43	52	66	34	-	-	-	-	-	-	-	-	53.00	30.00
Nb	<3	<3	<3	<3	<3	-	-	-	-	-	-	-	-	2.00	0.00
U	<2	8	<2	1	<2	-	-	-	-	-	-	-	-	1.00	2.00
Th	21	17	17	4	18	-	-	-	-	-	-	-	-	20.00	5.00

Note: half the value of the detection limit (e.g., 1.5 for <3) was used for calculating the mean and stdev.

The mean and stdev. for the Fe2O3/FeO ratios does not include the five (261.01-261.08) upper most oxidized samples in drill hole 261.

Major element values in percent: - = element not analyzed

Trace element values in ppm except Au in ppb

APPENDIX 17B

MAJOR AND TRACE ELEMENT ANALYSES OF ENDOSKARN SAMPLES COLLECTED FROM DDH's 195 AND 261: NICKEL PLATE DEPOSIT

Sample No.	261.03	261.04	261.05	261.11	261.25	261.27	195.02	195.04	195.05	195.06	195.10	195.14	Mean	Stdev.
Depth (m)	13.70	23.20	33.50	75.90	156.70	161.50	15.20	27.70	39.60	33.50	63.10	76.50	-	-
SiO2	59.23	61.24	63.55	57.32	59.96	55.50	71.65	54.78	55.02	55.68	55.51	56.02	58.79	4.93
TiO2	0.44	0.46	0.46	0.54	0.50	0.70	0.21	0.65	0.60	0.62	0.55	0.50	0.52	0.13
Al2O3	16.63	16.94	17.29	18.29	16.24	18.09	14.83	17.71	17.80	17.99	14.90	17.90	17.05	1.19
Fe2O3*	2.99	2.60	1.56	3.11	4.60	3.99	2.33	6.18	5.13	1.80	4.51	2.61	3.45	1.42
MnO	0.09	0.06	0.04	0.09	0.06	0.07	0.05	0.06	0.05	0.04	0.18	0.10	0.07	0.04
MgO	2.10	2.60	2.19	3.18	3.07	3.52	0.65	4.07	3.78	4.12	4.92	2.98	3.10	1.13
CaO	6.67	7.18	7.64	8.67	7.20	9.55	2.21	9.44	10.57	12.77	13.37	9.14	8.70	2.94
Na2O	1.73	3.75	4.37	5.24	3.66	3.41	5.14	3.53	3.50	3.50	2.62	2.86	3.61	0.99
K2O	9.88	3.84	2.94	2.05	2.25	3.49	1.47	1.92	2.32	1.86	2.66	5.33	3.33	2.32
K2O/Na2O	5.71	1.02	0.67	0.39	0.61	1.02	0.29	0.54	0.66	0.53	1.02	1.86	1.19	1.48
P2O5	0.12	0.11	0.12	0.14	0.13	0.18	0.09	0.19	0.18	0.18	0.13	0.16	0.14	0.03
CO2	0.21	0.36	0.14	0.48	1.03	0.72	0.15	0.18	0.15	0.15	0.64	0.99	0.43	0.34
FeO	2.57	2.14	1.36	2.63	3.97	3.36	1.89	5.11	4.33	1.58	3.58	2.18	2.89	1.17
Fe2O3	0.13	0.22	0.05	0.19	0.19	0.26	0.23	0.50	0.32	0.04	0.53	0.19	0.24	0.15
Fe2O3/FeO	0.05	0.10	0.04	0.07	0.05	0.08	0.12	0.10	0.07	0.03	0.15	0.09	0.08	0.04
LOI	0.59	0.70	0.65	1.01	1.32	1.42	0.79	1.22	1.07	1.16	0.71	1.50	1.01	0.32
Sum	100.47	99.48	100.81	99.64	98.99	99.92	99.42	99.75	100.02	99.72	100.06	99.10	99.78	0.52
Au	300	25	45	340	13	21	19	29	22	35	5070	29	496	1445
Ag	<10	<10	<10	<10	<10	<10	<0.5	0.5	0.6	<0.5	<0.5	0.0	3	2
Cu	5	6	4	235	210	156	2	180	274	18	4	7	92	109
Pb	18	7	12	16	8	13	9	11	18	25	8	166	26	44
Zn	53	32	40	54	30	31	28	49	44	52	63	135	51	29
Co	31	25	25	27	40	22	2	22	15	18	8	9	20	11
Ni	8	7	6	4	12	7	-	-	-	-	-	-	7	3
Cr	<25	<25	<25	47	51	26	-	-	-	-	-	-	27	18
As	649	18	<10	44	280	79	14	72	114	356	61	114	151	190
Ba	4700	2050	1700	847	1652	2200	-	-	-	-	-	-	2192	1316
Sr	850	729	816	804	803	1128	-	-	-	-	-	-	855	139
Rb	217	76	43	88	33	71	-	-	-	-	-	-	88	67
Y	10	9	9	7	13	13	-	-	-	-	-	-	10	2
Zr	71	67	80	57	77	67	-	-	-	-	-	-	70	8
Nb	<3	<3	<3	<3	<3	<3	-	-	-	-	-	-	2	0
U	<2	<2	<2	<2	<2	3	-	-	-	-	-	-	1	1
Th	18	19	19	29	24	21	-	-	-	-	-	-	22	4

Note: half the value of the detection limit (e.g., 1.5 for <3) was used for calculating mean and standard deviations. Sum excludes CO2, FeO and Fe2O3.

Major element values in percent; - = element not analyzed

Trace element values in ppm, except Au in ppb

APPENDIX 18A

REPRESENTATIVE CORE-TO-RIM MICROPROBE ANALYSES OF EXOSKARN GARNETS: FRENCH DEPOSIT

HD 170-2A (Garnet vein cutting biotite hornfels)

	Core									*Rim*
	1	*2*	*3*	*4*	*5*	*6*	*7*	*8*	*9*	*10*
SiO2	37.89	37.69	37.84	37.70	38.12	38.09	37.88	37.77	37.89	37.54
TiO2	0.20	0.17	0.32	0.44	0.53	0.48	0.48	0.31	0.49	0.40
Al2O3	17.51	17.85	17.65	18.16	18.45	18.38	18.31	17.41	16.81	16.56
Fe2O3	6.26	5.80	6.09	5.10	4.76	4.93	4.92	6.27	7.09	7.34
MgO	0.12	0.12	0.16	0.20	0.21	0.18	0.21	0.15	0.08	0.09
CaO	35.08	35.03	34.74	34.74	35.02	35.14	34.94	33.73	33.69	33.63
MnO	0.18	0.35	0.42	0.27	0.31	0.27	0.37	0.59	0.41	0.37
FeO	0.82	1.08	1.45	1.53	1.22	1.14	1.20	2.14	2.49	2.38
Total	98.06	98.09	98.67	98.14	98.62	98.61	98.31	98.37	98.95	98.31
Cations										
Si	5.9548	5.9258	5.9258	5.9155	5.9341	5.9342	5.9233	5.9436	5.9484	5.9385
Ti	0.0241	0.0199	0.0378	0.0521	0.0620	0.0563	0.0567	0.0370	0.0574	0.0476
Al	3.2433	3.3079	3.2575	3.3588	3.3884	3.3744	3.3751	3.2286	3.1107	3.0868
Fe+3	0.7400	0.6865	0.7170	0.6022	0.5574	0.5776	0.5690	0.7428	0.8370	0.8739
Mg	0.0282	0.0279	0.0395	0.0465	0.0481	0.0423	0.0486	0.0349	0.0189	0.0210
Ca	5.9074	5.8999	5.8280	5.8407	5.8415	5.8654	5.8542	5.6868	5.6665	5.6986
Mn	0.0243	0.0476	0.0553	0.0361	0.0403	0.0350	0.0495	0.0784	0.0552	0.0518
Fe+2	0.1074	0.1425	0.1894	0.2002	0.1592	0.1482	0.1567	0.2816	0.3264	0.3153
Total	16.0295	16.0571	16.0492	16.0520	16.0310	16.0335	16.0430	16.0337	16.0204	16.0335

HD 267-1A (Garnet in ore zone)

	Core							*Rim*
	1	*2*	*3*	*4*	*5*	*6*	*7*	*8*
SiO2	34.57	34.58	34.76	35.11	35.14	35.08	34.89	35.10
TiO2	0.00	0.00	0.00	0.00	0.00	0.00	0.02	0.02
Al2O3	0.05	0.05	0.00	0.24	0.12	0.11	0.05	0.00
Fe2O3	29.77	30.75	30.60	30.72	30.71	30.81	30.70	30.41
MgO	0.00	0.00	0.00	0.02	0.01	0.01	0.01	0.00
CaO	32.71	32.88	32.95	33.17	33.01	32.99	32.89	33.00
MnO	0.16	0.11	0.22	0.07	0.13	0.09	0.10	0.09
FeO	0.00	0.00	0.00	0.00	0.00	0.00	0.00	0.00
Total	97.26	98.37	98.53	99.33	99.12	99.09	98.66	98.62
Cations								
Si	6.0112	5.9589	5.9782	5.9784	5.9968	5.9889	5.9862	6.0174
Ti	0.0000	0.0000	0.0000	0.0000	0.0000	0.0001	0.0020	0.0029
Al	0.0109	0.0093	0.0002	0.0478	0.0238	0.0230	0.0101	0.0001
Fe+3	3.8953	3.9882	3.9597	3.9363	3.9434	3.9581	3.9638	3.9222
Mg	0.0000	0.0001	0.0001	0.0041	0.0016	0.0027	0.0023	0.0012
Ca	6.0944	6.0702	6.0719	6.0529	6.0353	6.0342	6.0464	6.0615
Mn	0.0238	0.0156	0.0319	0.0099	0.0186	0.0135	0.0139	0.0131
Fe+2	0.0000	0.0000	0.0000	0.0000	0.0000	0.0000	0.0000	0.0000
Total	16.0357	16.0423	16.0419	16.0295	16.0196	16.0204	16.0248	16.0185

HD 267-2B (Garnet in ore zone)

	Core							*Rim*
	1	*2*	*3*	*4*	*5*	*6*	*7*	*8*
SiO2	35.14	35.09	35.18	34.97	34.87	35.13	34.39	34.42
TiO2	0.08	0.01	0.00	0.09	0.04	0.02	0.00	0.03
Al2O3	3.06	2.75	2.36	2.75	2.68	3.39	0.01	0.01
Fe2O3	26.42	26.79	27.80	27.20	27.12	26.06	30.90	30.62
MgO	0.07	0.07	0.00	0.05	0.00	0.04	0.00	0.01
CaO	32.74	32.93	32.73	33.47	33.16	33.25	33.16	33.06
MnO	0.34	0.36	0.35	0.33	0.17	0.35	0.13	0.14
FeO	0.06	0.00	0.62	0.15	0.34	0.00	0.00	0.00
Total	97.91	98.00	99.04	99.01	98.38	98.24	98.59	98.29
Cations								
Si	5.9743	5.9727	5.9553	5.9121	5.9299	5.9493	5.9234	5.9415
Ti	0.0100	0.0019	0.0000	0.0115	0.0061	0.0037	0.0000	0.0044
Al	0.6139	0.5514	0.4700	0.5468	0.5383	0.6784	0.0027	0.0011
Fe+3	3.3807	3.4150	3.5399	3.4600	3.4705	3.3216	4.0060	3.9776
Mg	0.0172	0.0172	0.0000	0.0138	0.0000	0.0100	0.0050	0.0034
Ca	5.9640	6.0068	5.9362	6.0613	6.0410	6.0332	6.1205	6.1156
Mn	0.0492	0.0524	0.0503	0.0472	0.0249	0.0508	0.0191	0.0212
Fe+2	0.0090	0.0000	0.0879	0.0203	0.0488	0.0000	0.0000	0.0000
Total	16.0183	16.0174	16.0396	16.0730	16.0595	16.0470	16.0767	16.0648

Major element values in percent

APPENDIX 18B

REPRESENTATIVE CORE-TO-RIM ANALYSES OF EXOSKARN CLINOPYROXENE CRYSTALS: FRENCH DEPOSIT

HD 170-1A

	Core									*Rim*
	1	*2*	*3*	*4*	*5*	*6*	*7*	*8*	*9*	*10*
SiO2	48.66	48.33	48.16	48.24	48.69	48.46	48.47	48.02	48.46	48.60
TiO2	0.05	0.05	0.04	0.02	0.00	0.02	0.01	0.03	0.03	0.03
Al2O3	0.49	0.54	0.35	0.21	0.22	0.25	0.27	0.27	0.32	0.32
Cr2O3	0.00	0.02	0.00	0.00	0.03	0.03	0.00	0.00	0.00	0.01
Fe2O3	2.29	2.76	2.84	2.16	1.60	2.16	2.10	2.94	1.80	1.40
MgO	5.73	5.71	5.41	5.32	5.27	5.38	5.19	5.40	5.28	5.08
CaO	23.13	23.14	23.20	23.08	23.28	23.13	23.31	23.29	22.96	23.34
MnO	0.54	0.49	0.56	0.62	0.56	0.64	0.53	0.55	0.63	0.60
FeO	17.56	17.17	17.48	17.83	18.25	17.85	18.12	17.21	18.25	18.27
Na2O	0.06	0.07	0.05	0.04	0.04	0.05	0.04	0.04	0.05	0.07
Total	98.51	98.28	98.09	97.52	97.94	97.97	98.04	97.75	97.78	97.72
	Cations									
Si	1.9545	1.9464	1.9492	1.9630	1.9716	1.9623	1.9629	1.9496	1.9663	1.9725
Ti	0.0016	0.0014	0.0011	0.0005	0.0000	0.0006	0.0004	0.0008	0.0008	0.0009
Al	0.0232	0.0258	0.0166	0.0102	0.0104	0.0117	0.0129	0.0129	0.0151	0.0154
Cr	0.0000	0.0007	0.0000	0.0000	0.0011	0.0009	0.0000	0.0000	0.0000	0.0004
Fe+3	0.0693	0.0837	0.0863	0.0661	0.0486	0.0658	0.0639	0.0898	0.0550	0.0428
Mg	*0.3433*	*0.3426*	*0.3262*	*0.3225*	*0.3178*	*0.3247*	*0.3134*	*0.3270*	*0.3194*	*0.3070*
Ca	0.9953	0.9985	1.0059	1.0061	1.0098	1.0033	1.0113	1.0132	0.9983	1.0150
Mn	0.0183	0.0166	0.0191	0.0215	0.0193	0.0219	0.0181	0.0189	0.0217	0.0207
Fe+2	0.5899	0.5784	0.5917	0.6066	0.6179	0.6045	0.6138	0.5844	0.6192	0.6201
Na	0.0046	0.0058	0.0037	0.0035	0.0034	0.0042	0.0034	0.0034	0.0043	0.0058
Total	4.0000	4.0000	4.0000	4.0000	4.0000	4.0000	4.0000	4.0000	4.0000	4.0000

	HD 170-1B						**HD 170-3C**					
	Core					*Rim*	*Core*					*Rim*
	1	*2*	*3*	*4*	*5*	*6*	*1*	*2*	*3*	*4*	*5*	*6*
SiO2	48.20	48.16	48.25	48.40	48.26	48.54	48.43	48.25	48.35	48.31	48.13	47.96
TiO2	0.08	0.08	0.05	0.06	0.03	0.20	0.05	0.07	0.51	0.03	0.05	0.06
Al2O3	0.70	0.61	0.57	0.58	0.31	0.31	0.52	0.57	0.61	0.66	0.59	1.31
Cr2O3	0.01	0.01	0.01	0.00	0.06	0.00	0.00	0.00	0.00	0.21	0.00	0.00
Fe2O3	2.87	1.49	2.42	2.45	3.02	2.52	2.50	2.15	2.46	1.95	2.31	1.88
MgO	5.63	5.31	5.46	5.52	5.20	5.30	5.58	5.66	5.59	5.70	5.72	5.64
CaO	23.17	23.06	23.20	23.24	23.40	23.31	23.48	23.18	23.42	23.15	23.28	23.53
MnO	0.45	0.37	0.42	0.45	0.57	0.61	0.38	0.41	0.40	0.40	0.41	0.39
FeO	17.10	17.85	17.53	17.41	17.51	17.88	17.25	17.21	17.14	17.21	16.81	16.39
Na2O	0.09	0.09	0.07	0.09	0.09	0.05	0.06	0.73	0.08	0.07	0.08	0.08
Total	98.30	97.03	97.98	98.20	98.45	98.72	98.25	98.23	98.56	97.69	97.38	97.24
	Cations						**Cations**					
Si	1.9410	1.9636	1.9507	1.9507	1.9479	1.9559	1.9507	1.9543	1.9497	1.9560	1.9517	1.9414
Ti	0.0024	0.0023	0.0014	0.0017	0.0009	0.0006	0.0015	0.0022	0.0016	0.0010	0.0017	0.0019
Al	0.0329	0.0295	0.0270	0.0277	0.0150	0.0147	0.0246	0.0271	0.0289	0.0316	0.0285	0.0627
Cr	0.0003	0.0003	0.0002	0.0000	0.0022	0.0002	0.0000	0.0000	0.0000	0.0007	0.0000	0.0000
Fe+3	0.0870	0.0456	0.0739	0.0744	0.0918	0.0766	0.0757	0.0657	0.0746	0.0594	0.0706	0.0573
Mg	0.3384	0.3225	0.3290	0.3319	0.3129	0.3172	0.3350	0.3418	0.3358	0.3441	0.3456	0.3406
Ca	0.9997	1.0075	1.0053	1.0039	1.0122	1.0064	1.0137	1.0060	1.0119	1.0045	1.0116	1.0206
Mn	0.0156	0.0128	0.0145	0.0155	0.0195	0.0210	0.0130	0.0142	0.0134	0.0138	0.0142	0.0135
Fe+2	0.5758	0.6086	0.5927	0.5869	0.5912	0.6027	0.5812	0.5829	0.5783	0.5829	0.5701	0.5551
Na	0.0069	0.0073	0.0054	0.0071	0.0065	0.0046	0.0047	0.0058	0.0060	0.0058	0.0060	0.0067
Total	4.0000	4.0000	4.0001	3.9998	4.0001	3.9999	4.0001	4.0000	4.0002	3.9998	4.0000	3.9998

APPENDIX 19A

REPRESENTATIVE CORE-TO-RIM MICROPROBE ANALYSES OF EXOSKARN GARNETS: CANTY DEPOSIT (see Figure 26C)

HD 54-2-1

	Core				*Rim*
	1	*2*	*3*	*4*	*5*
SiO2	37.06	36.96	37.90	37.99	37.20
TiO2	1.85	1.80	0.33	0.71	0.74
Al2O3	12.91	13.17	15.27	15.77	12.00
Fe2O3	11.25	11.01	9.68	8.60	13.68
MgO	0.05	0.03	0.01	0.03	0.00
CaO	34.61	34.70	34.36	34.60	34.32
MnO	0.72	0.74	0.88	1.10	0.87
FeO	0.47	0.80	1.36	0.91	0.32
Total	98.92	99.21	99.79	99.71	99.13
	Cations				
Si	5.9066	5.8802	5.9475	5.9416	5.9546
Ti	0.2221	0.2151	0.0394	0.0836	0.0891
Al	2.4251	2.4695	2.8245	2.9077	2.2635
Fe+3	1.3489	1.3182	1.1433	1.0123	1.6475
Mg	0.0112	0.0081	0.0017	0.0072	0.0000
Ca	5.9098	5.9141	5.7775	5.7985	5.8856
Mn	0.0975	0.0991	0.1164	0.1454	0.1175
Fe+2	0.0631	0.1068	0.1788	0.1184	0.0428
Total	15.9843	16.0111	16.0291	16.0147	16.0006

HD 54-1-1

	Core				*Rim*
	1	*2*	*3*	*4*	*5*
SiO2	36.61	36.79	36.38	36.79	37.11
TiO2	0.54	0.51	0.55	0.58	0.70
Al2O3	10.13	10.12	10.34	10.55	13.20
Fe2O3	16.18	16.36	15.92	15.84	11.95
MgO	0.06	0.06	0.04	0.05	0.01
CaO	33.37	33.62	33.67	33.78	34.16
MnO	0.67	0.64	0.67	0.63	0.91
FeO	0.67	0.54	0.77	0.94	0.87
Total	98.23	98.64	98.34	99.16	98.91
	Cations				
Si	5.9698	5.9731	5.9322	5.9422	5.9288
Ti	0.0667	0.0627	0.0671	0.0707	0.0842
Al	1.9476	1.9374	1.9867	2.0091	2.4853
Fe+3	1.9851	1.9988	1.9538	1.9251	1.4369
Mg	0.0148	0.0139	0.0096	0.0127	0.0030
Ca	5.8299	5.8489	5.8833	5.8463	5.8485
Mn	0.0926	0.0880	0.0931	0.0866	0.1231
Fe+2	0.0909	0.0731	0.1046	0.1272	0.1159
Total	15.9974	15.9959	16.0304	16.0199	16.0257

HD 669-8A

	Core							*Rim*
	1	*2*	*3*	*4*	*5*	*6*	*7*	*8*	*9*
SiO2	36.39	36.31	36.42	36.19	35.59	36.20	36.15	36.44	36.07
TiO2	0.02	0.02	0.04	0.07	0.07	0.07	0.19	0.25	0.36
Al2O3	12.21	12.48	12.62	12.70	13.06	12.67	12.22	11.84	9.44
Fe2O3	13.82	13.48	13.30	12.97	12.03	13.15	13.63	14.22	17.40
MgO	0.00	0.00	0.01	0.00	0.02	0.02	0.01	0.02	0.02
CaO	34.86	35.16	35.21	35.06	34.47	34.97	34.98	34.74	33.73
MnO	0.20	0.23	0.22	0.21	0.22	0.27	0.22	0.24	0.37
FeO	0.59	0.49	0.45	0.48	0.94	0.86	0.68	0.79	1.14
Total	98.09	98.17	98.27	97.68	96.40	98.21	98.08	98.54	98.53
	Cations								
Si	5.9009	5.8796	5.8851	5.8795	5.8550	5.8632	5.8690	5.8945	5.9109
Ti	0.0028	0.0023	0.0046	0.0082	0.0092	0.0089	0.0234	0.0309	0.0449
Al	2.3331	2.3819	2.4031	2.4323	2.5330	2.4178	2.3382	2.2578	1.8237
Fe+3	1.6859	1.6424	1.6173	1.5854	1.4890	1.6027	1.6650	1.7313	2.1462
Mg	0.0000	0.0011	0.0019	0.0007	0.0045	0.0040	0.0025	0.0042	0.0051
Ca	6.0570	6.1006	6.0967	6.1038	6.0753	6.0673	6.0844	6.0213	5.9217
Mn	0.0277	0.0316	0.0300	0.0286	0.0301	0.0370	0.0309	0.0331	0.0507
Fe+2	0.0796	0.0666	0.0615	0.0650	0.1287	0.1169	0.0927	0.1069	0.1560
Total	16.0869	16.1060	16.1001	16.1035	16.1248	16.1177	16.1061	16.0800	16.0593

Major element values in percent

APPENDIX 19B
REPRESENTATIVE CORE-TO-RIM MICROPROBE ANALYSES OF EXOSKARN CLINOPYROXENES: CANTY DEPOSIT

HD 669-3A

	Core				*Rim*
	1	*2*	*3*	*4*	*5*
SiO2	47.37	48.04	44.29	44.67	47.01
TiO2	0.07	0.06	0.03	0.02	0.06
Al2O3	0.50	0.54	1.53	4.27	0.87
Cr2O3	0.01	0.00	0.00	0.00	0.02
Fe2O3	3.50	3.58	7.69	3.61	3.85
MgO	3.43	5.29	5.53	4.42	4.43
CaO	22.58	23.03	22.97	21.65	22.71
MnO	0.51	0.70	0.63	0.60	0.64
FeO	20.37	17.16	12.45	16.27	17.53
Na2O	0.17	0.15	0.13	0.20	0.24
Total	98.51	98.55	95.25	95.71	97.36
	Cations				
Si	1.9385	1.9370	1.8463	1.8472	1.9267
Ti	0.0021	0.0019	0.0008	0.0005	0.0020
Al	0.0243	0.0256	0.0750	0.2083	0.0422
Cr	0.0002	0.0000	0.0000	0.0000	0.0008
Fe+3	0.1077	0.1085	0.2414	0.1124	0.1187
Mg	0.2091	0.3178	0.3438	0.2724	0.2706
Ca	0.9900	0.9948	1.0260	0.9593	0.9971
Mn	0.0178	0.0240	0.0221	0.0210	0.0221
Fe+2	0.6972	0.5787	0.4341	0.5627	0.6007
Na	0.0132	0.0118	0.0106	0.0162	0.0191
Total	4.0000	4.0000	4.0000	4.0000	4.0000

HD 54-2-2

	Core					*Rim*
	1	*2*	*3*	*4*	*5*	*6*
SiO2	49.94	49.19	49.78	50.08	49.51	49.77
TiO2	0.02	0.03	0.10	0.00	0.01	0.00
Al2O3	0.23	0.25	0.07	0.16	0.22	0.21
Fe2O3	0.00	0.26	0.78	0.53	0.83	0.48
MgO	4.10	2.56	4.52	4.39	4.87	4.50
CaO	22.96	22.83	23.26	22.99	22.95	23.10
MnO	1.22	1.41	1.30	1.31	1.41	1.03
FeO	20.93	23.07	20.20	20.87	19.11	20.20
Na2O	0.10	0.11	0.03	0.08	0.13	0.14
Total	99.50	99.71	100.04	100.41	99.04	99.43
	Cations					
Si	2.0021	1.9935	1.9875	1.9916	1.9869	1.9933
Ti	0.0007	0.0008	0.0003	0.0000	0.0003	0.0000
Al	0.0107	0.0121	0.0036	0.0074	0.0104	0.0099
Fe+3	0.0000	0.0080	0.0233	0.0159	0.0251	0.0144
Mg	0.2450	0.1549	0.2693	0.2603	0.2915	0.2687
Ca	0.9864	0.9916	0.9929	0.9797	0.9868	0.9911
Mn	0.0413	0.0484	0.0439	0.0443	0.0478	0.0350
Fe+2	0.7017	0.7820	0.6746	0.6943	0.6413	0.6766
Na	0.0075	0.0087	0.0026	0.0065	0.0099	0.0109
Total	3.9955	4.0000	4.0000	4.0000	4.0000	4.0000

HD 54-1-5

	Core				*Rim*
	1	*2*	*3*	*4*	*5*
SiO2	49.12	49.42	49.59	49.52	49.76
TiO2	0.01	0.00	0.00	0.03	0.01
Al2O3	0.19	0.24	0.24	0.16	0.17
Fe2O3	0.27	0.00	1.15	0.59	0.66
MgO	2.96	2.93	3.39	3.80	4.56
CaO	22.50	22.74	22.97	22.82	23.12
MnO	1.37	1.40	1.69	1.48	1.40
FeO	22.80	22.87	21.33	21.21	19.95
Na2O	0.10	0.07	0.16	0.11	0.08
Total	99.32	99.672	100.52	99.72	99.71
	Cations				
Si	1.9950	1.9985	1.9834	1.9906	1.9887
Ti	0.0003	0.0000	0.0000	0.0010	0.0004
Al	0.0091	0.0116	0.0115	0.0076	0.0081
Fe+3	0.0083	0.0000	0.0345	0.0179	0.0199
Mg	0.1791	0.1764	0.2023	0.2278	0.2719
Ca	0.9791	0.9851	0.9846	0.9829	0.9902
Mn	0.0472	0.0478	0.0574	0.0505	0.0475
Fe+2	0.7742	0.7734	0.7135	0.7129	0.6669
Na	0.0079	0.0058	0.0128	0.0087	0.0063
Total	4.0000	3.9986	4.0000	4.0000	4.0000

HD 54-2-3

	Core					*Rim*
	1	*2*	*3*	*4*	*5*	*6*
SiO2	49.09	49.05	50.12	48.94	49.14	49.96
TiO2	0.02	0.00	0.02	0.00	0.00	0.03
Al2O3	0.22	0.24	0.04	0.24	0.26	0.17
Fe2O3	0.36	0.00	0.49	0.71	0.79	1.08
MgO	2.76	2.40	4.87	1.67	3.22	4.43
CaO	22.59	22.58	23.04	22.41	22.75	23.12
MnO	1.52	1.34	1.22	1.61	1.41	1.32
FeO	22.80	23.53	20.35	24.46	21.93	20.51
Na2O	0.11	0.09	0.04	0.13	0.11	0.09
Total	99.47	99.23	100.19	100.17	99.61	100.71
	Cations					
Si	1.9931	1.9995	1.9925	1.9886	1.9863	1.9824
Ti	0.0005	0.0000	0.0006	0.0000	0.0000	0.0008
Al	0.0106	0.0113	0.0018	0.0113	0.0122	0.0081
Fe+3	0.0110	0.0000	0.0148	0.0218	0.0241	0.0322
Mg	0.1671	0.1461	0.2886	0.1010	0.1938	0.2620
Ca	0.9826	0.9864	0.9811	0.9802	0.9854	0.9828
Mn	0.0522	0.0461	0.0412	0.0555	0.0481	0.0445
Fe+2	0.7742	0.8021	0.6767	0.8312	0.7412	0.6807
Na	0.0088	0.0068	0.0028	0.0104	0.0089	0.0066
Total	4.0000	3.9983	4.0000	4.0000	4.0000	4.0000

Appendix 19B (Continued)

HD 54-2-4

	Core			*Rim*
	1	*2*	*3*	*4*
SiO2	49.89	49.48	49.97	49.95
TiO2	0.01	0.02	0.00	0.00
Al2O3	0.18	0.22	0.19	0.20
Fe2O3	0.79	0.05	0.99	0.20
MgO	4.24	4.06	4.38	4.62
CaO	23.07	22.80	23.10	22.90
MnO	1.42	1.17	1.48	1.23
FeO	20.62	21.07	20.34	20.46
Na2O	0.11	0.11	0.11	0.10
Total	100.33	98.98	100.56	99.66
	Cations			
Si	1.9879	1.9974	1.9852	1.9960
Ti	0.0004	0.0007	0.0000	0.0000
Al	0.0083	0.0106	0.0088	0.0094
Fe+3	0.0236	0.0014	0.0295	0.0062
Mg	0.2516	0.2556	0.2592	0.2749
Ca	0.9849	0.9860	0.9831	0.9805
Mn	0.0479	0.0399	0.0498	0.0418
Fe+2	0.6871	0.7112	0.6756	0.6838
Na	0.0084	0.0082	0.0087	0.0075
Total	4.0000	4.0000	4.0000	4.0000

APPENDIX 20A

REPRESENTATIVE CORE-TO RIM MICROPROBE ANALYSES OF EXOSKARN GARNETS: GOOD HOPE DEPOSIT

HD 797-114-123

	Core									*Rim*
	1	*2*	*3*	*4*	*5*	*6*	*7*	*8*	*9*	*10*
SiO2	36.91	36.95	37.23	37.09	37.10	36.94	37.05	37.19	37.40	37.21
TiO2	0.34	0.08	0.16	0.05	0.00	0.04	0.06	0.02	0.12	0.12
Al2O3	15.32	15.61	15.30	16.26	15.77	15.57	15.15	15.62	16.00	15.65
Fe2O3	8.97	8.86	9.01	8.07	8.73	8.97	9.24	8.86	8.19	8.70
MgO	0.00	0.01	0.01	0.01	0.02	0.02	0.02	0.02	0.01	0.06
CaO	32.94	33.14	32.25	32.71	33.16	33.24	32.75	33.13	32.97	32.44
MnO	1.60	1.87	1.60	2.08	1.77	1.67	1.59	1.62	1.79	1.76
FeO	1.95	1.54	1.95	2.27	1.58	1.66	1.27	1.41	1.25	2.04
Total	98.03	98.06	97.51	98.54	98.13	98.11	97.13	97.87	97.73	97.98
	Cations									
Si	5.9126	5.9115	5.9786	5.9018	5.9226	5.9087	5.9711	5.9462	5.9686	5.9481
Ti	0.0407	0.0092	0.0192	0.0056	0	0.0045	0.0068	0.0022	0.0139	0.0144
Al	2.8927	2.9433	2.8954	3.0499	2.9683	2.9361	2.8786	2.9432	3.0083	2.9487
Fe+3	1.0815	1.0661	1.0881	0.9657	1.0488	1.0792	1.1203	1.0662	0.9832	1.0468
Mg	0.0001	0.0031	0.0025	0.0035	0.0055	0.0053	0.0049	0.0051	0.0029	0.015
Ca	5.6535	5.6812	5.5482	5.5754	5.6726	5.6968	5.6552	5.6751	5.6361	5.5554
Mn	0.2173	0.2535	0.2171	0.2803	0.2397	0.2267	0.2164	0.2194	0.2417	0.2381
Fe+2	0.2612	0.2066	0.2614	0.3026	0.2112	0.2218	0.1694	0.1894	0.167	0.2732
Total	16.0596	16.0746	16.0105	16.0848	16.0688	16.0792	16.0227	16.0469	16.0217	16.0397

HD 797-134-143

	Core									*Rim*
	1	*2*	*3*	*4*	*5*	*6*	*7*	*8*	*9*	*10*
SiO2	37.57	37.85	37.36	37.40	37.08	37.65	37.29	37.48	37.62	37.27
TiO2	0.04	0.07	0.11	0.14	0.14	0.22	0.23	0.19	0.19	0.22
Al2O3	16.11	15.24	17.41	17.41	13.82	15.16	15.35	15.54	15.83	16.03
Fe2O3	8.38	9.65	6.25	6.23	11.33	9.69	9.24	9.12	8.61	8.37
MgO	0.03	0.00	0.01	0.03	0.01	0.02	0.02	0.00	0.05	0.00
CaO	32.66	32.63	32.58	32.47	32.35	33.43	33.38	33.41	32.66	32.96
MnO	2.24	2.04	2.43	2.54	2.10	1.72	1.78	1.78	1.99	1.97
FeO	1.84	1.53	2.43	1.87	1.44	1.21	1.28	1.41	1.77	2.17
Total	98.87	99.01	98.58	98.09	98.27	99.10	98.57	98.93	98.72	98.99
	Cations									
Si	5.9397	5.9915	5.9066	5.9298	5.9631	5.9571	5.9319	5.9378	5.9606	5.9061
Ti	0.0042	0.0082	0.0129	0.0163	0.0169	0.0260	0.0275	0.0223	0.0229	0.0260
Al	3.0093	2.8435	3.2634	3.2538	2.6185	2.8272	2.8781	2.9018	2.9566	2.9943
Fe+3	0.9994	1.1492	0.7430	0.7437	1.3710	1.1535	1.1065	1.0873	1.0267	0.9976
Mg	0.0065	0.0009	0.0028	0.0067	0.0029	0.0055	0.0046	0.0001	0.0109	0.0004
Ca	5.5475	5.5344	5.5020	5.5155	5.5740	5.6673	5.6894	5.6707	5.5454	5.5953
Mn	0.3013	0.2741	0.3249	0.3414	0.2860	0.2304	0.2398	0.2387	0.2676	0.2639
Fe+2	0.2438	0.2020	0.3216	0.2480	0.1930	0.1595	0.1704	0.1868	0.2340	0.2882
Total	16.0517	16.0039	16.0773	16.0552	16.0253	16.0264	16.0483	16.0454	16.0248	16.0719

Appendix 20A (Continued)

HD 797-94-103

	Core							*Rim*
	1	*2*	*3*	*4*	*5*	*6*	*7*	*8*
SiO2	37.28	37.47	36.82	37.52	37.55	37.20	37.90	37.88
TiO2	0.30	0.07	0.29	0.06	0.13	0.03	0.22	0.15
Al2O3	16.30	16.71	19.16	16.50	16.60	16.87	16.08	16.46
Fe2O3	7.59	7.28	2.48	7.50	7.47	6.83	8.28	7.85
MgO	0.04	0.05	0.01	0.02	0.02	0.00	0.03	0.03
CaO	32.65	31.95	22.57	32.44	32.71	31.56	32.63	32.69
MnO	2.43	2.91	6.67	2.65	2.22	2.65	1.96	2.11
FeO	1.29	1.73	8.76	1.08	1.60	2.27	1.82	1.82
Total	97.88	98.17	96.76	97.77	98.30	97.41	98.92	98.99
	Cations							
Si	5.9420	5.9547	5.9738	5.9749	5.9541	5.9543	5.9800	5.9685
Ti	0.0360	0.0078	0.0353	0.0076	0.0152	0.0040	0.0266	0.0177
Al	3.0622	3.1303	3.6634	3.0977	3.1017	3.1831	2.9913	3.0561
Fe+3	0.9107	0.8711	0.3032	0.8994	0.8917	0.8225	0.9836	0.9312
Mg	0.0097	0.0108	0.0023	0.0039	0.0050	0.0000	0.0061	0.0073
Ca	5.5750	5.4397	3.9234	5.5348	5.5560	5.4120	5.5166	5.5182
Mn	0.3283	0.3922	0.9170	0.3572	0.2980	0.3587	0.2622	0.2819
Fe+2	0.1717	0.2302	1.1892	0.1433	0.2124	0.3041	0.2396	0.2392
Total	16.0356	16.0368	16.0076	16.0189	16.0340	16.0388	16.0059	16.0201

Major element values in percent

APPENDIX 20B
REPRESENTATIVE CORE-TO-RIM MICROPROBE ANALYSES OF EXOSKARN CLINOPYROXENES: GOOD HOPE DEPOSIT

HD 382-1A

	Core						*Rim*
	1	*2*	*3*	*4*	*5*	*6*	*7*
SiO2	45.57	46.31	46.66	47.26	46.57	46.69	47.31
TiO2	0.01	0.04	0.00	0.00	0.03	0.07	0.03
Al2O3	0.09	0.06	0.08	0.12	0.17	0.17	0.39
Fe2O3	2.48	2.92	1.48	2.09	3.77	2.84	1.42
MgO	0.62	0.44	0.33	0.28	0.52	0.59	0.25
CaO	21.94	21.21	20.79	22.25	22.37	22.25	22.36
MnO	6.60	4.31	4.74	4.24	6.08	5.71	4.32
FeO	20.78	22.78	23.53	22.87	19.58	20.40	22.74
Na2O	0.05	0.06	0.05	0.08	0.09	0.04	0.08
Total	98.14	98.13	97.66	99.19	99.18	98.76	98.90
	Cations						
Si	1.9607	1.0536	1.9766	1.9676	1.9392	1.9503	1.9707
Ti	0.0004	0.0013	0.0000	0.0001	0.0009	0.0023	0.0009
Al	0.0045	0.0027	0.0038	0.0057	0.0085	0.0084	0.0190
Fe+3	0.0769	0.0926	0.0472	0.0654	0.1183	0.0894	0.0446
Mg	0.0382	0.0278	0.0206	0.0173	0.0322	0.0365	0.0154
Ca	0.9689	0.9589	0.9438	0.9922	0.9979	0.9956	0.9979
Mn	0.2302	0.1541	0.1700	0.1495	0.2144	0.2019	0.1525
Fe+2	0.7164	0.8038	0.8336	0.7961	0.6818	0.7126	0.7923
Na	0.0037	0.0052	0.0043	0.0063	0.0069	0.0030	0.0067
Total	3.9999	3.1000	3.9999	4.0002	4.0001	4.0000	4.0000

HD 382-4C

	Core						*Rim*
	1	*2*	*3*	*4*	*5*	*6*	*7*
SiO2	46.80	47.07	46.80	46.88	47.00	46.70	46.03
TiO2	0.00	0.01	0.02	0.05	0.00	0.07	0.00
Al2O3	0.16	0.29	0.17	0.15	0.17	0.16	0.14
Fe2O3	2.62	2.46	2.71	2.57	2.09	2.72	3.35
MgO	0.35	0.36	0.32	0.32	0.31	0.36	0.36
CaO	21.25	21.93	21.42	21.70	21.32	21.50	21.50
MnO	4.05	3.91	4.20	4.27	4.22	4.78	4.51
FeO	23.63	23.27	23.34	23.00	23.75	22.35	23.04
Na2O	0.08	0.07	0.08	0.09	0.07	0.11	0.10
Total	98.94	99.37	99.06	99.03	98.93	98.75	99.03
	Cations						
Si	1.9582	1.9568	1.9557	1.9579	1.9656	1.9555	1.9483
Ti	0.0000	0.0005	0.0007	0.0015	0.0000	0.0022	0.0000
Al	0.0080	0.0144	0.0084	0.0073	0.0085	0.0079	0.0068
Fe+3	0.0824	0.0768	0.0852	0.0808	0.0658	0.0858	0.1043
Mg	0.0216	0.0226	0.0202	0.0198	0.0193	0.0226	0.0222
Ca	0.9528	0.9767	0.9591	0.9713	0.9551	0.9646	0.9542
Mn	0.1434	0.1376	0.1487	0.1511	0.1495	0.1697	0.1582
Fe+2	0.8267	0.8091	0.8155	0.8033	0.8307	0.7825	0.7982
Na	0.0068	0.0056	0.0065	0.0070	0.0054	0.0092	0.0078
Total	3.9999	4.0001	4.0000	4.0000	3.9999	4.0000	4.0000

Appendix 20B (Continued)

HD 382-6A

	Core						*Rim*
	1	*2*	*3*	*4*	*5*	*6*	*7*
SiO2	46.90	47.17	46.70	46.98	47.52	46.56	47.40
TiO2	0.03	0.01	0.07	0.04	0.00	0.00	0.00
Al2O3	0.15	0.14	0.10	0.25	0.34	0.16	0.20
Fe2O3	1.51	1.33	3.68	2.66	2.57	2.76	1.64
MgO	0.53	0.55	0.51	0.52	0.48	0.63	0.51
CaO	21.48	21.38	21.71	21.62	22.33	21.98	21.81
MnO	3.57	3.64	3.97	3.79	3.83	3.46	3.71
FeO	23.82	24.10	22.61	23.34	23.20	22.49	23.64
Na2O	0.05	0.06	0.12	0.09	0.06	0.14	0.09
Total	98.04	98.38	99.47	99.29	100.33	98.18	99.00
	Cations						
Si	1.9735	1.9776	1.9425	1.9546	1.9544	1.9581	1.9732
Ti	0.0008	0.0003	0.0023	0.0012	0.0000	0.0000	0.0000
Al	0.0075	0.0071	0.0048	0.0121	0.0165	0.0079	0.0098
Fe+3	0.0477	0.0420	0.1152	0.0833	0.0794	0.0871	0.0513
Mg	0.0330	0.0342	0.0314	0.0323	0.0296	0.0390	0.0313
Ca	0.9683	0.9601	0.9678	0.9640	0.9841	0.9864	0.9727
Mn	0.1272	0.1292	0.1397	0.1336	0.1333	0.1226	0.1311
Fe+2	0.8383	0.8449	0.7865	0.8121	0.7978	0.7877	0.8230
Na	0.0037	0.0048	0.0098	0.0069	0.0048	0.0112	0.0076
Total	4.0000	4.0002	4.0000	4.0001	3.9999	4.0000	4.0000

HD 382-6B

	Core				*Rim*
	1	*2*	*3*	*4*	*5*
SiO2	46.59	46.81	46.63	46.62	46.65
TiO2	0.02	0.00	0.04	0.00	0.04
Al2O3	0.07	0.04	0.09	0.06	0.09
Fe2O3	1.72	2.45	2.31	2.69	2.18
MgO	0.55	0.53	0.54	0.55	0.60
CaO	20.90	21.14	21.23	20.86	20.81
MnO	3.77	3.63	3.61	3.52	3.53
FeO	23.76	24.00	23.60	24.24	24.01
Na2O	0.09	0.06	0.08	0.05	0.11
Total	97.47	98.66	98.13	98.59	98.02
	Cations				
Si	1.9737	1.9627	1.9634	1.9582	1.9663
Ti	0.0006	0.0000	0.0012	0.0000	0.0012
Al	0.0036	0.0020	0.0046	0.0029	0.0046
Fe+3	0.0548	0.0773	0.0729	0.0850	0.0693
Mg	0.0348	0.0332	0.0340	0.0344	0.0375
Ca	0.9484	0.9497	0.9577	0.9388	0.9400
Mn	0.1354	0.1289	0.1287	0.1251	0.1259
Fe+2	0.8416	0.8414	0.8309	0.8513	0.8463
Na	0.0070	0.0048	0.0066	0.0043	0.0089
Total	3.9999	4.0000	4.0000	4.0000	4.0000

APPENDIX 21A
REPRESENTATIVE CORE-TO-RIM MICROPROBE ANALYSES OF EXOSKARN GARNETS: PEGGY SKARN

HD 670-1A

	Core			*Rim*	
	1	*2*	*3*	*4*	*5*
SiO2	37.38	37.10	37.21	36.71	36.49
TiO2	0.00	0.00	0.00	0.03	0.75
Al2O3	12.95	11.22	12.40	10.22	9.64
Fe2O3	13.26	15.63	13.75	16.87	16.49
MgO	0.04	0.00	0.00	0.00	0.01
CaO	34.62	35.31	34.36	34.35	34.42
MnO	0.49	0.13	0.08	0.37	0.29
FeO	0.94	0.00	0.95	0.57	0.00
Total	99.68	99.39	98.75	99.12	98.09
	Cations				
Si	5.9419	5.9512	5.9715	5.9453	5.9618
Ti	0.0000	0.0000	0.0000	0.0041	0.0918
Al	2.4263	2.1213	2.3459	1.9510	1.8555
Fe+3	1.5867	1.8680	1.6605	2.0567	2.0273
Mg	0.0100	0.0000	0.0011	0.0000	0.0033
Ca	5.8962	6.0682	5.9076	5.9612	6.0255
Mn	0.0662	0.0174	0.0109	0.0511	0.0398
Fe+2	0.1245	0.0000	0.1278	0.0774	0.0000
Total	16.0517	16.0448	16.0253	16.0468	16.0050

HD 670-3A

	Core							*Rim*
	1	*2*	*3*	*4*	*5*	*6*	*7*	*8*
SiO2	35.67	36.32	36.52	36.42	36.47	37.11	36.96	36.62
TiO2	0.01	0.01	0.00	0.24	0.08	0.23	0.43	0.88
Al2O3	5.04	8.40	8.19	8.10	8.92	12.82	11.53	11.64
Fe2O3	23.48	19.08	18.48	19.39	18.45	12.88	14.20	13.94
MgO	0.00	0.02	0.01	0.01	0.01	0.00	0.01	0.01
CaO	34.09	33.73	34.48	34.17	33.96	33.92	34.44	34.53
MnO	0.04	0.04	0.00	0.27	0.54	0.61	0.45	0.43
FeO	0.00	0.32	0.00	0.00	0.05	1.12	0.00	0.70
Total	98.33	97.92	97.68	98.60	98.48	98.69	98.02	98.75
	Cations							
Si	5.9725	5.9907	6.0300	5.9756	5.9728	5.9550	5.9821	5.9054
Ti	0.0014	0.0011	0.0000	0.0299	0.0100	0.0277	0.0527	0.1062
Al	0.9955	1.6335	1.5946	1.5665	1.7219	2.4240	2.1990	2.2115
Fe+3	2.9587	2.3673	2.2967	2.3936	2.2730	1.5552	1.7292	1.6916
Mg	0.0000	0.0045	0.0190	0.0031	0.0028	0.0000	0.0032	0.0032
Ca	6.1149	5.9609	6.1011	6.0081	5.9574	5.8320	5.9728	5.9671
Mn	0.0060	0.0059	0.0000	0.0376	0.0744	0.0835	0.0623	0.0584
Fe+2	0.0000	0.0438	0.0000	0.0000	0.0074	0.1502	0.0000	0.0937
Total	16.0490	16.0078	16.0253	16.0145	16.0197	16.0277	16.0012	16.0369

HD 670-3C

	Core							*Rim*
	1	*2*	*3*	*4*	*5*	*6*	*7*	*8*
SiO2	35.34	35.65	35.99	35.78	35.81	36.17	36.05	36.45
TiO2	0.01	0.00	0.03	0.03	0.04	0.00	0.38	0.14
Al2O3	5.41	6.32	7.30	7.03	7.14	7.48	8.04	8.46
Fe2O3	22.53	21.30	20.58	20.86	20.74	20.82	18.56	18.61
MgO	0.00	0.00	0.01	0.00	0.00	0.02	0.00	0.01
CaO	33.87	33.72	33.94	33.60	33.73	34.39	34.16	34.18
MnO	0.10	0.08	0.00	0.04	0.08	0.05	0.33	0.44
FeO	0.00	0.00	0.00	0.22	0.16	0.44	0.00	0.00
Total	97.26	97.07	97.85	97.56	97.70	99.37	97.52	98.29
	Cations							
Si	5.9709	5.9953	5.9759	5.9713	5.9664	5.6308	5.9779	5.9816
Ti	0.0012	0.0000	0.0042	0.0035	0.0044	0.0002	0.0476	0.0167
Al	1.0765	1.2530	1.4286	1.3830	1.4026	1.4464	1.5722	1.6557
Fe+3	2.8641	2.6952	2.5720	2.6195	2.6000	2.5687	2.3164	2.2978
Mg	0.0000	0.0000	0.0017	0.0010	0.0000	0.0055	0.0000	0.0014
Ca	6.1307	6.0750	6.0373	6.0086	6.0212	6.0424	6.0691	6.0106
Mn	0.0144	0.0121	0.0000	0.0060	0.0112	0.0066	0.0470	0.0613
Fe+2	0.0000	0.0000	0.0000	0.0311	0.0221	0.0606	0.0000	0.0000
Total	16.0577	16.0306	16.0197	16.0240	16.0279	16.0614	16.0302	16.0250

HD 670-3B

	Core							*Rim*
	1	*2*	*3*	*4*	*5*	*6*	*7*	*8*
SiO2	35.59	36.16	36.54	36.14	36.85	36.84	37.37	36.59
TiO2	0.08	0.17	0.08	0.15	0.15	0.12	0.10	0.75
Al2O3	6.36	8.28	9.46	9.92	14.56	12.15	13.23	11.30
Fe2O3	21.42	18.99	17.37	16.34	10.18	13.83	12.43	14.07
MgO	0.00	0.03	0.00	0.00	0.00	0.00	0.00	0.02
CaO	33.89	33.85	34.39	34.00	34.00	34.39	34.31	33.55
MnO	0.06	0.01	0.04	0.03	0.65	0.33	0.46	0.44
FeO	0.00	0.06	0.00	0.00	1.18	0.56	0.60	0.58
Total	97.40	97.55	97.88	96.58	97.57	98.22	98.50	97.30
	Cations							
Si	5.9697	5.9849	5.9892	5.9839	5.9308	5.9526	5.9812	5.9735
Ti	0.0102	0.0207	0.0101	0.0185	0.0179	0.0140	0.0110	0.0919
Al	1.2573	1.6155	1.8282	1.9364	2.7622	2.3131	2.4954	2.1748
Fe+3	2.7039	2.3649	2.1425	2.0361	1.2333	1.6819	1.4965	1.7290
Mg	0.0000	0.0060	0.0007	0.0000	0.0000	0.0000	0.0011	0.0037
Ca	6.0900	6.0017	6.0396	6.0319	5.8618	5.9526	5.8832	5.8690
Mn	0.0083	0.0015	0.0052	0.0045	0.0885	0.0453	0.0062	0.0613
Fe+2	0.0000	0.0089	0.0000	0.0000	0.1592	0.0763	0.0809	0.0796
Total	16.0394	15.9981	16.0155	16.0113	16.0537	16.0358	15.9555	15.9828

Major element values in percent

APPENDIX 21B
REPRESENTATIVE CORE-TO-RIM MICROPROBE ANALYSES OF EXOSKARN CLINOPYROXENES: PEGGY SKARN
(see Figures 21L and N)

HD 670-2A

	Core							*Rim*
	1	*2*	*3*	*4*	*5*	*6*	*7*	*8*
SiO2	47.73	47.77	47.29	47.20	47.89	47.21	47.98	48.10
TiO2	0.00	0.00	0.00	0.00	0.01	0.01	0.00	0.00
Al2O3	0.06	0.09	0.08	0.14	0.08	0.05	0.14	0.13
Fe2O3	1.09	1.88	3.26	2.37	2.09	2.80	1.93	0.61
MgO	2.45	2.33	2.31	2.36	2.30	2.84	3.09	2.33
CaO	22.61	22.54	22.81	22.37	22.72	22.55	22.86	22.33
MnO	1.08	1.07	1.21	1.11	0.99	1.03	1.04	0.99
FeO	22.40	22.62	21.62	21.91	22.70	21.18	21.12	23.49
Na2O	0.05	0.08	0.08	0.12	0.08	0.06	0.09	0.06
Total	97.47	98.38	98.66	97.58	98.86	97.73	98.25	98.04
	Cations							
Si	1.9836	1.9719	1.9505	1.9641	1.9683	1.9573	1.9704	1.9896
Ti	0.0000	0.0001	0.0000	0.0000	0.0004	0.0003	0.0000	0.0000
Al	0.0031	0.0043	0.0040	0.0069	0.0040	0.0025	0.0066	0.0064
Fe+3	0.0342	0.0584	0.1012	0.0741	0.0648	0.0873	0.0596	0.0190
Mg	0.1520	0.1436	0.1420	0.1465	0.1409	0.1753	0.1893	0.1435
Ca	1.0065	0.9969	1.0081	0.9972	1.0006	1.0017	1.0057	0.9896
Mn	0.0379	0.0373	0.0423	0.0392	0.0345	0.0361	0.0361	0.0348
Fe+2	0.7784	0.7809	0.7455	0.7627	0.7802	0.7345	0.7252	0.8126
Na	0.0044	0.0067	0.0063	0.0093	0.0062	0.0050	0.0071	0.0045
Total	4.0001	4.0001	3.9999	4.0000	3.9999	4.0000	4.0000	4.0000

HD 670-2B

	Core			*Rim*
	1	*2*	*3*	*4*
SiO2	47.39	47.64	48.18	46.79
TiO2	0.00	0.00	0.00	0.04
Al2O3	0.10	0.13	0.09	0.11
Fe2O3	2.95	1.78	1.25	4.47
MgO	2.99	3.31	2.36	2.95
CaO	22.54	22.78	22.66	22.98
MnO	1.01	0.94	1.05	1.28
FeO	20.96	20.51	22.90	19.44
Na2O	0.10	0.09	0.09	0.12
Total	98.04	97.18	98.58	98.18
	Cations			
Si	1.9558	1.9726	1.9821	1.9315
Ti	0.0000	0.0000	0.0000	0.0012
Al	0.0050	0.0064	0.0042	0.0054
Fe+3	0.0917	0.0555	0.0387	0.1388
Mg	0.1839	0.2043	0.1446	0.1813
Ca	0.9967	1.0107	0.9987	1.0162
Mn	0.0353	0.0331	0.0366	0.0448
Fe+2	0.7234	0.7103	0.7879	0.6710
Na	0.0082	0.0071	0.0071	0.0096
Total	4.0000	4.0000	3.9999	3.9998

HD 670-3B

	Core					*Rim*
	1	*2*	*3*	*4*	*5*	*6*
SiO2	47.73	47.81	47.10	47.13	47.56	47.67
TiO2	0.00	0.01	0.01	0.00	0.00	0.01
Al2O3	0.11	0.08	0.07	0.08	0.27	0.18
Fe2O3	0.71	3.15	2.37	1.84	1.43	1.32
MgO	2.11	1.93	2.70	2.58	1.98	2.45
CaO	22.29	22.94	22.59	22.10	22.45	22.06
MnO	1.05	1.44	1.27	0.95	1.17	1.18
FeO	23.29	22.09	20.86	22.16	22.87	22.68
Na2O	0.09	0.17	0.09	0.07	0.11	0.11
Total	97.38	99.62	97.06	96.91	97.84	97.66
	Cations					
Si	1.9897	1.9560	1.9645	1.9719	1.9757	1.9792
Ti	0.0000	0.0004	0.0003	0.0000	0.0000	0.0003
Al	0.0055	0.0038	0.0036	0.0040	0.0131	0.0087
Fe+3	0.0222	0.0971	0.0744	0.0580	0.0446	0.0412
Mg	0.1310	0.1177	0.1680	0.1606	0.1228	0.1513
Ca	0.9956	1.0056	1.0094	0.9906	0.9994	0.9814
Mn	0.0370	0.0497	0.0447	0.0338	0.0411	0.0414
Fe+2	0.8119	0.7558	0.7275	0.7753	0.7945	0.7875
Na	0.0071	0.0138	0.0076	0.0058	0.0089	0.0089
Total	4.0000	3.9999	4.0000	4.0000	4.0001	3.9999

HD 670-3G

	Core						*Rim*
	1	*2*	*3*	*4*	*5*	*6*	*7*
SiO2	47.37	46.75	47.05	48.03	47.99	47.72	47.45
TiO2	0.00	0.01	0.01	0.02	0.00	0.00	0.02
Al2O3	0.10	0.12	0.13	0.08	0.18	0.20	0.10
Fe2O3	1.20	2.51	1.94	1.04	0.64	2.55	2.78
MgO	2.67	2.55	2.44	2.52	2.38	2.42	2.29
CaO	21.79	22.46	22.45	22.36	23.04	22.85	22.92
MnO	1.19	1.19	1.19	1.25	1.02	1.47	1.32
FeO	22.64	20.95	21.48	22.62	22.10	21.58	21.51
Na2O	0.03	0.10	0.10	0.09	0.11	0.09	0.10
Total	96.99	96.64	96.79	98.01	97.46	98.88	98.49
	Cations						
Si	1.9797	1.9610	1.9700	1.9847	1.9899	1.9593	1.9578
Ti	0.0001	0.0004	0.0005	0.0007	0.0000	0.0001	0.0006
Al	0.0051	0.0060	0.0062	0.0041	0.0087	0.0097	0.0047
Fe+3	0.0378	0.0791	0.0611	0.0323	0.0199	0.0787	0.0865
Mg	0.1662	0.1594	0.1524	0.1555	0.1469	0.1478	0.1408
Ca	0.9757	1.0091	1.0071	0.9900	1.0239	1.0052	1.0134
Mn	0.0420	0.0424	0.0421	0.0437	0.0358	0.0512	0.0461
Fe+2	0.7911	0.7348	0.7523	0.7819	0.7664	0.7409	0.7422
Na	0.0024	0.0078	0.0082	0.0072	0.0085	0.0071	0.0080
Total	4.0001	4.0000	3.9999	4.0001	4.0000	4.0000	4.0001

HD 670-2C

	Core				*Rim*
	1	*2*	*3*	*4*	*5*
SiO2	47.87	48.22	46.99	47.39	47.57
TiO2	0.00	0.01	0.00	0.00	0.04
Al2O3	0.11	0.12	0.07	0.11	0.09
Fe2O3	1.44	1.70	2.37	1.48	2.32
MgO	2.75	2.49	2.55	1.88	2.63
CaO	22.79	22.54	22.68	22.29	22.58
MnO	1.20	1.10	1.05	0.99	1.14
FeO	21.54	22.94	21.22	23.57	21.72
Na2O	0.09	0.06	0.07	0.04	0.09
Total	97.79	99.18	97.00	97.75	98.18

	Cations				
Si	1.9783	1.9731	1.9638	1.9757	1.9643
Ti	0.0000	0.0003	0.0000	0.0000	0.0011
Al	0.0054	0.0059	0.0035	0.0056	0.0043
Fe+3	0.0448	0.0525	0.0745	0.0464	0.0721
Mg	0.1692	0.1518	0.1586	0.1167	0.1617
Ca	1.0091	0.9883	1.0153	0.9954	0.9991
Mn	0.0420	0.0380	0.0371	0.0350	0.0399
Fe+2	0.7444	0.7851	0.7415	0.8217	0.7501
Na	0.0069	0.0051	0.0057	0.0035	0.0073
Total	4.0001	4.0001	4.0000	4.0000	3.9999

APPENDIX 22A

CORE (1) TO RIM (23) MICROPROBE ANALYSES OF A ZONED GARNET CRYSTAL, MOUNT RIORDAN SKARN; (see Figure 26I).

HD 680-1A

	Core				
	1	*2*	*3*	*4*	*5*
SiO2	35.23	35.16	35.03	35.15	35.07
TiO2	0.01	0.04	0.04	0.03	0.02
Al2O3	0.68	0.70	0.72	1.45	1.18
Fe2O3	30.30	30.34	29.90	29.06	29.36
MgO	0.02	0.03	0.02	0.01	0.02
CaO	32.86	32.96	32.38	32.26	32.33
MnO	0.32	0.39	0.28	0.39	0.32
FeO	0.06	0.27	0.18	0.91	0.55
Total	99.48	99.89	98.55	99.26	98.85
	Cations				
Si	5.9786	5.9517	5.9939	5.9664	5.9782
Ti	0.0000	0.0049	0.0057	0.0045	0.0022
Al	0.1359	0.1406	0.1453	0.2905	0.2368
Fe+3	3.8689	3.8647	3.8498	3.7120	3.7656
Mg	0.0052	0.0074	0.0063	0.0021	0.0065
Ca	5.9754	5.9775	5.9356	5.8675	5.9035
Mn	0.0456	0.0560	0.0408	0.0561	0.0470
Fe+2	0.0094	0.0380	0.0253	0.1288	0.0786
Total	16.0190	16.0408	16.0027	16.0279	16.0184
	Mole %				
And*	96.15	95.49	96.25	92.06	93.64
Gross*	2.85	2.85	2.54	4.84	4.17
PyAlSp*	1.00	1.66	1.21	3.10	2.19

	6	*7*	*8*	*9*	*10*
SiO2	35.31	35.33	35.31	35.52	35.32
TiO2	0.05	0.03	0.01	0.04	0.02
Al2O3	1.36	1.95	2.20	2.06	2.01
Fe2O3	29.15	28.37	28.03	28.32	28.43
MgO	0.02	0.03	0.02	0.02	0.03
CaO	32.27	32.76	32.79	32.80	32.75
MnO	0.46	0.28	0.37	0.36	0.33
FeO	0.54	0.39	0.36	0.35	0.72
Total	99.16	99.14	99.09	99.47	99.61
Si	5.9903	5.9754	5.9701	5.9829	5.9555
Ti	0.0065	0.0044	0.0017	0.0053	0.0024
Al	0.2729	0.3903	0.4384	0.4085	0.3998
Fe+3	3.7220	3.6103	3.5663	3.5894	3.6075
Mg	0.0041	0.0079	0.0061	0.0057	0.0077
Ca	5.8665	5.9358	5.9399	5.9199	5.9160
Mn	0.0659	0.0404	0.0526	0.0511	0.0477
Fe+2	0.0774	0.0554	0.0506	0.0500	0.1019
Total	16.0056	16.0199	16.0257	16.0128	16.0385
	Mole %				
And*	92.99	89.77	88.47	89.47	89.14
Gross*	4.55	8.51	9.72	8.76	8.26
PyAlSp*	2.46	1.72	1.81	1.77	2.60

Appendix 22A (Continued)

	11	*12*	*13*	*14*	*15*
SiO2	35.23	35.58	35.36	35.20	36.33
TiO2	0.01	0.03	0.02	0.34	0.01
Al2O3	2.05	2.11	2.14	2.37	5.81
Fe2O3	28.41	28.28	28.15	27.82	23.13
MgO	0.01	0.03	0.01	0.03	0.02
CaO	33.10	32.58	32.79	32.98	34.31
MnO	0.39	0.32	0.32	0.29	0.16
FeO	0.40	0.69	0.45	0.52	0.00
Total	99.60	99.62	99.24	99.55	99.77
	Cations				
Si	5.9423	5.9857	5.9712	5.9446	5.9734
Ti	0.0000	0.0034	0.0022	0.0043	0.0000
Al	0.4060	0.4192	0.4266	0.4720	1.1264
Fe+3	3.6060	3.5801	3.5774	3.5355	2.8622
Mg	0.0012	0.0072	0.0037	0.0080	0.0041
Ca	5.9828	5.8726	5.9340	5.9668	6.0443
Mn	0.0555	0.0457	0.0465	0.0423	0.0219
Fe+2	0.0568	0.0972	0.0631	0.0738	0.0000
Total	16.0506	16.0111	16.0247	16.0473	16.0323
	Mole %				
And	88.73	89.25	88.79	87.17	70.72
Gross	9.41	8.26	9.34	10.79	28.85
PyAlSp	1.86	2.49	1.87	2.04	0.43

	16	*17*	*18*	*19*	*20*
SiO2	36.65	36.79	36.99	36.86	36.83
TiO2	0.01	0.01	0.00	0.01	0.02
Al2O3	7.75	7.95	10.17	8.39	9.20
Fe2O3	19.84	20.06	17.13	19.64	18.46
MgO	0.02	0.00	0.00	0.01	0.02
CaO	34.43	34.75	34.67	34.25	33.15
MnO	0.31	0.27	0.51	0.49	1.10
FeO	0.00	0.00	0.07	0.00	1.34
Total	99.01	99.83	99.54	99.65	100.12
	Cations				
Si	6.0002	5.9762	5.9612	5.9834	5.9632
Ti	0.0019	0.0004	0.0000	0.0002	0.0020
Al	1.4959	1.5225	1.9316	1.6036	1.7560
Fe+3	2.4444	2.4518	2.0771	2.3995	2.2499
Mg	0.0040	0.0005	0.0000	0.0034	0.0043
Ca	6.0381	6.0474	5.9861	5.9569	5.7514
Mn	0.0434	0.0374	0.0691	0.0678	0.1511
Fe+2	0.0000	0.0000	0.0095	0.0000	0.1538
Total	16.0279	16.0362	16.0346	16.0148	16.0317
	Mole %				
And	60.29	60.45	51.37	59.71	55.73
Gross	38.93	38.93	47.33	39.11	39.17
PyAlSp	0.78	0.62	1.30	1.18	5.10

Appendix 22A (Continued)

			Rim
	21	*22*	*23*
SiO2	36.66	36.51	36.15
TiO2	0.01	0.04	0.05
Al2O3	9.13	8.09	6.85
Fe2O3	18.41	19.82	21.52
MgO	0.05	0.04	0.04
CaO	33.12	33.45	33.18
MnO	0.72	0.68	0.67
FeO	1.25	0.57	0.69
Total	99.35	99.20	99.15
	Cations		
Si	5.9657	5.9724	5.9616
Ti	0.0012	0.0049	0.0063
Al	1.7517	1.5601	1.3312
Fe+3	2.2546	2.4406	2.6704
Mg	0.0121	0.0089	0.0104
Ca	5.7747	5.8634	5.8629
Mn	0.1001	0.0940	0.0941
Fe+2	0.1700	0.0780	0.0946
Total	16.0301	16.0223	16.0315
	Mole %		
And*	55.86	60.67	66.22
Gross*	39.48	36.33	30.50
PyAlSp*	4.66	3.00	3.28

**And = andradite*

**Gross = grossularite*

**PyAlSp = pyrope + almandine + spessartine*

Major element values in percent

CORE (1) TO RIM (11) MICROPROBE ANALYSES OF A ZONED GARNET CRYSTAL, MOUNT RIORDAN SKARN

HD680-3A

	Core										*Rim*
	1	*2*	*3*	*4*	*5*	*6*	*7*	*8*	*9*	*10*	*11*
SiO2	34.98	35.17	35.00	36.05	35.53	34.67	35.45	35.09	36.77	36.35	36.37
TiO2	0.02	0.05	0.02	0.00	0.00	0.00	0.00	0.01	0.03	0.00	0.06
Al2O3	2.05	2.05	1.38	4.93	1.49	1.05	0.84	1.26	8.30	8.12	7.79
Fe2O3	28.20	28.07	28.98	24.17	29.05	29.42	29.62	29.27	19.59	19.57	20.31
MgO	0.08	0.08	0.04	0.05	0.02	0.02	0.02	0.03	0.00	0.02	0.05
CaO	32.33	32.11	32.66	33.87	33.34	33.44	33.20	33.14	33.87	32.51	33.35
MnO	0.39	0.35	0.15	0.19	0.13	0.06	0.15	0.13	0.36	1.31	0.74
FeO	1.09	0.88	0.17	0.00	0.00	0.00	0.00	0.00	0.31	0.66	0.88
Total	99.14	98.76	98.40	99.26	99.56	98.66	99.28	98.93	99.23	98.54	99.55
	Cations										
Si	5.9338	5.9729	5.9789	5.9835	5.9890	5.9300	6.0097	5.9665	5.9939	5.9890	5.9514
Ti	0.0037	0.0059	0.0027	0.0003	0.0000	0.0000	0.0006	0.0012	0.0029	0.0000	0.0071
Al	0.4103	0.4114	0.2773	0.9647	0.2978	0.2127	0.1675	0.2528	1.5951	1.5766	1.5017
Fe+3	3.6003	3.5880	3.7244	3.0189	3.6856	3.7863	3.7797	3.7640	2.4030	2.4259	2.5012
Mg	0.0210	0.0219	0.0107	0.0061	0.0068	0.0063	0.0054	0.0077	0.0000	0.0048	0.0100
Ca	5.8763	5.8439	5.9766	6.0230	6.0208	6.1262	6.0307	6.0396	5.9173	5.7395	5.8465
Mn	0.0563	0.1516	0.0218	0.0279	0.0192	0.0091	0.0224	0.0185	0.0494	0.1824	0.1023
Fe+2	0.1556	0.1358	0.0252	0.0000	0.0000	0.0000	0.0000	0.0000	0.0425	0.0916	0.1198
Total	16.0573	16.1314	16.0176	16.0244	16.0192	16.0706	16.0160	16.0503	16.0041	16.0098	16.0400
	Mole %										
And*	88.49	89.2	92.64	74.77	91.43	92.48	93.6	92.8	60.05	60.46	61.87
Gross*	7.7	7.5	6.4	24.57	8.14	7.27	5.95	6.8	38.42	34.99	34.31
PyAlSp*	3.81	3.3	0.96	0.66	0.43	0.25	0.45	0.4	1.53	4.55	3.82

**And = andradite*

**Gross = grossularite*

**PyAlSp = pyrope + almandine + spessartine*

Major element values in percent

APPENDIX 22B
CORE TO RIM MICROPROBE ANALYSES OF FOUR PYROXENE CRYSTALS, MOUNT RIORDAN SKARN (see Figure 21Q)

HD 343-2C				**HD 343-2D**		
	Core		*Rim*	*Core*		*Rim*
	1	*2*	*3*	*4*	*5*	*6*
SiO2	50.19	50.13	49.65	50.12	49.68	49.68
TiO2	0.02	0.01	0.03	0.05	0.01	0.01
Al2O3	0.35	0.65	0.27	0.22	0.25	0.53
Fe2O3	3.42	2.52	3.07	2.58	3.1	2.45
MgO	10.09	9.95	9.08	9.25	9.24	7.12
CaO	23.96	23.85	24.11	23.82	23.71	23.65
MnO	0.96	0.96	0.98	0.97	0.93	1.12
FeO	9.82	10.27	10.96	11.63	11.28	13.55
Na2O	0.12	0.09	0.08	0.07	0.07	0.13
Total	98.93	98.43	98.23	98.71	98.27	98.24
	Cations					**Cations**
Si	1.9459	1.9513	1.9503	1.9585	1.9507	1.9591
Ti	0.0007	0.0002	0.0011	0.0014	0.0003	0.0000
Al	0.0161	0.0298	0.0125	0.0099	0.0118	0.0245
Fe+3	0.0998	0.0740	0.0907	0.0758	0.0918	0.0667
Mg	0.5831	0.5778	0.5318	0.5392	0.5406	0.4537
Ca	0.9953	0.9945	1.0149	0.9974	0.9976	0.9991
Mn	0.0315	0.0315	0.0327	0.0322	0.0309	0.0405
Fe+2	0.3184	0.3342	0.3600	0.3802	0.3705	0.4470
Na	0.0091	0.0067	0.0060	0.0054	0.0057	0.0094
Total	3.9999	4.0000	4.0000	4.0000	3.9999	4.0000
	Mole %					
Diopside	56.46	56.78	52.37	52.49	52.29	45.01
Hedenbergite	40.49	40.11	44.38	44.38	44.73	50.97
Johannsenite	3.05	3.11	3.25	3.13	2.98	4.02

HD 343-2E				**HD 343-3C**		
	Core		*Rim*	*Core*		*Rim*
	7	*8*	*9*	*1*	*2*	*3*
SiO2	49.82	49.22	50.39	49.99	49.74	49.61
TiO2	0.02	0.00	0.01	0.00	0.00	0.00
Al2O3	0.18	0.27	0.40	0.32	0.32	0.49
Fe2O3	3.42	4.59	3.24	3.33	2.34	3.50
MgO	9.02	9.09	10.70	9.72	8.89	9.20
CaO	23.97	24.14	24.22	23.85	23.62	23.86
MnO	1.08	1.30	0.67	0.87	0.96	1.08
FeO	11.27	10.12	9.22	10.45	12.14	10.84
Na2O	0.09	0.06	0.05	0.11	0.06	0.96
Total	98.87	98.79	98.90	98.64	98.07	99.54
	Cations					**Cations**
Si	1.9485	1.9285	1.9456	1.9482	1.9599	1.9408
Ti	0.0005	0.0000	0.0000	0.0000	0.0000	0.0000
Al	0.0083	0.0127	0.0183	0.0149	0.0152	0.0229
Fe+3	0.1008	0.1353	0.0944	0.0976	0.0694	0.1028
Mg	0.5261	0.5307	0.6158	0.5650	0.5219	0.5356
Ca	1.0044	1.0137	1.0019	0.9960	0.9972	1.0002
Mn	0.0357	0.0431	0.0220	0.0289	0.0320	0.0357
Fe+2	0.3687	0.3316	0.2979	0.3405	0.4001	0.3548
Na	0.0071	0.0095	0.0039	0.0089	0.0044	0.0073
Total	4.0001	4.0051	3.9998	4.0000	4.0001	4.0001
	Mole %					
Diopside	51.02	51	59.79	54.8	51.16	52.12
Hedenbergite	45.52	44.86	38.08	42.4	45.71	44.42
Johannsenite	3.46	4.14	2.13	2.8	3.13	3.46

Major element values in percent

APPENDIX 23
REPRESENTATIVE CORE-TO-RIM MICROPROBE ANALYSES OF EXOSKARN GARNETS: JJ SKARN

HD 679-6-1

	Core				*Rim*
	1	*2*	*3*	*4*	*5*
SiO2	37.47	37.82	37.58	37.27	37.51
TiO2	0.56	0.37	0.52	0.66	0.73
Al2O3	14.23	15.01	14.97	14.83	14.75
Fe2O3	10.78	9.94	9.76	9.76	9.74
MgO	0.05	0.07	0.06	0.09	0.10
CaO	34.63	34.60	34.31	34.37	33.96
MnO	0.65	0.63	0.85	0.79	0.84
FeO	0.86	1.00	1.20	1.28	1.26
Total	99.23	99.44	99.25	99.05	98.89
	Cations				
Si	5.9334	5.9514	5.9332	5.9054	5.9422
Ti	0.0672	0.0444	0.0616	0.0784	0.0876
Al	2.6559	2.7845	2.7864	2.7702	2.7545
Fe+3	1.2843	1.1770	1.1600	1.1638	1.1611
Mg	0.0122	0.0161	0.0147	0.0202	0.0239
Ca	5.8761	5.8347	5.8036	5.8357	5.7636
Mn	0.0870	0.0842	0.1139	0.1055	0.1124
Fe+2	0.1133	0.1312	0.1586	0.1702	0.1673
Total	16.0294	16.0235	16.0320	16.0493	16.0124

HD 679A-6-2

	Core				*Rim*
	1	*2*	*3*	*4*	*5*
SiO2	37.49	37.64	37.76	36.97	37.67
TiO2	0.53	0.49	0.48	0.71	0.75
Al2O3	14.86	14.84	14.54	13.00	15.15
Fe2O3	9.78	9.92	10.56	12.10	9.25
MgO	0.09	0.07	0.10	0.09	0.06
CaO	34.01	34.15	34.08	33.82	34.37
MnO	0.82	0.73	0.78	0.77	0.57
FeO	1.26	1.22	1.21	1.09	1.32
Total	98.84	99.06	99.51	98.55	99.14
	Cations				
Si	5.9423	5.9517	5.9593	5.9324	5.9398
Ti	0.0633	0.0578	0.0573	0.0855	0.0890
Al	2.7760	2.7656	2.7036	2.4589	2.8163
Fe+3	1.1665	1.1808	1.2418	1.4611	1.0982
Mg	0.0210	0.0168	0.0226	0.0207	0.0146
Ca	5.7759	5.7848	5.7621	5.8138	5.8064
Mn	0.1107	0.0979	0.1037	0.1041	0.0762
Fe+2	0.1676	0.1618	0.1603	0.1456	0.1736
Total	16.0232	16.0173	16.0107	16.0221	16.0140

HD 679A-6-3

	Core				*Rim*
	1	*2*	*3*	*4*	*5*
SiO2	37.84	37.47	37.31	37.67	37.41
TiO2	0.65	0.65	0.39	0.38	0.37
Al2O3	15.26	14.85	15.08	15.30	14.09
Fe2O3	9.27	9.68	9.47	9.34	11.06
MgO	0.08	0.09	0.07	0.05	0.09
CaO	34.39	34.35	34.26	34.12	33.98
MnO	0.69	0.81	0.63	0.71	0.70
FeO	1.15	0.84	1.12	1.32	1.26
Total	99.33	98.74	98.33	98.89	98.96
	Cations				
Si	5.9509	5.9399	5.9367	5.9539	5.9479
Ti	0.0768	0.0769	0.0467	0.0451	0.0440
Al	2.8287	2.7737	2.8281	2.8496	2.6399
Fe+3	1.0968	1.1542	1.1341	1.1105	1.3227
Mg	0.0184	0.0208	0.0166	0.0129	0.0222
Ca	5.7946	5.8333	5.8397	5.7778	5.7882
Mn	0.0920	0.1088	0.0852	0.0961	0.0939
Fe+2	0.1513	0.1116	0.1485	0.1749	0.1678
Total	16.0095	16.0192	16.0355	16.0209	16.0267

HD 679A-6-4

	Core		*Rim*	
	1	*2*	*3*	*4*
SiO2	37.44	37.60	37.35	37.60
TiO2	0.44	0.41	0.72	0.43
Al2O3	13.79	13.96	13.85	14.93
Fe2O3	11.46	11.34	11.02	9.81
MgO	0.07	0.07	0.05	0.06
CaO	34.24	34.29	33.71	34.04
MnO	0.66	0.75	0.72	0.67
FeO	1.02	0.99	1.60	1.42
Total	99.12	99.41	99.02	98.96
	Cations			
Si	5.9483	5.9529	5.9421	5.9512
Ti	0.0531	0.0489	0.0863	0.0509
Al	2.5822	2.6047	2.5976	2.7860
Fe+3	1.3704	1.3514	1.3193	1.1683
Mg	0.0161	0.0154	0.0112	0.0141
Ca	5.8281	5.8161	5.7458	5.7730
Mn	0.0892	0.0999	0.0972	0.0898
Fe+2	0.1351	0.1308	0.2135	0.1876
Total	16.0224	16.0202	16.0131	16.0208

APPENDIX 24A

ASSAY RESULTS ON ASSORTED MINERALIZED GRAB SAMPLES (ppm UNLESS STATED OTHERWISE)

Field No.	Property	Au	Ag	Cu	Pb	Zn	Co	Ni	Mo	As	Sb	Bi
HD 266	French mine	2.2	154	10%	8	103	27	37	<5	127	45	0.50%
HD 310	French mine	4.2	715	0.13%	170	139	214	110	<5	0.37%	<5	0.26%
HD 53	Canty mine	34.6	4	243	12	23	0.6%	850	52	28.90%	168	<5
HD 384	Good Hope mine	94	2	32	13	305	25	16	300	360	28	0.47%
HD 17	Peggy (1 & 2 adits)	3.1	1	55	25	135	65	157	<5	0.19%	<5	<5
HD 23	Peggy (1 & 2 adits)	6.2	3	0.22%	11	23	116	82	6	0.73%	<5	<5
HD 18	Peggy (McKinnon adit)	5.8	10	60	14	12	700	90	8	1.50%	10	<5
HD 284	Peggy (1 & 2 adits)	21	3	1.18%	< 3	56	NA	30	<5	0.76%	42	<5
HD 504	Kel	1.1	< 0.5	0.13%	5	103	NA	11	<5	2.69%	5	<5
HD 538	JJ	< 20 ppb	< 0.5	280	11	605	20	5	<5	1200	<5	12
HD 538A	JJ	< 20 ppb	< 0.5	34	14	182	27	104	<5	155	<5	22
HD 300	Red Mountain	498 ppb	< 0.5	0.13%	19	177	62	19	<5	0.73%	<5	0.26%
HD 312	Red Mountain	238 ppb	5	0.16%	23	131	67	15	<5	0.50%	43	40
HD 759	Golden Zone	23	100	16	88	14	49	2	<5	25.60%	286	420
HD 762	Mission Flint	3.3	370	450	0.18%	2.85%	11	2	<5	19.00%	620	205
HD 501	Patsy No. 2	5	14	13	9	7	NA	10	<5	14.70%	95	10

Footnote: NA = element not analysed

APPENDIX 24B

ANALYSES OF MINERALIZED GRAB SAMPLES FROM MOUNT RIORDAN

Field No.	W %	Cu ppm	Mo ppm	Au ppb	Ag ppm	Zn ppm
HD 357	0.1	850	5	475	7	75
HD 355	0.25	840	15	339	0.8	210
HD 350	5.0	600	250	187	0.7	105
HD 351	3.0	0.70%	106	<20	10	357
HD 352	0.1	0.30%	19	161	15	321
HD 353	0.5	0.20%	33	99	9	111
HD 354	0.35	75	310	498	0.5	270
HD 356	0.25	150	145	<20	0.5	258
HD 361	4.0	0.35%	152	122	5	106
HD 362	2.0	0.16%	36	37	1.3	50
HD 359	0.9	118	6	<20	0.6	159
HD 360	0.7	117	17	40	0.5	307
HD 358	0.1	45	5	<20	0.5	73
HD 363	0.1	84	30	<20	0.5	52
HD 365	<0.1	75	5	14	3	138
HD 366	<0.1	0.74%	7	1690	19	0.11%
HD 364	<0.1	0.13%	6	29	0.7	118

W by semi-quantitive emission spectrophotometry;
Cu, Mo, Au, Ag and Zn by AAS analysis
Sample HD357 contained 275ppm As;
all other samples contained <30ppm As

APPENDIX 25
UTM LOCATIONS OF LITHOGEOCHEMICAL SAMPLES LISTED IN APPENDICES 3 TO 14

Field# HD	Easting	Northing	Field# HD	Easting	Northing
50	707907	5469906	285	711350	5472550
52	707558	5469964	299	698695	5464111
60	711537	5472322	309	716367	5475072
60A	711537	5472322	313	716392	5471910
61	711930	5472772	332	283241	5474463
62	711930	5472771	333	282896	5474609
63	711825	5473005	334	282307	5473601
64	711770	5473042	335	282306	5473601
65	711562	5473143	346	716666	5471532
66	711419	5473242	381	287800	5475550
67	711319	5473346	406	288478	5476119
68	711212	5473415	409	287439	5475074
69	711096	5473809	411	287350	5475000
70	710966	5473907	424	698765	5464488
71	711100	5473350	510	699071	5472839
72	711100	5473300	511	699700	5472400
73	711000	5473320	521	700385	5454200
73A	711000	5473320	522	706060	5470132
77	715093	5468971	523	705870	5469954
78	715086	5469056	524	705755	5469666
79	715086	5469056	525	704891	5469562
80	715086	5469196	526	704753	5469332
84	714171	5472665	527	703502	5460444
85	714170	5472661	528	703772	5460808
130	715354	5471356	529	703834	5460913
131	715310	5471498	530	703409	5459828
150	708363	5462434	531	706268	5462426
151	708800	5462000	532	706356	5462517
152	708850	5461940	541	709058	5472049
154	708680	5462430	542	709058	5472049
155	713125	5470332	543	709059	5472049
156	712967	5470521	544	709059	5472049
157	712905	5470666	545	711404	5471276
158	712191	5471625	546	711405	5471276
159	712424	5472167	547	711404	5471276
160	714791	5470795	549	714780	5470717
160A	714791	5470795	550	714690	5470864
161	714497	5471068	551	714608	5470941
162	713668	5471111	700	699127	5463760
163	713725	5471489	701	699008	5466791
164	712174	5472219	702	698571	5466246
171	707726	5461155	717	715746	5470427
172	707744	5461223	720	715685	5473148
173	707602	5461355	722	715685	5473148
218	712750	5474600	767	711050	5474500

APPENDIX 26

DESCRIPTION OF LITHOGEOCHEMICAL SAMPLES LISTED IN THE FOLLOWING APPENDICES

Appendices 3A and 3B

HD313 and HD346: Massive, very dark green and mafic ash tuff containing abundant basaltic fragments, and some crystals of augite and hornblende.

Appendices 4A

HD285: Black, massive limestone; Chuchuwayha Formation.

HD542: Gritty, dark limestone; Stemwinder Formation.

HD549: Thin bed of black limestone; Stemwinder Formation.

HD550: Grey, massive limestone with shell fragments; Hedley Formation.

HD551: Grey, massive limestone; Hedley Formation.

Appendix 4B

HD541: Dark, thin bedded calcareous siltstone; Stemwinder Formation.

HD543: Light grey, bedded silty argillite with thin crystal tuff layers: Chuchuwayha Formation.

HD544: Black, thin bedded silty argillite; Stemwinder Formation.

HD545: Gritty, grey, thin bedded siltstone containing some very thin beds of feldspar crystal tuff; Chuchuwayha Formation.

HD546: Light grey, thin bedded calcareous siltstone; Chuchuwayha Formation.

HD547: Light grey calcareous siltstone; Chuchuwayha Formation.

Appendix 5

HD521 to HD526: Massive, light green, fine to medium-grained ash and crystal-lithic tuffs containing abundant crystals of plagioclase with lesser augite, hornblende and minor chlorite. HD526 and HD521 include minor and small fragments of feldspar-porphyritic basalt.

Appendix 6

HD151 and HD152: Ash tuff containing abundant fragments of devitrified dacitic and andesitic volcanic rock, together with crystals of angular plagioclase and rounded quartz.

HD171: Lapilli tuff containing angular fragments of andesite, together with broken quartz and plagioclase crystals.

HD172: Similar to HD171 except less lapilli fragments and more rounded quartz crystals.

HD173: Ash tuff with rare fragments of devitrified dacite, and abundant crystals of quartz and feldspar.

HD309: Crystal tuff with abundant plagioclase and lesser quartz in a chloritic matrix.

HD332: Lapilli tuff with dacitic fragments, broken crystals of orthoclase, plagioclase, calcite, quartz, and rare apatite. Abundant chlorite in groundmass.

HD333: Similar to HD332 except less dacitic fragments and more plagioclase crystals.

HD527: Green coloured crystal tuff containing >90% zoned plagioclase crystals up to 4 mm long. Minor sericite, carbonate, epidote and opaque minerals. Minor alteration.

HD528: Crystal-lithic tuff similar to HD527 except more altered and contains some lithic clasts of altered andesite.

HD529: Crystal tuff containing >90% plagioclase crystals with a few remnant, chloritic hornblende crystals.

HD530: Coarse-grained crystal tuff containing >95% plagioclase and rare, remnant augite crystals. Minor tremolite-actinolite, chlorite and opaque minerals.

HD531: Dark green crystal-lithic tuff with large altered plagioclase, and abundant tremolite-actinolite and opaque minerals.

HD532: Crystal-lithic tuff similar to HD532.

Appendix 7

HD299: Fine-grained rhyodacite flow containing euhedral phenocrysts of orthoclase and lesser plagioclase up to 2 mm, together with rare, highly altered remnants of ?mica. Ground mass contains abundant small quartz crystals and minor carbonate.

HD424: Devitrified rhyodacitic welded tuff. Abundant quartz crystals with inclusions of apatite, together with broken crystals of plagioclase and orthoclase. Some flattened dacitic lapilli and welded glassy shards. Minor epidote and chlorite.

HD700: Porphyritic andesitic volcanic flow containing coarse plagioclase (up to 2 mm) and augite in a fine-grained groundmass of plagioclase, epidote, carbonate, chlorite and opaque minerals.

HD701: Feldspar crystal tuff similar in mineralogy to HD700.

HD702: Porphyritic volcanic flow similar to HD700.

Appendix 8

HD510: Very dark volcanic containing flow-aligned plagioclase lathes (up to 0.3 mm) and phenocrysts of augite (up to 1 mm) set in a very fine grained, dark matrix. Minor tremolite and opaque minerals, with rare phenocrysts of embayed quartz and altered olivine.

HD511: Dark volcanic flow similar to HD510 except the more abundant rounded quartz phenocrysts are surrounded by coronas of pyroxene. Minor late biotite also present.

Appendix 9

HD50: Porphyritic hornblende diorite with 10% mafics. Primary amphibole up to 1 cm.

HD52: Porphyritic hornblende quartz diorite with 15% mafics. Weakly chloritic.

HD60: Equigranular, dark, coarse-grained biotite-hornblende quartz diorite (Stemwinder stock) with 20% mafic minerals.

HD62: Equigranular, dark, coarse-grained hornblende gabbro (Stemwinder stock) with 20-25% mafic minerals.

HD64: Equigranular, coarse grained hornblende-pyroxene quartz gabbro (Stemwinder stock).

HD65: Equigranular hornblende quartz diorite (Stemwinder stock) with 10% mafic minerals. Minor alteration to tremolite-actinolite.

HD66: Equigranular, dark, coarse-grained hornblende quartz gabbro (Stemwinder stock) with 20-25% mafic minerals).

HD67: Equigranular quartz gabbro (Stemwinder stock) with 20% amphibole and trace biotite.

HD68: Coarse, hornblende-porphyritic quartz diorite (Stemwinder stock) with 10-15% mafic minerals.

HD69: Porphyritic hornblende diorite (Stemwinder stock) with 12-15% amphibole and trace late sericite.

HD70: Equigranular biotite-hornblende gabbro (Stemwinder stock) with 20-25% mafic minerals. Some late alteration to tremolite-actinolite.

HD71: Equigranular biotite-hornblende quartz diorite (Stemwinder stock) with 20% mafic minerals.

HD72: Equigranular hornblende quartz diorite (Stemwinder stock) with 15% mafic minerals.

HD73: Equigranular biotite-hornblende quartz diorite (Stemwinder stock) with 15% mafic minerals).

HD60A: Equigranular mafic hornblende quartz diorite (Stemwinder stock) similar to HD60.

HD73A: Equigranular biotite-hornblende quartz diorite (Stemwinder stock) with 10% mafic minerals.

HD156: Porphyritic biotite-hornblende quartz diorite (small sill) with 10% mafic minerals. Minor biotite and chlorite alteration of amphibole.

HD157: Porphyritic biotite-hornblende quartz diorite (small sill) similar to HD156.

HD158: Porphyritic biotite-hornblende quartz diorite (small sill) similar to HD156 except no secondary biotite alteration.

HD159: Equigranular biotite-hornblende quartz diorite with 5% mafic minerals.

HD161: Coarsely porphyritic hornblende quartz gabbro with 5% amphibole. Hornblende phenocrysts up to 1 cm.

HD162: Coarsely porphyritic hornblende gabbro similar to HD161: Porphyritic biotite-hornblende quartz diorite with 10% mafic minerals.

HD163: Porphyritic biotite-hornblende quartz diorite with 5% mafic minerals. Extensive secondary biotite alteration of amphiboles.

HD164: Coarsely porphyritic hornblende quartz diorite with 8% mafic amphibole.

HD218: Equigranular biotite-hornblende quartz diorite with 8% mafic minerals.

HD767: Porphyritic hornblende diorite with minor chloritic alteration.

HD334: Coarsely porphyritic hornblende quartz diorite with 8% amphibole. Hornblende phenocrysts up to 1.25 cm.

Appendices 10A and 10B

HD84: Endoskarn hornblende-quartz diorite (Toronto stock) with abundant clinopyroxene and minor garnet.

HD85: Endoskarn hornblende-quartz diorite (Toronto stock) with abundant clinopyroxene.

HD130: Endoskarn hornblende-quartz diorite sill close to the Toronto stock with extensive clinopyroxene and minor garnet alteration.

HD131: Endoskarn hornblende-quartz diorite similar to HD130 from a sill close to the Toronto stock.

HD335: Endoskarn hornblende-quartz diorite with minor clinopyroxene and chlorite.

HD720: Bleached endoskarn porphyritic hornblende-quartz diorite sill, from Level 12, underground Nickel Plate mine, with 10% primary hornblende weakly altered to clinopyroxene and minor biotite. Altered feldspars highly optically zoned.

HD722: Similar sill rock as HD720

Appendices 10C and 10D

HD61: Coarse-grained biotite-hornblende-pyroxene diorite (Stemwinder stock) with 10-15% mafic minerals. Mafic minerals extensively chloritized; minor secondary biotite.

HD63: Bleached and silicified, medium grained biotite-hornblende quartz diorite (Stemwinder stock) with 10% mafic minerals. Hornblende phenocrysts are weakly altered to biotite

HD155: Coarse-grained hornblende-pyroxene-quartz diorite. Abundant silicification and primary hornblende and pyroxene replaced by biotite and minor chlorite.

HD160: Porphyritic hornblende quartz diorite; extensively silicified.

HD160A: Similar to HD160.

Appendices 11A and 11B

HD381: Porphyritic biotite-hornblende granodiorite similar to HD406.

HD406: Porphyritic biotite-hornblende granodiorite with 6-10% mafic minerals. Hornblende phenocrysts up to 0.5 cm.

HD409: Equigranular biotite-hornblende-quartz gabbro with 12% mafic minerals. Weakly altered.

HD411: Fine to medium-grained hornblende microgabbro with 20-30% hornblende. Some epidote veining.

Appendices 12A and 12B

HD77: Massive, equigranular granodiorite containing 5% weakly chloritized hornblende and 2% biotite.

HD78: Similar to HD77.

HD79: Massive, equigranular granodiorite with 8% hornblende and 2% biotite.

HD80: Similar to HD79 except weakly porphyritic with hornblende phenocrysts up to 4 mm.

HD717: Equigranular quartz monzodiorite with 5% hornblende and 3% biotite.

HD514-15: Equigranular quartz monzodiorite with 3% hornblende and 3% biotite. Weakly chloritized.

HD514-60: Similar to HD514-15 except less chloritized.

Appendices 13A and 13B

HD150 and HD154: Fine-grained, leucocratic feldspar porphyritic rhyodacitic intrusion. Groundmass of quartz and flow-aligned feldspar laths. Orthoclase phenocrysts up to 3 mm, together with rare, anhedral crystals of isotropic garnet and flakes of strongly altered biotite also occur.

Appendix 14

HD514-14 and HD514-40: Fine-grained, leucocratic weakly porphyritic intrusions with small phenocrysts of partially resorbed quartz and altered feldspar.

Appendices 16A and 16B

401-01 and 401-02: Skarn-altered Copperfield breccia with abundant fine-grained pyroxene, calcite, orthoclase and quartz, and trace wollastonite, clinozoisite and epidote. Up to 5% pyrrhotite.

401-03 and 401-04: Endoskarn (porphyritic diorite) with abundant pyroxene, plagioclase, quartz, calcite and epidote, and trace wollastonite, orthoclase and chlorite. Up to 10% pyrrhotite; trace arsenopyrite).

401-05 to 401-07: Exoskarn (siltstone) with abundant pyroxene, plagioclase, orthoclase, and calcite. Locally rich in garnet, scapolite and pyrrhotite (up to 10% each).

401-08: Exoskarn (altered tuff?). Abundant pyroxene, carbonate, quartz, orthoclase and plagioclase with trace scapolite, wollastonite and clinozoisite.

401-09 to 401-11: Strongly altered exoskarn (siltstone?). Abundant pyroxene, plagioclase, epidote, lesser orthoclase and up to 10% pyrrhotite. Trace idocrase, biotite and scapolite.

401-12 and 401-13: Endoskarn (porphyritic diorite) abundant plagioclase, carbonate and quartz, moderate pyroxene and scapolite, and trace wollastonite, biotite, and epidote. Up to 15% pyrrhotite.

401-14 and 401-15: Exoskarn (siltstone?). Abundant carbonate, plagioclase and pyrrhotite with moderate pyroxene and scapolite.

401-16: Endoskarn. Remnant amphibole phenocrysts replaced with pyroxene and epidote. Moderate pyroxene and pyrrhotite. Trace wollastonite

401-17: Pyroxene-garnet exoskarn (tuffaceous siltstone?). Garnet less than 2%. Minor scapolite.

401-18: Endoskarn (porphyritic hornblende diorite). Abundant plagioclase and calcite, and moderate pyroxene. Trace piedmontite and wollastonite. Some remnant hornblende phenocrysts.

401-19: Skarn-altered tuff with abundant scapolite and quartz, and moderate pyroxene, carbonate and pyrrhotite.

401-20: Biotite "hornfels" (altered argillite). Abundant fine-grained quartz, plagioclase and orthoclase with moderate biotite, pyroxene, scapolite, carbonate and pyrrhotite. Trace chlorite.

401-21: Weakly skarn-altered coarse porphyritic hornblende diorite (endoskarn). Abundant plagioclase and quartz with moderate pyroxene.

401-22: Wollastonite-rich (30%) exoskarn (calcareous siltstone with thin limestone beds) with abundant quartz and carbonate, pyroxene and epidote. Also trace remnant cordierite.

401-23 and 401-24: Weakly altered hornblende porphyritic diorite (endoskarn). Amphibole phenocrysts partially replaced with pyroxene and epidote. Feldspars intensely zoned.

401-25: Pyroxene-rich exoskarn (calcareous siltstone) with abundant carbonate and quartz, and trace axinite.

401-26: Massive, highly altered exoskarn? with abundant fine-grained plagioclase and quartz, and minor biotite, pyroxene and sericite.

401-27: Highly altered lapilli tuff with abundant carbonate, epidote and quartz and minor pyroxene. Trace remnant cordierite.

401-28 and 401-29: Exoskarn (calcareous siltstone with thin tuff beds) with abundant wollastonite, carbonate, quartz and pyroxene.

401-30: Coarse impure marble with 80% carbonate and minor quartz, and trace pyroxene and scapolite.

401-31 and 401-32: Weakly skarn-altered bedded tuff with abundant plagioclase and quartz and minor carbonate. Trace biotite, orthoclase and pyroxene.

Appendices 17A and 17B

195-01: Thinly layered pyroxene-garnet exoskarn (calcareous siltstone?) with abundant carbonate.

195-02: Endoskarn (hornblende-quartz diorite with rare partially resorbed quartz phenocrysts). Abundant albitic plagioclase and fine-grained quartz. Minor pyroxene and trace biotite.

195-03: Layered pyroxene and garnet-rich exoskarn (siltstone?) with abundant plagioclase and quartz. Minor orthoclase and scapolite.

195-04 to 195-06: Weakly skarn-altered, bleached hornblende-porphyritic diorite (endoskarn) with minor pyroxene.

195-07 to 195-09: Intensely altered pyroxene-garnet-carbonate exoskarn (locally garnet dominant) with abundant scapolite, pyrrhotite and arsenopyrite, and trace sphene, orthoclase and epidote. Some veins and patches of black chlorite.

195-10: Bleached endoskarn (porphyritic hornblende diorite) with abundant pyroxene and plagioclase, and minor garnet.

195-11 to 195-13: Layered pyroxene-garnet-carbonate exoskarn with abundant pyrrhotite and arsenopyrite, minor scapolite, and trace sphene.

195-14: Bleached endoskarn (porphyritic hornblende diorite) with veins of garnet and pyroxene.

261-01 and 261-02: Garnet-pyroxene-carbonate exoskarn (limestone and calcareous siltstone?) with 60-80% garnet. Trace pyrrhotite, orthoclase, biotite, wollastonite, scapolite and chlorite.

261-03 to 261-05: Intensely skarn-altered porphyritic diorite (endoskarn) with abundant plagioclase and quartz, minor pyroxene and carbonate, and trace sphene, scapolite, orthoclase, chlorite and pyrrhotite.

261-06 to 261-09: Garnet-pyroxene-carbonate exoskarn (calcareous siltstone with limestone beds?). Locally garnet dominant with abundant plagioclase, epidote, and quartz. Trace scapolite, biotite, orthoclase and sphene.

261-11: Bleached endoskarn (porphyritic diorite) with moderate pyroxene.

261-10 and 261-12 to 261-19: Garnet-pyroxene-carbonate exoskarn (calcareous siltstone?). Locally garnet dominant with abundant pyrrhotite and scapolite. Moderate orthoclase and trace wollastonite, sphene and chlorite.

261-20 to 261-22: Pyroxene exoskarn (calcareous siltstone?) with abundant carbonate, scapolite, pyrrhotite and arsenopyrite.

261-23: Marble with abundant wollastonite and pyrrhotite, and minor arsenopyrite. Trace orthoclase, pyroxene and tremolite-actinolite.

261-25: Weakly altered porphyritic diorite (endoskarn) with abundant plagioclase, moderate scapolite and trace pyroxene and sphene.

261-27: Intensely altered porphyritic diorite (endoskarn) with abundant plagioclase and quartz, minor hornblende and pyroxene, and trace tremolite-actinolite.

Appendix 24A

French mine: HD266: Pyroxene skarn with massive chalcopyrite and bornite, and minor pyrrhotite.

French mine: HD310: Pyroxene skarn with disseminated chalcopyrite and arsenopyrite.

Canty mine: HD53: Massive arsenopyrite with minor pyrrhotite.

Good Hope mine: HD384: Garnet-pyroxene-carbonate skarn with abundant pyrrhotite and trace chalcopyrite.

Peggy skarn: HD17: Pyroxene-garnet skarn with minor pyrrhotite and arsenopyrite.

Peggy skarn: HD18: Pyroxene skarn with disseminated pyrrhotite and arsenopyrite.

Peggy skarn: HD23: Pyroxene skarn with veinlets of chalcopyrite, pyrrhotite and arsenopyrite.

Peggy skarn: HD284: Massive pyrrhotite with minor chalcopyrite and arsenopyrite.

Kel: HD504: Fine-grained biotite-pyroxene skarn with arsenopyrite and chalcopyrite veins.

JJ: HD538 and HD538A: Schistose pyroxene- carbonate skarn with trace pyrite and pyrrhotite.

Red Mountain: HD300 and HD312: Garnet-pyroxene endoskarn with coarse veins of pyrrhotite and minor arsenopyrite and chalcopyrite.

Golden Zone: HD759: Massive arsenopyrite with minor white quartz and pyrite.

Mission Flint: HD762: Massive arsenopyrite with brown sphalerite.

Patsy No.2: HD501: Arsenopyrite-rich quartz-carbonate vein.

Queen's Printer for British Columbia©
Victoria, 1994